Springer Protocols

Terry J. McGenity
Kenneth N. Timmis
Balbina Nogales *Editors*

Hydrocarbon and Lipid Microbiology Protocols

Ultrastructure and Imaging

Springer

Springer Protocols Handbooks

More information about this series at http://www.springer.com/series/8623

Terry J. McGenity · Kenneth N. Timmis · Balbina Nogales
Editors

Hydrocarbon and Lipid Microbiology Protocols

Ultrastructure and Imaging

Scientific Advisory Board
Jack Gilbert, Ian Head, Mandy Joye, Victor de Lorenzo,
Jan Roelof van der Meer, Colin Murrell, Josh Neufeld,
Roger Prince, Juan Luis Ramos, Wilfred Röling,
Heinz Wilkes, Michail Yakimov

Springer

Editors
Terry J. McGenity
School of Biological Sciences
University of Essex
Colchester, Essex, UK

Kenneth N. Timmis
Institute of Microbiology
Technical University Braunschweig
Braunschweig, Germany

Balbina Nogales
Department of Biology
University of the Balearic Islands
and Mediterranean Institute
for Advanced Studies
(IMEDEA, UIB-CSIC)
Palma de Mallorca, Spain

ISSN 1949-2448 ISSN 1949-2456 (electronic)
Springer Protocols Handbooks
ISBN 978-3-662-49132-4 ISBN 978-3-662-49134-8 (eBook)
DOI 10.1007/978-3-662-49134-8

Library of Congress Control Number: 2016938230

© Springer-Verlag Berlin Heidelberg 2016
This work is subject to copyright. All rights are reserved by the Publisher, whether the whole or part of the material is concerned, specifically the rights of translation, reprinting, reuse of illustrations, recitation, broadcasting, reproduction on microfilms or in any other physical way, and transmission or information storage and retrieval, electronic adaptation, computer software, or by similar or dissimilar methodology now known or hereafter developed.
The use of general descriptive names, registered names, trademarks, service marks, etc. in this publication does not imply, even in the absence of a specific statement, that such names are exempt from the relevant protective laws and regulations and therefore free for general use.
The publisher, the authors and the editors are safe to assume that the advice and information in this book are believed to be true and accurate at the date of publication. Neither the publisher nor the authors or the editors give a warranty, express or implied, with respect to the material contained herein or for any errors or omissions that may have been made.

Printed on acid-free paper

This Springer imprint is published by Springer Nature
The registered company is Springer-Verlag GmbH Berlin Heidelberg

Preface to Hydrocarbon and Lipid Microbiology Protocols[1]

All active cellular systems require water as the principal medium and solvent for their metabolic and ecophysiological activities. Hydrophobic compounds and structures, which tend to exclude water, although providing *inter alia* excellent sources of energy and a means of biological compartmentalization, present problems of cellular handling, poor bioavailability and, in some cases, toxicity. Microbes both synthesize and exploit a vast range of hydrophobic organics, which includes biogenic lipids, oils and volatile compounds, geochemically transformed organics of biological origin (i.e. petroleum and other fossil hydrocarbons) and manufactured industrial organics. The underlying interactions between microbes and hydrophobic compounds have major consequences not only for the lifestyles of the microbes involved but also for biogeochemistry, climate change, environmental pollution, human health and a range of biotechnological applications. The significance of this "greasy microbiology" is reflected in both the scale and breadth of research on the various aspects of the topic. Despite this, there was, as far as we know, no treatise available that covers the subject. In an attempt to capture the essence of greasy microbiology, the *Handbook of Hydrocarbon and Lipid Microbiology* (http://www.springer.com/life+sciences/microbiology/book/978-3-540-77584-3) was published by Springer in 2010 (Timmis 2010). This five-volume handbook is, we believe, unique and of considerable service to the community and its research endeavours, as evidenced by the large number of chapter downloads. Volume 5 of the handbook, unlike volumes 1–4 which summarize current knowledge on hydrocarbon microbiology, consists of a collection of experimental protocols and appendices pertinent to research on the topic.

A second edition of the handbook is now in preparation and a decision was taken to split off the methods section and publish it separately as part of the Springer Protocols program (http://www.springerprotocols.com/). The multi-volume work *Hydrocarbon and Lipid Microbiology Protocols*, while rooted in Volume 5 of the Handbook, has evolved significantly, in terms of range of topics, conceptual structure and protocol format. Research methods, as well as instrumentation and strategic approaches to problems and analyses, are evolving at an unprecedented pace, which can be bewildering for newcomers to the field and to experienced researchers desiring to take new approaches to problems. In attempting to be comprehensive – a one-stop source of protocols for research in greasy microbiology – the protocol volumes inevitably contain both subject-specific and more generic protocols, including sampling in the field, chemical analyses, detection of specific functional groups of microorganisms and community composition, isolation and cultivation of such organisms, biochemical analyses and activity measurements, ultrastructure and imaging methods, genetic and genomic analyses, systems and synthetic biology tool usage, diverse applications, and

[1] Adapted in part from the Preface to *Handbook of Hydrocarbon and Lipid Microbiology*.

the exploitation of bioinformatic, statistical and modelling tools. Thus, while the work is aimed at researchers working on the microbiology of hydrocarbons, lipids and other hydrophobic organics, much of it will be equally applicable to research in environmental microbiology and, indeed, microbiology in general. This, we believe, is a significant strength of these volumes.

We are extremely grateful to the members of our Scientific Advisory Board, who have made invaluable suggestions of topics and authors, as well as contributing protocols themselves, and to generous *ad hoc* advisors like Wei Huang, Manfred Auer and Lars Blank. We also express our appreciation of Jutta Lindenborn of Springer who steered this work with professionalism, patience and good humour.

Colchester, Essex, UK — Terry J. McGenity
Braunschweig, Germany — Kenneth N. Timmis
Palma de Mallorca, Spain — Balbina Nogales

Reference

Timmis KN (ed) (2010) Handbook of hydrocarbon and lipid microbiology. Springer, Berlin, Heidelberg

Contents

About the Editors

Terry J. McGenity is a Reader at the University of Essex, UK. His Ph.D., investigating the microbial ecology of ancient salt deposits (University of Leicester), was followed by postdoctoral positions at the Japan Marine Science and Technology Centre (JAMSTEC, Yokosuka) and the Postgraduate Research Institute for Sedimentology (University of Reading). His overarching research interest is to understand how microbial communities function and interact to influence major biogeochemical processes. He worked as a postdoc with Ken Timmis at the University of Essex, where he was inspired to investigate microbial interactions with hydrocarbons at multiple scales, from communities to cells, and as both a source of food and stress. He has broad interests in microbial ecology and diversity, particularly with respect to carbon cycling (especially the second most abundantly produced hydrocarbon in the atmosphere, isoprene), and is driven to better understand how microbes cope with, or flourish in hypersaline, desiccated and poly-extreme environments.

Kenneth N. Timmis read microbiology and obtained his Ph.D. at Bristol University, where he became fascinated with the topics of environmental microbiology and microbial pathogenesis, and their interface pathogen ecology. He undertook postdoctoral training at the Ruhr-University Bochum with Uli Winkler, Yale with Don Marvin, and Stanford with Stan Cohen, at the latter two institutions as a Fellow of the Helen Hay Whitney Foundation, where he acquired the tools and strategies of genetic approaches to investigate mechanisms and causal relationships underlying microbial activities. He was subsequently appointed Head of an Independent Research Group at the Max Planck Institute for Molecular Genetics in Berlin, then Professor of Biochemistry in the University of Geneva Faculty of Medicine. Thereafter, he became Director of the Division of Microbiology at the National Research Centre for Biotechnology (GBF)/now the Helmholtz Centre for Infection Research (HZI) and Professor of Microbiology at the Technical University Braunschweig. His group has worked for many years, *inter alia*, on the biodegradation of oil hydrocarbons, especially the genetics and regulation of toluene degradation, pioneered the genetic design and experimental evolution of novel catabolic activities, discovered the new group of marine hydrocarbonoclastic bacteria, and conducted early genome sequencing of bacteria that

became paradigms of microbes that degrade organic compounds (*Pseudomonas putida* and *Alcanivorax borkumensis*). He has had the privilege and pleasure of working with and learning from some of the most talented young scientists in environmental microbiology, a considerable number of which are contributing authors to this series, and in particular Balbina and Terry. He is Fellow of the Royal Society, Member of the EMBO, Recipient of the Erwin Schrödinger Prize, and Fellow of the American Academy of Microbiology and the European Academy of Microbiology. He founded the journals *Environmental Microbiology*, *Environmental Microbiology Reports* and *Microbial Biotechnology*. Kenneth Timmis is currently Emeritus Professor in the Institute of Microbiology at the Technical University of Braunschweig.

Balbina Nogales is a Lecturer at the University of the Balearic Islands, Spain. Her Ph.D. at the Autonomous University of Barcelona (Spain) investigated antagonistic relationships in anoxygenic sulphur photosynthetic bacteria. This was followed by postdoctoral positions in the research groups of Ken Timmis at the German National Biotechnology Institute (GBF, Braunschweig, Germany) and the University of Essex, where she joined Terry McGenity as postdoctoral scientist. During that time, she worked in different research projects on community diversity analysis of polluted environments. After moving to her current position, her research is focused on understanding microbial communities in chronically hydrocarbon-polluted marine environments, and elucidating the role in the degradation of hydrocarbons of certain groups of marine bacteria not recognized as typical degraders.

Ultrastructure and Imaging

Manfred Auer

Abstract

Most characterization techniques use bulk approaches to study microbes in either their planktonic or their biofilm state. Such bulk analysis methods however ignore the large heterogeneities that exist with respect to protein expression and metabolism. Visualizing the cell-to-cell differences in protein and metabolite abundance that exist in planktonic cultures as well as regional differences that can be found in biofilms require imaging approaches with adequate resolving power and spatial coverage. Various optical light and electron microscopy techniques are most frequently employed, often in a correlative manner. Samples must be faithfully preserved, and imaging often requires the use of affinity-based or genetically encoded tag-based specific labeling approaches, however label-free imaging is a promising developing field. Light and electron microscopy, particularly when well integrated, have excellent potential to allow mechanistic insight into biological processes in hydrocarbon and lipid research.

Keywords Biofilms, Electron microscopy, Heterogeneity, Imaging, Light microscopy

Most characterization techniques studying microbes in planktonic culture or in biofilms are bulk approaches resulting in measurements of an averaged characteristics or response. It is now widely accepted that the assumption of homogeneity in a cell culture is incorrect, instead that even monocultures display heterogeneities possibly stemming from the fact that different cells in solution are likely in a different stage in their life cycle and show vastly different protein expression profiles. This heterogeneity is augmented when considering microbial communities, where different cells face different micro-niche environments. Likewise, the proximity to a hydrocarbon liquid or solid surfaces is likely to affect microbial physiology and further complicates the idealized view of a unified homogenous response and/or metabolic and protein expression profile.

Imaging is one of the most promising routes to deal with such heterogeneities, as imaging in principle allows the study of individual microbes and the interaction with their respective micro-niche environment. Given that the size of the microbes being typically in its shortest dimension is less than 1 μ, only a small window of the

T.J. McGenity et al. (eds.), *Hydrocarbon and Lipid Microbiology Protocols*, Springer Protocols Handbooks (2016) 1–3,
DOI 10.1007/8623_2015_154, © Springer-Verlag Berlin Heidelberg 2015, Published online: 19 December 2015

electromagnetic and/or discrete subatomic particle spectrum can be utilized for imaging, and thus it is no surprise that the vast majority of contributions in this volume/chapter is based on fluorescence light microscopy and electron microscopy. Often these two approaches are employed in a correlative manner or at least consecutively, since they probe different aspects of the system, and if planned carefully with adequate controls can yield comprehensive insight into microbial function.

To be clear, in most cases, the task goes beyond the simple taking of image snapshots that may serve as eye candy for an otherwise solid scientific story. Instead, the imaging itself is the vehicle that allows to test hypotheses and to reveal mechanistic insight. Therefore, adequate experimental controls, extensive optimization of probes, labeling schemes, contrasting schemes, and sample preservation all are crucial in order to provide adequate spatiotemporal context to microbial responses and physiological properties.

Sample preparation, the often unsung hero, obviously is key for any meaningful analysis: avoiding the trash-in/trash-out trap cannot be overstated. This ranges from resolution-faithful preservation of 2D and 3D (biofilm or protein) organization, over the elimination or reduction of background noise, e.g., autofluorescence of the abiotic surface area or through minimizing out-of-focus contributions.

Furthermore, devising adequate and specific molecular targeting schemes that exploit distinctions in microbial phylogenetic identity, metabolic activity, or functional protein inventory is at the heart of label-dependent imaging, whereas label-free imaging approaches at the optical microscopy level may be affected by nuisances like high autofluorescence or spectral overlap.

Naturally, it is important to obtain statistically sufficient data, either by high-throughput imaging of individual cells or by large area/volume imaging, in order to reveal a comprehensive picture of microbial properties or response, ideally by clustering the heterogeneous observations into a small set of interpretable categories through computer-assisted image analysis. All optical microscopy imaging approaches are designed to yield information at the level of individual cells or clusters of cells in microbial communities localizing to different micro-niches or biofilm regions.

For information at the subcellular level, one typically needs to resort to the high-resolution imaging capability ensured by electron microscopy (EM). However, careful sample preparation is even more important for EM studies of hydrocarbon-rich samples in order to preserve both the hydrocarbon-rich sample portion as well as the microbial ultrastructure. Cryogenic and/or correlative sample preparation approaches offer a solution but can be more difficult to implement, with some approaches being limited to very few labs around the world, whereas other approaches can be

mastered by a wider community. For certain applications, it may be desirable to combine fluorescence and electron microscopy imaging, whereas with others, they appear somewhat mutually exclusive or somewhat difficult to combine (e.g., CARD-FISH and EM).

All in all, it seems clear that an integrated approach that combines several of these approaches is superior to conventional approaches and will yield a more complete picture of microbial physiology in the presence of hydrocarbons and lipids. Beside architectural imaging and localization imaging, one would like to have a strong footprint in label-free compositional imaging, such as FTIR, Raman, or mass spectrometry imaging, but hydrocarbons are not always very easy to detect and visualize or technical issues like autofluorescence can be problematic, and this there is clearly room for innovation and technology improvement.

In summary, some of the more frequently encountered techniques like fluorescence microscopy are widely accessible and can be readily adapted by a novice researcher, whereas others are so specialized that only few people will have access to it; however, we believe that they make a useful contribution as they demonstrate the potential that ultrastructure and imaging have in the context of hydrocarbon and lipid research.

Electron Microscopy Protocols for the Study of Hydrocarbon-Producing and Hydrocarbon-Decomposing Microbes: Classical and Advanced Methods

Kamna Jhamb and Manfred Auer

Abstract

One of the fascinating areas of hydrocarbon microbiology biology is the quest for an ultratstructural understanding of (macro)-molecular mechanisms underlying the degradation, synthesis, and intracellular storage of hydrocarbons, which due to their hydrophobic characteristics continuously threaten the integrity of biological membranes. Here we review classical and novel advanced electron microscopy approaches, including correlative light and electron microscopy that in combination with genetics and biochemical experimentation can be utilized to study such hydrocarbon–cell interactions.

Keywords: Cellular inclusion, Correlative microscopy, Cryo-EM, Electron microscopy, Hydrocarbon, Lipid

1 Introduction

1.1 Significance

All life on Earth relies on the unique properties of water, and thus to carry out biochemical reactions efficiently, evolution has created lipid-enclosed membranes compartments, which allow (bio)chemical reactions to take place in a defined chemical environment. For this reason any lipophilic solvents, such as hydrocarbons, are of great danger to the integrity of these membranous compartments and thus to the integrity of its metabolism. It is therefore surprising that certain microorganism not only can exist in the presence of hydrocarbon but also can grow and strive under such conditions, using the high energy density stored in hydrocarbon to fuel their metabolism. Hydrocarbons are the Earth's most important natural energy resources, being the main constituents of petroleum and natural gas reserves. They are formed abiotically through pressure and appropriate temperature condition-mediated reduction of fossilized organic material such as zooplankton and algae in sediments. Petroleum and natural gas are critical to all human economic activities, including transportation, and energy and are therefore of high

T.J. McGenity et al. (eds.), *Hydrocarbon and Lipid Microbiology Protocols*, Springer Protocols Handbooks (2016) 5–28,
DOI 10.1007/8623_2015_96, © Springer-Verlag Berlin Heidelberg 2015, Published online: 05 July 2015

geostrategic significance, and thus, any biotic mechanisms (e.g., caused by microorganisms residing in oil wells), by which such petroleum reservoirs may be affected, are of great importance to the petroleum industry. The very question by which mechanisms microorganisms can exist and even strive in hydrocarbon-rich environment is fascinating, as it touches on tolerance toward presumably toxic chemical conditions and the microbial strategies employed to deal with the destabilizing effect of a lipophilic solvent. This question not only concerns the biodegradation of hydrocarbons but also the effective synthesis and storage of lipid moieties such as triacylglycerols (TAGs) and wax esters, which are used as storage reservoirs for energy, leading to the recognition of an entirely new branch of science called as "hydrocarbon microbiology."

1.2 Hydrocarbon Microbiology

Certain systematic groups of microorganisms are characterized by specific composition of the hydrocarbon fractions; for instance, cyanobacteria are unique in their ability to produce 7- and 8-methylheptadecanes; photosynthetic bacteria are distinguished by the synthesis of cyclic hydrocarbons (pristane and phytane), whereas in fungi, long-chain hydrocarbons are predominant. It was assumed that the hydrocarbon composition of microorganisms could be used as a chemotaxonomic criterion. Microbial hydrocarbons appear to regulate the cell development; act as causative agents in the plant–microorganism, predator–prey, and interspecies interactions; and play an important ecological and physiological role [1].

There are at least four different aspects of hydrocarbon microbiology that go beyond an academic curiosity in hydrocarbon microbiology and thus are of industrial interest:

1. **Biodegradation of petroleum reserves**: Degradation of oil results in a decrease in its hydrocarbon content and an increase in oil density, sulfur content, acidity, and viscosity. These changes have negative economic consequences for oil production and refinery operations. Recent studies [2, 3] have concluded that in addition to aerobic bacteria in the shallow on-shore oil fields, a variety of anaerobic bacteria, including sulfate-reducing bacteria, iron oxide-reducing bacteria, and bicarbonate-reducing bacteria are capable of biodegrading oils. Most biodegrading organisms negatively impact the economics of the oil drilling process by generating carbon dioxide as a by-product when they degrade the hydrocarbons [4]. The knowledge of the microbiology of hydrocarbon degradation in petroleum reservoirs and of the microorganisms involved and the pathways by which these microbes utilize oil components as well as the conditions under which they thrive is critical and can save time for the exploration of new oil reserves [5].
2. **Bioremediation**: Oil spills that occur during drilling operations or other accidental oil spills are catastrophic for the fragile marine life in the affected areas. Microbes have long been

known to naturally degrade oil and its constituents [6]. The literature is filled with numerous reports and reviews, highlighting the exploitation of microorganisms for bioremediation [7–12]. Emergency response guidelines from the Environmental Protection Agency (EPA) for cleanup of oil spills consider biological agents (microorganisms) crucial for successful bioremediation approaches [13]. However, recently, Kostka and colleagues have highlighted the fact that despite the available advances in technologies for oil drilling, strategies to respond to oil spills and to assess environmental impacts of oil contamination have lagged behind. It is imperative that we develop a detailed understanding of the impacts of oil on indigenous microbial communities and pave the way for identification of oil-degrading microbial groups that are prerequisite for directing the management and cleanup of oil contaminated beach ecosystems [14].

3. **Biosynthesis of hydrocarbons**: Traditionally, hydrocarbon biomarkers have been used to constrain the age of the ancient bacteria, archaea, and eukaryotes owing to their long-term stability [1]. Gas and liquid chromatography as well as ultrastructural visualization by electron microscopy [15] has led to the discovery of intracellular hydrocarbons in microbes, which given the fact that microorganisms can be efficiently cultivated in bioreactors has led to a growing interest in using biotechnology for the production of fuels and chemicals, which to this date are largely derived from petroleum hydrocarbon reservoirs that are becoming scarcer and more expensive to exploit. Thus, it comes as no surprise that one goal of commodity biotechnology is to produce hydrocarbons via bacterial metabolism [16]. The major polymeric lipids produced by prokaryotes are poly (3-hydroxybutyrate) (PHB) or other polyhydroxyalkanoates (PHAs), whereas accumulation of triacylglycerols (TAGs) and wax esters (WEs) in intracellular lipid bodies is a property of only a few prokaryotes. The formation of PHAs, TAGs, and WEs is also promoted in response to stress imposed on the cells and during imbalanced growth, for example, by nitrogen limitation, if an abundant carbon source is present at the same time. All these lipids act as storage compounds for energy and carbon needed for maintenance of metabolism and synthesis of cellular metabolites during starvation [17–19]. The literature has since been growing on the studies conducted on the formation and mechanisms of hydrocarbon biosynthesis, accumulation, and transport in microbial cells [15, 16, 20, 21].
4. **Biofuels**: Ever-growing demands for crude oil and concerns about carbon emissions from fossil fuels contributing to the climate change and alternative renewable resources for transport fuel are urgently needed. Biofuels, in particular biodiesel,

which is produced from renewable biomass by transesterification of triacylglycerols, yielding monoalkyl esters of long-chain fatty acids with short-chain alcohols, for example, fatty acid methyl esters (FAMEs) and fatty acid ethyl esters (FAEEs), has gained considerable attention in this regard, even more so as it contributes no net carbon dioxide or sulfur to the atmosphere and emits less gaseous pollutants than normal diesel [22]. Plant oils and animal fats have been used to generate biodiesel worldwide. Ethanol, made mostly from corn starch from kernels, today is by far the most significant biofuel in the United States, accounting for 94% of all biofuel production in 2012. Most of the remainder is biodiesel, which is made from vegetable oils (chiefly soy oil) as well as animal fats, waste oils, and greases [23]. However, considering the economics of the production of biofuels and the amount of area required for cultivation of plants, researchers are now looking for other viable options. Oleaginous microorganisms such as yeasts, fungi, microalgae, and some bacteria are known to accumulate intracellular lipids, mainly triacylglycerols and some wax esters, which may prove to be become promising alternatives [24]. Developing "high lipid content" microorganisms or engineered strains for biodiesel production would be becoming a potential and promising way in the future [22].

All the aspects of hydrocarbon microbiology discussed above highlight the need to understand microbial oil/lipid catabolism and anabolism and strategies for withstanding the solvent properties of these substances, threatening the integrity of cell membranes. Specifically, we would like to understand the exact mechanisms of biodegradation of oil and the microbial communities that are involved in this process and the synergistic behavior of community members. Also, we know very little about how the lipid inclusions/bodies accumulate inside the cell, their ultrastructure (shape and size), and how this process is controlled, as well as the transport mechanisms to and from the cell to extracellular medium. A combination of genetic, cell biological, biochemical, and biophysical (including ultrastructural) studies will yield insight on the cellular and molecular base of lipid bodies and the regulation of their accumulation and mobilization and thus could lead to the use of these organisms as a renewable energy resource [19, 25].

Direct imaging of hydrocarbons and lipids inside (or in the presence of) microorganism by light and electron microscopy allows the study of heterogeneous processes, where not all microorganism will contain the same amount of hydrocarbon and lipids, or where the hydrocarbons and lipids are found in (or are associated with) particular intracellular compartments. A few examples from our own research will illustrate the various approaches that are further detailed below. For example a variety of commercially available

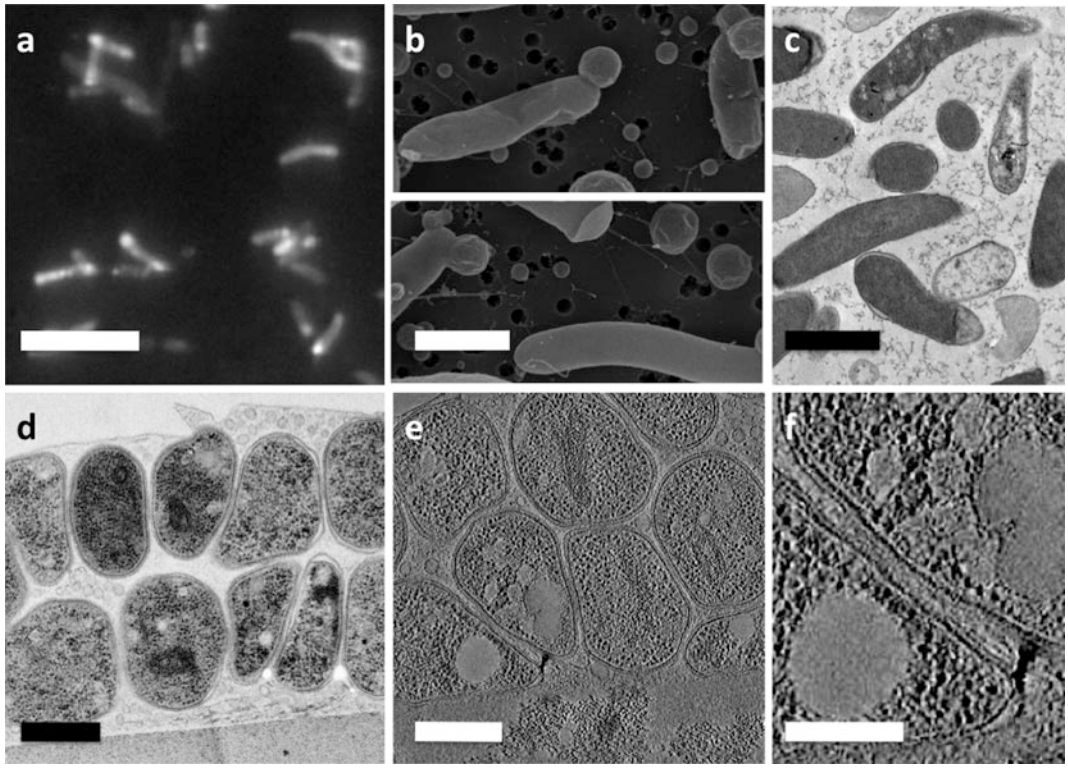

Fig. 1 Hydrocarbon/lipid storage in bacteria. Biodiesel producing *Escherichia coli* imaged by (**a**) fluorescence microscopy, revealing polar distribution of biodiesel, (**b**) scanning electron microscopy, showing ball-like structure most likely enclosing biodiesel, and (**c**) ultrathin-section transmission electron microscopy, revealing extracted polar regions. (**d**)–(**f**) High-pressure frozen, freeze-substituted *Myxococcus xanthus* biofilms as imaged by transmission electron microscopy of 100 nm ultrathin sections (**d**). Upon 3D imaging by electron tomography, single or merged drop-like empty compartments and their ultrastructural relationship to the bacterial cytoplasm can be studied in 1 nm slices of the 3D tomograms in exquisite detail. Scale bars: $a = 5$ μm; $b = 1$ μm; $c = 1$ μm; $d = 500$ nm; $e = 500$ nm; $f = 250$ nm

lipophilic dyes can be used to visualize such hydrocarbon and lipid distributions, e.g., when screening biodiesel-producing bacteria (Fig. 1a). Such biodiesel-producing bacteria can also be visualized for unusual morphology using scanning electron microscopy (SEM) revealing ball-like objects emerging typically at the poles of the bacterial cells (Fig. 1b) or transmission electron microscopy (TEM), where the pole regions are often found depleted of material due to hydrocarbon extraction during lengthy sample preparation (Fig. 1c). Hydrocarbon deposits can be visualized also in biofilms using 2D (Fig. 1d) and 3D TEM (Fig. 1e,f) as the absence of material in resin-embedded samples that have been faithfully preserved by ultrarapid freezing and freeze substitution (see below). A close-up look reveals that such "empty" compartments that contained hydrocarbons prior to freezing are not bound by a membrane but appear like an oil-drop in a watery emulsion, sometimes

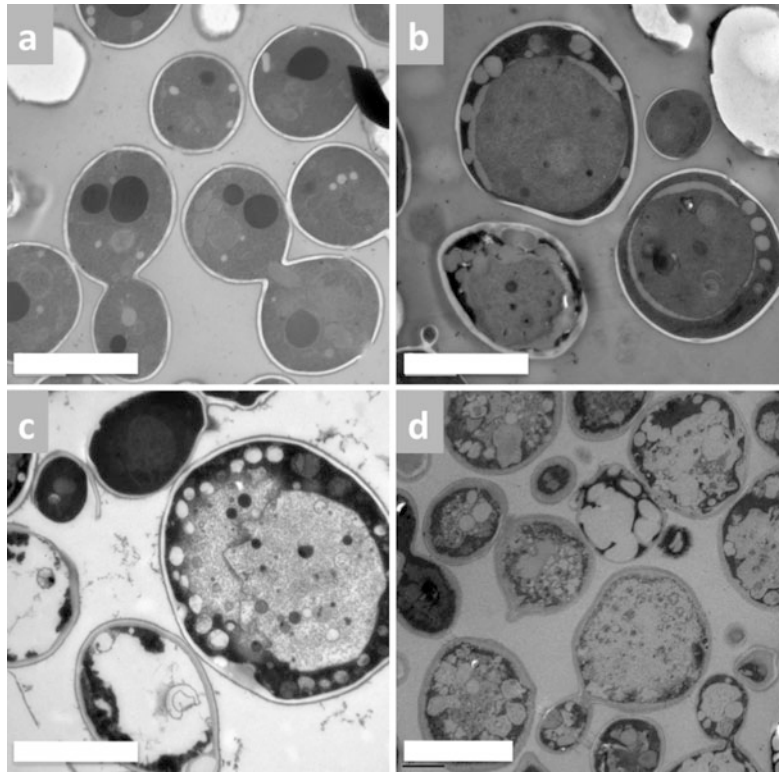

Fig. 2 Hydrocarbon-producing yeast (*Saccaromyces cerevisiae*). (**a**) Wild-type yeast strain prepared by high-pressure freezing and freeze substitution. (**b**)–(**d**) Yeast strain producing increasing amounts of hydrocarbons. Note the increasing number and size of droplet-like compartments, indicating the location of hydrocarbon prior to extraction. Scale bars: 5 μm

with several of such droplets partially merging, resulting in deviations from a simple ball-like geometry (Fig. 1f). Ultrastructural characterization of yeast cells producing different amounts of hydrocarbon (Fig. 2) not only reveals an increased amount of hydrocarbon production but also reveals the effect such increased hydrocarbon production has on cellular morphology and architectural organization. Cells that produce a high titer are often found to be abnormally shaped and appear highly stressed (Fig. 2d), compared to cells with moderate (Fig. 2c), low (Fig. 2b), and no (Fig. 2a) hydrocarbon production.

Resin section electron microscopy yields high-resolution ultrastructural information not visible by other means, leading to the discovery of intracellular lipid bodies [15, 26], which are formed in methane-utilizing bacteria and other hydrocarbon-utilizing bacteria and have been found in a variety of microbial species: Only hydrocarbon-grown *Acinetobacter* sp. cultures possessed intracellular lipid inclusion bodies [27]. Hydrocarbon-degrading *Rhodococcus opacus* strain PD630 possesses electron-transparent inclusions, the fatty acid composition of which depended on the substrate used [28]. Ultrathin sections of the strain DE2007 grown in the

presence of crude oil showed highly electro-dense (HE) inclusions of different sizes distributed throughout the cytoplasm of the bacterium [29]. Similarly, microbodies that have a homogeneous matrix and are surrounded by single unit membranes appeared profusely in various strains of *Candida* yeasts grown in *n*-alkanes. For a detailed review of the electron microscopic methods used for visualization of hydrocarbon-utilizing yeasts, *see* [30].

Traditionally, *osmium tetroxide* (OsO_4) is used as the major contrasting agent as it reacts with the carbon–carbon double bonds of unsaturated polymers, therefore staining the polymer and also fixing it in place, chemically cross-linking the sample, and causing hardening and increased density [31]. Wigglesworth as early as 1957 showed that tissues fixed with osmium tetroxide and then treated with ethyl gallate aided essentially in visualization of lipids since un-denatured proteins take up relatively little osmium, and nucleic acids and carbohydrates are completely unreactive [32]. Contrast of lipid-rich structures can be further enhanced by a saturated solution of monoterpene hydrocarbon myrcene, with or without the addition of 0.1% ethyl gallate in 70% ethanol, followed by osmium tetroxide, which allowed the visualization of both saturated and unsaturated lipids, including waxes [32]. Since osmium tetroxide will react predominantly with unsaturated lipids, Trent introduced *ruthenium tetroxide* (RuO_4) as a far more vigorous oxidant than OsO_4 to stain both aromatic and unconjugated unsaturated organic compounds, as well as some unsaturated polymers [33], which allowed visualization of microphase-separated saturated hydrocarbon diblock copolymers [34]. After this contrast-generating step, samples are typically dehydrated in either a graded ethanol or acetone series, with less lipid loss typically being observed when acetone was used instead of ethanol.

Freeze-fracture electron microscopy is powerful technique that has revolutionized our understanding of lipid structures, although it is rarely used these days. The hydrophobic fats and oils are non-etchable unlike water-containing materials, and therefore in freeze-fractured specimens, they can be readily recognized after etching. Frequently one encounters non-crystallized, lipid droplet-like fats in biological samples, which appear amorphous, e.g., droplets of olive oil [35] or lipid droplets (chylomicrons) in the human blood [36] in contrast to lipid granules (fat droplets) in yeast cells, which appear as laminated structures [37, 38].

Freeze etching, a variant of the freeze-fracture approach, has enabled the viewing of cells without prior chemical treatment, thereby avoiding the potential artifacts encountered in processing specimens for resin embedding and ultrathin sectioning, and has provided evidence for the presence of a smooth-surfaced limiting membrane for the hydrocarbon inclusions [39]. In another study, freeze-fracture studies demonstrated the presence of the rectangular intracellular inclusions and intracytoplasmic membranes in hexadecanol-grown cells of *Acinetobacter* sp. [17].

Quick-freezing replica microscopy was employed as a tool to study the structure of the disk-shaped inclusion bodies in *Acinetobacter* sp. strain M-1 cells, which had a smooth surface, and grew to almost the same diameter as the cells. However, in this case no intracytoplasmic membrane structures or limiting membranes surrounding these inclusions were observed [40]. It is worth noting that although this approach offers a complementary perspective to thin-section analysis, one does not image the native structure but a metal replica of the fractured surface, with metal decoration artifacts having been described, making freeze-fracture images not always easy to interpret [41]. Another limitation of the freeze-fracture technique is the need to identify the chemical nature of the structural components visualized. Thus the combination of cytochemistry with freeze fracture led to the introduction of a new method called as freeze-fracture replica immunolabeling technique (FRIL) [42]. In this technique, samples are frozen, fractured, and replicated with platinum carbon as in standard freeze fracture and then carefully treated with sodium dodecylsulfate to remove all the biological materials except a fine layer of molecules attached to the replica itself. Immunogold labeling of these molecules permits their distribution to be seen superimposed on high-resolution planar views of membrane structure, leading an improved understanding of lipid droplet biogenesis and function [43, 44].

Negative-stain electron microscopy employing phosphotungstic acid as a rapid and simple technique allows the visualization of hydrocarbon inclusions in bacterial cells and their membrane fractions [27, 45], permitting the study of morphology of these particles albeit the danger of artifacts such as a rouleau forms in lipid-bound forms of apoE4 persists.

1.2.1 Water-Compatible Durcupan Resin Infiltration

Conventional electron microscopy sample preparation methods can lead to the loss of osmicated hydrocarbon bodies during organic solvent-based dehydration and epoxy resin embedding, leaving behind electron-lucent halo [27, 41, 46]. However, hydrocarbon inclusions, e.g., in alk-1-ene grown bacteria, were retained by employing water-compatible infiltration (water-Durcupan graded series) procedures [27]. Durcupan infiltration of hexadecane-grown cells has been shown to minimize extraction of the hydrocarbon, whereas the remainder of the cellular ultrastructure appeared similar to ethanol-dehydrated cells, with the interesting finding that hexadecane inclusions often appeared membrane bound in the Durcupan-infiltrated cells [39].

1.2.2 Advanced EM Imaging Approaches

Apart from the more traditional imaging approaches, some less commonly used and/or newer and thus more advanced imaging approaches have been applied to hydrocarbon microbiology, including cryogenic sample preparation and correlative light and electron microscopy approaches:

1.2.3 High-Pressure Freezing–Freeze Substitution (HPF–FS)

Ultra-rapid freezing followed by low-temperature dehydration has long been recognized as resulting in significantly improved cellular ultrastructure [47–49] by immobilizing within milliseconds the cellular scenery and subsequently gently replacing the cellular water ice by an organic solvent, thus circumventing a variety of macromolecular aggregation and extraction artifacts typically encountered during conventional sample processing. After vitrification, the sample can either be freeze-substituted, resin embedded prior to room-temperature ultrathin sectioning, or sectioned (cryo-ultramicrotomed) directly in its frozen-hydrated state [50], an approach (CEMOVIS) that is technically extremely challenging and thus not well suited for most investigators not specialized in this technique. Using freeze substitution, Paul and Beveridge [51] demonstrated that OsO_4 provides strong covalent interaction with the lipids preventing their leaching during the solvent washes.

1.2.4 Cryo-Electron Microscopy of Vitreous Sections (CEMOVIS)

In this approach that is only mastered in a handful or two of labs in the world and is technically quite challenging, sample are often vitrified by high-pressure freezing and cryo-sectioned in their frozen-hydrated state instead of freeze substitution and resin embedding [52]. Apart from the technical challenge to cut ultrathin sections from a frozen block surface at liquid-nitrogen temperature and to effectively transfer the frozen section to an electron microscope grid with an eyelash in the absence of a solvent onto which the section could be floated and to make the sections stick to the grid without melting and/or drying out of the section, there are a variety of issues such as compression artifacts that render this approach somewhat limited to a more general set of scientists.

1.2.5 Tokuyasu Sectioning

In this approach the sample is typically infiltrated by comparatively high concentrations of sugar, which acts like a cryoprotectant and also as an agent to mitigate any effects from drying by providing a hydration shell and possibly the retention of small amounts of water during the drying out of the sections. The advantage over CEMOVIS is that this approach is relatively easy and robust and allows (together with the HPF–FS approaches) immuno-affinity labeling.

A systematic study was carried out where different protocols, including (1) conventional, (2) Tokuyasu cryo-sectioning, (3) HPF–FS with room-temperature epoxy resin embedding, (4) HPF–FS with low-temperature Lowicryl HM20 embedding and ultraviolet (UV) polymerization, as well as (5) cryo-electron microscopy of vitreous sections (CEMOVIS), were tested for the visualization of *Mycobacterium smegmatis* cell structures along with lipid bodies [41]. HPF–FS avoided the artifacts encountered by conventional protocols, but displayed difficulties to visualize the monolayer boundary of the lipid bodies, which could be detected by CEMOVIS and which are thought to exist (*see* [19]).

1.2.6 Whole-Mount Cryo-Electron Microscopy (Cryo-EM)

Cells smaller than about 0.5–1 μm in diameter can be vitrified by plunge freezing into liquid ethane and studied as whole-mount samples, circumventing the need for organic solvents, resin, and ultrathin sectioning, thus allowing the entire cells to be imaged in their native frozen-hydrated state. This approach is widely considered as the gold standard for transmission electron microscopy imaging and upon 3D tomographic imaging can yield unprecedented insight into the bacterial large macromolecular complexes and organelles, such as PHA and polyphosphate inclusions in *Caulobacter crescentus* [53]. However, cryo-EM is technically demanding, including rapid plunge-freezing sample vitrification to avoid freeze-damage, liquid-nitrogen temperature grid handling to avoid contamination, as well as low-dose cryo-EM imaging, rendering this technique beyond the scope of this chapter.

1.2.7 Wet Scanning Transmission Electron Microscopy

A rather new and somewhat exotic approach is the use "wet scanning transmission electron microscopy" (STEM) to study polyhydroxyalkanoate and triacylglycerol carbon storage inclusions in bacterial cells [54]. Sample preparation is relatively fast and uncomplicated as only cooling to ~1°C during imaging is required. Given their lower density compared to the cytoplasm, hydrocarbon inclusions (PHA and TAG) are readily observed as relatively electron-lucent inclusions within cells, demonstrating the utility of wet STEM for imaging such structures without staining albeit at somewhat poor resolution compared to traditional TEM methods.

1.2.8 Correlative Light and Electron Microscopy (CLEM)

While the approaches above mostly rely on direct ultrastructural detection of the inclusions, correlative light and electron microscopy approaches allow the visualization of the dynamics of cellular hydrocarbon inclusions followed by ultrastructural analysis, either through image registration or via photoconversion, where the fluorescence signal is turned into a osmiophilic precipitate. Both Nile Red and BODIPY FL have been employed as lipophilic fluorophores. *Nile Red*, a phenoxazine dye, is almost nonfluorescent in water and other polar solvents but undergoes fluorescence enhancement and large absorption and emission blue shifts in nonpolar environments [55]. Nile Red has previously been used to screen bacteria, cyanobacteria, and microalgae for those producing fatty acids and esters [56]. A high-throughput method for detection of bacterial hydrocarbons in the form of PHA inclusions using Nile Red fluorescence was described recently [16]. *BODIPY 505/515* (4,4-difluro-1,3,5,7-tetramethyl-4-bora-3a,4adiaza-s-indacene) is a highly lipophilic neutral fluorophore used to label a wide range of hydrophobic compounds such as fatty acids, phospholipids, cholesterol, cholesteryl esters, and ceramides [57] and has been used to evaluate lipid droplets in microalgae [58]

determine cellular localization of bacterial lipids [21]. Fluorophores that can be bleached are well suited for correlative light and electron microscopy through *photooxidation of diaminobenzidine* (*DAB*) that results in the formation of brown DAB precipitate that is osmiophilic and thus readily visible at the electron microscopic level [59, 60]. Lipid prebodies of *R. opacus* PD630 were found after DAB photoconversion of BODIPY FL C_{12}-stained cells to correspond to the observed peripheral lipid domains observed in fluorescence microscopy [21].

1.2.9 Possible Future Directions

Not currently exploited very much, but potentially very interesting, is the correlative optical spectral data imaging (Fourier transform infrared spectroscopy or Raman microspectroscopy) with ultrastructural imaging, as the former is nondestructive and sensitive to chemical nature of the hydrophobic compounds and thus can be applied prior to the somewhat destructive electron microscopy imaging. This combination of chemical specificity with ultrastructural architectural sensitivity could prove to be of high value to the increasingly interesting and important field of hydrocarbon microbial research, but their synergy has yet to be demonstrated.

2 Materials

2.1 Preparation of Hydrocarbon-Grown Microbial Cells for Standard Transmission Electron Microscopy (TEM)

2.1.1 Primary Fixation (Use Electron Microscopy or Analytical-Grade Reagents)

1. Electron microscopy grade glutaraldehyde, 2.5%:

   CAUTION: Fixatives are poisonous irritants; work in a fume hood and wear gloves.

   Glutaraldehyde fixatives are easily prepared from 25% solutions of electron microscopy grade glutaraldehyde in sealed glass ampoules by making a 1:10 dilution in the buffer of choice.

   To make 100 mL of 2.5% glutaraldehyde with 0.1 M $CaCl_2$:

   50 mL 0.2 M buffer stock solution at proper pH

   10 mL 25% glutaraldehyde (electron microscopy grade)

   2 mL 0.1 M $CaCl_2$ (IMPORTANT: do not use $CaCl_2$ with phosphate buffer as a precipitate will form)

   40 mL distilled water

2. Sodium cacodylate ($(NaCH_3)_2AsO_2.3H_2O$) buffer (0.2 M):

   CAUTION: Cacodylate buffer contains arsenic and poisonous, carcinogenic substances that can be absorbed through the skin; wear gloves.

   Cacodylate buffer consists of a 0.2 M stock solution of sodium cacodylate in distilled water (4.28 g/100 mL) and the pH is adjusted by adding the appropriate volume of 0.2 M HCl (1.7 mL concentrated HCl/100 mL distilled water) to the 100 mL stock as shown in Table 1.

Table 1
Preparation of cacodylate buffer (0.2 M)

pH	6.2	6.4	6.6	6.8	7.0	7.2	7.4
0.2 M HCl, mL	47.6	36.6	26.6	18.6	12.6	8.4	5.5

Table 2
Preparation of PBS (0.1 M, pH 7.3)

Reagent	Formula weight	Quantity	Final concentration
Sodium chloride (NaCl)	58.44	80 g	1.37 M
Potassium chloride (KCl)	74.56	2 g	26.8 mM
Sodium phosphate (Na_2HPO_4)	142	14.2 g	0.1 M
Potassium phosphate ($KHPO_4$)	136.1	2.4 g	17.6 mM
Hydrochloric acid (HCl), 1 N	NA	NA	1 N

To 100 mL of 0.2 M cacodylate solution (4.28 g/100 mL distilled water), add the appropriate amount of 0.2 N HCl (1.7 mL concentrated HCl/100 mL distilled water) to obtain the desired pH.

3. Phosphate-buffered saline (PBS):

   Dissolve the chemicals listed in Table 2 in 800 mL of distilled water by stirring in a beaker.
   Adjust pH to 7.3 with 1 N HCl.
   Transfer to a graduated cylinder and adjust volume to 1 L with distilled water.
   Sterilize by filtering through a 0.2-μm filter flask or autoclaving.

2.1.2 Washing

1. 5% w/v sucrose: Dissolve 5 g per 1 L of the buffer used. Adjust the weight of sucrose required accordingly, such as, for 100 mL of buffer used, dissolve 0.5 g of sucrose.

2.1.3 Postfixation

1. Osmium tetroxide (OsO_4), 1%:

   CAUTION: Osmium tetroxide is toxic, and the volatile fumes are very corrosive, especially to mucous membranes. It is essential that osmium solutions are handled in a fume hood and used osmium solutions be disposed of properly.

   Prepare a 2% aqueous solution (1 g of osmium tetroxide in 50 mL of distilled water). A working fixative of 1% is prepared

just before use by mixing equal parts of 2% aqueous stock osmium tetroxide solution with an equal part of 0.2 M buffer.

2.1.4 Embedding of Cells in Agar Blocks (Optional)

1. Noble agar, 2%: Noble agar is the highest purity agar available. It is obtained after being washed in accordance with the Noble and Tonney method which removes trace impurities, ash, and minerals that interfere with many sensitive applications. To prepare, weigh 2 g of agar in 100 mL of distilled water or buffer. Bring to a boil and heat until it completely dissolves. Bring down the temperature to about 45°C and then pour desired amount over the bacterial cells. Allow to solidify without disturbing the tube.

2.1.5 Dehydration Series

1. Ethanol–water series:

   CAUTION: flammable

   Prepare 30, 50, 70, 90, 96% v/v ethanol in distilled water according to Table 3.

   Keep 100% (absolute) ethanol in sealed pint containers.

2. Durcupan–water series:

   CAUTION: Take great care when working with Durcupan, as this substance may cause skin irritation and allergic reactions. Work always with rubber gloves.

   Durcupan, a water-soluble epoxy resin produced by the Fluka subsidiary of Sigma-Aldrich, is commonly used for embedding electron microscope samples. However, from the perspective of this paper, the employment of Durcupan dehydration has been shown to minimize extraction of the hydrocarbon in the preparation of specimens for thin sectioning [39]. The recipe for dehydration series containing component A (a water-soluble aliphatic polyepoxide) with water can be prepared as mentioned in Table 4.

Table 3
Preparation of ethanol–water dehydration series for 100 mL final volume

Volume of ethanol (mL)	Volume of water (mL)	Final % of ethanol
30	70	30
50	50	50
70	30	70
90	10	90
96	4	96

Table 4
Preparation of Durcupan–water dehydration series for 100 mL final volume

Volume of Durcupan (component A) (mL)	Volume of water (mL)	Final % of Durcupan
50	50	50
70	30	70
90	10	90

2.1.6 Embedding Resins

CAUTION: Both are hyper-allergenic and VCHD is carcinogenic.

1. Epoxy resin 812: Epoxy resin 812 consists of epoxy resin (originally designated Epon 812), the hardeners dodecenylsuccinic anhydride and methyl nadic anhydride, and an accelerant such as benzyldimethylamine (BDMA) or 2,4,6-tris(dimethylaminomethyl) phenol. Prepare epoxy resin 812 embedding medium by pouring measured amounts (usually volumes) into a graduated, disposable polypropylene tube such as a 50 mL centrifuge tube with a tight-sealing cap. A mixture of medium hardness consists of the following components:

   Epoxy resin 812 20 mL (24.0 g)

   Dodecenylsuccinic anhydride 16 mL (16.0 g)

   NMA 8 mL (10.0 g)

   BDMA 1.3 mL (1.5 g)

   Mix the resins thoroughly to obtain satisfactory results by inverting the tube end over end for 5–10 min.

2. Spurr's resin: The classical formulation of Spurr's resin consists of vinylcyclohexene dioxide (VCHD) or another cycloaliphatic epoxide ERL-4221, diglycidyl ether of polypropylene glycol (DER 736, Dow Epoxy Resin 736), nonenylsuccinic anhydride, and an accelerant such as BDMA or dimethylaminoethanol. Spurr's embedding medium is prepared by weighing components in a 50 mL graduated centrifuge tube on a top-loading balance. Prepare Spurr's resin of firm hardness resin as follows:

   VCHD (or ERL-4221) resin 10.0 g

   DER 736 6.0 g

   Nonenylsuccinic anhydride 26.0 g

   Dimethylaminoethanol 0.4 g

   In order to prepare the mixtures of resin–water, mix thoroughly the appropriate volume of resin and water in 50 mL polypropylene tubes, and keep them capped until needed.

2.1.7 Staining

CAUTION: Uranium compounds are toxic and radioactive. Contact your safety officer or local authorities for appropriate handling and disposal protocols.

1. Uranyl acetate, 1%: Weigh 0.1 g uranyl acetate and dissolve in 10 mL of pre-warmed distilled water in a polypropylene tube and mix until all the crystals dissolve. Make aliquots by filtering through a 0.22 μ syringe filter and store them in dark at 4°C.
2. Lead citrate:
   Place 1.33 g lead nitrate and 1.76 g sodium citrate into a 50 mL volumetric flask and add 30 mL water. Shake vigorously for 1 min. Allow to stand at room temperature for 30 min with intermittent shaking. Solution will be a milky white color. Add 8.0 mL of 1 N sodium hydroxide and mix. Solution will turn clear. Make up to 50 mL with boiled, cooled, and filtered double-deionized water. Store in a tightly sealed volumetric flask. Seal stopper with Parafilm. Do not use until the following day.

2.2 Preparation of Microbial Cells for Visualization by Negative Staining

1. Phosphotungstic acid, 1.5%:
   Dissolve 1.5 g phosphotungstic acid in 100 mL distilled water. Adjust the pH to 7.0 with KOH. Store at 2–8°C.

2.3 Preparation of Microbial Cell Samples for High-Pressure Freezing–Freeze Substitution (HPF–FS)

1. Microbial cells resuspended in hexadecane
2. Membrane carriers (100 μm deep, Leica) coated with 100 mg/mL lecithin (dissolved in chloroform), dried
3. High-pressure freezer (Leica EMPACT2-RTS, Leica Microsystems, Vienna, Austria)
4. Freeze-substitution medium: 1–2% osmium tetroxide (OsO_4) plus 0.5% uranyl acetate (UA) in acetone
5. Cryovials with o-ring seal (Genesee Scientific)

2.3.1 Quick Freeze Substitution Method: Preparation of Microbial Cell Samples for High-Pressure Freezing–Quick Freeze Substitution (HPF–QFS)

1. A modular heating block with 13 mm holes (VWR International, PA).
2. A foam box of dimensions (15 cm W × 11 cm D × 8 cm H, approx.) filled with liquid nitrogen. Walls of the box were around 2.5 cm thick.
3. A type T thermocouple temperature probe wrapped around a cryovial filled with 1.5 mL acetone and connected to a datalogger. Place it in one of the holes of the heating block.

2.4 Diaminobenzidine (DAB) Photoconversion

1. Fluorescent staining solution:
   Prepare DMSO stock solution of 0.5 mg/mL Bodipy FL C12 (Molecular Probes, United States).
2. Primary fixative:

2% (w/v) paraformaldehyde and 0.5% (w/v) glutaraldehyde in PBS.

3. Chilled 0.5 mg/mL DAB solution in PBS
4. Conventional fluorescence microscope with a fluorescein filter setting (BP530-560), a 50 W mercury lamp, and a 10X objective.
5. Postfixative:
   1% (w/v) OsO_4 in PBS (use caution while using osmium tetroxide)

3 Methods

3.1 Preparation of Hydrocarbon-Grown Microbial Cells for Standard Transmission Electron Microscopy (TEM)

The protocol described below is a general method for visualization of lipid bodies in microbial cells in particular, bacteria. Hydrocarbon microbiology has been gaining importance from the point of view of biofuel production or exploitation of microorganisms for bioremediation. In either scenario, visualization of accumulated lipids can provide an insight into the mechanisms of hydrocarbon metabolism, the pathways to its degradation, or the complex transport mechanisms involved. This protocol is a compilation of several protocols and should be optimized for best conditions.

3.1.1 Primary Fixation

Exponential-phase hydrocarbon-grown microbial cells are fixed in glutaraldehyde alone (2.5–6.25%) or containing calcium chloride (*see* **Note 1**) in a suitable buffer for 45 min to 1 h at room temperature. The buffer employed is generally sodium cacodylate (0.01–0.2 M, pH 7.2) or PBS (0.1 M, pH 7.3).

1. Pellet the cells by centrifuging at 7,000–10,000 rcf (*see* **Note 2**) for 5–10 min and remove most of the culture medium using a pipette.
2. Fix the cells by adding an excess volume (5–10 times the cell volume) of fixative and resuspend the cells in the fixative. A wide-bore pipette can be employed to gently resuspend the cells.
3. Incubate at room temperature for 45 min to 1 h with gentle shaking on a rotary shaker.
4. The cells are then pelleted in a microfuge tube (3–5 min at max rpm). Fixative removed. Leave a few drops in the cells so that they do not dry up.

3.1.2 Washing

Fixed cells should be washed in distilled water or more preferably in the same buffer that was used in the primary fixation step. Washing should be as thorough as possible, at least three times, each step for 20 min. Five percent wt/vol sucrose can also be added to the buffer in this step.

1. For the first washing step, resuspend the cells in ten times the cell volume of washing buffer or distilled water and shake gently on a rotary shaker for 20 min.
2. Pellet the cells by centrifugation at max speed for 5 min.
3. Resuspend the cells in the washing buffer and shake gently for 20 min.
4. Repeat the centrifugation and rinsing with the buffer at least one more time.
5. Finally pellet the cells for addition of postfixative.

3.1.3 Postfixation

The cells are then postfixed with 1.0% osmium tetroxide in the same buffer that was used in first fixation step (i.e., either PBS or cacodylate) for 90 min.

1. To the cell pellet, add 1% buffered osmium fixative and incubate for 90 min at room temperature, in the dark.
2. Carefully collect the cells by centrifugation.

3.1.4 Washing

The cells are again washed at least three times in the appropriate buffer (0.1 M cacodylate or PBS) by following the steps listed in Sect. 3.1.2.

3.1.5 Embedding of Cells in Agar Blocks (Optional)

The fixed cells are suspended in 2.0% (wt/vol) noble agar. Agar blocks (1 mm^3) containing fixed cells are then further processed. It is important that the cell pellet is loose for this step.

1. Using a warmed plastic pipette (*see* **Note 3**), quickly transfer a few μL of warm agar onto the loose cells and gently stir the cells with the tip of the plastic pipette to suspend the cells in the warm agar. Do not dilute the cells in the agar.
2. Let the agar solidify. Do not touch or disturb the tube during the solidification process, or it will not harden properly.
3. Very carefully cut open the tube using a sharp razor blade to remove the agar plug containing cells.
4. Transfer them in a petri dish containing buffer and trim the agar into 1 mm cubes using a sharp razor blade.

3.1.6 Staining (Optional)

En bloc stain with 1% aqueous uranyl acetate (UA) for ~2 h at 4°C IN DARK (must be carried out in the dark as UA is photoreductive and will precipitate).

3.1.7 Dehydration

From the perspective of hydrocarbon visualization, Durcupan dehydration of hexadecane-grown cells has been shown to minimize extraction of the hydrocarbon in the preparation of specimens for thin sectioning [39]. The routine followed by Staubli (1963) was Durcupan–water series (50, 70, and 90% Durcupan, each step

for 15–30 min; two changes of 100% Durcupan, each step for 30–60 min) [61].

However, ethanol–water dehydration has also been routinely employed.

1. Dehydrate the cell pellet/cubes in graded water – ethanol series (30, 50, 70, 90, 96, and 100% ethanol) each step for 15 min.
2. Follow up with three changes of absolute ethanol, 10 min each. In case embedding medium to be used is epoxy resin 812, further perform three changes of propylene oxide (*see* **Note 4**), each for 15 min.
3. Remove most of the propylene oxide from the specimen cubes but leave a trace to prevent the cells from drying out.

3.1.8 Resin Embedding

A number of resins have been employed in the literature such as Spurr [21], Vestopal [26], Epon Araldite [17], epoxy resin 812, and Maraglas [27]. However, the most commonly used resins have been Spurr and epoxy resin 812, the methods for which have been described below. Spurr's embedding medium is recommended for bacterial cells since it infiltrates the bacterial cells better than epoxy resin 812. It has been suggested that to extend the times in the propylene oxide: Spurr's resin mixtures to 2 h each and the pure Spurr's resin mixture to overnight. Keep the capsules capped since this resin will absorb moisture and give an improper polymerization.

1. Prepare three mixtures of absolute ethanol: epoxy resin 812 embedding medium consisting of 3:1, 1:1, and 1:3 parts, each in 10 mL of graduated, disposable polypropylene tubes with tight fitting lids. Care should be taken to avoid air bubbles while mixing (*see* **Note 5**).
2. After the final change of absolute ethanol, gently pour on the 3:1 mixture of absolute ethanol/epoxy resin 812 embedding medium. Gently swirl the culture vessel five to six times over a period of 60 min to assist infiltration of the mixture into the cells. Similarly, repeat this procedure with the 1:1 and 1:3 mixtures.
3. Finally add pure epoxy resin 812 embedding medium and let it infiltrate for 60 min. Repeat this step one more time.
4. Replace the second epoxy resin 812 embedding medium with one final change and leave overnight, uncovered to facilitate evaporation of any residual ethanol.

A suggested infiltration schedule for Spurr resin in case of Durcupan–water dehydration method is Durcupan–Spurr (50:50, v/v), 5 h; Durcupan–Spurr (25:75, v/v), 8 h; and 100% Spurr, 5 h (twice) [39].

3.1.9 Polymerization

Polymerize epoxy resin 812 embedding medium for 48 h at 60°C. Polymerization of Spurr can be performed at 70°C for 48 h.

3.1.10 Sectioning and Post-staining

1. Cut thin sections (70–80 nm) with an ultramicrotome using a diamond knife and place them on a 200 mesh copper grid.
2. Stain the sections with aqueous uranyl acetate (20 min) followed by lead citrate (2 min) (*see* **Note 6**) [63].
3. The sections are now ready for imaging in an electron microscope.

3.2 Preparation of Microbial Cells for Visualization by Negative Staining

Negative staining has been employed to visualize electron-transparent hydrocarbon inclusions in hydrocarbon-grown bacteria. A general protocol using staining with phosphotungstic acid by the drop-by-drop method has been described here:

1. Obtain formvar carbon film-coated copper EM grids with medical tweezers with clamping ring, putting the carbon film side up on a clean glass microscope slide, and place the slide on a clean filter paper in a petri dish and cover it.
2. Place ~3 μL of the cell sample on the EM grid carbon film side and incubate for 3–5 min.
3. Remove excess solution by gently touching the edge of the grid with filter paper wicks.
4. Wash the grid by briefly placing the surface of the grid with a drop (~35 μL) of deionized water on Parafilm and then blot with filter paper to remove the excess solution. The touching and blotting steps are to be performed quickly three times, each with a clean drop of deionized water.
5. Stain the grid immediately with 1.5% (w/v) phosphotungstic acid for 1 min and blot the extra solution from the edge of the grid using filter paper.
6. Subsequently, a thin film of this mixture is allowed to air-dry. Image the grid in EM or store it in a grid storage box for future imaging.

3.3 Preparation of Microbial Cell Samples for High-Pressure Freezing–Freeze Substitution (HPF–FS)

1. For high-pressure freezing, resuspend the microbial cells in hexadecane or 2% agarose as filler and introduce the mixture in 100 μm deep membrane carriers. Freeze the cells in a Leica EMPACT2-RTS high-pressure freezer.
2. Transfer the rapidly frozen samples, under liquid nitrogen, to cryotubes containing the freeze substitution medium.
3. Place the cryotubes in the freeze substitution apparatus (automatic FS system 1, AFS-1, Leica) with a temperature maintained at −90°C.

4. Let the samples sit at this temperature for 48 h, and during this time, the solvent mixture slowly replaces the cellular water.
5. Slowly warm up the temperature of the samples (5°C per hour) until it reaches −30°C. Hold at this point for 3 h followed by increase to 0°C (in increments of 5°C per hour.
6. Wash the samples three times with pure acetone on ice and incubate with increasing epoxy/acetone mixture, each step for 2 h.
7. Infiltrate with pure epon overnight, followed by polymerization.

*3.3.1 Quick Freeze Substitution Method: Preparation of Microbial Cell Samples for High-Pressure Freezing–Quick Freeze Substitution (HPF–QFS) (see **Notes 7–10**)*

This protocol is an improvement over the traditional time-consuming protocol and requires only basic laboratory tools. The results with this method have been found to be similar to those with traditional method [62]:

1. Place a modular heating block (with holes) in a foam box filled with liquid nitrogen.
2. Place a Type T thermocouple temperature probe connected to a data logger in one of the holes.
3. Then add the frozen samples at the liquid-nitrogen temperature. Start the datalogger.
4. Next, pour out the liquid nitrogen from the foam box and rotate the dry block heater with the samples at 100 rpm so that the cryotubes are horizontal. In around 2 h, the samples should have reached 0°C.
5. Remove the samples from the foam box and allow to warm to room temperature on a rocker. Stop the datalogger at this point.
6. Rinse out the fixative with pure acetone and continue with resin infiltration and embedding.

3.4 Diaminobenzidine (DAB) Photoconversion [21, 59]

1. Harvest the cell suspension by centrifugation at 13,000 rpm for 5 min and resuspend in the same volume of the fluorescent staining buffer (Bodipy FL C12).
2. Incubate in the dark, on ice for 30 min.
3. After staining, wash the cells three times in PBS buffer.
4. Fix the washed cells in primary fixative at 4°C for 3 days. Rinse again three times in PBS for 10 min.
5. At this stage, the cells can be embedded in 3.5% (w/v) agarose, sections of about 200 nm cut with a razor blade, followed by overnight fixation in 2% (w/v) paraformaldehyde in PBS or cell suspension can be used as such.
6. Preincubate the washed sections or the cell suspensions in prechilled 0.5 mg/mL DAB solution for 30 min (*see* **Note 11**).

7. Photoconvert the microbial cells for 1.5 h using a conventional fluorescence microscope with a fluorescein filter setting, a 50 W mercury lamp, and a 10 X objective.
8. Add fresh DAB solution every 15 min.
9. Monitor the development of the brown DAB reaction product. Excise those agarose sections and rinse three times in PBS for 10 min.
10. Postfix for 30 min in 1% (w/v) OsO_4 in PBS. Wash the fixed sections/cells in PBS again and use for TEM preparation (dehydration, resin infiltration, embedding, and polymerization) as described in Sects. 3.1.7, 3.1.8, 3.1.9, and 3.1.10.

4 Notes

1. Addition of calcium chloride (1–3 mM) to the glutaraldehyde fixation can minimize lipid loss during dehydration steps.
2. The formula for relative centrifugal force is $RCF = 11.2r(RPM/1{,}000)^2$, where r = radius in centimeters and RPM = revolutions per minute.
3. Glass pipettes can be used but they should be fire-polished to prevent the release of small chips of glass in the specimen. Such glass chips will damage the knives used in ultramicrotomy.
4. Acetonitrile can be used instead of propylene oxide due to carcinogenic nature of propylene oxide.
5. Do not shake the tube containing the resin components too vigorously or bubbles will be introduced that will interfere with the embedding. The few bubbles that form during the inversion process will rise to the surface and not pose a problem.
6. The Reynolds' lead citrate will react with carbon dioxide in the air to form a lead carbonate precipitate, so it must be stored in a tightly sealed volumetric flask.
7. It is important to note that for high-pressure freezing methods to work most effectively, the high-pressure frozen material should be removed from the freezer specimen cups before resin infiltration.
8. While using cryotubes with O-ring seal, it is a good idea to do a test run on the cryovials filled with acetone only to make sure they do not leak before using them with fixatives.
9. Liquid nitrogen expands about 700-fold in going from the liquid to gaseous state. Even a small amount of liquid sealed in a cryotube could cause it to explode. It is imperative that liquid nitrogen is not sealed in a cryotube.

10. It is best to have the lids of the cryotubes at room temperature just before putting them on, so the O-ring is pliable and gives a good seal.
11. The DAB solution must be made fresh and should be pre-chilled. The low temperature maintains high oxygen content and supports effective and specific DAB polymerization.

References

1. Ladygina N, Deyukhina EG, Veinshtein MB (2006) A review on microbial synthesis of hydrocarbons. Process Biochem 41:1001–1014
2. Head I, Aitken C, Gray N et al (2010) Hydrocarbon degradation in petroleum reservoirs. In: Timmis K (ed) Handbook of hydrocarbon and lipid microbiology. Springer, Berlin/Heidelberg
3. Sierra-Garcia I, de Oliveira V (2013) Microbial hydrocarbon degradation: efforts to understand biodegradation in petroleum reservoirs. In: Chamy R (ed) Biodegradation – engineering and technology. InTech, ISBN: 978-953-51-1153-5, doi:10.5772/55920
4. Wenger L, Davis C, Isaksen G 2002 Multiple controls on petroleum biodegradation and impact on oil quality. In: Society for petroleum engineers (SPE) reservoir evaluation and engineering, pp 375–383
5. Roling W, Head I, Larter S (2003) The microbiology of hydrocarbon degradation in subsurface petroleum reservoirs: perspectives and prospects. Res Microbiol 154:321–328
6. Atlas R, Bartha R (1993) Microbial ecology - fundamentals and applications. Benjamin-Cummings, Redwood City
7. Atlas R (1981) Microbial degradation of petroleum hydrocarbons: an environmental perspective. Microbiol Rev 45(1):180–209
8. Van Hamme J, Singh A, Ward O (2003) Recent advances in petroleum microbiology. Microbiol Mol Biol Rev 67(4):503–549
9. Muthuswamy S, Binupriya A, Baik S, Yun S (2008) Biodegradation of crude oil by individual bacterial strains and a mixed bacterial consortium isolated from hydrocarbon contaminated areas. Clean 36(1):92–96
10. Martins L, Piexoto R (2012) Biodegradation of petroleum hydrocarbons in hypersaline environments. Braz J Microbiol 43(3):865–872
11. Hazen T, Dubinsky E, De Santis T, Andersen G et al (2010) Deep-sea oil plume enriches indigenous oil-degrading bacteria. Science 330(6001):204–208
12. Baelum J, Borglin S, Chakraborty R, Fortney J et al (2012) Deep-sea bacteria enriched by oil and dispersant from the deepwater horizon spill. Environ Microbiol 14(9):2405–2416
13. Biological Agents. http://www2.epa.gov/emergency-response/biological-agents. Accessed 24 Nov 2014
14. Kostka J, Prakash O, Overholt W, Green S et al (2011) Hydrocarbon degrading bacteria and the bacterial community response in Gulf of Mexico beach sands impacted by the deepwater horizon oil spill. Appl Environ Microbiol 77 (22):7962
15. Scott C, Finnerty W (1976) A comparative analysis of the ultrastructure of hydrocarbon – oxidizing microorganisms. J Gen Microbiol 94:342–350
16. Pinzon N, Aukema K, Gralnick J et al (2011) Nile red detection of bacterial hydrocarbons and ketones in a high throughput format. MBio 2 (4):e00109-11. doi:10.1128/mBio.00109-11
17. Singer M, Tyler S, Finnerty W (1985) Growth of *Acinetobacter* sp. strain HO1-N on n-hexadecanol: physiological and ultrastructural characteristics. J Bacteriol 162(1):162
18. Alvarez H, Steinbuchel A (2002) Triacylglycerols in prokaryotic microorganisms. Appl Microbiol Biotechnol 60:367–376
19. Waltermann M, Steinbuchel A (2005) Neutral lipid bodies in prokaryotes: recent insights into structure, formation and relationship to eukaryotic lipid depots. J Bacteriol 187 (11):3607
20. Marin M, Pedregosa A, Laborda F (1996) Emulsifier production and microscopical study of emulsions and biofilms formed by the hydrocarbon-utilizing bacteria *Acinetobacter calcoaceticus* MM5. Appl Microbiol Biotechnol 44:660–667
21. Waltermann M, Hinz A, Robenek H et al (2005) Mechanism of lipid body formation in

prokaryotes: how bacteria fatten up. Mol Microbiol 55(3):750–763
22. Meng X, Yang J, Xu X, Zhang L, Nie Q, Xian M (2009) Biodiesel production from oleaginous microorganisms. Renew Energy 34:1–5
23. U.S. Bioenergy Statistics. http://www.ers.usda.gov/data-products/us-bioenergy-statistics. Accessed 10 Oct 2014
24. Shi S, Valle-Rodriguez J, Siewers V, Nielsen J (2011) Prospects for microbial biodiesel production. Biotechnol J 6:277–285
25. Suzuki R, Ito N, Uno Y, Nishii I et al (2013) Transformation of lipid bodies related to hydrocarbon accumulation in a green alga, *Botryococcus braunii* (Race B). PLoS One 8(12), e81626. doi:10.1371/journal.pone.0081626
26. Davies S, Whittenbury R (1970) Fine structure of methane and other hydrocarbon-utilizing bacteria. J Gen Microbiol 61:227–232
27. Kennedy R, Finnerty W, Sudarsanan K, Young R (1974) Microbial assimilation of hydrocarbons. I. The fine-structure of a hydrocarbon oxidizing *Acinetobacter* sp. Arch Microbiol 102:75–83
28. Alvarez H, Mayer F, Fabritius D, Steinbüchel A (1996) Formation of intracytoplasmic lipid inclusions by *Rhodococcus opacus* strain PD630. Arch Microbiol 165(6):377–386
29. Diestra E, Esteve I, Burnat M, Maldonado J, Sole A (2007) Isolation and characterization of a heterotrophic bacterium able to grow in different environmental stress conditions, including crude oil and heavy metals. In: Méndez-Vilas A (ed) Communicating current research and educational topics and trends in applied microbiology. Formex, Badajoz
30. Osumi M (2012) Visualization of yeast cells by electron microscopy. J Electron Microsc 61 (6):343–365
31. Li Z (ed) (2002) Industrial application of electron microscopy. CRC Press, Boca Raton, p 362
32. Wigglesworth V (1975) Lipid staining for the electron microscope: a new method. J Cell Sci 19:425–437
33. Trent J (1984) Ruthenium tetraoxide staining of polymers: new preparative methods for electron microscopy. Macromolecules 17:2930–2931
34. Khandpur A, Macosko C, Bates F (1995) Transmission electron microscopy of saturated hydrocarbon block copolymers. J Polym Sci B Polym Phys 33:247–252
35. Richter H, Sleytr U (1971) Fettextraction bei −78°C: nachweis im Gefrieratzbild. Z Naturforsch 26b:470–473
36. Meyer H, Winkelmann H (1970) Die Darstellung von lipiden bei der gefrieratzpraparation und ihre beziehung zur strukturanalyse biologischer membranen. Exp Pathol 4:47–59
37. Moor H, Muhlethaler K (1963) Fine structure in frozen etched yeast cells. J Cell Biol 17:609–628
38. Meyer H, Richter W (2001) Freeze-fracture studies on lipids and membranes. Micron 32:615–644
39. Scott C, Finnerty W (1976) Characterization of intracytoplasmic hydrocarbon inclusions from the hydrocarbon-oxidizing *Acinetobacter* Species HO1-N. J Bacteriol 127 (1):481–489
40. Ishige T, Tani A, Takabe K, Kawasaki K et al (2002) Wax ester production from n-Alkanes by *Acinetobacter* sp. strain M-1: ultrastructure of cellular inclusions and role of acyl coenzyme A reductase. Appl Environ Microbiol 68 (3):1192–1195
41. Bleck C, Merz A, Gutierrez M, Alther P et al (2010) Comparison of different methods for thin section EM analysis of *Mycobacterium smegmatis*. J Microsc 237:23–28
42. Fujimoto K (1995) Freeze-fracture replica electron microscopy combined with SDS digestion for cytochemical labeling of integral membrane proteins - application to the immunogold labeling of intercellular junctional complexes. J Cell Sci 108:3443–3449
43. Severs N (1995) Freeze-fracture cytochemistry: an explanatory survey of methods. In: Severs N, Shotton D (eds) Rapid freezing, freeze fracture, and deep etching. Wiley-Liss, New York, pp 173–208
44. Robenek H, Severs N (2008) Recent advances in freeze-fracture electron microscopy: the replica immunolabeling technique. Biol Proced Online 10:9–19
45. Scott C, Makula S, Finnerty W (1976) Isolation and characterization of membranes from a hydrocarbon-oxidizing *Acinetobacter* sp. J Bacteriol 127(1):469–480
46. Kellenberger E, Johansen R, Maeder M, Bohrmann B et al (1992) Artefacts and morphological changes during chemical fixation. J Microsc 168:181–201
47. Mc Donald K, Auer M (2006) High-pressure freezing, cellular tomography, and structural cell biology. Biotechniques 41(2):137, 139, 141
48. Djaczenko W, Muller M, Benedetto A (1990) Ultra-rapid high pressure freezing in high resolution EM of cell-cell and cell-substrate interactions. Cell Biol Int Rep 14

49. Dubochet J (1995) High-pressure freezing for cryoelectron microscopy. Trends Cell Biol 5 (9):366–368
50. Hurbain I, Sachse M (2011) The future is cold: cryo-preparation methods for transmission electron microscopy of cells. Biol Cell 103:405–420
51. Paul T, Beveridge T (1994) Preservation of surface lipids and determination of ultrastructure of *Mycobacterium kansasii* by freeze substitution. Infect Immun 62(5):1542–1550
52. Al-Amoudi A, Chang J, Leforestier A, McDowall A et al (2004) Cryo –electron microscopy of vitreous section. EMBO J 23 (18):3583–3588
53. Comolli L, Kundmann M, Downing K (2006) Characterization of intact subcellular bodies in whole bacteria by cryo-electron tomography and spectroscopic imaging. J Microsc 223:40–52
54. Thomson N, Channon K, Mokhtar N, Staniewicz L et al (2011) Imaging internal features of whole, unfixed bacteria. Scanning 33(2):59–68
55. (2010) Probes for lipids and membranes. In: The molecular probes® handbook: a guide to fluorescent probes and labeling technologies, 11th edn. http://www.lifetechnologies.com/us/en/home/references/molecular-probes-the-handbook/probes-for-lipids-and-membranes.html
56. Chen W, Zhang C, Song L, Sommerfeld M, Hu Q (2009) A high throughput Nile red method for quantitative measurement of neutral lipids in microalgae. J Microbiol Methods 77:41–47
57. Elle I, Olsen L, Pultz D, Rødkær S, Færgeman N (2010) Something worth dyeing for: molecular tools for the dissection of lipid metabolism in *Caenorhabditis elegans*. FEBS Lett 584:2183–2193
58. Govender T, Ramanna L, Bux R (2012) BODIPY staining, an alternative to the Nile Red fluorescence method for the evaluation of intracellular lipids in microalgae. Bioresour Technol 114:507–511
59. Dantuma N, Pijnenburg M, Diederen J, Van der Horst D (1998) Electron microscopic visualization of receptor–mediated endocytosis of DiI–labeled lipoproteins by diaminobenzidine photoconversion. J Histochem Cytochem 46 (9):1085–1089
60. Cortese K, Diaspro A, Taccheti C (2009) Advanced correlative light/electron microscopy: current methods and new developments using Tokuyasu cryosections. J Histochem Cytochem 57(12):1103–1112
61. Staubli W (1963) A new embedding technique for electron microscopy, combining a water soluble epoxy resin (Durcupan) with water insoluble Araldite. J Cell Biol 16:197–199
62. Mc Donald K, Webb R (2011) Freeze substitution in 3 hours or less. J Microsc 243 (3):227–233
63. Reynolds ES (1963) The use of lead citrate at high pH as an electron-opaque stain for electron microscopy. J Cell Biol 17:208

Protocol for Laser Scanning Microscopy of Microorganisms on Hydrocarbons

Thomas R. Neu and John R. Lawrence

Abstract

Microbial communities in their fully hydrated state can be imaged in space and time (4-dimensionally) by laser scanning microscopy using 1-photon or 2-photon excitation. In this protocol, we provide guidance on how to examine microorganisms associated with liquid, viscous and solid hydrocarbons. Practical aspects are discussed including the material and sources, microscopy consumables, software programs and time constraints. The details of mounting samples for the upright and inverted microscope as well as options for fluorescence staining of bacteria and hydrocarbons are presented. Suggestions are made for recording images and subsequent digital image analysis. Finally, notes are added and a guideline for troubleshooting is supplied.

Keywords: Bacteria, Biofilms, Colonisation of hydrocarbons, Confocal laser scanning microscopy, Deconvolution, Degradation of hydrocarbons, Digital image analysis, Fluorescence techniques, Fluorochromes, Hydrophobicity, Image analysis, Imaging, Imaging techniques, Laser scanning microscopy, Lectins, Microorganisms, Quantification, Two photon laser scanning microscopy, Visualisation

1 Introduction

Laser scanning microscopy (LSM) represents an established technique for structure–function studies of microbial aggregates and films. The main advantage of LSM is its 3-dimensional sectioning capability of fully hydrated, living microbial communities. The LSM approach allows multichannel imaging of cellular constituents and extracellular polymeric substances (EPS). In addition, the microenvironment can be examined using a variety of fluorescent probes. With state of the art instruments, up to six different parameters can be recorded simultaneously or sequentially. The digital image series recorded may then be used for visualisation and quantification. The basics of LSM and details of how to apply LSM in order to examine a microbiological sample in general are out of the scope of this protocol. However, there is an extensive series of reviews describing the applicability of LSM with focus on microbial

T.J. McGenity et al. (eds.), *Hydrocarbon and Lipid Microbiology Protocols*, Springer Protocols Handbooks (2016) 29–47,
DOI 10.1007/8623_2014_30, © Springer-Verlag Berlin Heidelberg 2014, Published online: 30 December 2014

communities such as biofilms and bioaggregates (*see* **Note 1**). The focus of this review is on LSM and its suitability to examine the interaction of microorganisms with hydrocarbon interfaces.

The interaction of microorganisms with hydrocarbons may occur directly or via surface active compounds. In fact, microbial surface active compounds maybe involved not only in the degradation of hydrocarbons but also in the interaction of microorganisms (adhesion and detachment) with interfaces [1]. In many cases, the microbial communities degrading hydrocarbons are located in close proximity to the hydrophobic substrate which at the same time may serve as a substratum. Consequently, the microorganisms adhere to solid hydrocarbons as well as to liquid hydrocarbons and develop into a microbial biofilm. Thereby microorganisms, especially if they possess a hydrophobic cell surface, may stabilise oil–-water emulsions [2]. The necessity to image the adhesion of bacteria to hydrocarbons at different depths of focus is apparent from an example recorded by conventional light microscopy (*see* Fig. 1 in Rosenberg and Doyle [3]). They showed bacteria colonising a spherical hydrocarbon droplet and demonstrated the ability to focus in one optical layer only, thereby indicating the need for 3D imaging of fully hydrated samples. Nevertheless, microbial colonisation of hydrocarbons has been investigated by LSM in a few studies only.

For example, Whyte et al. studied the degradation of hexadecane and diesel fuel by a *Rhodococcus* strain at low temperature [4]. They could show the bacteria colonising the water–hydrocarbon interface of the microdroplets. By fluorescence lectin-binding analysis (FLBA) the different glycoconjugates produced were related to the temperature and carbon source employed. They finally demonstrate that the strain can assimilate both solid and liquid hydrocarbons. Some of the data was impressively visualised 3-dimensionally in a later review article [5]. The group of Baldi investigated the interaction of *Acinetobacter venetianus* with diesel fuel droplets [6]. It was shown that adhesion to the hydrocarbon droplets involved a glycoconjugate which was stained by lectins. Using LSM time series, they were able to demonstrate two types of interactions: (1) cell–cell interactions before colonising the hydrocarbon and (2) incorporation of nanodroplets into the capsular polysaccharide. Another manuscript by the same group reported the growth of a yeast strain, *Rhodosporidium toruloides*, on dibenzothiophene and orimulsion [7]. By means of LSM, the growth of yeast on hydrocarbons, the changes in morphology and the production of glycoconjugates were followed. Macedo et al. employed LSM to follow the colonisation of polychlorinated biphenyls (PCB) droplets by a microbial community isolated from PCB-contaminated soil [8]. For this purpose, they used a variation of the hanging drop cultivation method. For examination by LSM, the PCB droplets on plastic slides were

studied using an upright LSM system with water-immersible lenses. Thereby pronounced stages of microbial colonisation could be established which correlated with the degradation of the complex PCB mixture. In a follow-up manuscript, the adaptation of the community to different PCB levels was studied [9]. LSM assessment of the PCB samples showed different types of biofilms, starting from thin layers on the PCB droplets towards more aggregated layers containing dense microcolonies. In both studies, the extracellular hydrocarbon phase was stained with Nile Red, whereas in a study on bacterial hydrocarbon production, Nile Red was used to stain the cellular hydrocarbon fraction [10]. The colonisation of polycyclic aromatic hydrocarbons (PAH) in flow cells was investigated with triple-species biofilms. For LSM imaging of bacterial species, a combination of GFP (*Sphingomonas*), DsRed (*Pseudomonas*) and Syto 62 (*Mycobacterium*) was employed. PAH was imaged via its autofluorescence under UV excitation [11]. Similarly, the tolerance of bacteria against solvents can be studied using LSM. For this purpose, *Pseudomonas* biofilms were exposed to styrene and examined with respect to biofilm structure, membrane damage and glycoconjugate production [12]. In a field study, the in situ bioremediation of a hydrocarbon-polluted site was stimulated by adding hydrogen peroxide, an oleophilic fertiliser and a surfactant. The experiment was followed by chemical analysis of hydrocarbons, traditional enrichment techniques for bacteria and LSM [13].

Most of the studies used a similar LSM approach to examine the interaction of the microorganisms with hydrocarbons. For fluorescence staining, Nile Red was used for the liquid hydrocarbon phase, a nucleic acid stain (e.g. Syto 9) for the bacteria and various lectins for visualisation of the glycoconjugates. The details of the staining procedures are described below.

2 Materials

2.1 Internet Sites and Sources

2.1.1 Microscopy Supplies

- http://www.marienfeld-superior.com/index.php/cover-glasses/articles/precision-cover-glasses-thickness-no-15h-for-high-performance-microscopes.html
- https://de.vwr.com/app/catalog/Product?article_number=737-0013
- http://www.gracebio.com
- http://www.thermoscientific.com/en/product/nunc-lab-tek-chambered-coverglass.html
- http://www.emsdiasum.com/microscopy/products/preparation/imaging-microscopy.aspx
- http://www.finescience.de/index.asp?verified=true

2.1.2 Fluorochromes and Lectins

Fluorochromes

- http://www.lifetechnologies.com/de/de/home/brands/molecular-probes.html
- http://www.biostatus.com
- http://www.dyomics.com/
- http://www.atto-tec.com/
- http://www.biotium.com
- http://www.abberior.com

Lectins

- http://www.sigmaaldrich.com/life-science/biochemicals/biochemical-products.html?TablePage=17904091
- http://www.eylabs.com/index.php?page=shop.browse&category_id=6&option=com_virtuemart&Itemid=79
- https://www.vectorlabs.com/catalog.aspx?catID=31&locID=0

2.1.3 Commercial Visualisation and Deconvolution Programs

Visualisation

- Imaris – http://www.bitplane.com
- Amira – http://www.amiravis.com
- Volocity – http://www.improvision.com
- Image-Pro – http://www.mediacy.com/index.aspx?page=Image_Pro_Software
- MetaMorph – http://www.moleculardevices.com/Products/Software/Meta-Imaging-Series/MetaMorph.html

Deconvolution

- Huygens – http://www.svi.nl/HomePage
- AutoQuant – http://www.mediacy.com/index.aspx?page=autoquant
- Volocity – deconvolution as option
- CLSM software – most companies offer a deconvolution option

2.1.4 Freely Available Programs

General

- ImageJ – http://rsb.info.nih.gov/ij/
- Fiji – http://fiji.sc/fiji

Developed for Microbiological Data Sets

- Comstat 1 and 2 – http://www.comstat.dk/
- Phlip – http://sourceforge.net/projects/phlip/
- Daime – http://www.microbial-ecology.net/daime/

Visualisation

- BioImageXD – http://www.bioimagexd.net/
- ImageSurfer – http://imagesurfer.cs.unc.edu/
- VolViewer – http://cmpdartsvr3.cmp.uea.ac.uk/wiki/BanghamLab/index.php/VolViewer

Deconvolution

- Plug-in for ImageJ – http://bigwww.epfl.ch/algorithms/deconvolutionlab
- BiaQIm – http://www.deconvolve.net/index.html

3 Methods

The procedures will describe how to examine microbial communities growing on hydrocarbons by using LSM. A differentiation is made in terms of studying bacteria on liquid, viscous and solid hydrocarbons. The approach is split into sample mounting, staining, collecting images and data analysis.

3.1 Growing Microorganisms on Hydrocarbons with Respect to LSM

There are different approaches regarding how to grow microbial communities on hydrocarbons. The main issue in terms of growth and LSM examination is the consistency of the hydrocarbon, meaning whether it is liquid, viscous or solid at the temperature employed for cultivating the microorganisms.

1. If the hydrocarbon is liquid, the culture can be performed in a normal Erlenmeyer flask containing a simple mineral medium.
2. If the hydrocarbon is viscous, a variation of the hanging drop method maybe used. For this purpose, a droplet of the hydrocarbon is put onto a hydrophobic plastic slide which is exposed to the microbial community.
3. If the hydrocarbon is used in the form of waxy material or solid crystals, they also may be added to an Erlenmeyer flask with mineral medium. Another option may be flow-through cells, e.g. in those applications where dissolved hydrocarbons are studied [14]. For hydrocarbons which are solid at room temperature, the substratum may be coated by the dissolved hydrocarbon with subsequent evaporation of the solvent [11]. Another option would be that solid crystals are mounted in a flow-through cell in order to follow biofilm development over time, although this, to the best of our knowledge, has not been published.

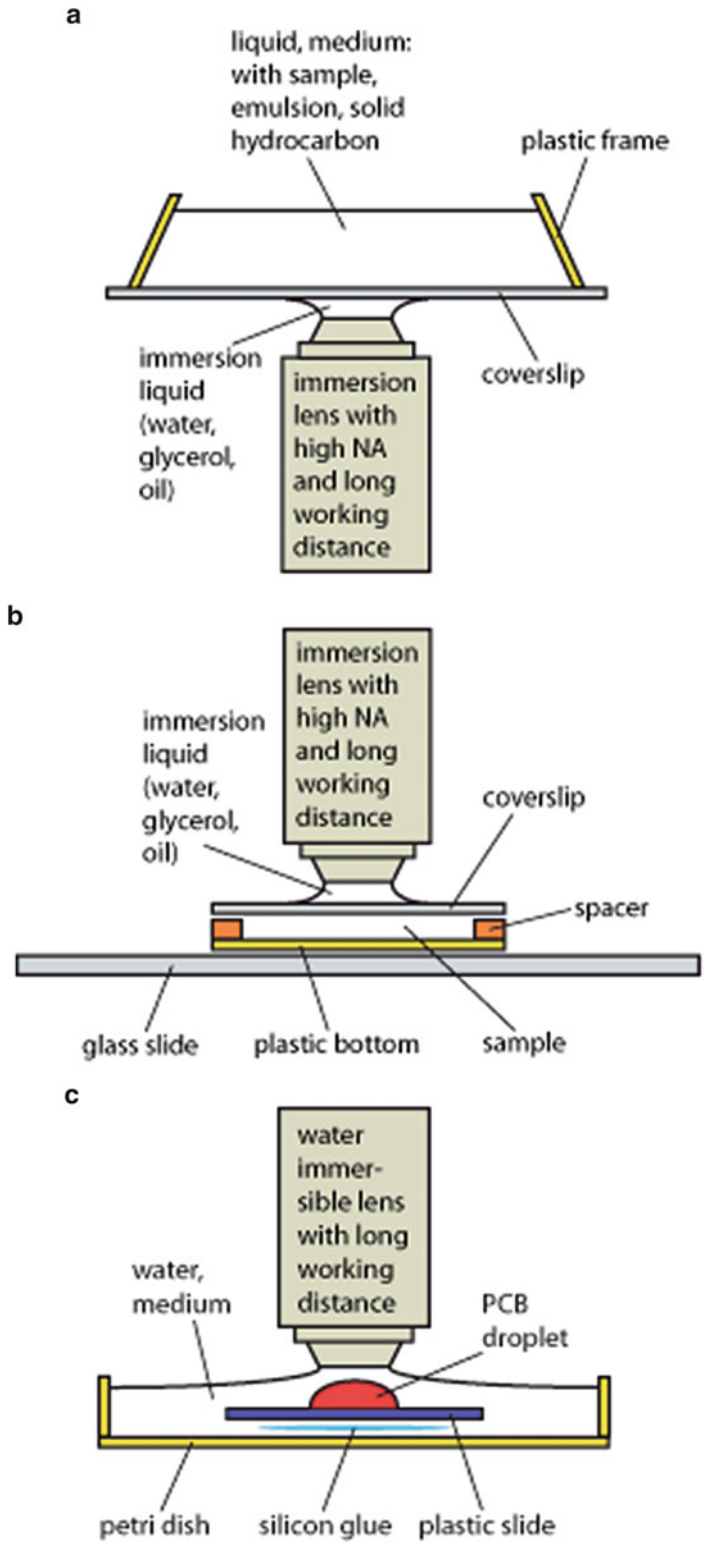
a
liquid, medium: with sample, emulsion, solid hydrocarbon
plastic frame
immersion liquid (water, glycerol, oil)
immersion lens with high NA and long working distance
coverslip
b
immersion lens with high NA and long working distance
immersion liquid (water, glycerol, oil)
coverslip
spacer
glass slide
plastic bottom
sample
c
water immer-sible lens with long working distance
water, medium
PCB droplet
petri dish
silicon glue
plastic slide

3.2 Mounting of the Sample for LSM

1. First, a subsample of the culture matching the LSM requirements has to be collected. In liquid cultures, collect the emulsified hydrocarbon with the associated bacteria using an inverted glass pipette (5 or 10 mL) in order to apply as little shear force as possible. Place the emulsion in the appropriate chambers, commercial or self-made (*see* **Note 1**). The same procedure can be used if the bacteria grow on solid hydrocarbons. In that case, a few hydrocarbon crystals with the attached bacteria are transferred into a suitable chamber.
2. The mounting of the sample will be determined by the LSM type available, upright or inverted microscope (Fig. 1). For both microscope types, apply the staining in the chamber used. For the *inverted* setup, place the sample in a coverslip chamber and image it from below (Fig. 1a). The chambers are available with 1, 2, 4 or 8 wells having different sizes. In this case, the free working distance of the objective lens maybe a problem if hydrocarbon droplets are rather large or due to the fact that hydrocarbons will float on the aqueous phase or sorb to the chamber frame made from plastic. For the *upright* setup, place the sample in a cover well chamber, cover it with a coverslip and put it on a slide (Fig. 1b). It is a good idea to put a droplet of water on the slide to prevent the chambers from gliding off the slide. These chambers are available with different spacers of 0.2, 0.5, 1 and 2 mm thickness. Be aware that the hydrocarbon droplets may sorb to the coverslip. The upright setup has more flexibility and also allows mounting of larger samples, e.g. hydrocarbon-contaminated objects, in a 5 cm Petri dish. In this case, the observation can be made using water-immersible objective lenses. They have the advantage of an extra-long working distance (*see* **Note 2**).
3. For bacteria growing on viscous hydrocarbons, the plastic slide with the hydrocarbon droplet is transferred into a 5 cm Petri dish. The slide is placed in the dish with the droplet facing upwards. In order to avoid floating of the plastic slide, it can be glued to the Petri dish using silicon adhesive (RTV silicone, WPI, Sarasota, FL). This type of mounting is suitable for imaging with the upright microscope only (Fig. 1c). For an inverted microscope, it is more difficult as the plastic slide has

Fig. 1 Mounting options for examination of hydrocarbon-associated microorganisms by means of LSM. (**a**) Setup for the inverted microscope by using coverslip chambers. The rectangular chambers are available with plastic frames creating wells of different sizes. (**b**) Setup for the upright microscope by using cover well chambers. The square chambers are available with spacers of different height. (**c**) Special setup for the upright microscope which was used to image biofilms developing on PCB droplets [8]. A similar setup maybe used to image bacteria or fungi growing on solid hydrocarbons

to be mounted upside down in a coverslip chamber using self-made spacers. The spacers may be of different materials (*see* below) and have to be used in order to avoid squeezing of the droplet with the attached bacteria.

3.3 Staining Solutions: Nucleic Acids (Bacteria)

1. Nucleic acid-specific fluorochromes (e.g. Syto 9, Life Technologies) are usually delivered in vials containing 100 µL at a concentration of 5 mM in DMSO. Prepare aliquots of 2 µL and store at −20°C for later use (*see* **Notes 3** and **5**).
2. For staining, take an aliquot and dilute it in 2 mL of appropriate buffer, medium or, e.g. filtered river water. Staining of bacteria is done by adding a few droplets to the sample and incubating for 5 min; the sample can then be examined visually or by laser microscopy without any destaining step.
3. The staining solution may be used up for a few days. Be aware that all fluorochromes must be handled with care. Most of them have not been investigated in terms of their toxicity or carcinogenicity.

3.4 Stains: Liquid/Viscous Hydrocarbons

1. As a general stain for hydrocarbon compounds, the lipophilic fluorochrome Nile Red (Sigma-Aldrich) can be used. Prepare stock solution of 1 mg Nile Red in 1 mL acetone. For staining, dilute at 1:1,000 with water and incubate for 15 min (*see* **Note 3**).
2. Be aware that Nile Red will also stain lipophilic compartments, e.g. in eukaryotic microorganisms and bacteria (*see* **Note 4**).

3.5 Probes for Glycoconjugates: Lectins

1. Lectins dissolved in buffer are either supplied as solution (1 mg/mL) or freeze-dried in 1 mg portions. Freeze-dried lectins are prepared at 1 mg/mL by just adding water. From the stock solution, prepare aliquots of 100 µL and freeze at −20°C. Take 100 µL and dilute 1:10 with filter-sterilised water, buffer or medium. For staining, add a few droplets to the sample and incubate for 20 min. Carefully wash the sample 3–4 times in order to remove unbound lectins.
2. Warning – some lectins are extremely toxic and have to be handled with caution. Ideally, lectins are only handled in solution.

3.6 Fluorescence Staining Strategies

The staining approach depends on the sample properties and the aims of the study. In any case, usually the bacteria will be stained using a nucleic acid-specific fluorochrome. For this purpose, there is a choice of many fluorochromes with different excitation and emission characteristics. A particularly suitable one is Syto 9 which has been successfully employed for many different sample types. Similarly SYBR Green may be applied. In addition, it is useful to differentially image the hydrocarbon phase. If the hydrocarbon is liquid or viscous, it can be stained with a lipophilic fluorochrome such as Nile Red (Fig. 2a, b). This combination would result in a

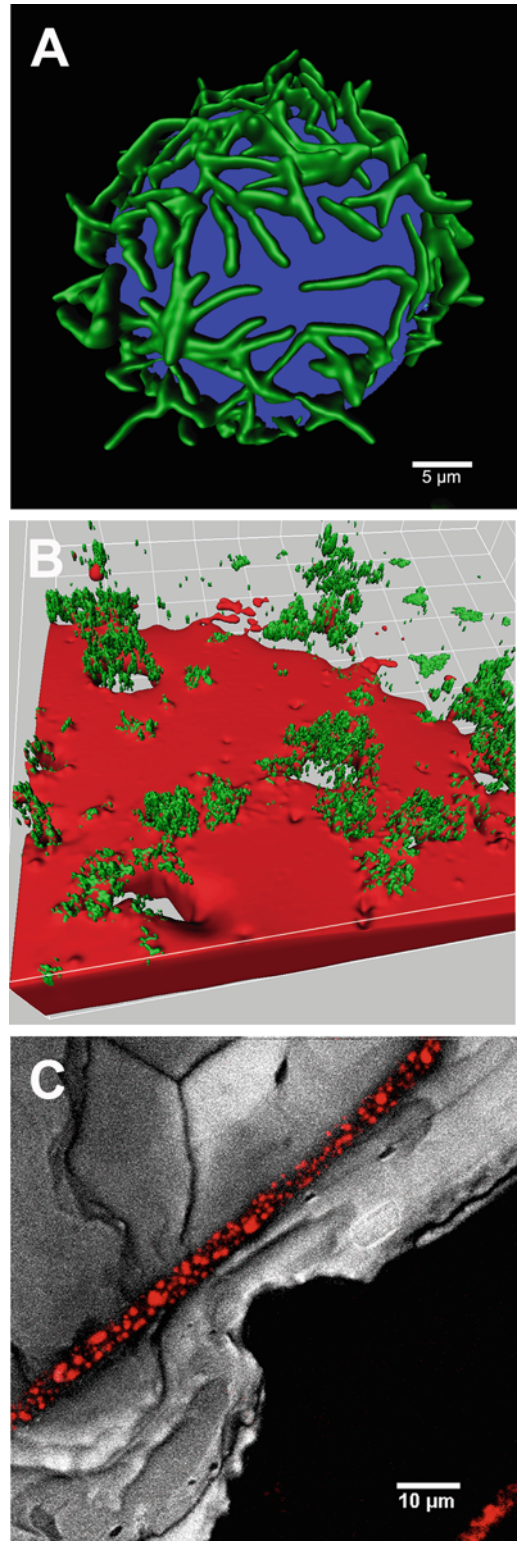
A
5 µm
B
C
10 µm

dual-channel image with the hydrocarbon stained red and the bacteria stained green. In the case of solid hydrocarbons, the surface of the crystals can be imaged in the CLSM reflection mode (Fig. 2c). If a UV laser or a two-photon laser is available, the autofluorescence of many hydrocarbons can be imaged and recorded in a separate channel. This makes sure that the nucleic acid-stained bacteria are not lost in space but can be related to a matrix or surface. A critical issue is the potential application of fluorescence in situ hybridisation (FISH) as the chemicals used for fixation and dehydration may interfere with the hydrocarbon phase.

1. First, stain the hydrocarbon droplets with Nile Red (about 15 min), and then apply the nucleic acid-specific counterstain for the bacteria. After staining with Syto 9, you can use the sample directly for imaging. If fluorescence lectin-binding analysis (FLBA) is employed, the Syto 9 counterstaining is done last.
2. Depending on the sample properties, additional stains can be applied. For example, the glycoconjugates of the extracellular polymeric substances (EPS) maybe stained using lectins [15]. The detailed procedure of fluorescence lectin-binding analysis (FLBA) has been described elsewhere [5]. In this case, the lectin staining is done first, and then the nucleic acid-specific counterstain is added.

3.7 Collecting Images by Laser Scanning Microscopy

Laser scanning microscopy can be done in many different ways. There is not one correct way of doing LSM, but it rather depends on the purpose of imaging. Ideally the user should consult a laser microscopy specialist in order to discuss the options for collecting

Fig. 2 Laser scanning microscopy of bacteria and fungi associated with hydrocarbons of different consistency (liquid, viscous and solid). (**a**) Bacteria adhering to a suspended liquid hydrocarbon droplet. The bacteria at the hydrocarbon–water interface were stained with the nucleic acid-specific fluorochrome Syto 9. The image series of the nucleic acid signal is shown as an isosurface projection. The diesel droplet in the centre is indicated by an artificial projection of a sphere. Related images showing different projections have been published [4]. (**b**) PCB-degrading microbial community isolated from soil. The viscous PCB droplet absorbed to a plastic slide was stained with Nile Red (*red*); the bacteria were stained with SYBR Green (*green*). The data set is presented as an isosurface projection. Take notice of the microcolonies above the PCB lesions indicating the degradation of PCB by the microbial community. Grid size = 50 μm. Further details on the pronounced stages of PCB colonisation may be found in Macedo et al. [8]. (**c**) Fungal filament of *Pythium ultimum* adhering to a solid phenanthrene crystal. The fungus was stained with Nile Red indicating intracellular hydrophobic vesicles. The image was collected by means of two-photon laser scanning microscopy. Excitation was at 800 nm; the emission was recorded in two channels at 400–502 nm (autofluorescence of phenanthrene) and 587–800 nm (Nile Red)

images. A sound basis for understanding the advantages and disadvantages of laser microscopy is usually "taking the course". From experience, it is known that it may take several weeks or even months before one can use a laser scanning microscope properly and effectively. In the following, the main issues which are important for doing laser scanning microscopy are listed. For more details, *see* references in Table 1.

1. In many imaging facilities, the instrument has to be booked in advance. Usually there is a short introduction to the instrument. There might be a charge for using the microscope. Stains may have to be purchased from your own budget.
2. Look up the technical details of the laser scanning microscope. Check for upright/inverted microscope, existing lasers and laser lines for excitation, number of photomultipliers/detection

Table 1
Review articles and book chapters (only) describing laser scanning microscopy and fluorescence techniques as tools for examination of microbial communities associated with interfaces

Focus of article	References
LSM of adherent microorganisms	Gorman et al. [16]
Imaging of biofilms	Lawrence et al. [17]
Confocal laser scanning microscopy	Lawrence and Neu [15]
Fluorescence lectin-binding analysis	Neu and Lawrence [18]
In situ detection of EPS	Neu and Lawrence [19]
Confocal and other approaches	Palmer and Sternberg [20]
Structured LSM approach	Neu and Lawrence [21]
LSM with focus on immunofluorescence	Schmid et al. [22]
1-Photon versus 2-photon LSM	Neu and Lawrence [5]
Spatiotemporal approaches	Palmer et al. [23]
LSM of aggregates and flocs	Lawrence and Neu [24]
LSM applications in microbiology	Lawrence and Neu [25]
Analytical imaging	Lawrence et al. [26]
LSM of microorganisms on hydrocarbons	Neu and Lawrence [27]
LSM of biofilm matrix	Neu and Lawrence [28]
LSM of biofilm structure	Neu and Lawrence [29]

channels, objective lenses available and suitable sample chambers for microscopy (*see* **Note 6**).

3. At this stage, it might be a good idea to discuss possible software to be used for subsequent digital image analysis. Issues for directly using these programs include file loading and import of instrument parameters. Especially check the bit depth of the recorded data. Often it is 8 bit (0–255 pixel intensities) which can be handled by most image analysis programs. Many sources claim that 12 bit or 16 bit is required for scientific image data sets. However, this may cause problems in terms of the image analysis programs used at a later stage.
4. Be aware of the number of samples and the time needed for imaging (*see* comments at the end of the chapter). Usually recording one data set per sample is not enough. Often an overview is imaged and then several locations are examined at high resolution. Mostly the quality of image data is increased during recording by continuously optimising the settings. Be aware that if you work fast for a full day at the LSM, you may create 1–2 or even more GB of data.
5. Become familiar with using the laser scanning microscope. For that purpose, a variety of fluorescent beads maybe employed as test samples. Try single and multichannel imaging. Take notes of the main instrument settings (*see* **Note 7**).
6. Think about the purpose of imaging. What is the aim of collecting images? For example, 2D, 3D or 4D data sets, visualisation only, one perfect image, routine imaging of many samples, quantification, statistics and deconvolution. These aspects will determine the approach to recording images and the settings to be used.

3.8 Analysis of 3-Dimensional Image Data Sets

Digital image analysis comprises *firstly*, *visualisation* and projection of data, and *secondly*, *quantification* and extraction of numbers. For these goals, different software packages are required. Furthermore, commercial software and freely available software may have to be considered and evaluated. In addition, deconvolution may be applied in order to increase the resolution. Although it is often very appropriate to do, in most (microbiological) cases, deconvolution has not been used due to several critical issues.

1. *File formats*
   Make sure that the microscopy file format of the images is compatible with the program used for digital image analysis. Most often, the first problem encountered is the impossibility of loading the data into a particular program. Many commercial programs will have a reader for the microscopy format of the main laser microscopy companies. However, sometimes, the readers are not up to date as the microscope companies

keep changing their file formats. With most LSM software, the data can be stored in a neutral file format. Another frequent requirement is renaming of the image series. Free programs for renaming of image series can be found in the Internet.

2. Digital image analysis is a multistep procedure. One major step is thresholding of the images (*see* **Note 8**). By this procedure, a grey level image (e.g. 8 bit having 0–255 pixel intensities) is transformed into a binary image with only black and white pixels (0 and 255 pixel intensities). The thresholded image series is then used for visualisation or quantification. This key step in the procedure is considered controversially, and as a result several publications from the microbiology field should be consulted to understand the issues [30–33].

3. *Visualisation*
   Currently, most programs controlling and running the LSM instrument have several basic tools available for visualisation of the data recorded. In addition, several advanced programs specifically developed for LSM data sets are available including Amira, Imaris and Volocity, among others. They usually can be purchased as a basic program with additional add-on tools as options for specific analyses. Furthermore, there are programs freely available including, e.g. ImageJ [34] and its extension for biological imaging called Fiji [35] as well as BioImageXD [36].

4. *Quantification*
   The most popular program is again the freely available software ImageJ developed at the National Institutes of Health (NIH). At the NIH website and due to the many users, a long list of macros and plug-ins are available. Other free software developed for microbiological data include Comstat, Phlip and Daime. However, these three programs were developed for a specific microscopy file format, for certain types of samples and for special analysis procedures. As a consequence, they may be not suitable for all types of data sets. Again, often loading the data is an issue, and renaming the files may be required if these software packages are employed.

5. *Deconvolution*
   Deconvolution is applied in order to (a) remove noise from an image data set, (b) to enhance the resolution in XY and (c) to improve axial (XZ) elongation. However, for correct calculations, the images have to be recorded at the Nyquist rate, meaning at a pixel resolution of 50 nm and a step size of about 150 nm. Both will lead to dramatic bleaching if an image stack with a large number of sections has to be recorded. In addition, the point spread function of the instrument has to be measured, ideally inside the actual sample to be analysed. As

a consequence, deconvolution has been applied in only a few studies. Nevertheless, a comparison of the two major software packages has been published [37].

3.9 Time Considerations

Laser microscopy is a 3-step procedure: (1) sample mounting and staining, (2) recording of images and (3) digital image analysis (quantification and visualisation). With fresh samples, mounting and staining are straightforward and can be done quickly (time frame 5–30 min). If samples have to be fixed, embedded and sectioned, it may take 1–2 days. The use of cryo-sectioning techniques may reduce this time to half a day. A similar time frame is needed for fluorescence in situ hybridisation (FISH). Recording images takes time. The time which is needed for collecting an image series is dependent upon the number of sections, necessity for averaging, resolution in pixels, simultaneous or sequential scanning mode. The user should be aware of these constraints if many samples have to be examined within 1 day.

Image analysis is usually done at a later stage, most often using a different computer in order to have the LSM instrument available for recording data. For quick visualisation, it is a good idea to produce, e.g. a maximum intensity projection (MIP) which results in a 2D image of the image series (*see* **Note 9**). The MIP is usually good enough if every single section contains limited information. The MIP looks overloaded if every single section contains a lot of signal/information. That does not mean the data set has low quality, but in this case, other modes for projection may be better choices such as XYZ projection, 3D orthogonal view, 3D volume view, 3D isosurface view. Projecting images in 3D with a variety of tools and options using a sophisticated program requires more time in order to achieve good results. Quantification – programs which only count pixels (2D) or voxels (3D) work fast (seconds). However, programs recognising objects need a much longer time for calculation (hours).

3.10 Troubleshooting

1. Low signal
   (a) Staining OK?
   (b) Coverslip clean?
   (c) Front lens of objective lens clean?
   (d) Air bubbles in front of lens?
2. No signal
   (a) Microscope settings OK?
   (b) Laser settings OK?
   (c) Check focus and staining using visual epifluorescence or transmitted light.
   (d) Control if laser is visible, light path OK, excitation wavelength right and emission detection setting matching fluorochrome.

(e) Double check settings at microscope (mechanical in older types) and in software.

3. Preventive maintenance
   (a) Check the alignment of the system periodically (e.g. using focal check fluorescent beads).
   (b) Use reference samples and reference images to assess instrument performance.
   (c) Check accuracy of stage movement using fluorescent beads of known size.
   (d) Have periodic (annual) alignment by the manufacturer.

4 Research Needs

Given the tremendous advances in laser microscopy imaging over the last 20 years, it is somewhat surprising that so few studies have applied the different LSM approaches in hydrocarbon research. In general, there is substantial opportunity to carryout microscopy-based studies of microbial interactions with hydrocarbons including:

- Expanded application of fluorescent probes to cover a range of parameters including the micro-environmental conditions associated with hydrocarbon degradation
- Further use of time-course studies of events including the degradation of the hydrocarbon
- Greater attention to calibration of imaging and quantification of events
- Ground truth of events associated with microbial colonisation and transformation of hydrocarbons
- Use of correlative microscopy where possible to study events

5 Notes

1. Spacers of different but defined height can be cut from glass slides, coverslips, plastic material, thin plastic sheets, O-rings, etc.. Spacers may be also purchased from microscopy equipment suppliers.
2. Depending on the mounting procedure and microscopy supplies used, floating of the hydrocarbon droplet at the water surface may be critical in terms of the working distance (inverted microscope). Another issue is sorption of the liquid hydrocarbon to, e.g. the coverslip or spacers, resulting in either deformation of the droplet or even loss during placement of the coverslip (upright microscope). It may also be useful to have a

temperature-controlled stage or use warm or cold packs on the stage to regulate temperature for bacterial growth and fluidity of the hydrocarbon.

3. Control – make sure that the unstained sample is checked for possible autofluorescence. In certain samples, a specific autofluorescence can be used for imaging. This maybe the case for cells, e.g. cyanobacteria or algae, as well as for specific hydrocarbons having ring structures.
4. Apart from Nile Red, there are many other lipophilic fluorochromes available, e.g. DiI-C_{18}, DiO-C_{18} or membrane-specific ones, e.g. FM1-43 and FM4-64. They have different HLB values (hydrophilic–hydrophobic balance) as well as different excitation and emission characteristics.
5. Due to sample properties and potential quenching effects, it is a good idea to check other nucleic acid-specific fluorochromes such as SYBR Green.
6. Most important is the proper selection of the objective lens. There are two contradictory issues to consider: resolution and working distance. Resolution is determined by the numerical aperture (NA) of the lens and not by the magnification! The magnification only determines the area you look at. However, high NA means short working distance or vice versa; long working distance means low NA. Nevertheless, for samples extending into axial direction (thick samples or objects on a 3D topography), lenses with a long working distance are necessary. An ideal solution is using water immersion or water-immersible lenses. They are available in two forms: (1) corrected for a coverslip or not corrected for a coverslip (both with high NA) and (2) as long working distance objective lens to be used without a coverslip (low NA). All objective lenses produce bright images and have been used for many different sample types.
7. Always write a protocol and take notes of all the settings used. For this purpose, a spreadsheet is quite useful. In the future, it will allow one to quickly look up the details without going back to the microscope which is usually occupied by someone else, and there is no need of time-consuming searching and loading of the images. The spreadsheet will allow listing of sample preparation and details of the settings used for each image series. The main points are mounting, staining, laser lines, filters, magnification, resolution, pixel/voxel size, thicknesses, number of images, step size, zoom, average, channels, PMT voltage, image number *and most important comments*. These details are used later to judge image quality, assess suitability of images for specific projections, select images for publication, ensure proper scaling and comprehend what and why things were done in that particular way.

8. It is very important in digital image analysis to be aware of (1) what has been seen visually in the (epifluorescence) microscope attached to the LSM, (2) what has been recorded as raw data (on screen) and (3) what changes were applied to the raw data during visualisation. Always apply changes to a copy of the data set, and always compare changes with what has been seen in the microscope. Please consult the following publications on critical issues in scientific imaging [38].
9. The MIP represents only an intermediate result! In fact, it is the image to be remembered. It has a small file size and can be carried away on a USB stick. The MIP may then serve together with the laser microscopy protocol as a basis for discussion and subsequent image analysis. The latter of course is done with the original raw image data set (3D series).

Acknowledgements

Image courtesy: A. Macedo and W.-R. Abraham (Fig. 2b), S. Furuno and L. Wick (Fig. 2c). Support of the Canada–Germany collaboration by Environment Canada and Helmholtz Centre for Environmental Research – UFZ. Excellent technical support was provided over many years by Ute Kuhlicke and George Swerhone.

References

1. Neu TR (1996) Significance of bacterial surface-active compounds in interaction of bacteria with interfaces. Microbiol Rev 60:151–166
2. Dorobantu LS, Yeung AKC, Foght JM, Gray MR (2004) Stabilisation of oil–water emulsions by hydrophobic bacteria. Appl Environ Microbiol 70:6333–6336
3. Rosenberg M, Doyle RJ (2005) Microbial cell surface hydrophobicity: history, measurement and significance. In: Doyle RJ, Rosenberg M (eds) Microbial cell surface hydrophobicity. American Society for Microbiology, Washington, DC, pp 1–37
4. Whyte LG, Slagman SJ, Pietrantonio F, Bourbonniere L, Koval SF, Lawrence JR, Inniss WE, Greer CW (1999) Physiological adaptations involved in alkane assimilation at a low temperature by *Rhodococcus* sp. strain Q15. Appl Environ Microbiol 65:2961–2968
5. Neu TR, Lawrence JR (2005) One-photon versus two-photon laser scanning microscopy and digital image analysis of microbial biofilms. Methods Microbiol 34:89–136
6. Baldi F, Ivosevic N, Minacci A, Pepi M, Fani R, Svetlicic V, Zutic V (1999) Adhesion of *Acinetobacter venetianus* to diesel fuel droplets studied with in situ electrochemical and molecular probes. Appl Environ Microbiol 65:2041–2048
7. Baldi F, Pepi M, Fava F (2003) Growth of *Rhodosporidium toruloides* strain DBVPG 6662 on dibenzothiophene crystals and orimulsion. Appl Environ Microbiol 69:4689–4696
8. Macedo AJ, Kuhlicke U, Neu TR, Timmis KN, Abraham W-R (2005) Three stages of a biofilm community developing at the liquid-liquid interface between polychlorinated biphenyls and water. Appl Environ Microbiol 71:7301–7309
9. Macedo AJ, Neu TR, Kuhlicke U, Abraham W-R (2007) Adaptation of microbial communities in polychlorinated biphenyls contaminated soil leading to the transformation of higher chlorinated congeners in biofilm communities. Biofilms 3:37–46
10. Pinzon NM, Aukema KG, Gralnick JA, Wackett LP (2011) Nile Red detection of bacterial hydrocarbons and ketones in a high throughput format. MBio 4:1–5

11. Wouters K, Maes E, Spitz JA, Roeffaers MBJ, Wattiau P, Hofkens J, Springael D (2010) A non-invasive fluorescent staining procedure allows confocal laser scanning microscopy based imaging of Mycobacterium in multispecies biofilms colonizing and degrading polycyclic aromatic hydrocarbons. J Microbiol Methods 83:317–325
12. Halan B, Schmid A, Buehler K (2011) Real-time solvent tolerance analysis of Pseudomonas sp. Strain VLB120ΔC catalytic biofilm. Appl Environ Microbiol 77:1563–1571
13. Menendez-Vega D, Gallega JLR, Pelaez AI, de Cordoba GF, Moreno J, Munoz D, Sanchez J (2007) Engineered in situ bioremediation of soil and groundwater polluted with weathered hydrocarbons. Eur J Soil Biol 43:310–321
14. Möller S, Pedersen AR, Poulsen LK, Arvin E, Molin S (1996) Activity and three-dimensional distribution of toluene-degrading *Pseudomonas putida* in a multispecies biofilm assessed by quantitative in situ hybridization and scanning confocal laser microscopy. Appl Environ Microbiol 62:4632–4640
15. Lawrence JR, Neu TR (1999) Confocal laser scanning microscopy for analysis of microbial biofilms. Methods Enzymol 310:131–144
16. Gorman SP, Mawhinney WM, Adair CD (1993) Confocal laser scanning microscopy of adherent microorganisms, biofilms and surfaces. In: Denyer SP, Gorman SP, Sussman M (eds) Microbial biofilms: formation and control. Blackwell, London, pp 95–107
17. Lawrence JR, Wolfaardt G, Neu TR (1998) The study of microbial biofilms by confocal laser scanning microscopy. In: Wilkinson MHF, Shut F (eds) Digital image analysis of microbes. Wiley, Chichester, pp 431–465
18. Neu TR, Lawrence JR (1999) Lectin-binding analysis in biofilm systems. Methods Enzymol 310:145–152
19. Neu TR, Lawrence JR (1999) In situ characterization of extracellular polymeric substances (EPS) in biofilm systems. In: Wingender J, Neu TR, Flemming H-C (eds) Microbial extracellular polymeric substances. Springer Verlag, Berlin, pp 21–47
20. Palmer RJ Jr, Sternberg C (1999) Modern microscopy in biofilm research: confocal and other approaches. Curr Microbiol 10:263–268
21. Neu TR, Lawrence JR (2002) Laser scanning microscopy in combination with fluorescence techniques for biofilm study. In: Bitton G (ed) The encyclopedia of environmental microbiology. Wiley, New York, pp 1772–1788
22. Schmid M, Rothballer M, Assmus B, Hutzler P, Lawrence JR, Schloter M, Hartmann A (2004) Detection of microbes by scanning confocal laser microscopy (SCLM). In: Kowalchuk GA, de Bruijn FJ, Head IM, Akkermans ADL, van Elsas JD (eds) Molecular microbial ecology manual. Kluwer Academic Publishers, Dordrecht, pp 875–910
23. Palmer RJ Jr, Haagensen J, Neu TR, Sternberg C (2006) Confocal microscopy of biofilms – spatiotemporal approaches. In: Pawley JB (ed) Handbook of biological confocal microscopy. Springer, New York, pp 882–900
24. Lawrence JR, Neu TR (2007) Laser scanning microscopy for microbial flocs and particles. In: Wilkinson KJ, Lead JR (eds) Environmental colloids: behavior, structure and characterisation. Wiley, New York, pp 469–505
25. Lawrence JR, Neu TR (2007) Laser scanning microscopy. In: Reddy CA, Beveridge TJ, Breznak JA, Marzluf GA, Schmidt TM, Snyder LR (eds) Methods for general and molecular microbiology. American Society for Microbiology, Washington, DC, pp 34–53
26. Lawrence JR, Korber DR, Neu TR (2007) Analytical imaging and microscopy techniques. In: Hurst CJ, Crawford RL, Garland JL, Lipson DA, Mills AL, Stetzenbach LD (eds) Manual of environmental microbiology. American Society for Microbiology, Washington, DC, pp 40–68
27. Neu TR, Lawrence JR (2010) Examination of microbial communities on hydrocarbons by means of laser scanning microscopy. In: Timmis KN (ed) Microbiology of hydrocarbons, oils, lipids and derived compounds. Springer, Heidelberg, pp 4073–4084
28. Neu TR, Lawrence JR (2014) Advanced techniques for the in situ analysis of the of the biofilm matrix (structure, composition, dynamics) by means of laser microscopy. In: Donelli G (ed) Microbial biofilms: methods and protocols, vol 1147. Springer, New York, pp 43–64
29. Neu TR, Lawrence JR (2014b) Investigation of microbial biofilm structure. Adv Biochem Eng Biotechnol
30. Sieracki ME, Reichenbach SE, Webb KL (1989) Evaluation of automated threshold selection methods for accurately sizing microscopic fluorescent cells by image analysis. Appl Environ Microbiol 55:2762–2772
31. Xavier JB, Schnell A, Wuertz S, Palmer R, White DC, Almeida JS (2001) Objective threshold selection procedure (OTS) for segmentation

of scanning laser confocal microscope images. J Microbiol Methods 47:169–180

32. Yang X, Beyenal H, Harkin G, Lewandowski Z (2001) Evaluation of biofilm image thresholding methods. Water Res 35:1149–1158
33. Yerly J, Hu Y, Jones SM, Martinuzzi RJ (2007) A two-step procedure for automatic and accurate segmentation of volumetric CLSM biofilm images. J Microbiol Methods 70:424–433
34. Schneider CA, Rasband WS, Eliceiri KW (2012) NIH Image to ImageJ: 25 years of image analysis. Nat Methods 9:671–675
35. Schindelin J, Arganda-Carreras I, Frise E, Kaynig V, Longair M, Pietzsch T, Preibisch S, Rueden C, Saalfeld S, Schmid B, Tinevez JY, White DJ, Hartenstein V, Eliceiri K, Tomancak P, Cardona A (2012) Fiji: an open-source platform for biological-image analysis. Nat Methods 9:676–682
36. Kankaanpaa P, Paavolainen L, Tiitta S, Karjalainen M, Paivarinne J, Nieminen J, Marjomaki V, Heino J, White DJ (2012) BioImageXD: an open, general-purpose and high-throughput image-processing platform. Nat Methods 9:683–689
37. Model MA, Fang J, Yuvaraj P, Chen Y, Zhang Newby BM (2011) 3D deconvolution of spherically aberrated images using commercial software. J Microsc 241:94–100
38. Rossner M, Yamada KM (2004) What's in a picture? The temptation of image manipulation. J Cell Biol 166:11–15

Fluorescence Microscopy for Microbiology

Gabriella Molinari

Abstract

Fluorescence microscopy allows selective recognition of a particular component from biomolecular complex structures for the investigation of biological processes. It is frequently used to image specific microbial features. The rapid development of new fluorescent probes that can be easily adapted for a wide array of biological applications, coupled to the extraordinary technical improvements in microscope systems and software, strongly supports the sustained development and exploitation of fluorescence microscopy as a powerful research tool.

Fluorescence microscopy in microbiology can investigate the localization and levels of molecules and can provide information about their distribution, dynamics, and interactions, both in living and fixed samples. The preparation of high-quality samples for microscopic observation is the starting point for obtaining good resolution and optimum imaging results. This chapter attempts to provide basic methods for the application of conventional fluorescence and immunofluorescence microscopy for microbiology.

Keywords: Fluorescence microscopy, Fluorochrome, Fluorophore, Immunofluorescence

1 Introduction

Fluorescence imaging, a combination of detection and visualization, is a powerful tool to investigate biological processes. Although in use for several decades, it is nowadays in a state of rapid evolution. The exceptional technical improvements in microscopes coupled with the constant development of new fluorescent probes and the software advancement for exceptional imaging acquisition and documentation make the progress in fluorescence microscopy very valuable for research.

Fluorescence microscopy is based on the property of some substances called fluorophores, fluorochromes, or fluorescent dyes to produce fluorescence after absorbing energy. Fluorescence is the emission of light that occurs as a result of the absorption of the excitation light. Thus, excitation and emission are two different wavelength values, being the absorbed energy emitted at longer wavelengths [1]. The molecules that are fluorescent are seen

T.J. McGenity et al. (eds.), *Hydrocarbon and Lipid Microbiology Protocols*, Springer Protocols Handbooks (2016) 49–69,
DOI 10.1007/8623_2015_108, © Springer-Verlag Berlin Heidelberg 2015, Published online: 19 June 2015

through filters that filter the excitation light permitting the observation of only the emitted light.

Fluorescence microscopy can be exploited for a wide range of applications. The combination of several factors determines the success of the experiments. There are many variables which must be recognized and optimized for each individual study. Among them, the selection of a suitable fluorescent probe, the labeling strategy, the fluorescence microscope system, and the imaging acquisition technology are fundamental for the achievement of good images.

The genetically encoded fluorescent labels, such as green or cherry fluorescent proteins, will be not discussed in this chapter [2]. For the successful use of fluorescent proteins for imaging, other requirements need to be fulfilled. For example, the efficiency of protein expression, the lack of toxicity for the investigated pathway, and the brightness and stability of the fluorescence protein when expressed as a fusion to the protein of interest need to be considered. Furthermore, although representing a powerful tool for tracking processes in live cell imaging, the work with a fusion protein has its limitations. Among them, the required genetic manipulation and the observation of artificial fusion proteins may induce changes on the protein localization, function, and expression levels. Thus, these issues are covered in a specific chapter (*see* Chapter "Localization of proteins within intact bacterial cells using fluorescent protein fusions" from VW Rowlett and W Margolin).

Microorganisms and cellular structures can be stained with a fluorescence dye, a fluorochrome, in order to be observed through a fluorescence microscope and produce fluorescence images where the target structures will look colored or shiny (Fig. 1a). Many fluorochromes are specific for cell components and are widely used in microbiology [3]. Dyes bind to DNA, RNA, intracellular lipids [4], or membrane lipids [5]. Furthermore, fluorophore-conjugated antibiotics such as vancomycin and cephalosporin are powerful tools for studies on the peptidoglycan cell wall, penicillin-binding proteins, and bacterial cell division [6, 7].

In immunofluorescence (IF) microscopy, the specificity of antigen-antibody reactions is exploited for the observation of structures (antigens, targets) that react with their specific antibody, which would deliver the fluorophore directly or when further tagged with another dye-coupled antibody for increasing signal intensity. The dye-coupled antibody will produce fluorescence and shine under the fluorescence microscope allowing the detection, visualization, and localization of specific antigens. The use of indirect labeling enables the use of a limited number of commercial conjugates with a variety of primary antibodies, avoiding the conjugation procedure, which is cumbersome and could also affect the binding activities of the primary antibody (Fig. 1b, c). Protein candidates to be studied by microscopy analyses can be purified

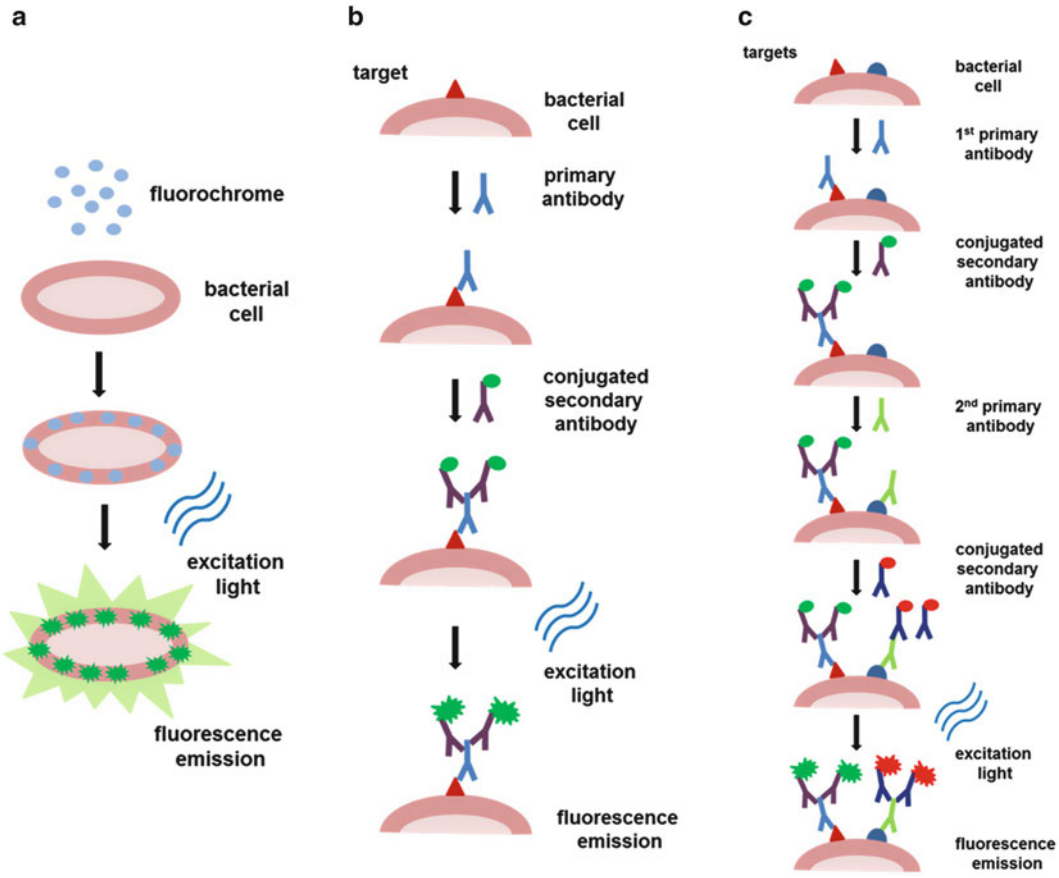

Fig. 1 Fluorescence labeling for microscopy. (**a**) Bacterial labeling with a fluorochrome, (**b**) indirect immunofluorescence labeling, (**c**) indirect double immunofluorescence labeling

from bacterial cells overproducing them. The purified protein is injected into animals (e.g., rabbits) to produce a specific polyclonal antiserum in enough quantities. In order to test the specificity of the antisera raised and exclude a possible cross-reactivity with other bacterial proteins, the serum should be tested by immunoblotting using total cell extracts of the bacteria. Alternatively, synthetic peptides derived from the native protein are also used for the generation of antibodies [8].

Generally, the large spectral range of available fluorophores is described in the context of imaging different cellular, subcellular, and molecular components from eukaryotic cells. Regarding available commercial products, less is reported for bacteriological applications. Fluorescence and IF reagents and protocols for imaging bacteria need to be accessed from the outstanding publications containing high-level quality of fluorescence images. However, when describing the staining techniques applied for labeling, publications are not always sufficiently specific in their account of the procedures used.

Recently, new developments in the design of new microscopes have extended their abilities by surpassing the diffraction limit in optical microscopy to see more detail with greater resolution [9]. The new super-resolution microscopy includes an array of advancing techniques as the stimulated emission depletion microscopy (STED), stochastic optical reconstruction microscopy (STORM), fluorescence photoactivation localization microscopy (PALM), structured illumination microscopy (SIM), and total internal reflection fluorescence microscopy (TIRFM). These microscopes are the new "nanoscopes," and they have broken the 200 nm resolution limit from the light microscopy offering higher resolution, sensitivity, field and depth of view, and speed than conventional light microscopy. However, although this new instruments have advantages, they have also their limitations, and it is not easy for biologist to choose which new technologies to explore. The application of some of these new super-resolution techniques are discussed in other chapters.

The aim of this chapter is to provide fluorescence and IF methods containing sufficient technical information to implement and further improve fluorescence imaging for microbiological applications.

2 Materials

2.1 Bacterial Cultures for IF Studies

2.1.1. Bacterial strains *Escherichia coli* Nissle 1917, *Pseudomonas aeruginosa* PA14, *Staphylococcus aureus* Sa02 [10], and *Streptococcus pyogenes* A40 [11] were obtained from our Central Collection of Strains.

2.1.2. Growth media specific for the organism and the condition of interest (*see* **Note 1**). Here was used LB agar and broth (*see* Subheading 2.6.1).

2.2 Fixation of Bacterial Cells

2.2.1. Phosphate-buffered saline (PBS) (Subheading 2.6.2).

2.2.2. 3% and 6% paraformaldehyde (PFD) solution in PBS (*see* Subheading 2.6.3), 50 ml aliquots stored at −20°C, the aliquot "in use" stored at 4°C.

2.3 Microscopic Observation of Live Bacterial Cells

2.3.1. Low-melt agarose 2% solution in LB broth (*see* Subheading 3.2.1). The low-melt agarose is commercially available from several vendors.

2.3.2. Microscope slides pre-cleaned and ready to use (Thermo Scientific (http://www.thermoscientific.com)).

2.3.3. Small square glass slides 26 × 26 mm and 1.0 mm thick.

2.3.4. FM® 4-64 dye (N-(3-triethylammoniumpropyl)-4-(6-(4-(diethylamino) phenyl) hexatrienyl) pyridinium

dibromide) (Life Technologies (http://www.lifetechnologies.com)). A freshly prepared 100 μg/ml solution is prepared in DMSO (Sigma (http://www.sigmaaldrich.com)). (*See* **Note 2**.)

2.3.5. Phosphate-buffered saline (PBS) (*see* Subheading 2.6.2).

2.3.6. SlowFade Gold antifade reagent (Life Technologies (http://www.lifetechnologies.com)).

2.3.7. Cover slips 22 × 22 mm #1 (Thermo Scientific (http://www.thermoscientific.com)).

2.3.8. Immersol 518 F, immersion oil for fluorescence microscopy fluorescence-free (Zeiss (http://www.micro-shop.zeiss.com)) (*see* **Note 3**).

2.4 Preparation of Fixed Bacterial Cells for Fluorescence Labeling

2.4.1. Coverslip circles 12 mm (Thermo Scientific (http://www.thermoscientific.com)).

2.4.2. Poly-L-lysine 0.1% solution in water (Sigma P8920, http://www.sigmaaldrich.com) stored at room temperature (*see* **Note 4**).

2.4.3. PBS (*see* Subheading 2.6.2).

2.4.4. 24-well plates. They can be purchased from different suppliers.

2.5 Immunofluorescence Labeling

2.5.1. PBS (*see* Subheading 2.6.2).

2.5.2. 0.1% Triton X-100 detergent in PBS (*see* Subheading 2.6.4).

2.5.3. Heat-inactivated fetal calf serum (FCS), Gibco (Life Technologies (http://www.lifetechnologies.com)) or bovine serum albumin (BSA) (Sigma (http://www.sigmaaldrich.com)).

2.5.4. Primary antibodies: rabbit anti-protein A from *S. aureus* (Sigma (http://www.sigmaaldrich.com)). The polyclonal antibodies anti-*S. aureus* Sa02 and anti-group A Streptococci GAS123 were raised in rabbit against heat-killed bacteria strains from our laboratory collection. The rabbit polyclonal antibodies obtained against the hyperexpressed DnaK protein and against different synthetic peptides from the FliC flagellar protein from *P. aeruginosa* PA14 were generated by Metabion International AG (http://www.metabion.com).

2.5.5. Goat anti-rabbit IgG secondary antibody and Alexa Fluor 488 and Alexa Fluor 568 conjugates (Life Technologies (http://www.lifetechnologies.com)).

2.5.6. Microscope slides pre-cleaned, ready to use, and with frosted end (Thermo Scientific (http://www.thermoscientific.com)).

2.5.7. ProLong Gold antifade reagent with or without DAPI (Life Technologies (http://www.lifetechnologies.com)).

2.5.8. Nail polish.

2.5.9. Immersol 518 F, immersion oil for fluorescence microscopy fluorescence free (Zeiss (http://www.micro-shop.zeiss.com)) (*see* **Note 3**).

2.6 Media, Buffer, and Reagents

2.6.1. Bacterial growth media. These may be purchased from any supplier of common bacterial growth medium components. In our lab we use the Becton-Dickinson (http://www.bd.com/) products. LB broth: 5 g yeast extract, 10 g tryptone, 5 g NaCl per 1 L. To prepare the LB agar, add 15 g agar to the LB broth components per L.

2.6.2. Phosphate-buffered saline (PBS): 8 g NaCl, 0.2 g KCl, 1.44 g Na_2HPO_4, 0.24 g KH_2PO_4 per L, pH 7.4. The reagents were purchased in Merck & Co. (http://www.merck.com).

2.6.3. 3% and 6% paraformaldehyde (PFD) solution in PBS: paraformaldehyde (Sigma (http://www.sigmaaldrich.com)) is prepared as described in **Note 5**, and 50 ml aliquots are stored at −20°C; an aliquot is thawed and kept at room temperature before using for fixation.

2.6.4. The 0.1% Triton X-100 detergent solution in PBS (Sigma (http://www.sigmaaldrich.com)) is prepared from a 1% stock solution Triton X-100 detergent in water (*see* **Note 6**).

3 Methods

Fluorescence microscopical localization of specific microbial and cellular structures is possible when cellular components are stained with a fluorescence dye and observed through a fluorescence microscope to produce fluorescence images where the target structures will look colored or shiny (Fig. 1a). In microbial fluorescence imaging, fluorochromes are frequently used to stain DNA, intracellular lipids [4], membrane lipids [5], and the cell wall.

There are several classes of nucleic acid stains, showing different binding modes to DNA and differences in cell membrane permeability. They are used in microscopy, in addition to stain the bacterial cells, to distinguish between live and dead bacteria or for direct enumeration of total bacteria in environmental and clinical samples. The commonly used DAPI (4′,6-diamidino-2-phenylindole) and Hoechst dyes bind to the DNA minor groove at A-T-rich sites. In addition, DAPI also intercalates at G-C sites [12]. The bisbenzimide Hoechst dyes are cell membrane-permeant bright stains, whereas the DAPI dye shows higher photostability. This

dye shows blue fluorescence and is commercially available in combination with mounting media permitting simultaneous staining, protecting, and conservation of samples for microscopy. The DAPI staining of bacterial and cellular DNA was used coupled to immunofluorescence labeling methods described later on in this chapter. The SYTO nucleic acid stain series of cyanine dyes [3, 13] penetrate only cells with compromised membrane and will not cross the membranes of live cells, being extremely useful to stain both Gram-positive and Gram-negative death cells. The red fluorescent nucleic acid stain propidium iodide, which only penetrates bacterial cells with damaged membranes, in combination with the SYTO 9 dye, which passively diffuses through membranes, allows the visualization of dead and live bacterial cells in the widely used LIVE/DEAD BacLight Viability Kits [3, 14].

Bacteria that accumulate polyhydroxyalkanoic acid (PHA) and other lipid storage compounds can be screened and monitored with the lipophilic Nile red dye, which stains large cytoplasmic lipid bodies, and the amphiphilic BODIPY FL C12 dye, which stains lipid domains at peripheral areas of the bacterial cell [4, 15]. Furthermore, the fluorescent fatty acid analogs from the BODIPY group may be also used as direct probes for membranes or for metabolic incorporation by live cells [3, 16, 17]. Their lipid tail causes their insertion into membranes in a similar way as it has been shown for other lipophilic dyes as the FM dyes. Particularly, the FM 4-64 and FM 1-63 bind rapidly and reversibly to membranes with strong fluorescence [5, 18]. These are just some examples of fluorescent lipid probes used in bacterial membrane research [19]. Furthermore, fluorophore-conjugated antibiotics such as vancomycin, cephalosporin, and daptomycin are powerful tools for studies on the peptidoglycan cell wall, penicillin-binding proteins, bacterial cell division, and bacterial susceptibility and resistance to antibiotics [5–7, 20, 21].

Many fluorochromes stain their targets brilliantly either in fixed or in living bacterial cells. In this chapter, the staining of membrane lipids with the fluorochrome FM4-64 was performed in live bacteria, and the DNA staining with DAPI was performed in fixed bacterial cells.

Live cell imaging methods are used with fluorescence dyes that act on live cells. The samples need to be observed after the required incubation times and images should be immediately obtained. These processes are highly demanding because the preparation of the material and bacteria, staining, microscopic observation, and imaging need to be done successively. On the contrary, fluorescence staining on fixed cells permits the mounting of the samples with anti-bleaching and anti-fading reagents to increase photostability and allow long-term storage. This allows dedicating longer times for observing and imaging the samples. In addition, some mounting formulations include a nuclear stain, such as DAPI, to achieve

counterstaining during the mounting process in one step. Our laboratory has used these protocols successfully with a variety of bacteria and Gram-negative and Gram-positive environmental and pathogenic microorganisms. However, some optimization may be required, and different conditions may be necessary for other bacteria. Furthermore, fixed cells on coverslips, if not used immediately for labeling, can be stored in 24-well plates immersed in 3% PFD in PBS and sealed with Parafilm at 4°C.

3.1 Preparation of Bacteria for Fluorescence Studies on Live (See Subheading 3.2) or Fixed Bacteria (See Subheading 3.4)

3.1.1. Streak the bacteria on the appropriate agar and incubate overnight at the indicated temperature for optimal growth.

3.1.2. Inoculate a 5 ml broth and grow overnight at the recommended temperature and shaking speed.

3.1.3. Dilute the overnight culture 1:10 or 1:100 in the same broth and grow under the same condition as above during 3 h or until an OD_{600} of approx. 0.5.

3.1.4. The bacteria are ready to follow the live-cell imaging method or to be fixed for immunofluorescence labeling (*see* **Note** 7).

3.2 Slide Preparation Technique for Observation of Live Bacteria in Agarose Pads

3.2.1. The agarose medium should be freshly prepared for each set of experiments and kept melted at 70°C. The 2% low-melt agarose in LB (*see* Subheading 2.3.1) is first dissolved in a beaker on a stirring hotplate (or microwave) and allowed to boil for 5 min stirring continuously, until the agarose dissolves completely. Cool the solution to approx. 70°C before pouring it in 1.5 ml microcentrifuge tubes, placing them immediately in a heat block pre-heated at 70°C.

3.2.2. To prepare the agarose pads, we use our self-pre-prepared microscope slides with two 26 × 26 small square glasses 1 mm thick sealed with spray sealer on each side. These slides are reused after washing and drying. The "chamber" in the middle of the slide, created by the two squared small glasses, will be used to make the agar pad (an agarose "sandwich" of even thickness). Alternatively, tape could be used wrapped around each side of a slide, to create a "chamber" with a thickness of 1 mm.

3.2.3. Add approximately 200 μl of the molten LB low-melt agarose to the "chamber" of each slide and cover immediately with a new microscope slide pressing to obtain a homogeneous distribution of the agar in the free space between the two slides. We place a 250 ml bottle on top of each slide and let solidify for an hour.

3.2.4. After solidification and when the bacterial sample is ready for observation, the two slides are separated using a scalpel, leaving the agar pad attached to the top microscope slide.

Flip the microscope slide with the agarose pad, now on top of it. The transfer of the pads from one surface to another can be done with a scalpel carefully to not damage the agarose surface.

3.2.5. Seed the bacteria on agarose pads by pipetting 3 µl of the bacterial samples onto individual agarose pads.

3.3 Labeling of Bacterial Membranes with the Lipophilic Dye FM4-64

The following protocol describes an example of the labeling schematized in Fig. 1a. The lipophilic dye *N*-(3-triethylammoniumpropyl)-4-(*p*-diethylaminophenyl-hexatrienyl) pyridinium dibromide (FM 4-64) is a vital stain and fluoresces red only in living cells; therefore, bacterial cells cannot be fixed. The dye intercalates into the membrane without permeabilizing it and was used to label a wide range of Gram-positive and Gram-negative bacteria, *Mycoplasma*, and yeasts. Recently, it has been used to discriminate between compounds that have different effects on the *E. coli* cell envelope [5] and to study the mechanism of action of the *Bacillus subtilis* SDP cannibalistic toxin membranes [22]. Here, it was used for the visualization of *E. coli* Nissle and *P. aeruginosa* PA14 membranes in Fig. 2a and b, respectively.

3.3.1. The bacteria are prepared as described in Subheading 3.1.

3.3.2. While the bacteria are growing, the small agarose pads are prepared as described in Subheading 3.2.

3.3.3. After 2–3 h of incubation (Subheading 3.1.3), prepare parallel microcentrifuge tubes with each 100 µl bacterial culture.

3.3.4. Add 5 µl from the 100 µg/ml FM4-64 solution (Subheading 2.3.4) to each tube. One sample is prepared for immediate microscopic observation. The other ones are incubated in a Thermoblock at 37°C with shaking and protected from light during 30 min and 1 h (*see* **Note 8**).

3.3.5. After each incubation time, spin cells for 30 s at high speed in a microcentrifuge, discard the supernatant, and resuspend the pellet in 10 µl PBS.

3.3.6. Pipette 3 µl of cells onto the agarose pad prepared as described in Subheading 3.2.

3.3.7. Add a small drop of SlowFade Gold antifade reagent (Subheading 2.3.6) and place a cover slip (Subheading 2.3.7) on top and immersion oil (Subheading 2.3.8). The sample is ready for microscopic observation.

The FM4-64 dye stains the membranes with red fluorescence (excitation/emission maxima ~ 515/640 nm). Figure 2a shows the *E. coli* strain Nissle stained with FM4-64 for 15 min. Some bacterial cells and generally all filaments are stained stronger than the rest of the bacterial population. Figure 2b shows *P. aeruginosa* PA14 cells stained with FM4-64 for 30 min.

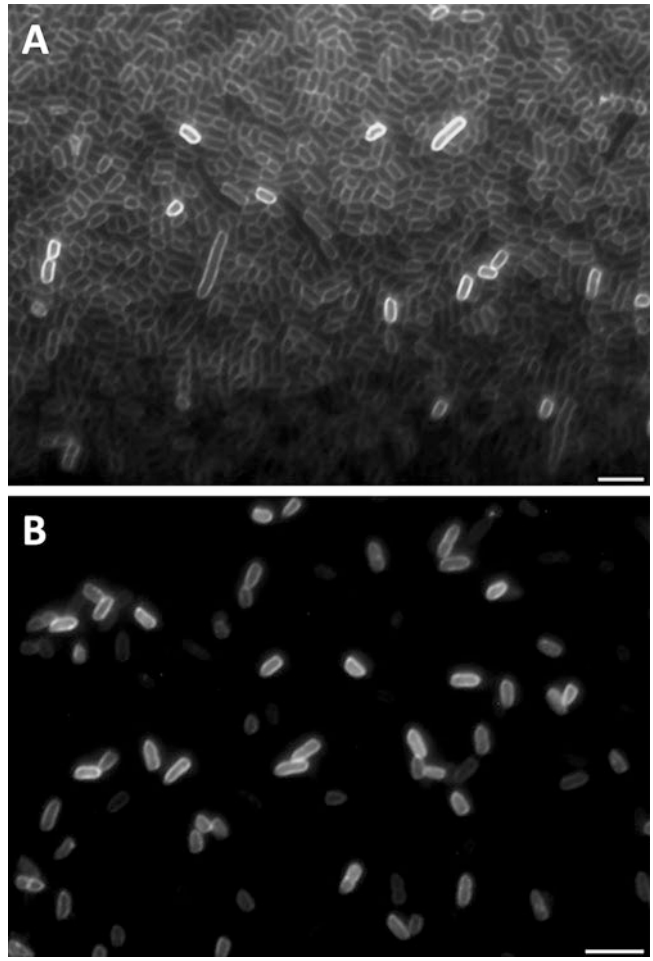

Fig. 2 Fluorescence microscopy images of live *E. coli* (**a**) and *P. aeruginosa* (**b**) bacterial cells stained with FM4-64. The majority of the *E. coli* bacterial cells show the same strong staining pattern and only fewer cells are overstained. *P. aeruginosa* cells depict a much more irregular staining pattern; many cells show weaker staining or lack of labeling. Scale bar represents 10 μm

3.4 Preparation of Fixed Bacterial Cells on Poly-L-Lysine-Coated Coverslips for Immunofluorescence Staining

In the immunofluorescence staining methods showed in Fig. 1b and c, the bacterial cells are labeled after fixation on poly-L-lysine-coated coverslips.

3.4.1. Prepare the bacteria as described in Subheading 3.1.

3.4.2. While the bacterial cells are growing to the early exponential phase, the poly-L-lysine-coated coverslips are prepared.

3.4.3. Use clean coverslips, previously sterilized by dry autoclaving (*see* **Note 9**).

3.4.4. Place a piece of Parafilm large enough to accommodate all coverslips on a flat surface (*see* **Note 10**).

3.4.5. Before use, a fresh 0.01% poly-L-lysine solution is prepared in sterile distilled water (*see* Subheading 2.4.2 and **Note 4**). For each coverslip, place 60 µl of the poly-L-lysine 0.01% solution on the Parafilm. Be careful to leave enough space between drops.

3.4.6. Use fine tweezers to place a coverslip onto each drop (it is recommended to prepare always some extra coverslips). Incubate the coverslips at room temperature for 5–15 min (*see* **Note 4**).

3.4.7. Remove the coverslips from the Parafilm with tweezers and eliminate the excess of the poly-L-lysine solution with the help of a tissue paper. Tranfer the coverslips, now the coated side up, to a clean Parafilm surface to dry for approximately 30 min (*see* **Note 11**).

3.4.8. When the bacterial cells reached the desired bacterial density, add the same volume of 6% PFD in PBS (*see* Subheading 2.2.2) for fixation (3% PFD final concentration). Invert/rotate the tubes and incubate at room temperature for 20 min. Fixed cells could be stored at 4°C and used within a week.

3.4.9. Prepare one or more 1 ml aliquots in sterile microcentrifuge tubes and centrifuge for 3 min at 10,000 rpm. After washing with 1 ml of PBS, discard the supernatant and resuspend the pellet in 100 µl of PBS.

3.4.10. For each coverslip, pipette 50 µl of fixed bacterial cells on a clean Parafilm surface and place the coverslips on top with the coated side in contact with the cells. Incubate at room temperature for 15–30 min.

3.4.11. To remove the coverslips from the Parafilm, pipette 100 µl of PBS onto the edge of the coverslip; the liquid will flow under the coverslip elevating it, allowing easy access for the tweezers.

3.4.12. Handle the coverslips carefully with the tweezers, remove the excess of liquid with the help of a tissue paper, and wash the coverslips immersing them in a small beaker with PBS. Remove the excess of liquid. The coverslips are ready for antibody labeling (*see* Subheadings 3.5 and 3.6). The coverslips with the attached bacteria, if not used immediately, can be stored each in a well from a 24-well plate (the bacteria side up), filled with 3% PFD solution in PBS. Seal the plate with Parafilm and store at 4°C.

3.5 Immunofluorescence Staining for the Observation of Bacteria and Bacterial Proteins

IF labeling uses a primary and a secondary antibody conjugated to a fluorochrome (*see* Fig. 1b, c). The primary antibody will bind to your chosen target antigen or protein. It can be purchased, if commercially available, or custom produced against heat-inactivated bacteria, purified bacterial proteins, or synthetic peptides and small molecules. The custom process for the generation of antibodies takes time, about 3 months, which include the required animal immunization protocol, but will then generate sufficient serum for years of research. The secondary antibody conjugated to a fluorochrome will react with the first antibody; thus it will be raised against the host species used to generate the primary antibody. For a rabbit primary antibody, an anti-rabbit secondary antibody is obtained in a host species other than rabbit (e.g., goat or donkey). The fluorescent dyes are chosen for their emission color and the filter available on the fluorescence microscope that will be used for the sample observation (*see* **Note 12**). For multiple antibodies labeling, when primary antibodies from different species are available, they can be used in the same first incubation step as their related secondary antibodies in the second incubation step. Alternatively, two primary antibodies from the same species can be used in independent labeling steps, as the double staining showed in Fig. 1c and described in Subheading 3.6.

Once the cells have been fixed on coverslips (Subheading 3.4), there are some pretreatments that may be considered before starting the immunolabeling.

The aldehyde fixatives, particularly glutaraldehyde, react with amines and proteins generating fluorescent and may become a problem for microscopic observation. As only formaldehyde is used in the methods described here, a quenching step to reduce autofluorescence is unnecessary. However, if necessary, a 20 min treatment of the coverslips with a 20 mM glycerin solution in PBS (quenching buffer) could be used to quench any unreacted fixative. This treatment is performed after the coverslips have been washed following fixation.

Bacterial permeabilization to improve antigen accessibility is performed when intracellular proteins are labeled. If the protein is exposed to the external surface of the bacterial membrane, a permeabilization step is unnecessary. It is also possible to perform the permeabilization after an extracellular protein was labeled to reach a second antigen intracellular localized.

A blocking buffer could be used to block nonspecific interactions of antibodies. Blocking buffers used are (a) 1% BSA in PBS, (b) 5% pre-immune serum from the same animal that was used to raise the secondary antibody in PBS, and (c) 10% fetal calf serum (FCS) in PBS. In addition, the blocking buffer is used to prepare the antibody dilutions. However, the blocking solution might increase the background and should not be necessary if the antibodies are working efficiently.

The last issue that needs to be discussed is how to perform the labeling using small volumes of antibodies (no more than 25–40 μl antibody dilution for each coverslip). A low number of coverslips can be handled in two ways: (a) in a glass plate with a water-soaked paper filter covered by a piece of Parafilm where the coverslips are placed with the cell side up and the antibody dilutions are pipetted onto each coverslip. For washing, after aspiration of the antibody solution, PBS is added on top, repeating the procedure at least three times; (b) a small layer of Parafilm is first fixed with some water drops on the bench surface, the antibody solutions are pipetted onto the Parafilm, and the coverslip is placed on top of the drop (cell side down). For washing, permeabilization, and blocking, use the strategy described in Subheading 3.4.11, adding and aspirating the solutions the necessary times. Alternatively, in both (a) and (b), the coverslips can be washed in a beaker containing PBS. In our laboratory, as we handle a large number of samples, we work with coverslips placed (cell side up) in the center from each well from a 24-well plate. The antibody solutions (25 μl) are pipetted onto each coverslip; during treatments (200 μl) and washing (500 μl), the liquids are covering the coverslip and are removed by aspiration using a vacuum system (*see* **Note 13**).

The description of the simple IF staining method, as schematized in Fig. 1b, follows.

3.5.1. The bacteria were previously fixed on poly-L-lysine coverslips as indicated in Subheading 3.4 and stored, if necessary, in 3% PFD in PBS at 4°C.

3.5.2. Rinse twice with PBS.

3.5.3. Permeabilization, if necessary, with 0.1% Triton X-100 in PBS (Subheading 2.6.4) for no longer than 5 min (*see* **Note 14**).

3.5.4. Rinse twice with PBS.

3.5.5. Blocking with 10% FCS in PBS (an alternative blocking solution is 1% BSA) for 30–45 min.

3.5.6. Incubation with the primary antibody: aspirate the blocking solution and without washing, cover the coverslips with a dilution of the primary antibody made in blocking buffer (*see* **Note 15**). In Figure 3a and b, respectively, anti-protein A (1:100) and anti-*S. aureus* Sa 02 (1:100) antibodies were used; *see* Subheading 2.5.4. Incubate for 1 h at room temperature.

3.5.7. Rinse twice with PBS.

3.5.8. Incubation with the secondary antibody: the coverslips are incubated with a secondary antibody conjugated to a fluorochrome that is selected depending on the donor species of the primary antibody and the desired fluorochrome.

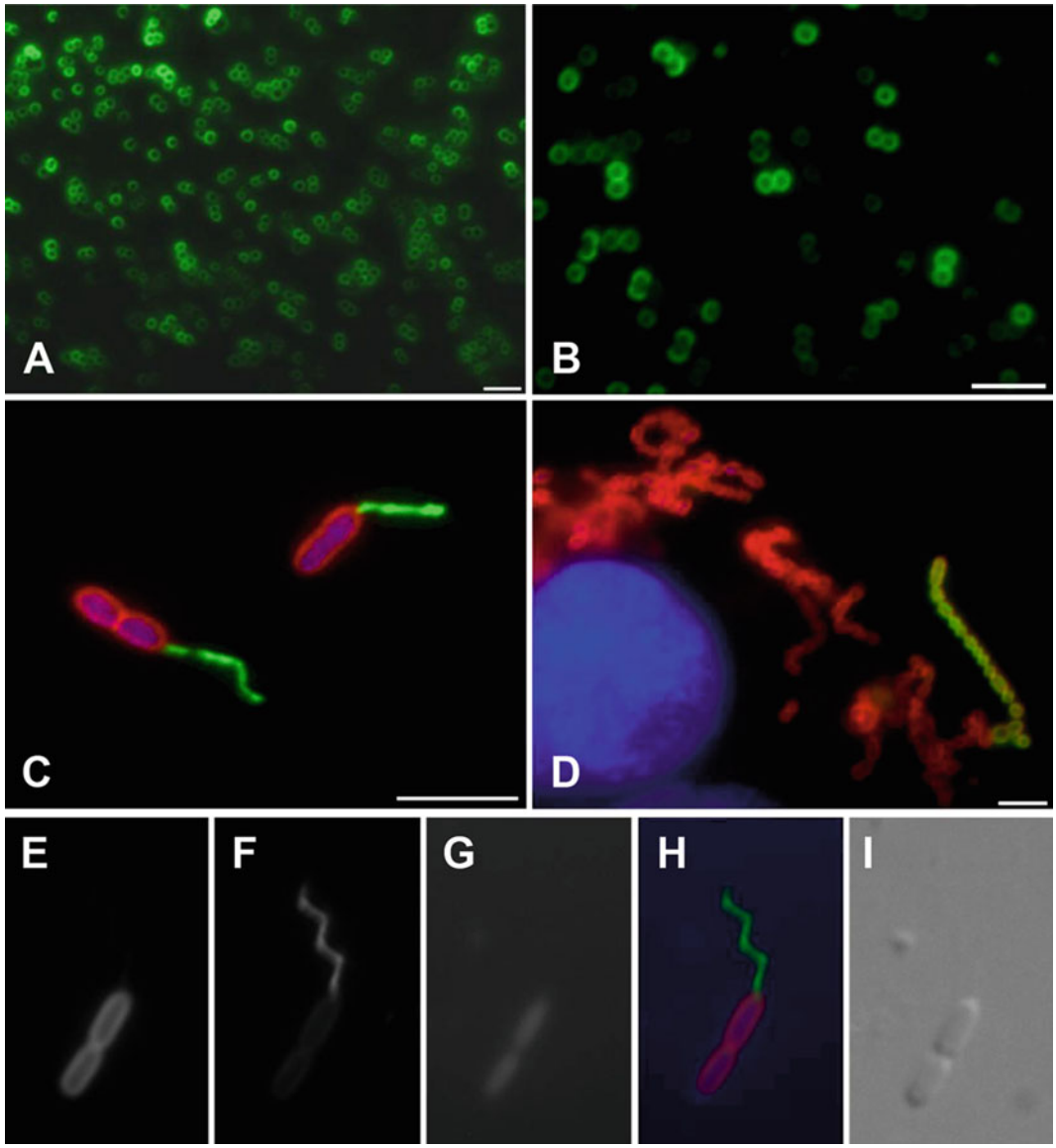

Fig. 3 Immunofluorescence staining. In (**a**) and (**b**) *S. aureus* cells were labeled using two different primary rabbit antibodies: anti-*S. aureus* serum obtained against heat-killed bacteria from the same Sa02 strain in (**a**) or a commercial anti-protein A antibody in (**b**). Goat anti-rabbit IgG Alexa Fluor 488 was the secondary antibody used in both images (green fluorescence). (**c**) and (**h**) show the merge images from a double immunofluorescence staining of *P. aeruginosa* PA14 for the visualization of the flagellum structure and the bacterial cells. The primary antibody used was rabbit anti-FliC followed by goat anti-rabbit Alexa Fluor 488 (green). A second staining with anti-DnaK antibody was performed followed by goat anti-rabbit Alexa Fluor 568 (red). The cover slips were mounted with ProLong Gold DAPI which counterstained the DNA in blue. The independent channel acquisitions from the merge image showed in (**h**) are shown in (**e**) for red, (**f**) green, and (**g**) blue fluorescence. The DIC image is depicted in (**i**). The interaction between *S. pyogenes* and HEp2 eukaryotic cells after 2 h of infection is observed in (**d**). The extracellular and intracellular streptococci were labeled with the same primary antibody, rabbit anti-group A, followed by goat anti-rabbit Alexa Fluor 488 and 568 (before and after permeabilization). The extracellular bacteria are double stained in green and red (yellow), and the intracellular bacteria are stained only in red. The nucleus from the HEp2 cell is stained with DAPI (blue). Scale bar represents 10 μm

As the primary antibodies used here were all generated in rabbit, the secondary antibody will be a goat anti-rabbit antibody conjugated with, e.g., FITC, TRITC, Cy3, or one of the brighter and photostable Alexa Fluor dyes (*see* Subheading 2.5.5 and **Note 12**). In Fig. 3a and b, goat anti-rabbit IgG Alexa Fluor 488 was used. Incubate for 45 min at room temperature protected from light.

3.5.9. Rinse three times with PBS.

3.5.10. Mounting of coverslips on microscope slides: apply a small amount (~5 μl) of mounting media ProLong Gold (Subheading 2.5.7) to a slide, take up the coverslip with tweezers and blot the excess PBS on a tissue paper (cleaning the surface of the non-sample side), and invert the coverslip onto the mounting medium.

3.5.11. Curing time: leave the coverslips protected from light overnight to cure. If using another mounting media, follow the manufacturer's indications for mounting and curing time.

3.5.12. After the overnight mounting process, seal the coverslip with nail polish around the edges to prevent drying and movement under microscope.

3.5.13. The sample is ready for microscopic observation. Use immersion oil for fluorescence microscopy (Subheading 2.3.8 and **Note 8**). After viewing, wipe off the oil from the slides before keeping them in a microscope slide box, at 4°C.

Figure 3 shows the same *S. aureus* strain labeled with either an anti-*S. aureus* antibody obtained against heat-killed bacteria from the same strain (Fig. 3a) or a commercial anti-protein A antibody (Fig. 3b). The protein A is a membrane-associated protein from *S. aureus* [23], and its antibodies label very well the *S. aureus* bacterial cells, resulting in almost the same staining and fluorescence brightness observed when bacteria are labeled with the antibodies raised against the whole cells.

3.6 Double Immunofluorescence Staining for the Observation of Two Different Bacterial Targets, P. aeruginosa *PA 14 Bacterial Cell and Flagellum*

In the example described here, the double staining of *P. aeruginosa* with anti-FliC and anti-DnaK, following separate antibody incubations as showed in Fig. 1c, was performed after permeabilization of the bacterial cells. Figure 3c, e–i shows the double immunofluorescence staining of FliC, the structural protein component of the flagellar filament, and DnaK, a molecular chaperone, in *P. aeruginosa* PA14 cells. Particularly in this *Pseudomonas* strain, the DnaK protein is localized and well distributed in the membrane area, allowing a clear staining of the bacterial cells. The samples were counterstained for DNA with the DAPI contained in the mounting reagent; thus the cells are seen blue (DNA) and red (DnaK), whereas the flagella (FliC) are seen green. The labeling obtained

with the anti-DnaK antibody showed in Fig. 3e can be compared with the fluorescence pattern observed when labeling the *Pseudomonas* membrane with FM4-64, as showed in Fig. 2b.

3.6.1. The bacteria were previously fixed on poly-L-lysine coverslips as indicated in Subheading 3.4 and stored, if necessary, in 3% PFD in PBS at 4°C.

3.6.2. Rinse twice with PBS.

3.6.3. Permeabilization with 0.1% Triton X-100 in PBS (Subheading 2.6.4) for no longer than 5 min.

3.6.4. Rinse twice with PBS.

3.6.5. Blocking with 1% FCS in PBS (or another different blocking solution as described above and in Subheading 3.5.5) for 30–45 min.

3.6.6. Incubation with the first primary antibody to stain the bacterial flagella: a rabbit polyclonal anti-FliC antibody (1:100) (*see* Subheading 2.5.4) is used following the indications from the Subheading 3.5.6. Incubate for 1 h at room temperature.

3.6.7. Rinse twice with PBS.

3.6.8. Incubation with the secondary antibody goat anti-rabbit IgG conjugated with Alexa Fluor 488 (1:100) (*see* Subheading 2.5.5) for 45 min at room temperature.

3.6.9. Rinse twice with PBS.

3.6.10. Incubation with the second primary antibody to label the *P. aeruginosa* cells for 1 h at RT. In this example, a rabbit polyclonal anti-DnaK antibody (1:50) is used (*see* Subheading 2.5.4).

3.6.11. Rinse twice with PBS.

3.6.12. Incubation with the second secondary antibody goat anti-rabbit IgG conjugated with Alexa Fluor 568 (1:100) (Subheading 2.5.5) for 45 min at room temperature.

3.6.13. Rinse three times with PBS.

3.6.14. Mounting of coverslips on microscope slides as described in Subheading 3.5.10. The mounting media used here, ProLong Gold DAPI, contains a DAPI which is a counterstain for DNA and eliminates the need for a separate step to stain DNA (*see* **Note 16**).

3.6.15. Follow steps described in Subheadings 3.5.11–3.5.13.

Double IF staining is also extensively used in microbial pathogenicity, when the interaction of microbial pathogens with eukaryotic cells is investigated in vitro. The double labeling of bacteria, using twice the same primary antibody in combination with two different conjugated secondary antibodies, allows

distinguishing attached and internalized bacteria [11, 24]. In this case, the bacterial staining is performed twice, before and after permeabilization of the eukaryotic cells. An example of this strategy is showed in Fig. 3d, where epithelial cells attached to coverslips were infected with *S. pyogenes* during 2 h. Extracellular bacteria are labeled twice in green and red during the first and second immune staining. In contrast, intracellular bacteria are only labeled once (in red), after the permeabilization of the eukaryotic cells with a detergent as Triton X-100, when the antibodies are able to reach the internalized bacterial cells. In this case, the DAPI (blue) stains much stronger the nucleus from the eukaryotic cells than the bacterial DNA.

4 Imaging

All our samples were examined using a Zeiss Axio Imager A1 fluorescence microscope equipped with a HXP 120 lamp and the Zeiss filters 20, 44, and 49 used to observe the signals from the fluorochromes Alexa Fluor 568 and FM4-64, Alexa Fluor 488, and DAPI, respectively (*see* **Note 17**). The images were obtained with the microscope camera AxioCam MRm and the Zeiss AxioVision or ZEN image acquisition software. The multichannel fluorescence microscopy enables the acquisition and processing of different fluorescent and transmitted light (differential interference contrast (DIC)) images in independent channels, as showed in Fig. 3e–i. Merge images are also generated, as showed in Fig. 3c, d, and h. All the images were analyzed with the Zeiss AxioVision or ZEN software and prepared for publication with Adobe Photoshop CS5.

State-of-the-art microscopes with sensitive cameras and powerful software, paired with good prepared microscopic samples, are the basis for high-quality images. Conventional fluorescence microscopy is the most versatile and accessible method for the observation of labeled structures. Advances in labeling methods are constantly improving the ability to simultaneously image multiple structures and macromolecules. However, its primary limitation is that diffraction prevents structures closer than approximately half the wavelength of light from being resolved from one another. The physical diffraction limit is ~200 nm for light microscopy [25].

In confocal microscopy, a laser is used to provide the excitation light that reflects in a system of mirrors that scan the laser across the sample. The system has a confocal pinhole that rejects the out-of-focus fluorescent light, and only one point of the sample is observed, detected, and used to build the image by the computer attached to the detector. The image is obtained from a thin section of the sample, increasing the optical resolution by reducing the impact of out-of-focus light in order to approach the diffraction limit. This is particularly advantageous in thick samples like

mammalian tissues. Furthermore, by scanning many thin sections through a sample, a very clean three-dimensional image of the sample can be obtained. However, this powerful method provides little advantages for very thin samples such as microbes [25]. In our experience, carefully performed protocols and good mounting reagents are sufficient for obtaining very good images of microbes using conventional fluorescence microscopy.

Recent advances in microscope technology allowed to improve the resolution, throughput, and quantitative analysis of fluorescence microscopy. Super-resolution methods break the diffraction limit to image the localization and dynamics of proteins and molecules at molecular scales. Some of the new microscopes, described in the Introduction, were implemented in microbial research yielding exciting discoveries [25].

Imaging has been utilized to gain detailed knowledge about many different microbial processes [26]. Nowadays the application of fluorescence microscopy is evolving to previous unimaginable levels. However, new advances in microscopy technologies need to be coupled to advances in computational analysis of images [26] for exploring all the possibilities of fluorescence microscopy for deep investigation of biological processes.

5 Notes

1. For fluorescence studies on live bacteria, the use of a defined minimal medium is generally recommended, to minimize the interference of autofluorescence compounds. It is usually said that yeast extract should be avoided. However, we used LB to grow bacteria for the staining described in 3.2, and no problems were observed with regard to the quality of the fluorescence images obtained. Furthermore, it is documented that FM4-64 does not efficiently label cells in minimal medium.
2. The lyophilized FM4-64 dye is stable at room temperature if stored protected from the light; on the other hand, the stock solution is unstable. In our lab we use the FM4-64 special packaging with ten vials of 100 μg each. The dye is dissolved in 1 ml of DMSO (solution 100 μg/ml), fractionated in small aliquots, stored at −20°C, and used within a week.
3. Our microscopes are from Zeiss; hence we buy Zeiss immersion oil for fluorescence microscopy.
4. Note poly-L-lysine. Many protocols are available on the poly-L-lysine coating of coverslips; they use different concentrations and incubation times. In our lab we use the higher molecular weight poly-L-lysine (150,000–300,000) which should provide more attachment sites per molecule. No differences were observed when using the 0.1% or 0.01% w/v solution.

We prefer to prepare a fresh dilution (0.01%), coat only one side from the coverslips, and avoid the washing steps before drying.

5. To prepare the 3% PFD solutions in PBS, first be aware to perform all the steps in the hood because PFD is toxic. Avoid breathing the power during weighting and during the preparation of the solution. Heat 400 ml of distilled water in a beaker to 60°C. Add 15 g of PFD and stir. Add drops of 1N NaOH under stirring until the solution is completely clear. Add 50 ml of 10x PBS. Complete the volume to 500 ml and allow the solution to reach room temperature before adjusting the pH to 7.4. Filter through a 0.2 μm filter. Prepare 50 ml aliquots in tubes and store at −20°C. Aliquots are thawed before use and kept at room temperature before using for fixation. The rest of the solution can be stored at 4°C for short time. To prepare the 6% solution, just double the amount of PFD power.
6. The Triton X-100 10% stock solution is prepared in water and stored, after sterilization, protected from light. From this solution is obtained the 0.1% working solution in PBS.
7. Incubation time and growth conditions can be modified as necessary in relation to the bacteria, bacterial structures, or processes to be monitored by fluorescence imaging.
8. Incubation time periods may be increased in relation to the bacteria observed. A 20 min stabilization of the stained bacteria seeded onto the agar before observation is recommended. In our experience, the stabilization did not improve the intensity of the fluorescence.
9. One package of 100 round coverslips is placed in a glass petri dish wrapped in aluminum foil before dry sterilization.
10. Place first some drops of water on the clean bench surface, place a piece of Parafilm with the protection paper, push with your hand until the Parafilm will remain attached to the surface, and remove the protection paper.
11. To handle the coverslips, in addition to use fine pointed curved tweezers, we use a regular needle with a self-made curved tip at the end (i.e., like a tiny hook) that is very useful in helping the tweezers to pick up the coverslips from the Parafilm or plastic surfaces. Alternatively, you can raise the coverslips off the Parafilm by pipetting PBS at the edge of the coverslip and lift them with the tweezers.
12. The fluorescent dyes are chosen for their emission color and the filter available on the fluorescence microscope that will be used for the sample observation. Green common fluorophores are fluorescein FITC and Alexa Fluor 488. Red common fluorophores are tetramethylrhodamine TRITC, Texas Red, Cy3, and Alexa Fluor 568 and 594.

13. In our laboratory, we handle a large amount of coverslips and it is faster to perform all the treatment steps and labeling in 24-well plates. A vacuum system is used to remove the liquids and the coverslips are not moved or touched. We use a multipipette to fill the wells with 500 µl PBS/each for washing and 200 µl for blocking. Before the antibody incubations, all the liquid is aspirated from the well, and with a needle (*see* **Note 11**), the coverslips are placed in the center of each well (avoiding contact with the well sides) and 25 µl of antibody dilution is placed on top of each coverslip. For mounting the coverslips, they are carefully lifted with the needle, allowing access to the tweezers, to transfer them from the 24 wells to the microscope slides.
14. Another milder detergent used is saponin, which acts preferentially on membranes rich in cholesterol.
15. The optimal antibody concentration to be used depends on the affinity of the antibody and the abundance of the antigen. Serial antibody dilutions (from 1:25 to 1:1000) are tested when using a new purchased or generated antibody on multitest well slides. The highest dilution that results in good fluorescence (highest signal) and lowest background is the optimal concentration to be used.
16. Other mounting media with or without DAPI are commercially available and are also good for preventing fluorescence from fading (photobleaching) during fluorescence microscopy and for storage. ProLong Diamond antifade reagent is a new superior antifade and mountant that provides additional protection (http://www.lifetechnologies.com).
17. The information about each number filter set (excitation and emission) is found in the filter assistant from Zeiss (http://www.micro-shop.zeiss.com). A list with the excitation and emission data from an overview of dyes is also available.

References

1. Lichtman JF, Conchello J-A (2005) Fluorescence microscopy. Nat Methods 2:920–931
2. Shaner NC, Steinbach PA, Tsien RY (2005) A guide to choosing fluorescent proteins. Nat Methods 2:905–909
3. Johnson I, Spence MTZ (eds) (2010) The molecular probes handbook. A guide to fluorescent probes and labeling technologies, 11th edn. Life Technologies, Carlsbad
4. Bassas-Galia M, Nogales B, Arias S, Rohde M, Timmis KN, Molinari G (2012) Plant original *Massilia* isolates producing polyhydroxybutyrate, including one exhibiting high yields from glycerol. J Appl Microbiol 112:443–454
5. Nonejuie P, Burkart M, Pogliano K, Pogliano J (2013) Bacterial cytological profiling rapidly identifies the cellular pathways targeted by antibacterial molecules. Proc Natl Acad Sci U S A 110:16169–16174
6. Gee CL, Papavinasasundaram KG, Blair SR, Baer CE, Falick AM, King DS, Griffin JE, Venghatakrishnan H, Zukauskas A, Wei J-R, Dhiman RK, Crick DC, Rubin EJ, Sassetti CM, Alber TM (2012) A phosphorylated pseudokinase complex controls cell wall synthesis in mycobacteria. Sci Signal 5:ra7
7. Kocaoglu O, Calvo RA, Sham LT, Cozy LM, Lanning BR, Francis S, Winkler ME, Kearns

DB, Carlson EE (2012) Selective penicillin-binding protein imaging probes reveal substructure in bacterial cell division. ACS Chem Biol 7:1746–1753

8. Trier NH, Hansen PR, Houen G (2012) Production and characterization of peptide antibodies. Methods 56:136–144
9. Toomre D, Bewersdorf J (2010) A new wave of cellular imaging. Annu Rev Cell Dev Biol 26:285–314
10. Molinari G, Rohde M, Wilde C, Just I, Aktories K, Chhatwal GS (2006) Localization of the C3-like ADP-ribosyltransferase from *Staphylococcus aureus* during bacterial invasion of mammalian cells. Infect Immun 6:3673–3677
11. Molinari G, Rohde M, Guzman CA, Chhatwal GS (2000) Two distinct pathways for the invasion of *Streptococcus pyogenes* in non-phagocytic cells. Cell Microbiol 2:145–154
12. Blackburn GM (ed) (2006) Nucleic acids in chemistry and biology. Royal Society of Chemistry, Cambridge
13. Joux F, Lebaron P (2000) Use of fluorescent probes to assess physiological functions of bacteria at single-cell level. Microbes Infect 2:1523–1535
14. Stiefel P, Schmidt-Emrich S, Maniura-Weber K, Ren Q (2015) Critical aspects of using bacterial cell viability assays with the fluorophores SYTO9 and propidium iodide. BMC Microbiol 15:36
15. Wältermann M, Hinz A, Robenek H, Troyer D, Reichelt R, Malkus U et al (2005) Mechanism of lipid-body formation in prokaryotes: how bacteria fatten up. Mol Microbiol 55:750–763
16. Hachmann AB, Sevim E, Gaballa A, Popham DL, Antelmann H, Helmann JD (2011) Reduction in membrane phosphatidylglycerol content leads to daptomycin resistance in *Bacillus subtilis*. Antimicrob Agents Chemother 55:4326–4337
17. Johnson L, Mulcahy H, Kanevets U, Shi Y, Lewenza S (2012) Surface-localized spermidine protects the *Pseudomonas aeruginosa* outer membrane from antibiotic treatment and oxidative stress. J Bacteriol 194:813–826
18. Lewenza S, Vidal-Ingigliardi D, Pugsley AP (2006) Direct visualization of red fluorescent lipoproteins indicates conservation of the membrane sorting rules in the family Enterobacteriaceae. J Bacteriol 188:3516–3524
19. Trevors JT (2003) Fluorescent probes for bacterial cytoplasmic membrane research. J Biochem Biophys Methods 57:87–103
20. Kashyap DR, Wang M, Liu LH, Boons GJ, Gupta D, Dziarski R (2011) Peptidoglycan recognition proteins kill bacteria by activating protein-sensing two-component systems. Nat Med 17:676–683
21. Tran TT, Panesso D, Mishra NN, Mileykovskaya E, Guan Z, Munita JM et al (2013) Daptomycin-resistant *Enterococcus faecalis* diverts the antibiotic molecule from the division septum and remodels cell membrane phospholipids. MBio 4:e00281–13
22. Lamsa A, Liu W-T, Dorrestein PC, Pogliano K (2012) The *Bacillus subtilis* cannibalism toxin SDP collapses the proton motive force and induces. Mol Microbiol 84:486–500
23. Graille M, Stura EA, Corper AL, Sutton BJ, Taussig MJ, Charbonnier JB, Silverman GJ (2000) Crystal structure of a *Staphylococcus aureus* protein A domain complexed with the Fab fragment of a human IgM antibody: structural basis for recognition of B-cell receptors and superantigen activity. Proc Natl Acad Sci U S A 97:5399–53404
24. Molinari G, Chhatwal GS (1998) Invasion and survival of *Streptococcus pyogenes* in eukaryotic cells correlates with the source of the clinical isolates. J Infect Dis 177:1600–1607
25. Gitai Z (2009) New fluorescence microscopy methods for microbiology: sharper, faster, and quantitative. Curr Opin Microbiol 12:341–346
26. van Teeffelen S, Shaevitz JW, Gitai Z (2012) Image analysis in fluorescence microscopy: bacterial dynamics as a case study. Bioessays 34:427–436

Imaging Bacterial Cells and Biofilms Adhering to Hydrophobic Organic Compound–Water Interfaces

Alexis Canette, Priscilla Branchu, Régis Grimaud, and Murielle Naïtali

Abstract

Assimilation of hydrophobic organic compound (HOC) entails frequently the formation of biofilm at the HOC–water interface. Knowledge on the behavior of cells at the oil–water interface and within the structured biofilm is therefore important to understand the degradation of the HOC in ecosystems. The adhesion and biofilm formation on oil–water interface are best documented by microscopic observations. In this chapter we thus describe two methods for observation of bacterial cells and biofilms growing at the HOC–water interface. The first method uses CLSM (confocal laser scanning microscopy) to obtain in situ images of biofilm developing on thin paraffin strip which offers a flat transparent surface allowing imaging directly through the bottom of the culture dish without sampling. Alternatively, the biofilm can be grown on a paraffin strip deposited on a glass microscope slide and then imaged from the top when high resolution is needed. The second method addresses the problem of the ultrastructure of biofilm developing on HOC. It enables to obtain by TEM (transmission electron microscopy) images of cross sections of biofilms with identification of the side in contact with the HOC.

Keywords: Adhesion, Biofilm, CLSM, Hydrocarbons, Lipids, Oleolytic bacteria, TEM

1 Introduction

Hydrophobic organic compounds (HOC), including the chemical classes of lipids and hydrocarbons, are ubiquitous components of the organic matter in ecosystems. The so-called oleolytic bacteria have the ability to use members of either one or both classes as a substrate [1, 2]. However, they have to face the very low water solubility of these substrates. Adhesion to the HOC–water interface and the subsequent formation of biofilms (3D architectures of bacterial cells embedded within matrixes of biopolymers) are strategies shared by many oleolytic bacteria to overcome the low solubility of their substrates [3–5]. Different mechanisms have been proposed for the stimulation of the rate of mass transfer from the oily phase to cell surface. The localization of cell in the vicinity of the interface results in reduction of the length of the diffusion

T.J. McGenity et al. (eds.), *Hydrocarbon and Lipid Microbiology Protocols*, Springer Protocols Handbooks (2016) 71–83,
DOI 10.1007/8623_2015_80, © Springer-Verlag Berlin Heidelberg 2015, Published online: 15 April 2015

pathway of the hydrocarbon from the interface to the cell surface which in turn increases the mass transfer rate [6]. Extracellular matrixes of biofilms provide confined environments where biosurfactants can be accumulated and contribute to hydrocarbon uptake by substrate emulsification or pseudo-solubilization. A direct contact of bacteria with hydrocarbons is also possible via the modification of the cell surface [7] offering the possibility of direct uptake from the hydrocarbon–water interface, although this remained to be demonstrated. In the case of lipids which must undergo hydrolysis into fatty acids by extracellular lipases before uptake by the cell, adhesion and biofilm formation at the water–lipid interface provide the advantage to retain together the exoenzymes, the lipids, the hydrolysis products, and the cells, thus preventing them from rapid transportation to bulk water. The behavior of cells at the oil–water interface and within the structured biofilm is therefore one important aspect of the degradation of the HOCs in ecosystems.

The adhesion and biofilm formation at the oil–water interface are best studied by microscopic observations. Although a huge number of HOCs degrading strains have been isolated over the past decades, adhesion of these strains to their substrate is rarely documented. Only few authors provided images of bacterial cells that adhered to HOC–water interface using light microscopy, scanning electron microscopy, and confocal laser scanning microscopy (CLSM) [8–13]. Studies of the behavior of bacteria at the HOC–water interface and within biofilms often involve examination and comparison of different strains (wild type versus mutants or different species). This can be only achieved if the HOC–water interfaces generated are compatible with the quantitative measurement of the adhesion or biofilm formation that is hardly the case with spherical or hemispherical droplets of HOC and crystals of irregular shape. To fulfill these requirements, we propose a methodology using thin films of paraffin (15 μm) to generate a substratum to grow biofilms. Ultrathin paraffin films are obtained by slicing solid paraffin with a microtome. Paraffin films pasted to the bottom of a culture dish offer a flat surface and are thin enough to allow in situ observation by CLSM through the bottom of the culture dish avoiding thus disruption of the biofilm structure. Any solid substrate at the experiment temperature and that can be cut by microtome into slices thin enough to allow laser penetration can be employed in place of paraffin. A better definition of imaging can be obtained using a microscope glass slide as solid substratum to paste the paraffin; the biofilm is then observed upside down through a coverslip. This latter approach can also be used for substrates which cannot allow laser penetration.

Determination of the ultrastructure of biofilms that adhered to HOC–water interface is also of great interest. In general, biofilm cells exhibit heterogeneity in their physiology which can be reflected by the presence of different morphotypes. In the case of

biofilm developing on hydrocarbons, intracellular inclusions of storage lipids have been often observed [14]. For instance, biofilm cells of *Marinobacter hydrocarbonoclasticus* SP17 growing on hexadecane accumulate wax ester in their cytoplasm. These storage lipids persist after detachment from the biofilm and provide cells with energy for colonization of unoccupied interfaces [15]. Lipid inclusions can be investigated using CLSM using specific fluorescent dye. However, the ultrastructure of growing cells on HOCs is best studied using transmission electron microscopy (TEM) [1, 16]. The distribution and arrangement of cells containing inclusions within the biofilm can be investigated by TEM provided that the biofilm structure is preserved and the orientation of the biofilm in respect to the HOC surface is traceable. Here, we describe a method where the biofilm is grown in a Petri dish whose bottom has been coated with paraffin. TEM requires sectioning the biofilm included in epoxy resin. Because paraffin would melt during epoxy polymerization at high temperature, the biofilm is first removed from the paraffin surface by embedding it in agarose. Melting of paraffin before complete resin polymerization would result in biofilm disorganization and contamination of the resin with the paraffin which would thereafter hinder polymerization and cutting. Protocols to remove paraffin from samples for TEM experiments exist, but they are rather long and can cause disorganization of the biofilms [17]. Agarose embedding can be bypassed in the case of a substrate compatible with epoxy resin. Then agarose pieces are processed for TEM by paying attention to keep track of the side bearing the biofilm. This procedure enables to obtain images of cross sections of biofilms with identification of the side in contact with the paraffin. Other substrates can be employed for TEM experiments. When incompatible with epoxy resin, they have to be solid at a temperature above the jelling point of agarose in order to prevent mixing between both compounds and biofilm destructuration. The imaging methods were both applied on a marine Gram-negative bacterium, *Marinobacter hydrocarbonoclasticus* SP17, and on a Gram-positive bacterium, *Rhodococcus* sp. NapRu1.

2 Materials

2.1 Observation of Biofilms Grown on Paraffin by CLSM

2.1.1 Strains, Culture Media, and Substratum for Biofilm Growth

1. The protocol described here has been developed with the bacterial strains *M. hydrocarbonoclasticus* SP17 [18] and *Rhodococcus* sp. NapRu1 [3] (**Note 1**).
2. Synthetic seawater (SSW): NaCl 0.2 mol.L^{-1}, KCl 10 mmol.L^{-1}, Tris–HCl 50 mmol.L^{-1} pH 7.8, NH_4Cl 56 mmol.L^{-1}, K_2HPO_4 427 μmol.L^{-1}, $FeSO_4$ 8 μmol.L^{-1}, $MgSO_4$ 65 mmol.L^{-1}, and $CaCl_2$ 13 mmol.L^{-1} (**Note 2**).
3. Sodium lactate 2 mol.L^{-1} adjusted to pH 7.

4. Paraffin Normal Q Path® (VWR International, France) (**Note 3**).
5. Petri dishes (55 and 90 mm diameter) (**Note 4**).
6. Washed glass microscopic slides (25 × 75 mm) (**Note 5**).
7. Ultramicrotome (Leica RM2245, Leica Microsystems, Germany).

2.1.2 CLSM Observation of the Biofilm

1. Fluorescent dye: Syto®9 (L-10316, Life Technologies, France), Syto®61 (S-11343, Life Technologies), BODIPY® (D-3922, Life Technologies) (**Note 6**)
2. Glass coverslips N° 1.5 (Knittel Gläser, Germany)
3. Silicon spacer for coverslip, Press-to-Seal™, 1 mm thick (Invitrogen™, Life Technologies)
4. Inverted confocal laser scanning microscope, Leica TCS SP8 AOBS (Leica Microsystems, Germany) (**Note 7**)
5. Image analysis software IMARIS 7.7.2 software (Bitplane, Switzerland) and Fiji (Fiji.sc/Fiji) (**Note 8**)

2.2 Observation of Biofilms Grown on Paraffin by TEM

See Subheading 2.1.1.

2.2.1 Strains, Culture Media, and Substratum for Biofilm Growth

2.2.2 TEM Observation of the Biofilm

1. Sodium cacodylate buffer 0.15 or 0.1 mol.L^{-1}, pH 7.4 (Sigma-Aldrich, France) (**Note 9**). The pH is adjusted with HCl.
2. Fixative solution (prepared extemporaneously): 2.5% glutaraldehyde (from glutaraldehyde solution Grade I, 25% in H_2O, Sigma-Aldrich) in 0.15 M sodium cacodylate buffer at pH 7.4 or 0.10 M sodium cacodylate buffer at pH 7.4 (**Note 9**).
3. Post-fixative solution (prepared extemporaneously): 1% osmium tetroxide (Electron Microscopy Sciences, France) in 0.15 M sodium cacodylate buffer at pH 7.4 or 0.10 M sodium cacodylate buffer pH 7.4 (accordingly to the fixative solution).
4. 2.5% agarose solution in distilled water (Seakem® LE agarose, Lonza, France). Agarose solution must be maintained at 50°C in an incubator, for example (**Note 10**).
5. Ethanol 99.8% (AnalaR NORMAPUR, VWR International).
6. Fresh or thawed epoxy resin (R1165, low-viscosity resin, medium grade, Agar Scientific, France) (**Note 11**).
7. A filtered solution of 0.05% oolong tea extract (OTE) in distillated water (OTE, Eloïse, France) (**Note 12**).
8. Whatman® grade n°1 cellulose filter paper (Sigma-Aldrich).

9. 2 mL Eppendorf® microcentrifuge tubes (Eppendorf, France) (**Note 13**).
10. Rotator for Eppendorf microcentrifuge tubes.
11. Vacuum desiccator.
12. Diamond knife for ultrathin sectioning (35° angle, DU3520 Diatome 2 mm) and ultramicrotome (UC6, Leica Microsystems, Germany).
13. 200 and 300 mesh copper grids (G200-Cu and G300-Cu, Electron Microscopy Sciences).
14. Flat embedding molds for TEM (70900 silicone clear Electron Microscopy Sciences or 70907 Dykstra blue, Electron Microscopy Sciences) (**Note 14**).
15. HT7700 transmission electron microscope (Hitachi, Japan) equipped with an eight million pixels format CCD camera driven by the image capture engine software AMT version 6.02.

3 Methods

3.1 Observation of Biofilms Grown on Paraffin by CLSM

3.1.1 Pre-culture of Bacteria

1. Inoculate 100 µL of a glycerol stock of bacteria (strain SP17 or NapRu1) stored at −80°C into 10 mL of SSW supplemented with 20 mmol.L^{-1} sodium lactate as a carbon source in a 50 mL tube and incubate overnight at 180 rpm, 30°C.
2. Transfer 100 µL of the culture in 10 mL of SSW plus 20 mmol.L^{-1} sodium lactate and incubate overnight at 180 rpm, 30°C.
3. Centrifuge the overnight culture at 20°C, 10,000*g* for 15 min, wash the cell pellet twice in SSW, and resuspend the cells in SSW at an $OD_{600nm} = 0.01$.

3.1.2 Biofilm Culture

1. Prepare the substratum.
   Melt the paraffin at 65°C and pour it into cassettes for microtome. Let the paraffin cool down on a cool top board to allow solidification. Cut the solid paraffin with a microtome in 15-µm-thick strips. Strips must be transported on ice (e.g., in a Petri dish) then stored at 4°C until use. A thin strip of paraffin is placed on a microscope glass slide within a Petri dish (90 mm) or directly on the bottom of a Petri dish (55 mm). Put the Petri dish in an incubator at 45°C for 10 min to soften the paraffin and make it adhere to the solid support. Before use, decontaminate by exposing the Petri dish to UV light for 5 min.
2. Inoculate the solid support.
   Pour 30 mL of the bacterial suspension ($OD_{600nm} = 0.01$) in the Petri dish (90 mm) containing the thin paraffin strip stuck on a microscopic slide or 5 mL in a Petri dish (55 mm) containing the thin paraffin strip stuck on the bottom. Make sure that

the bacterial suspension covers the whole surface of the solid substratum. Incubate at 30°C without shaking for 5 days (**Note 15**).

3.1.3 CLSM Observation of the Biofilm

1. Biofilm staining with fluorescent markers (**Note 16**).
   Remove the culture medium leaving about 1 mL to keep the biofilm wet. It is important to avoid dehydration to conserve the biofilm structure. Add the selected fluorescent makers to the recommended concentration (see manufacturer's instructions) and incubate at room temperature in dark for 15 min. Here, either Syto®9 (diluted 1:1,000) or the mixture Syto®61 (1:1,000)/BODIPY® (final concentration 0.05 $mg.mL^{-1}$) are used.
2. Biofilm observation.
   Biofilms grown on paraffin thin film deposited on the bottom of the Petri dish are imaged directly, without mounting, through the bottom of the Petri dish with an inverted microscope. This approach is preferred when biofilms are loosely attached to paraffin and mounting would result in loss in the biofilm integrity. However, if a maximal resolution is desired, the biofilm is grown on paraffin film pasted on a microscope slide. Then the biofilm is mounted between the slide and a coverslip with a silicon spacer to avoid compressing it and observed upside down on the inverted microscope. Biofilms mounted or not are observed with a water immersion HCX APO L, 0.80 NA, W U-V-I, Leica 40 X objective with a working distance of 3.3 mm. Adjust the laser excitation and fluorescence signal recuperation according to the characteristic of the markers (absorption and fluorescence emission maxima Syto®9: 482/500 nm, Syto®61: 628/645 nm, BODIPY® : 493/503 nm).
3. Aquire *xy* image or 3D *xyz* stack and process the image series using IMARIS 7.7.2 software and Fiji (Fig. 1).

3.2 Observation of Biofilms Grown on Paraffin by TEM

The basic principles and techniques of electron microscopy for biological applications are described elsewhere [19]. This protocol is designed to visualize more specifically the spatial distribution in the biofilm of cells containing intracytoplasmic inclusions. In order to visualize the extracellular matrix, bacterial capsules, or appendixes, other fixative cocktails and other electron microscopy techniques have to be used [20, 21].

3.2.1 Pre-culture of Bacteria

See Subheading 3.1.1.

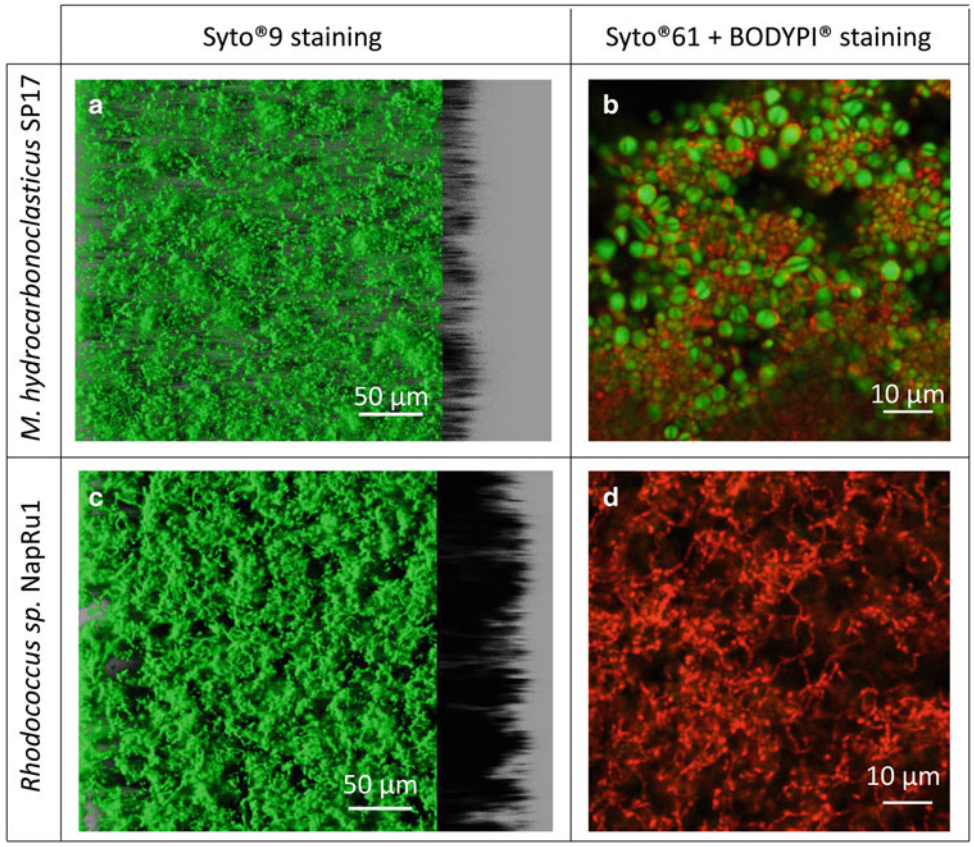

Fig. 1 Observation of paraffin-grown biofilms by CLSM. Biofilm of *M. hydrocarbonoclasticus* SP17 and of *Rhodococcus* sp. NapRu1 stained by Syto®9 observed directly through the bottom of a plastic Petri dish and paraffin strip (optical lens ×40, numerical zoom 1) (**a** and **c**). Biofilm of the same strains stained by the mixture BODIPY®/Syto®61 observed upside down through a microscopic coverslip (optical lens ×40, numerical zoom 4) (**b** and **d**). Syto®9 and Syto®61 are, respectively, green and red nucleic acid stains and BODIPY® green labels neutral and nonpolar lipid components (**Note 6**). Images in (**a**) and (**c**) are three-dimensional projections of biofilm structures reconstructed using the easy 3D function (in blend mode) of the IMARIS 7.7.2 software. The shadow projection on the right is a virtual top–bottom *z* sectioning, which materializes the section of the biofilm and provides thickness information. (**b**) and (**d**) are *xy* images for which the overlay of the two channels and the scale bar were performed using Fiji software. The coffee bean-like structures stained by BODIPY® in (**b**) were not due to paraffin as they were not observed neither in non-inoculated paraffin or in *Rhodococcus* NapRu1 biofilm. They are most likely intracytoplasmic lipid inclusions that were shown abundant in *M. hydrocarbonoclasticus* SP17 growing on alkanes [1]. These intracytoplasmic inclusions swelled within the duration of the experiment (data not shown)

3.2.2 Biofilm Culture

1. Coat the bottom of Petri dishes with paraffin by pouring 15 mL of liquid paraffin heated at 50°C. Let the paraffin solidify by cooling at room temperature.
2. Twenty milliliters of bacterial suspension prepared as described in Subheading 3.1.1 is used to inoculate the paraffin-coated Petri dishes. Make sure that the whole surface of the solid paraffin is covered by the cell suspension. Incubate at 30°C without shaking for 5 days (**Note 15**).

3.2.3 TEM Observation of the Biofilm

To prevent dehydration, the samples must be kept immersed in solution during the all procedure, except for step 3. During the change of solutions, it is therefore recommended to not discard all the solution from the previous step. Addition and removal of solutions must be performed with extreme care to avoid biofilm alteration. Be aware of the toxicity of the compounds used (**Note 17**).

1. Fix the biofilm.
   Remove the culture medium from the Petri dish and pour 20 mL of the fixative solution and incubate at room temperature for 1 h. The cacodylate buffer concentration in fixative solution is 0.15 mol.L^{-1} for *M. hydrocarbonoclasticus* SP17 and 0.10 mol.L^{-1} for *Rhodococcus* sp. NapRu1. At this stage samples can be stored few months in the fixative solution, at 4°C. Wash three times during 5 min with the cacodylate buffer at the corresponding concentration.
2. Post-fix the biofilm.
   Remove the fixative solution, add 20 mL of post-fixative solution, and incubate at room temperature for 1 h. Wash twice for 10 min in distillated water. At this stage samples can be stored few days maximum, at 4°C.
3. Embed the biofilm in agarose (**Note 18**).
   Discard the distilled water and quickly embed the fixed biofilm in 30 mL of a 2.5% agarose solution maintained above its gel point at 50°C (**Note 10**). Tilt the Petri dish and carefully swirl the melted agarose to obtain a homogenous surface. Let the agarose jellify for 1 h at 4°C.

   Detach the agarose gel from the Petri dish wall by moving all around the edges of the dish a thin blade inserted between the agarose and the dish wall. Unmold carefully the agarose by detaching it from the paraffin. The biofilm normally separates easily from the paraffin staying in the agarose layer. Check visually that all the biofilm has been removed from the surface of the paraffin. Transfer the agarose slab, biofilm facing down, in a Petri dish containing the first solution of dehydration (30% ethanol). Make sure that the biofilm bearing face is always immersed in the solution. Cut the agarose slab into big pieces (1 cm^3) with a scalpel and choose pieces where the biofilm seems thicker and homogeneous (**Note 19**).
4. Dehydrate the agarose pieces in ethanol solutions series: 50, 70, 90, and 2 × 100% v/v, 15 min for each step at room temperature. Removal and addition of ethanol solution must be carried out with care to not damage the biofilm. Dehydration procedure can be stopped at the stage of 70% ethanol. Samples are stable for few days maximum, at 4°C.

After dehydration reduce the thickness of the agarose layer above the biofilm to 1 mm and cut small pieces of 3 mm long by 1 mm wide. Transfer each piece in an Eppendorf™ microcentrifuge tube containing 700 µL of a 100% ethanol (third bath).

5. Impregnate successively the dehydrated samples with epoxy resin solutions in ethanol of increasing concentrations: 25 and 33% for 10 min, 50% overnight, then 66 and 75% for 10 min. Impregnations are performed at room temperature under rotary shaking (**Notes 20** and **21**). Then impregnate with pure (100%) fresh resin, for 10 min up to few hours, with the caps of the microcentrifuge tubes opened to let evaporate the last traces of ethanol. Impregnate once more with pure fresh resin overnight on rotary shaking. Finally, impregnate with pure fresh resin with the caps of the microcentrifuge tubes opened in under vacuum to maximize resin penetration (from 10 min to few hours). After dehydration and impregnation, the biofilm bearing face of agarose pieces can be easily recognized by its black coloration.
6. Include samples in epoxy resin.
   Pour a thin layer of pure fresh epoxy resin into TEM molds and allow to polymerize for 2 h at 60°C. Place each impregnated sample, in a mold, on the top of the polymerized epoxy layer in such a way that the biofilm black layer is below and parallel to the bottom of mold. The viscous thin layer of resin in the bottom of the mold will help to stabilize the sample during polymerization (**Note 22**).

   Fill completely the cavity with pure fresh epoxy resin, considering volume reduction during polymerization. Put the mold under vacuum for 10 min up to few hours to maximize resin penetration and eliminate air bubbles. Polymerize at 60°C, during 16–18 h, depending on the resin hardness preferred for the cutting. Resin blocks can be stored *ad vitam æternam* in a temperate and dry place.
7. Make ultrathin sections (60–80 nm) with a diamond knife and an ultramicrotome. Deposit on 200 or 300 mesh copper grids (**Note 23**). Stain each grid with one drop of 0.05% OTE solution for 30 min, washed with four successive drops of distilled water and dried on Whatman grade n°1 cellulose filter paper.
8. Observe in a TEM microscope between 80 and 120 kV (Fig. 2). Resolution increases with the accelerating voltage. Contrast increases when accelerating voltage is decreased and objective aperture is more closed [22].

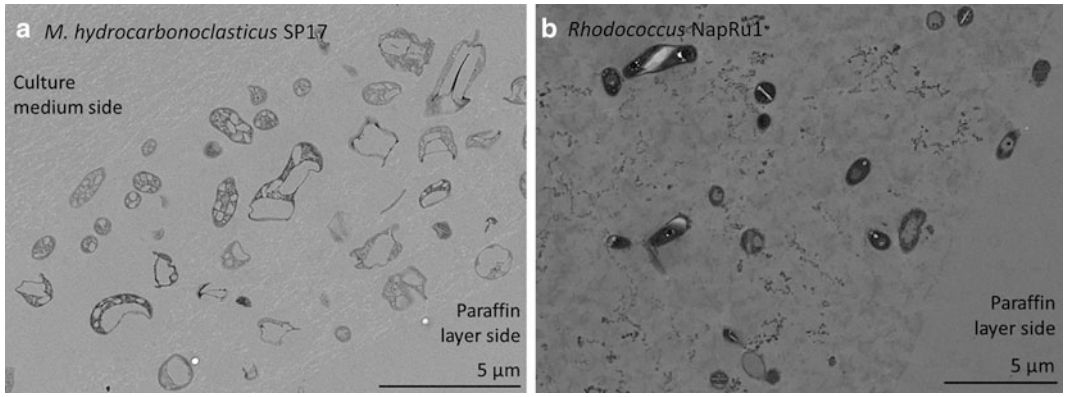

Fig. 2 TEM observation of *M. hydrocarbonoclasticus* SP17 and *Rhodococcus* sp. NapRu1. Only the bottom of the *Rhodococcus* sp. NapRu1 biofilm (i.e., the side in contact with paraffin during growth) is shown as the biofilm is very thick with no stratification within the ultrastructure of cells. Cells in *Rhodococcus* sp. NapRu1 biofilm (**b**) are less numerous and more distant from each other than in biofilm of *M. hydrocarbonoclasticus* SP17 (**a**). In contrast to *Rhodococcus* sp. NapRu1 cells, many cells of *M. hydrocarbonoclasticus* SP17 contain large lipidic inclusions. These observations are in agreement with CLSM imaging (**b**, **d**). The size of the inclusions observed by CSLM as well as by TEM is not homogenous but rather appears evenly distributed over a size continuum

4 Notes

1. Although this method was originally developed for *M. hydrocarbonoclasticus* SP17 and *Rhodococcus* sp. NapRu1, it can be adapted, by using the appropriated culture medium, to any strain that is able to form biofilm on paraffin (or other HOCs; *see* **Note 3**).
2. Any other medium that allows the studied strain to grow, adhere, and form biofilm on HOC can be employed.
3. The method was originally developed for paraffin which is a mixture of alkane molecules containing between 20 and 40 carbon atoms. Its solid state (melting point between 50 and 57°C) enables to slice paraffin into thin strips that make substrata suitable for the growth and the in situ observation by CLSM of oleolytic biofilms. Other substrates, hydrocarbons, or lipids, as far as they are sliceable, can be employed to observe biofilms by CLSM. They must be soft enough to be cut in very thin slices to allow laser penetration. Crystallized (like pure alkanes or aromatic hydrocarbons) or liquid (like unsaturated hydrocarbons and lipids) compounds are not suitable. The biofilms developing on solid substrates which cannot be cut into slices thin enough have to be observed more classically, upside down through a coverslip, as also described here.
4. Classical Petri dishes are employed. Other diameters can be used. If the biofilm is observed directly through the bottom of the dish, specific Petri dishes with a bottom designed for

high-end microscopic analyses have to be used (μ-Dish 50 mm, low, Ibidi) for higher-resolution imaging.

5. Microscopic slides and coverslips are cleaned by acetone/ethanol (50/50 V/V), dried, and stored in sterile conditions in Petri dishes until used.
6. Syto®9 (green fluorescent dye) and Syto®61 (red fluorescent dye) labels give a bright fluorescent signal, upon binding to nucleic acids. The nonpolar BODIPY® (green fluorescent dye) labels neutral and nonpolar lipids. Other fluorescent dyes can be used according to the structures to be observed as previously described [23].
7. The use of an inverted CLSM is required to observe directly biofilms in situ without perturbing their architecture during staining and mounting.
8. Various software can be used as previously described [23].
9. Adapt and control the osmolarity of the buffer for each type of sample.
10. The agarose solution is maintained at the liquid state at a temperature above its gel point but not too high to avoid the paraffin from melting or any damage to the biofilm.
11. This resin is prepared accordingly to the manufacturer's instructions, aliquoted, and stored at −20°C.
12. OTE is a nonhazardous reagent used instead of the hazardous uranyl acetate [24].
13. Smaller microcentrifuge tubes are not suitable for dehydration and next steps.
14. Pay attention to the compatibility between the type of resin and the mold materials.
15. Time and temperature depend on the strain cultivated and on the conditions studied. If incubation is very long, prevent the evaporation by humidifying the atmosphere.
16. Wear a lab coat and gloves to manipulate fluorescent markers. Use specific disposal bins. Read the material safety data sheet (MSDS) of the products.
17. Work under a fume hood wearing lab coat, gloves, and glasses. Use specific disposal bins. Read the MSDS of the products before use.
18. The method was originally developed for paraffin wax that is incompatible with epoxy resin. Other substrates can be employed for biofilm growth; their compatibility with the epoxy resin has to be verified. If the substrate is compatible with the epoxy resin, this step is not necessary. If not, the method has to be implemented as for paraffin which requires that the substrate is solid at a temperature above the gel point of agarose in order to prevent mixing between both compounds and biofilm destructuration.

19. Small pieces increase the "surface/volume" ratio and thus the penetration of reagents (solvents and resins). This is important for Gram-positive strains that are particularly difficult to impregnate. Furthermore, it saves reagents by transferring samples in smaller containers
20. While facilitating the early stages of impregnation, propylene oxide traditionally employed is not used in this protocol. It is a hazardous product (boiling point at 34°C) that reacts with many plastics. Instead, ethanol is used for mixed baths with epoxy resin although they mix less easily.
21. Number and length of the impregnation steps are adjusted to our models and our epoxy resin. They can be adapted in case of troubles during the sample cutting (block too soft to an ultrathin cut, dissolution of the ultrathin section in the water tank of the knife) or during TEM observations (holes visible in the ultrathin section). Other standardized protocols describing impregnation steps with other resins can be found [17].
22. When placing the samples into the cavities of the molds, it is possible to reference them by adding a small paper with a printed code (pen ink diffuses in the resin) on the opposite side of the sample.
23. Use the lowest possible mesh copper grids to maximize the observation area (i.e., 200 mesh copper grids). Use 300 mesh copper grids for unstable sections under electron beam.

Acknowledgment

We thank the MIMA2 platform (www.jouy.inra.fr/mima2) for its expertise and access to microscopy equipments and Michael Trichet (Institut de Biologie Paris-Seine, Université P. et M. Curie) for his advices and comments for TEM. We gratefully acknowledge the French National Research Agency, project AD'HOC ANR-11-BSV7-0002, for financial support.

References

1. Klein B, Grossi V, Bouriat P, Goulas P, Grimaud R (2008) Cytoplasmic wax ester accumulation during biofilm-driven substrate assimilation at the alkane–water interface by *Marinobacter hydrocarbonoclasticus* SP17. Res Microbiol 159(2):137–144
2. Tanaka D, Takashima M, Mizuta A, Tanaka S, Sakatoku A, Nishikawa A, Osawa T, Noguchi M, Aizawa SI, Nakamura S (2010) *Acinetobacter* sp. Ud-4 efficiently degrades both edible and mineral oils: isolation and characterization. Curr Microbiol 60:203–209
3. Bouchez-Naïtali M, Rakatozafy H, Marchal R, Leveau JY, Vandecasteele JP (1999) Diversity of bacterial strains degrading hexadecane in relation to the mode of substrate uptake. J Appl Microbiol 86(3):421–428
4. Grimaud R (2010) Biofilm development at interfaces between hydrophobic organic compounds and water. In: Timmis KN, McGenity T, de Lorenzo V, van der Meer JR (eds) Handbook of hydrocarbons and lipid microbiology. Springer, Berlin, pp 1491–1499

5. Mounier J, Camus A, Mitteau I, Vaysse PJ, Goulas P, Grimaud R, Sivadon P (2014) The marine bacterium *Marinobacter hydrocarbonoclasticus* SP17 degrades a wide range of lipids and hydrocarbons through the formation of oleolytic biofilms with distinct gene expression profiles. FEMS Microbiol Ecol 90:816–831
6. Harms H, Smith KEC, Wick LY (2010) Introduction: problems of hydrophobicity/bioavailability. In: Timmis KN, McGenity T, de Lorenzo V, van der Meer JR (eds) Handbook of hydrocarbons and lipid microbiology. Springer, Berlin, pp 1437–1450
7. Heipieper HJ, Cornelissen S, Pepi M (2010) Surface properties and cellular energetics of bacteria in response to the presence of hydrocarbons. In: Timmis KN, McGenity T, de Lorenzo V, van der Meer JR (eds) Handbook of hydrocarbons and lipid microbiology. Springer, Berlin, pp 1615–1624
8. Whyte LG, Slagman SJ, Pietrantonio F, Bourbonnière L, Koval SF, Lawrence JR, Inniss WE, Greer CW (1999) Physiological adaptations involved in alkane assimilation at a low temperature by Rhodococcus sp. strain Q15. Appl Environ Microbiol 65:2961–2968
9. Eriksson M, Dalhammar G, Mohn WW (2002) Bacterial growth and biofilm production on pyrene. FEMS Microbiol Ecol 40:21–27
10. Wick LY, De Munain AR, Springael D, Harms H (2002) Responses of *Mycobacterium* sp. LB501T to the low bioavailability of solid anthracene. Appl Microbiol Biotechnol 58:378–385
11. Rodrigues AC, Brito AG, Wuertz S, Melo LF (2005) Fluorene and phenanthrene uptake by *Pseudomonas putida* ATCC 17514: kinetics and physiological aspects. Biotechnol Bioeng 90:281–289
12. Macedo AJ, Kuhlicke U, Neu TR, Timmis KN, Abraham WR (2005) Three stages of a biofilm community developing at the liquid-liquid interface between polychlorinated biphenyls and water. Appl Environ Microbiol 71:7301–7309
13. Wouters K, Maes E, Spitz JA, Roeffaers MBJ, Wattiau P, Hofkens J, Springael DA (2010) A non-invasive fluorescent staining procedure allows confocal laser scanning microscopy based imaging of *Mycobacterium* in multispecies biofilms colonizing and degrading polycyclic aromatic hydrocarbons. J Microbiol Methods 83:317–325
14. Manilla-Perez E, Reers C, Baumgart M, Hetzler S, Reichelt R, Malkus U, Kalscheuer R, Waltermann M, Steinbuchel A (2010) Analysis of lipid export in hydrocarbonoclastic bacteria of the Genus *Alcanivorax*: identification of lipid export-negative mutants of *Alcanivorax borkumensis* SK2 and *Alcanivorax jadensis* T9. J Bacteriol 192:643–656
15. Vaysse PJ, Sivadon P, Goulas P, Grimaud R (2011) Cells dispersed from Marinobacter hydrocarbonoclasticus SP17 biofilm exhibit a specific protein profile associated with a higher ability to reinitiate biofilm development at the hexadecane-water interface. Environ Microbiol 13:737–746
16. Kalscheuer R, Stöveken T, Malkus U, Reichelt R, Golyshin PN, Sabirova JS, Ferrer M, Timmis KN, Steinbüchel A (2007) Analysis of storage lipid accumulation in *Alcanivorax borkumensis*: evidence for alternative triacylglycerol biosynthesis routes in bacteria. J Bacteriol 189 (3):918–928
17. Graham L, Orenstein JM (2007) Processing tissue and cells for transmission electron microscopy in diagnostic pathology and research. Nat Protoc 2(10):2439–2450
18. Gauthier MJ, Lafay B, Christen R, Fernandez L, Acquaviva M, Bonin P, Bertrand JC (1992) *Marinobacter hydrocarbonoclasticus* gen. nov., sp. nov., a new, extremely halotolerant, hydrocarbon-degrading marine bacterium. Int J Syst Bacteriol 42:568–576
19. Hayat MA (2000) Principles and techniques of electron microscopy - biological applications. Cambridge University Press, Cambridge
20. Erlandsen SL, Kristich CJ, Dunny GM, Wells CL (2004) High-resolution visualization of the microbial glycocalyx with low-voltage scanning electron microscopy: dependence on cationic dyes. J Histochem Cytochem 52:1427–1435
21. Hammerschmidt S, Wolff S, Hocke A, Rosseau S, Müller E, Rohde M (2005) Illustration of pneumococcal polysaccharide capsule during adherence and invasion of epithelial cells. Infect Immun 73(8):4653–4667
22. Dykstra MJ, Reuss LE (2003) Biological electron microscopy: theory, techniques, and troubleshooting, 2nd edn. Kluwer Academic/ Plenum, New York
23. Bridier A, Dubois-Brissonnet F, Briandet R (2014) Methods for biofilms constituents and turnover, Section 1. Destructive and nondestructive methods. In: Dobretsov S, Thomason JC, Williams DN (eds) Biofouling methods. Wiley, Oxford, pp 139–152
24. Carpentier A, Abreu S, Trichet M, Satiat-Jeunemaitre BJ (2012) Microwaves and tea: new tools to process plant tissue for transmission electron microscopy. J Microsc 247(1):94–105

Bacteria-Mineral Colloid Interactions in Biofilms: An Ultrastructural and Microanalytical Approach

Heinrich Lünsdorf

Abstract

Simple reproducible experimental set-ups are described to study initial growth and interactions of bacteria with clay colloids and soil nanoparticles or with dissolved metal ions as primordial biofilms. These bacteria-nanoparticle constructs, exemplified by so-called clay hutches, are accessible to ultrastructural and microanalytical electron microscopical analysis. By this, the spatial arrangements and in part the physiological state of the involved autochthonous bacteria can be studied, leading to an estimate of the mineral-organic nutritional sphere the bacteria need for growth. It further leads to an entry to additional chemical, microbial and macromolecular traits of experimental follow-ups to analyse the mineral-organic chemistry, to isolate pollutant-adapted bacteria and to get information on the complex community structure of this kind of biofilms.

Keywords: Electron energy loss spectroscopy (EELS), 'In situ/in vitro' biofilms

1 Introduction

Clay minerals and other nanoparticles are known constituents of most soils and in the case of clay minerals encompass the smallest size fraction of clastic sediments, i.e. < 2 μm [1]. Because of their known high specific surface from 50 and more than 130 m^2/g [2, 3] and their high surface charge, they are broadly used for diverse sorption needs and applications in different industries. For instance, bentonite is widely used in purification of mineral oils, mineral fats and waxes or in water protection as sorbent of oil, floating on the water [4].

'Clay hutches' are an exemplifying term to describe a homogeneous arrangement of soil colloids and indigenous microorganisms attached to a hydrophobic surface of a suitable support (substratum). Originally, these associations of bacteria with soil colloids were grown from polychlorinated biphenyl (PCB)-contaminated soils as early biofilms [5, 6]. As such, they represent a closer, more detailed view to the general interaction and degradation of PCBs

T.J. McGenity et al. (eds.), *Hydrocarbon and Lipid Microbiology Protocols*, Springer Protocols Handbooks (2016) 85–101,
DOI 10.1007/8623_2015_62, © Springer-Verlag Berlin Heidelberg 2015, Published online: 04 April 2015

with soil constituents as this has been observed, for instance, in river sediments [7]. Ultrastructural analysis revealed the existence of particulate clusters of colloidal constituents associated with bacteria which were built up from a bacterial extracellular matrix, i.e. extracellular polymeric substances (EPS) and clay leaflets, occasionally accompanied by ironoxohydroxide colloids (Fig. 1). These studies showed that the experimental set-up is applicable to different analytical traits to analyse soil-microbe interaction with organic pollutants, i.e. polychlorinated biphenyls or polycyclic aromatic hydrocarbons (PAHs) [8].

In general, a sterile support with low surface energy (Permanox® slides, Melinex® stripes; see sketch of the construction in 'Notes') can be exposed to a natural environment, either submerged within the water column or placed on the sediment floor of a natural pond. Even when stuck into water-saturated soil, these supports should be good tools and opportunities to breed biofilms. Biofilms can be regarded as 'microbial landscapes' [9], grown autochthonously under natural conditions during a distinct period of time within a specific unique environmental milieu. Specific interactions such as metal cation adsorption by EPS can be monitored and studied as a trait of initial mineralogenesis.

The advantage of this simple experimental approach, i.e. a sterile, strict hydrophobic support either swimming on the water surface or submerged within the water of a pond, running water of a creek or buried into the soil, is based on its 'close-to-nature' character. It is the purpose of this methodological description of biofilm formation from the initial state to final confluent growth, thus to get high-resolution ultrastructural information of the intrinsic interactions between autochthonous bacteria with soil matrix colloids.

Hydrophobic surfaces, characterized by low surface energy, show short-term settlement and biofilm growth in contrast to high surface energies of hydrophilic glass slides. Nevertheless, floating, submerged or buried slides used as hydrophobic supports are to some extent selective for planktonic soil bacteria, which has to be considered.

The clarified bulk water of a before homogeneously and intensely mixed soil suspension in the experimental set-up contains the free porewater of soil, inhabited by planktonic, free-living bacteria and protozoa. It thus includes all autochthonous bacteria and further ingredients similarly needed for bacterial growth in soil. Thus, sterile floating supports are open for bacterial settlement and surface-associated growth. Since bacteria as well as clay phyllosilicates and other soil colloids are statistically distributed within the water body, multiples of swimming supports can be located on the water surface, suitable to get biofilms in parallel to characterize diverse state-of-the-art analytical traits [10]. As such, biofilms,

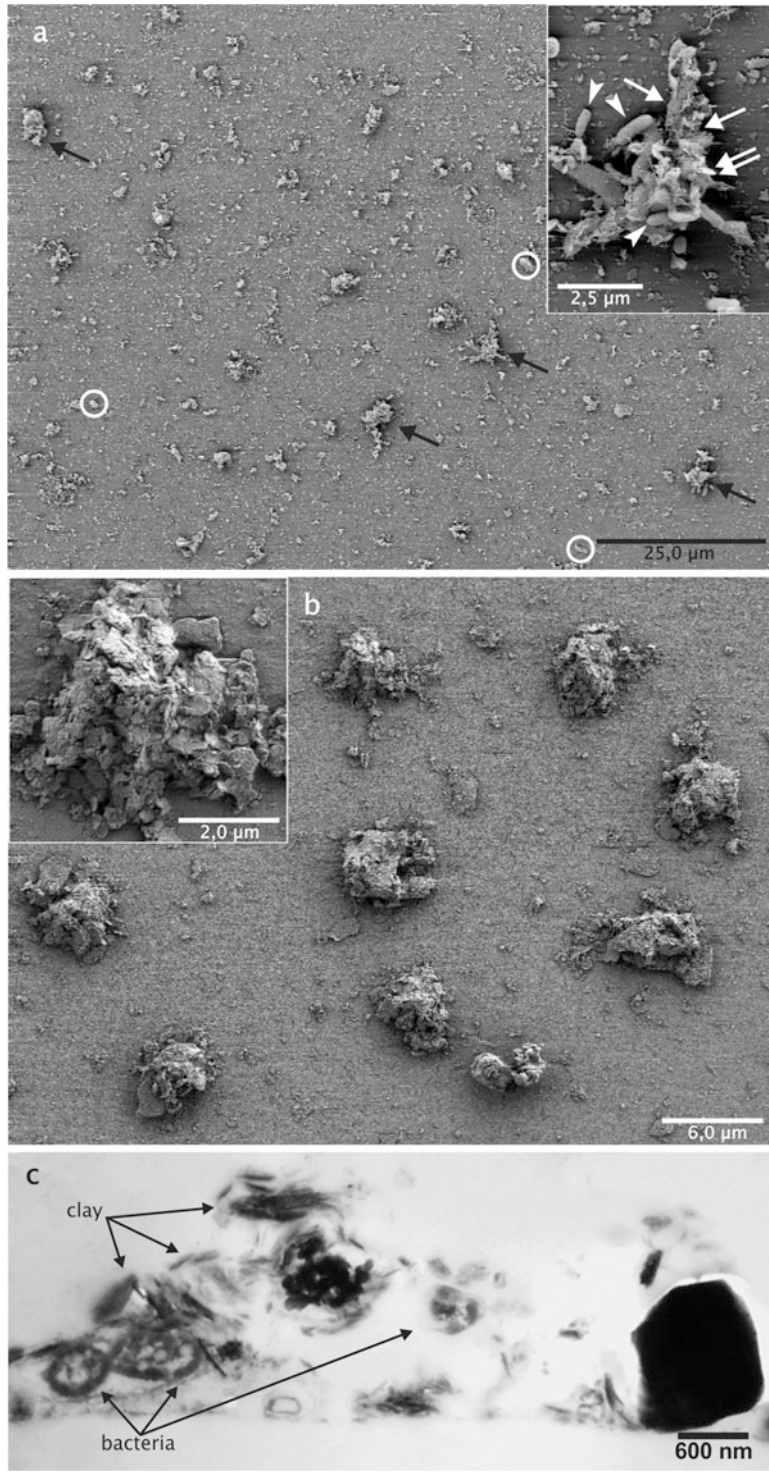

Fig. 1 Scanning micrographs of 'clay hutches'. (**a**) Initial state of 'clay hutch' formation; few bacteria are docked to the substratum (*circles*). 'Clay hutches' are indicated by *arrows*. A detailed view (*inset*) shows bacteria of different cell size (*white arrowheads*), which appear associated with a filigree EPS network (*white arrows*); only a few clay leaflets are visible (*double arrows*). (**b**) Compact 'clay hutches' after 14 days of exposition. No bacteria are visible in the periphery of the 'clay hutches'; here, a thin layer of particulate matter of different size covers the substratum background. *Inset* reveals the tight package of leaflets and compactness of a 'clay hutch'. (**c**) Corresponding ultrathin section, cut normally through a 'clay hutch', which shows the arrangement of bacteria and clay leaflets

highly similar and homogeneous in quality, can be analysed at the level of (a) their ultrastructure by light and electron microscopy; (b) elemental analysis by energy-dispersive X-ray (EDX) and/or electron energy loss spectroscopic analysis (EELS, ESI); (c) environmental nucleic acid analysis by SCCP, T-RFLP, DGGE and/or other macromolecular techniques [11–13]; and (d) finally isolation of bacteria, which are able to grow with hydrocarbons and other lipophilic substrates/pollutants.

In this chapter, I describe the making of 'in situ/in vitro' biofilm preparates for ultrastructure and microanalysis which describe microbial life in its close-to-natural context.

Though the experimental set-up for 'clay hutch' formation (and similarly the submerged hydrophobic supports in bulk water, e.g. of a pond, creek) is rather simple, it is not an easy task to proceed with the analysis of these microbe-soil colloid interactions on a micro- or even nanoscale. It would thus be of interest to study and understand the basics of communications, possibly by 'quorum sensing' of many bacteria or crosstalk at a drastic smaller level of only few, i.e. three to five, bacteria, within a settlement focus when attached to the hydrophobic substratum.

The question of how bacteria sense the specificity and quality of cargo from soil colloids in the water body as relevant for nutrition is of general interest in understanding bacterial life in context of the soil matrix. There is enough substantial reason for speculation but with the aid of optical tweezers or micromanipulators and suitable handling of individual 'clay hutches' with microcapillaries and/or bacterial consortia, this could be a further goal to study bacterial interactions, supplementing the primary view of light and electron microscopy.

2 Materials

2.1 General Material

250 ml Erlenmeyer flasks or glass Petri dishes of 5 cm height and of 10–12 cm diameter (www.neolab.de)

500 ml sterile glass beaker (www.neolab.de)

Sterile Teflon stirring rod (www.neolab.de)

Magnetic stirrer (www.neolab.de)

2 × 2 mm sieve for soil sieving (www.neolab.de)

Spoon or spatula (www.neolab.de)

Melinex® foil, sterile Permanox® slides (26 × 76 mm; www.thermofisher.com.au)

For submerged exposure of slides:

Suitable inert plastic ware (e.g. polypropylene; www.neolab.de)

Sterile 6.0–7.0 cm in diameter and 5.0 cm in height rubber plugs, used for clamping/fixing Permanox® slides for submerged substratum exposition (www.neolab.de)

Gelatine capsules, flat embedding moulds, forceps (for grid handling), Ni and/or Cu electron microscopic grids, 300 and 700 mesh size, thin bar (http://scienceservices.eu)

2.2 Reagents

Fixation buffer (1% (v/v) glutaraldehyde – 10 mM Hepes, pH 7.0)

Acidic, cationic ThO_2 colloid (0.04% (w/v) ThO_2 – 100 mM Na acetate, pH 3.0 (*see* **Note 1**))

Acidic washing buffer (100 mM Na acetate, pH 3.0)

Washing buffer 1 (20 mM Hepes, pH 7.0)

Washing buffer 2 (100 mM Na cacodylate, pH 7.2)

5% (w/v) aqueous osmium tetroxide

Dried acetone (over $CuSO_4$)

All chemicals are p.a. grade from Merck, Darmstadt, Germany (www.merck.de)

Spurr-epoxy resin (for embedment) (http://scienceservices.eu)

2.3 Microscopes (see Note 2)

Inverse light microscope

Scanning electron microscope (= SEM) (electron microscopic laboratory)

In-column energy filter transmission electron microscope (= EF−TEM), post-column filter with general TEM (electron microscopic laboratory) (*see* **Note 3**)

3 Methods

3.1 Soil Sample Preparation

Site material of interest should be rather fresh. It should be sufficiently dried and rough sieving at 2 mm mesh size is appropriate to get rid of plant materials and bigger sand granules. In order to get homogenized and mixed soil, samples should be additionally passed through a sieve of 0.5–1.0 mm mesh size. As such, an aliquot should be frozen and stored at −80°C for additional stock for total DNA extraction, needed for microbial community analysis. Doing so, the fraction of microorganisms, capable in soil-colloid hydrocarbon interactions and biofilm production, can be related to the total soilborne microbial community. Details of the soil type and soil horizon of the sampling site should be addressed. Treatment of the soil sample as is described below will lead to homogeneous starting conditions of statistical relevance, necessary for scaling up and/or multiplicity.

3.1.1 Preparation of the Soil Slurry

Four to six aliquots per type of soil (i.e. about 20 g per Erlenmeyer flask or glass Petri dish, suspended within 10–20 ml of sterile reverse osmosis purified water) are homogeneously mixed with the aid of a magnetic stirring bar at 50–150 rpm for 15–30 min at ambient temperature. One such aliquot of suspended soil should be sterilized by three to four heating-cooling cycles in an autoclave. This sterile soil sample is used to check for abiotic, physico-chemical interactions of the soil colloids with the substratum (when doing submerged experiment in resting or floating natural waters, this control cannot be done). The 'soil assays' are used as doubles or triplicates in Erlenmeyer flasks or adequate glass Petri dishes.

3.1.2 Handling of Permanox® Slides and Substratum-Grown Biofilms

Start the experiment by gentle floating sterile Permanox® slides on top of the water surface. This should only be done when the turbid bulk water has clarified after a resting period of 24 h at ambient temperature. In general, it is useful to only put in one slide per Erlenmeyer flask for a one-step experiment but – depending on the diameter of the glass Petri dishes – two or more may be layered on the water surface. This will be useful if samples have to be taken at different states of biofilm development. Slides have to be placed within an area of clean water surface, free from floating fine residual root or plant debris from the soil matrix which has passed soil sample sieving. If necessary, suck them off with a sterile vacuum pipette under a clean bench.

As such, biofilm growth of autochthonous, planktonic bacteria (and fungi) can start and a corresponding microbial community will be established within 7–14 days at ambient temperature in the laboratory without direct artificial or sunlight illumination. Development of 'clay hutch' biofilms can be roughly judged by inspection with the naked eye and is visible (under oblique illumination) as a faint turbid layer on the floating substratum surface. (Caution before picking up the biofilm-grown slide with a sterile forceps: if meanwhile neustonic biofilm has developed at the water-air interface in the vicinity of the floating slides or further plant-/root-derived debris or other aggregates, recognizable by eye, have accumulated, these have to be carefully sucked off first with a vacuum pipette in order not to contaminate the sample by partially flipping over and superimpose to the substratum-bound biofilms.) It is not recommended to intermittently take out the slides for light microscopical examination of unsterile handling and surface pressure impact or drying of the biofilm surface.

Sufficient biofilm substrata used for chemical, especially for microbial and community analysis, are gently picked up from the water surface with the aid of a suitable sterile forceps. Adhesive bulk water is shortly drained off from the short edge of the Permanox® slide with filter paper before they are frozen in liquid nitrogen for storage at −20°C until use for non-ultrastructural analysis

(those biofilms used for ultrastructural/elemental analysis never should be frozen and stored because this will lead to severe damage to ultrastructural details.)

3.2 Sample Handling and Preparation for Ultrastructural Analysis

3.2.1 Precheck of Biofilms

For ultrastructural analysis by either transmission (TEM) or scanning electron microscopy (SEM) (*see* Fig. 1), a floating Permanox® slide is picked up with a sterile forceps from the water surface, drained softly over the short edge in contact with filter paper and is roughly cleaned on its 'ungrown' backside with soft cleaning household paper to get rid of dust and other contaminants. As such, the slide is mounted on an inverse light microscope stage with its 'biofilm side' up and a few drops of clarified bulk water are added to prevent the biofilm to fall dry. Quality and dimensions of biofilm growth, i.e. development and density of 'clay hutches', can be observed with x20 to x40 (x63) objective lens at phase contrast-imaging conditions. Thus, the actual state can be observed and documented with the aid of a CCD camera. This light microscopic analysis will accurately show the unique growth and distribution of 'clay hutches' and/or the degree of biofilm heterogeneity or cluster formation by inhomogeneous growth. Further, a rough estimate will be given at x400 magnification on the amount and frequency of individual bacteria, not associated with soil aggregates.

3.2.2 Fixation, Dehydration, Embedment and Sectioning of Biofilms

Next, aliquots of the biofilm-grown substratum are cut as stripes, 1 × 2.6 cm in size, for electron microscopic analysis and are immediately transferred to a suitable Petri dish, partially filled with 20–25 ml fixation buffer, and let them float with biofilm side down. Glutaraldehyde fixation is performed at least for 20 min at ambient temperature and samples are stored and kept floating at 4°C until further processing up to 1 week.

For general embedding and ultrathin sectioning, subdivide the fixed biofilm in equal parts and process one half (as it is described in detail by [14]). For ultrastructural analysis, postfixation with 1% (w/v) OsO_4 – 100 mM cacodylate, pH 7.4 – is done for 30–60 min at ambient temperature after the sample has been washed for 10 min at ambient temperature in washing buffer 2. (Postfixation with osmium tetroxide is omitted if elemental analysis is done. Then, samples are washed twice in washing buffer 1 for 10 min at ambient temperature after glutaraldehyde fixation.) They are then dehydrated in an aqueous acetone series at ambient temperature. For this, submerge the Permanox® cutoffs with the biofilm side up in aqueous acetone in a glass dish (10%/30 min; 30%/10 min; 50%/10 min; 70%/10 min), stain with 1% (w/v) uranyl acetate in 70% acetone for 20 min at ambient temperature (this staining step is omitted when elemental analysis is done) and complete dehydration (100%/2 × 10 min). Infiltrate in an acetone-epoxy resin mixture (2 parts acetone + 1 part resin/30 min; 1 part acetone + 2 parts resin/60 min), followed by pure resin (2 × 30 min;

12 h/overnight). After transfer of samples to gelatine capsules or flat embedding moulds, prefilled with resin monomer, samples are degassed for some time with a rotary pump linked to a suitable glass exsiccator at residual pressure so air bubbles can come up smoothly from the resin, looking like foam, and care is taken by pressure handling not to make the resin overrun the gelatine capsule. The glass exsiccator is gently aerated and samples are polymerized at 70°C for 16 h in a laboratory oven/incubator.

General information of fixation of biological samples and resin embedment can be found in [14–17].

For conventional TEM, ultrathin sections (70–90 nm, also recognized as silver to golden shining sections) are cut with a diamond knife (*see* **Note 4**) with an Ultracut E® ultramicrotome (Leica, Austria). Sections, picked up with 300 mesh Cu-hexagonal Formvar-coated grids, are post-stained with aqueous uranyl acetate (4% (w/v); 5 min at ambient temperature) and lead citrate (0.3% (w/v): 5 min at ambient temperature) [18] and are analysed with an EF-TEM (CEM 902 or Libra 120; Zeiss, Oberkochen, Germany).

3.2.3 Sample Preparation for SEM

For SEM analysis process, use the second half of the biofilm sample, as is described in detail by [14].

In short, biofilm-grown Permanox® stripes, dehydrated in acetone, are transferred to a pressure chamber of a critical point drying unit (CPD030; Bal-Tec, Liechtenstein) filled with acetone at 10°C. After three to four washes with liquid CO_2 for each 10 min of equilibration time, raise temperature to 40°C and pressure to finally 80 bars. Within a period of 30 min, reduce pressure at constant temperature (40°C) to normal atmospheric. Mount the dried biofilms on aluminium stubs. In a sputter-coat unit (SCU040; Balzer Union, Liechtenstein), they then are coated with gold in an argon atmosphere (0.06 mbar; target distance, 10 cm; sputter current, 45 mA) for 54 s.

3.3 Submerged Exposition of Substratum in the Water Column

Similar to soil-derived biofilm growth on floating Permanox® slides on top of a water column which experimentally is defined by soil constituents, biofilm development and growth from bulk water, either from resting water of a pond or streaming water from a creek, are of general interest to study interactions of autochthonous microorganisms with solved or nanoparticulate minerals. Biofilm growth on submerged substrata with low surface energy can be studied over time, and thus, initial states of mineralogenesis, catalysed or initialized by bacterial impact, can be observed. These experiments to some extent simulate development of biofilms as these will grow on many submerged solid surfaces, such as inorganic stones or organic plant material, such as wood or leaves.

To do such experiments, submerged sterile Permanox® slides, fixed to 5.0 cm high rubber plugs (6.0–7.0 cm in diameter;

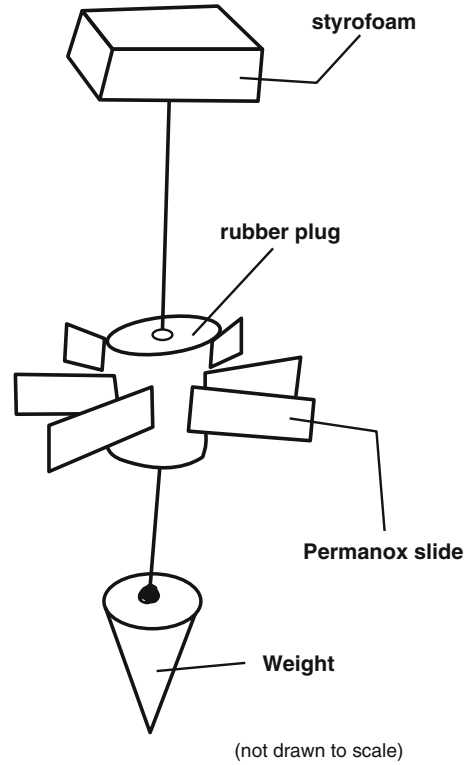

Fig. 2 Construction of rubber plug-based slide holdfast for submerged biofilm acquisition (Sketch). In order to position and fasten the slides, about 10 mm deep cuts are set into the rubber plug to a length of 30 mm by a short scalpellum

see Fig. 2), are exposed to different heights under the water surface in a resting pond or lake or laid down on the floor of a creek. Attention should be paid to keep these constructions in a stable position, not to get lost during the exposure period. Multiple slides should be inserted by their short edges to a rubber plug at sufficient distance, i.e. 10–15 mm, in order to prevent 'functional shading'. This way, a series of time points can be set and substrata with adhering biofilms can be sampled sequentially and fixed as is described for the 'clay hutch' set-up above.

3.4 Labelling of Acidic Groups in Biomatrices by Cationic ThO_2 Nanoparticles

3.4.1 Synthesis of Hydrous Cationic Thorium Dioxide Nanocolloids

According to [19], take 10 g of thorium nitrate hydrate (MM 480.06; Fluka, Switzerland) and dissolve in 50 ml water (distilled or reverse-osmophorese water) at ambient temperature to get a 20% (w/v) solution of pH 2.4 in a flask.

To 20 ml of this solution in a 250 ml round-bottomed flask, 0.4 ml aliquots of 25% (w/v) ammonium hydroxide are added dropwise under continuous stirring until pH 3.0 is reached and the solution turns slightly turbid.

Add more 0.4 ml NH_4OH so at pH 4.0, the solution turns intense turbid; further 0.4 ml NH_4OH are added to completely precipitate thorium hydroxide at pH 11.0.

In a flat funnel laid with filter paper (grade 3 hw; Sartorius, Göttingen, Germany), filter the milky suspension under slight vacuum.

Residual electrolytes are removed completely by washing with 100–150 ml distilled/reverse-osmophorese water until no ammonia is smelled.

Transfer thorium hydroxide paste with the aid of a spatula into a 100 ml Erlenmeyer flask and with 5–8 ml wash and add residual precipitate to the bulk.

Stir the slurry hydroxide and bring it to boil under reflux for 5 min (with the aid of a 40 cm Dimroth condenser).

Then, add 0.2 ml of 20% (w/v) thorium nitrate solution and continue to boil under reflux. Repeat this reflux boiling every time 0.2 ml thorium nitrate solution has been added.

Turbidity clarifies when two times 0.2 ml thorium nitrate has been added.

A final addition of 0.2 ml thorium nitrate did not increase turbidity and this is the last step in colloid peptization (1.2–1.6 ml of thorium nitrate on the whole will be sufficient), leaving the solution slightly opalescent at roughly 50% (w/v) colloidal ThO_2 solution at pH 2.0–2.5.

3.4.2 Acidic Group Labelling with ThO_2 Nanocolloids

For ultrastructural analysis of acidic extracellular polymeric substances (EPS), float a suitable cut-off segment of the Permanox® slide face down on acidic washing buffer in a small Petri dish and wash twice for 10 min at ambient temperature. Transfer to 0.04% (w/v) cationic colloidal thorium dioxide and let float and incubate for 30–60 min at ambient temperature or at 4°C overnight, to stain acidic EPS residues (for detail, *see* [19]). Next, float-wash the biofilm face down or submerge twice on 10 mM Na acetate, pH 3.0, as is described above. Start sample dehydration in an acetone-water series, according to [14].

3.5 Electron Energy Loss Spectroscopy

The presence of inorganic soil nanoaggregates as sorbents of organic substances and/or the formation of 'clay hutches' as active on growth on a low surface energy substratum gives the opportunity to study the interplay of soilborne indigenous bacteria with soil-derived colloids. These interactions, though on a static level in the fixed and embedded state, can be analysed by electron energy loss spectroscopy (EELS), applied in the (1) EELS mode to acquire spectra of an area/structure of interest or (2) in the electron spectroscopic imaging mode (ESI), which leads to elemental maps with high spatial resolution of key elements, such as Si, O, Al, Fe, etc. EELS is a useful means to get a nanometre-scaled view to individual bacteria-clay/nanoparticle associates (*see* Fig. 3).

30 to 40 nm ultrathin sections of unstained embedded biofilms are picked up with 700 mesh bare grids and are observed natively without post-staining. Either 'zero-loss elastic bright-field' images or 'inelastic images' at a corresponding electron energy loss of the element of interest are obtained by EF-TEM [20]. The specific settings for ESI recording in order to reveal high resolution of these spatial arrangements are described by [14, 19, 20]. Tracing cationic thorium dioxide colloids by ESI here outlines the distribution and local densities of negative charges of clay, EPS and the cell surfaces, directly observed at and linked to the macromolecular level.

Besides element mapping with ESI, electron energy loss spectra (EELS) can be acquired from dedicated areas of interest. This reveals insight into the chemistry and spatial coordination of the element of interest and shows EELS features next to the ionization edge (energy loss near edge structures; ELNES) as a fingerprint of the local chemistry, which can be used for comparison and differentiation of different 'clay hutches' (*see* **Note 3**).

3.5.1 Practice of EELS Acquisition with an 'In-Column' EF-TEM

As a rough guide to EF-TEM practice, the following steps should be addressed. In order to get suitable EEL spectra and elemental maps (electron spectroscopic imaging; ESI), it is a prerequisite to have the electron microscope perfectly adjusted according to the manual's instructions.

First, an unstained 30–40 nm ultrathin section, picked up by a 400 or 700 mesh 'thin bar' grid, is introduced into the EF-TEM. At low magnification (e.g. x3,000 to x5,000) and low beam intensities (beam current, 1–2 μA; illumination aperture, 80–200 mrad) to minimize beam damage, the sample is examined for 'biofilm features of interest' suitable. Generally, an electron dense motif (in the 'image mode') is centred and Gaussian-focused on the screen with the objective aperture, e.g. 60 μm in size, set precisely before (in the 'diffraction mode'). The image has been checked to be free/corrected from astigmatism. In the 'image mode', the 'spectrometer entrance aperture', which fits best to the motif's dimensions, is selected and centred to the 'index point' on the screen (this in general is the central small hole in small viewing screen of the EF-TEM). Then, the 'spectrum mode' is selected and the 'energy-selecting slit aperture' is removed by anticlockwise turns to the stop. The EEL spectrum now should be visible and is set to a suitable 'spectrum magnification', e.g. x100. It then has to be centred with its highest intensity edge, i.e. the 'zero-loss peak', to the 'index point' by the aid of x-y (spectrum shifting) knobs. Now, the CCD camera is started by the integrated application software for EEL spectrum registration. (See the 'EELS registration software manual', e.g. iTEM software

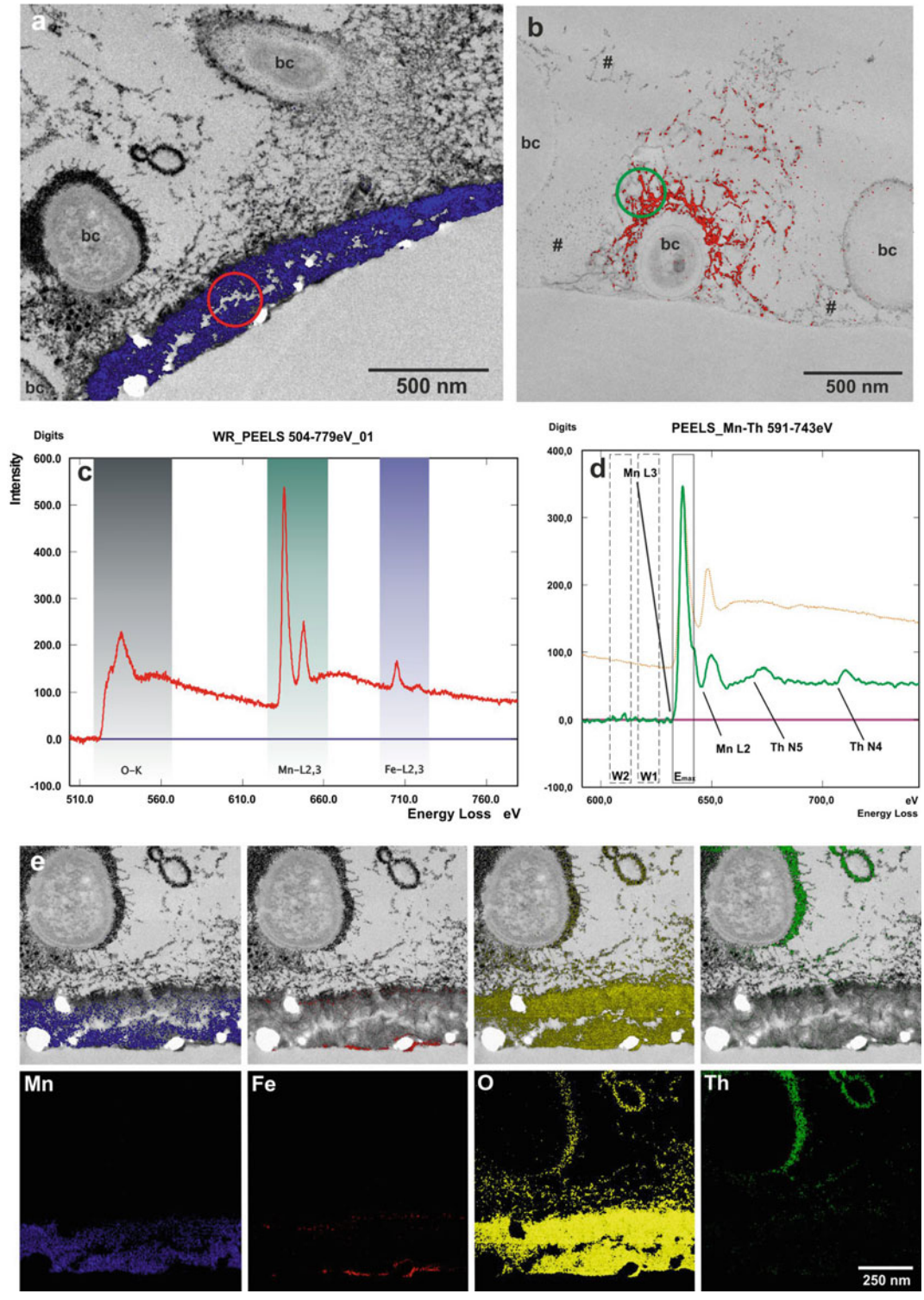

Fig. 3 Electron energy loss spectroscopic analysis of mineralogenesis in autochthonous biofilm. (**a**) Survey view of a biofilm, showing three bacterial cells (*bc*) in context with the heterogeneous EPS matrix, intensely

with the Zeiss Libra120Plus, used in our lab, for exact details and description to start this process. Further, suitable camera calibrations and settings have been done accordingly – see 'camera instruction manual' and 'EELS registration software'.) In the 'Wide Range PEELS' mode from about 2,500–0 eV spectrum, registration is done to get a rough overview of elements present within this range of electron energy loss (it is highly recommended to follow the instructions of the 'EELS registration software manual', since doing full-width spectrum registration takes some few minutes, i.e. 20–45 min [burning all the time with relatively high beam intensities on your sample motif]). If you look for and know the presence of 'indicator elements', characteristic for your sample, i.e. Fe, Mn, Al, etc., you can do short-time registration on the characteristic ionization energy range of your 'indicator element', the energy settings of which can be taken from the online 'EELS atlas'. After EELS registration, it is mandatory to switch back to the 'image mode' and check whether the motif has moved out of the spectrometer aperture partially or in total or not at all to be sure that your spectrum is valid. If not, you have to repeat the procedure with WR-PEELS registrations set at suitably smaller energy intervals, i.e. in the 'high energy loss' within 200–400 eV, 500–800 eV in the 'medium energy loss' and 600–1,200 eV from the 'low energy loss'.

A well-registered spectrum will (1) give you the exact elemental presence in your sample/motif and (2) show you the precise ionization energies and ELNES features (for instance, the suitable energy width of a maximum intensity peak, i.e. Mn-L3, Fe-L3, O-K edges; *see* Fig. 3d), which are mandatory for ESI parameters, set for high-resolution element mapping.

Element mapping or ESI can then be done in detail on your motif, used either at the same scale as during WR-PEELS

Fig. 3 (Continued) stained with ThO_2 nanocolloids. The *red encirled area* indicates the measuring area, used to WR-PEELS analysis and the corresponding spectrum shown in (**c**). The *deep blue* overlay at the contact interface of the biofilm with the Permanox substratum represents manganese distribution, as is additionally shown in part as the Mn elemental map in (**e**). (**b**) Further motif of Mn deposition within the EPS of an individual bacterial cell (*bc*), coloured in *red*. The *green circle* indicates the measuring and position of a PEEL spectrum, shown in (**d**). (**c**) Wide Range Parallel Electron Energy Loss Spectrum (WR-PEELS) of the encircled motif in (**a**). *Coloured rectangular areas* indicate the ionization edges and the corresponding ELNES features of oxygen, manganese and iron as shown in (**e**). (**d**) PEEL spectrum of the *green circled area* in (**b**). The *dashed line spectrum* shows the Mn-L2,3 reference. Spectra in (**c**) and (**d**) all have been background-subtracted according to the power law method. *Rectangular boxes* (E_{max}, W_1 and W_2) represent the energy slit width, set to 10 eV, and the positions along the energy axis (energy loss, eV), used to calculate the net elemental map of Mn-L3, according to the 'Three-Window Method' (after subtraction of background images (W_1, W_2) from the maximum intensity image (E_{max}) according to 'power law'). See Mn elemental map, colour-coded in *red* in (**b**) accordingly. (**e**) Gallery of unique biofilm motif, overlaid with the elemental maps (*first row*), as they are shown as colour-coded intensity signal maps (*second row*)

measurements or at lower magnification thus to encompass the motif's vicinity. Precise settings of the maximum intensities of the ionization edges of interest on the energy axis and the suitable energy width of the slit aperture should be set according to 'EELS acquisition software' manual. Before starting the ESI acquisition, the motif is set with appropriate magnification in the elastic bright-field mode; to get it precisely set to Gaussian focus, the low-loss range of 60–80 eV with suitable image intensities is chosen and ultrastructural features (partially in inverted contrast) are used for focusing, which are optimally Gaussian when recognized as sharp, detailed structures. With this focus fixed, the elastic bright field (= zero-loss image) is used for precisely positioning a 'detail of interest' close to the centre of the CCD detector (which is always readdressed for further element settings if further elements are constituents of the motif). Choosing the suitable ionization energy of the element's ionization edge to be mapped after starting the ESI application, follow/adjust parameter settings according to the 'EELS acquisition software' before the start of image registration. Acquisition of the ESI image stack (four images on the hole, one optimally set as elastic 'zero-loss' image at the end of registration) can be done within a few seconds (in the high-intensity 'low-loss' region) or can take up to 5–30 or more minutes at 'medium-electron energy loss' (finally, the strength of the sample/section will dictate how long and how many data sets can be acquired; but it is possible to collect data sets of different elements from one single motif up to more than 120 min; here, it is mandatory to check each ESI image stack on image drift; this is to decide whether the data set finally leads to a high-quality element map or whether ESI registration has to be repeated with different setting for that very element). The manual has to be followed in computational working out the 'background-corrected' element maps, either according to the 'Three-Window Method' with suitable mathematical models for background subtraction, i.e. 3 window power law, 3 window exponential law, etc., or with the 'Two-Window Method' as 'ratio imaging' (here, it is obligatory to learn more/get familiar with EELS theory, which is fundamentally given in [21]).

4 Notes

1. Cationic ThO_2 nanocolloids can be synthesized in a normal laboratory. A prerequisite however is the official permission from your local/institutional authorities to work with this radioactive compound. Synthesis of nanocolloids (from thorium nitrate × 5 H_2O; http://www.merck.de) is described in short under Sect. 3.4 and in detail by [19], and no special radiation protection is needed since Th is an alpha emitter and is non-toxic but has to be handled in a professional

manner, according to 'good chemical practice'. There can be a problem to get thorium nitrate hydrate as the starting compound because of its radioactivity.

2. Microscopical inspection, documentation and analysis at either low or high resolution should be done in an appropriate laboratory. Here, you can be trained in sample preparation if you are a novice.

   Further suitable equipment and expertise can be found in electron microscopic units, which should be equipped with sample preparation hardware such as a critical point drying apparatus and a sputter-coat unit for SEM analysis. An SEM equipped with FEG beam source is quite opportune to get images at high resolution (in our laboratory, we use a Zeiss Merlin for these purposes).

   Transmission electron microscopy (TEM) of ultrathin sections (70 nm thickness, bright silver interference colour) of embedded samples is a prerequisite to see and analyse interactions of bacteria with clay and other soil colloids. Sections should be post-stained with uranyl acetate for optimum contrast, thus making it possible to explore and understand the microbial motive. If this is understood and documented by medium (about x4,000 to x7,000) and high magnification (about x12,000 to x30,000), ultrathin sections 30–40 nm are cut with the same motive for elemental analysis by EELS. Either a post-column filter (Gatan system) or an in-column filter (Zeiss, JEOL) is suitable for electron energy loss spectroscopy. (EELS data presented in this article have been acquired with (in-column) energy filter transmission electron microscopes (EF-TEM) Zeiss CEM902 and Libra 120Plus (Zeiss, Oberkochen, Germany).)

   Further, you should be well trained and know how to adjust the optical instruments and how to work with them or you should get well trained for optical operations/observations or you should cooperate with the staff of a light or electron microscopical laboratory. Especially, electron spectroscopic analysis with an EF-TEM is not basic routine electron microscopy.

3. Theory of EELS is a sophisticated item and profound knowledge of electron scattering and ionization energies associated with energy levels of the outer valence electrons of the atom of interest should be understood in order to do right interpretation of spectrum features. It should be mentioned that X-ray absorption spectroscopy (XAS) and data obtained with this analytical methodology are highly similar and of good help as an alternative to EELS. A suitable entrance to the field of EELS is given by [21].

4. Though a diamond knife for cutting ultrathin sections is rather expensive, the use of self-made glass knives, as a much cheaper alternative, cannot be recommended. Here, the presence of soil colloids, such as clays and Fe and/or Mn containing colloidal aggregates, will immediately crash the sharpness of the knife and no fruitful sections will be obtained. These ingredients however should generally be withstood by the diamond, but extreme care should be taken not to include any sand granules (= quartz; Mohs's mineral hardness scale = 7; in comparison, diamond = 10) which immediately will destroy the sharpness and function of the diamond knife.

References

1. Heim D (1990) Tone und Tonminerale – Grundlagen der Sedimentologie und Mineralogie. Ferdinand Enke, Stuttgart
2. Hepper EN, Buschiazzo DE, Hevia GG, Urioste A, Antón L (2006) Clay mineralogy, cation exchange capacity and specific surface area of loess soils with different volcanic ash contents. Geoderma 135:216–223
3. Schwertmann (1984) Tonminerale. In: Scheffer, Schachtschabel, Lehrbuch der Bodenkunde. Enke, Stuffgart, pp 23–28
4. Lagaly G (1993) Praktische Verwendung und Einsatzmöglichkeiten von Tonen. In: Jasmund K, Lagaly G (eds) Tonminerale und Tone. Steinkopff, Darmstadt, pp 358–427
5. Nogales B, Moore ERB, Abraham WR, Timmis KN (1999) Identification of the metabolically- active members of a bacterial community in a polychlorinated biphenyl-polluted moorland soil. Environ Microbiol 1:199–212
6. Nogales B, Moore ERB, Llobet-Brossa E, Rossello-Mora R, Amann R, Timmis KN (2001) Combined use of 16S ribosomal DNA and 16S rRNA to study the bacterial community of polychlorinated biphenyl-polluted soil. Appl Environ Microbiol 67:1874–1884
7. Harkness MR, McDermott JB, Abramowicz DA, Salvo JJ, Flanagan WP, Stepens ML, Mondello FJ, May RJ, Lobos JH, Carroll KM, Brennan MJ, Bracco AA, Fish KM, Warner GL, Wilson PR, Dietrich DK, Lin DT, Morgan CB, Gately WL (1993) In situ stimulation of aerobic PCB biodegradation in Hudson river sediments. Science 259:503–507
8. Lünsdorf H, Erb RW, Abraham WR, Timmis KN (2000) 'Clay hutches': a novel interaction between bacteria and clay minerals. Environ Microbiol 2:161–168
9. Perfil'ev BV, Gabe DR (1969) Capillary methods of investigating micro-organisms. Oliver and Boyd, Edinburgh, Great Britain
10. Marcedo A, Kuhlicke U, Neu T, Timmis KN, Abraham WR (2005) Three stages of a biofilm community developing at the liquid-liquid interface between polychlorinated biphenyls and water. Appl Environ Microbiol 71:7301–7309
11. Valentin K, John U, Medlin L (2005) Nucleic acid isolation from environmental aqueous samples. Methods Enzymol 395:15–37
12. MacGregory BJ, Amann R (2006) Single-stranded conformational polymorphism for separation of mixed rRNAS (rRNA-SSCP), a new method for profiling microbial communities. Syst Appl Microbiol 29:661–670
13. Smalla K, Oros-Sichler M, Milling A, Heuer H, Baumgarte S, Becker R, Neuber G, Kropf S, Ulrich A, Tebbe CC (2007) Bacterial diversity of soils assessed by DGGE, T-RFLP and SSCP fingerprints of PCR-amplified 16S rRNA gene fragments: do the different methods provide similar results? J Microbiol Methods 69:470–479
14. Lünsdorf H, Strömpl C, Osborn AM, Bennasar A, Moore ERB, Abraham WR, Timmis KN (2001) Approach to analyze interactions of microorganisms, hydrophobic substrates, and soil colloids leading to formation of composite biofilms, and to study initial events in microbiogeological processes. Methods Enzymol 336:317–331
15. Glauert AM (1975) Fixation, dehydration and embedding of biological specimens. Volume 3, part 1 in the Glauert series. Elsevier, Amsterdam
16. Glauert AM (1991) Epoxy resins: an update on their selection and use. Microsc Anal 25:15–20

17. Spurr AR (1969) A low viscosity epoxy resin embedding medium for electron microscopy. J Ultrastruct Res 26:31–43
18. Reynolds ES (1963) The use of lead citrate at high pH as an electron-opaque stain in electron microscopy. J Cell Biol 17:208–212
19. Lünsdorf H, Kristen I, Barth E (2006) Colloidal hydrous thorium dioxide colloids – a useful tool for staining negatively charged surface matrices of bacteria for use in energy-filtered transmission electron microscopy. BMC Microbiol 6:59
20. Kapp N, Studer D, Gehr P, Geiser M (2010) Electron energy-loss spectroscopy as a tool for elemental analysis in biological specimens. Methods Mol Biol 369:431–447
21. Egerton RF (1996) Electron energy-loss spectroscopy in the electron microscope. Plenum Press, New York/London

Identification of Microorganisms in Hydrocarbon-Contaminated Aquifer Samples by Fluorescence In Situ Hybridization (CARD-FISH)

Schattenhofer Martha, Valerie Hubalek, and Annelie Wendeberg

Abstract

High loads of petroleum hydrocarbons in contaminated soils and sediments make these ecosystems difficult to study with molecular techniques. Among these sites, aquifers – environments with low turnover rates and, hence, slow-growing microbial communities–pose a great challenge for microbial ecologists.
Fluorescence produced by petroleum hydrocarbons coating sediment particles can be so strong that microscopic techniques are made impossible. Low microbial cell numbers pose further limitations for molecular analyses such as fluorescence in situ hybridization (FISH).
Here, we present a protocol for the separation of microbial cells from sediment samples of highly petroleum-contaminated aquifers. By excluding the strongly autofluorescing sediment particles, by concentrating microbial cells on membrane filters, and by using signal amplification in combination with FISH (CARD-FISH), we were able to quantify various microbial populations in this intriguing ecosystem.

Keywords: Aquifer, CARD-FISH, Cell quantification, Hydrocarbon contamination, Microbial community

1 Introduction

Contamination of aquatic and terrestrial ecosystems with hydrocarbons occurs worldwide and represents a major threat to the environment and human health. Alongside cost- and labor-intensive technological approaches, natural attenuation strategies exploiting microorganisms have become an alternative way to clean up those contaminated sites [1, 2]. Yet our understanding of the physiology and ecology of the natural microbial communities found at polluted sites is limited as the sites themselves often pose a challenge even to common analysis techniques.

Aquifers, like most nutrient-poor water bodies, are characterized by a low number of small-sized planktonic cells, with more than 90% of the microorganisms attached to sediment particles [3, 4]. Hence, studying microbes indigenous to an aqua-terrestrial

T.J. McGenity et al. (eds.), *Hydrocarbon and Lipid Microbiology Protocols*, Springer Protocols Handbooks (2016) 103–113,
DOI 10.1007/8623_2014_9, © Springer-Verlag Berlin Heidelberg 2014, Published online: 20 November 2014

ecosystem necessitates the enrichment of the planktonic fraction by filtering large amounts of water [5–7] or by directly analyzing sediment samples [8–10]. Most studies include both approaches [11–13]. Since particle-attached communities are often more active than their planktonic counterpart [14–17], sediment samples are likely to be more relevant when focusing on microbial processes, such as biodegradation [18]. However, background fluorescence and autofluorescence caused by sediment particles (i.e., clay) and especially hydrocarbons present a major challenge to any kind of microbial visualization technique in this environment. One of the techniques thus affected is fluorescence in situ hybridization (FISH) of rRNA – at large, a widely used cultivation-independent method to investigate population dynamics and interspecies relationships at the single-cell level [19–21]. This fact is also reflected in the very low number of published studies using FISH in contaminated aquifer sediments (six in total: [22–27]).

The FISH procedure generally consists of four parts:

1. *Fixation* of the sample containing the target cells.

   Fixation stabilizes macromolecules and cytoskeletal structures thus preventing lysis of the cells during hybridization. At the same time fixation permeabilizes the cell walls for the fluorescently labeled oligonucleotide probe molecules.

2. *Hybridization* of target cells with specific oligonucleotide probes.

   The fixed cells are incubated (hybridized) in a buffer containing the labeled probe at a specified temperature that favors the specific binding of the probe to the target. Ideally, only those probe/rRNA pairs will form which have no mismatches in the hybrid. Consequently, only target cells that contain the full signature sequence on their rRNA will be stained.

3. *Washing* to remove unbound probe.

   The subsequent washing step will remove all unbound probe molecules.

4. *Enumeration/quantification* of stained target cells.

   Finally, the hybridized cells are counted by epifluorescence microscopy.

Further developments of the FISH assay introduced additional steps to the common protocol, for example, signal amplification by catalyzed reporter deposition with horseradish peroxidase (HRP)-labeled oligonucleotides (CARD-FISH, [28]). A study on marine planktonic and benthic microbial assemblages showed that the quantification efficiency of FISH can be significantly enhanced by using the more sensitive CARD-FISH assay [29].

Alternative approaches for the quantification of certain target organisms in an environment are of course available (though without cell visualization) and used in many areas of microbial diversity research. Some of these methods require prior DNA extraction, and regardless of the chosen protocol, one has to keep in mind that this step will already have an influence on the outcome of the microbial composition study [30]. Some more bias is likely to be introduced when applying polymerase chain reaction (PCR)-based methods (e.g., quantitative real-time PCR [31–33]). In addition, setting up PCR protocols for samples from petroleum-contaminated samples can be rather challenging, as not only the hydrocarbons but humic substances are known to at least partly inhibit the PCR [34]. One technique for cell quantification without prior DNA extraction and amplification steps is flow cytometry. This approach works well for cell cultures [35], single-cell sorting [36], and also in combination with FISH [37]. However, hydrocarbons and particles in the sediments that remain in the sample even after physical/chemical cell separation techniques cause strong autofluorescence, leading to erroneous cell counts with the flow cytometer. Another issue with cytometry is the potential clogging and contamination of the fine tubings by such fine particles and hydrocarbons.

The challenge to visualize microbes in contaminated aquifers with (CARD)-FISH is to minimize both background fluorescence and the number of false-positive (CARD)-FISH signals caused, for example, by particle-bound probes. One way to reduce background fluorescence and false-positive signals is by detaching cells from sediment through physical and/or chemical means and density gradient centrifugation. However, the disadvantage with this procedure is that spatial distribution patterns of microbes are disrupted and steric partnerships are disintegrated. Thus, this method is commonly more suited to analyze the presence/absence and abundance of target organisms.

The CARD-FISH protocol we present here has been developed and optimized for hydrocarbon-contaminated aquifers, in particular heavily polluted aquifers containing large plumes of methyl tertiary butyl ether (MTBE) and benzene, toluene, ethylbenzene, and xylenes (BTEX) [38]. We obtained considerable improved permeabilization and hybridization efficiency (2- to 20-fold) by applying a laboratory microwave. In fact, permeabilization with Tris-EDTA buffer (1× TE) in the conventional oven resulted in CARD-FISH signals below the detection limit, whereas a short treatment with the histological microwave resulted in CARD-FISH signals with well-preserved cell morphologies. Additionally, using a histological microwave decreased hybridization time when compared to hybridization in a conventional oven. The latter usually requires two to twelve hours for the hybridization reaction, while hybridization using controlled microwave irradiation needs only 20 min to 2 h.

The detection efficiency of FISH in contaminated aquifers lies reportedly between 23 and 72% for *Bacteria* and *Archaea* together [24, 25, 27]. Depending on the degree of hydrocarbon contamination, we achieved an efficiency ranging from 100% in aquifer samples with lower hydrocarbon concentrations to 15% closest to the center of the contaminant plume being the least biologically active part [39, 40].

2 Materials

2.1 Sample Fixation

Formaldehyde (37%): best stored dark, stable for several months at room temperature.
Phosphate buffered saline (1× PBS): 137 mM NaCl, 2.7 mM KCl, 4 mM Na_2HPO_4, 2 mM KH_2PO_4, pH 7.6.
Ethanol 96%.

2.2 Cell Separation

Tris-EDTA buffer (1× TE): 10 mM TrisHCl, 5 mM EDTA, pH 9.0.
Natrium pyrophosphate: 1 M.
Tween 80 (Reagent purchased from SERVA (http://www.serva.de)).
Sonication device: ultrasonic liquid processor.
Phosphate buffered saline (1× PBS) (*see* Sect. 2.1).
Nycodenz solution: 1.3 g ml^{-1}; 60% (w/v) in Milli-Q water; if autoclaved and stored at 4°C, stable for several weeks (Axis-Shield PoC, http://www.axis-shield.com).
Cellulose nitrate support filters: pore size 0.45 μm, diameter 47 mm (The filters were purchased from Sartorius (http://www.sartorius.com)).
Polycarbonate filters type GTTP: pore size 0.2 μm, diameter 47 mm. (The filters were purchased from Millipore (http://www.millipore.com)).

2.3 Cell Permeabilization

Low gelling point agarose: 0.1% [w/v], gel strength should be approx. 1,000 g cm^{-2} (Reagent purchased from Biozym (http://www.biozym.com)).
Ethanol 50%.
Tris-EDTA buffer (1× TE) (*see* Sect. 2.2).
Formaldehyde (37%) (*see* Sect. 2.1).
Hydrogen peroxide (H_2O_2): 0.1%, store at 4°C.

2.4 CARD-FISH Procedure and Counterstaining

Horseradish peroxidase (HRP)-labeled oligonucleotide probes: working solutions are prepared at a concentration of 50 ng μl^{-1} and stored in small portions (50–100 μl) in the dark at −20°C. Once thawed, HRP-labeled probes should be stored at 4°C where they are stable for up to 6 months (all probes were purchased from biomers.net (https://www.biomers.de) (*see* **Note 1**).

Hybridization buffer: 0.9 M NaCl, 20 mM TrisHCl (pH 8), 10% dextran sulfate, 0.02% sodium dodecyl sulfate (SDS), 1% blocking reagent, × ml formamide and × ml Milli-Q water; stable for 12 months if stored at −20°C. (Blocking reagent was purchased from Roche (https://www.roche-applied-science.com)) (*see* **Note 2**).
Phosphate buffered saline (1× PBS) (*see* Sect. 2.1).
Amplification buffer: 1× PBS (pH 7.6), 2 M NaCl, 10% dextran sulfate, 0.1% blocking reagent; stable for 12 months if stored at −20°C, at 4°C stable for 4 weeks (Blocking reagent was purchased from Roche (https://www.roche-applied-science.com) (*see* **Note 3**).
Hydrogen peroxide (H_2O_2): 0.0015% make fresh as required.
Fluorescein-labeled tyramide (Fluorochromes purchased from Invitrogen (www.invitrogen.com); custom labeled, see [28]; light sensitive, store at −20°C (*see* **Note 4**).
Ethanol series: 50%, 70%, and 96%.
Mounting medium containing a general DNA stain (i.e., 4′,6-diamidino-2-phenylindole, DAPI), light sensitive, store at 4°C.
Microscope glass slides and cover slips.

3 Methods

3.1 Sampling Procedure and Fixation

1. Take sediment sample and fix with formaldehyde (2% volume/volume [v/v] final concentration) at 4°C for 12–24 h (*see* **Note 5**).
2. Wash samples twice with a 1:1 mix of 1× PBS and 96% ethanol by pelleting at 15,000×*g* for 5 min and resuspend. For centrifugation we use 5810R centrifuge with swing-out rotor A-4-62 (Eppendorf (http://ww.eppendorf.com)).
3. Store washed samples in 96% ethanol at −80°C.

3.2 Cell Separation

1. Mix 200 µl of sediment sample with 700 µl 1× TE buffer and 100 µl of 1 M Na-pyrophosphate in a 1.5 ml tube.
2. Place tube into a water bath and heat it to 55°C for 5 min at 200 W in a laboratory microwave. For microwaving we use the laboratory microwave BP-111-RS (Microwave Research and Applications, Inc. (http://www.microwaveresearch.com)).
3. Cool sample down to room temperature.
4. Add 1 µl Tween 80 and vortex for 15 min at RT.
5. Sonicate on ice. For sonication we use Sonifier Model 250 (Branson (http://www.emersonindustrial.com)).
6. To separate dislodged cells from sediment particles, transfer sample to 50 ml tube and mix thoroughly with 22.5 ml 1× PBS and 2.5 ml 0.1 M Na-pyrophosphate.

7. Place 2 ml of Nycodenz solution at the bottom of the 50 ml tube using a syringe with a long needle.
8. Centrifuge at 4,000 rpm for 15–17 h at 4°C. For centrifugation we use 5810R centrifuge with swing-out rotor A-4-62 (Eppendorf (http://www.eppendorf.com)).
9. Transfer supernatant and Nycodenz layer to a clean 50 ml tube and mix sample.
10. Filter sample onto white polycarbonate filter. For filtration we use filter type GTTP, size 47 mm, pore size 0.2 μm (Millipore (http://www.millipore.com) together with cellulose nitrate support filter, size 47 mm, pore size 0.45 μm (Sartorius (http://www.sartorius.com)).
11. Wash filter twice with autoclaved Milli-Q water, air-dry, and store at −20°C. It is possible to store filters at −20°C for several months. Labeling of filters should be done using a lead pencil only.

3.3 Cell Permeabilization

1. To prevent cell loss during permeabilization, place filters facing down into 200 μl low gelling point agarose (0.1%) onto a Parafilm covered, even surface (i.e., glass plate) and dry filters in an oven at 35°C (*see* **Note 6**).
2. Remove filters from Parafilm by wetting with 50% ethanol and gently peel filters off, air-dry filters.
3. Section filters into pieces (and label sections with a lead pencil if necessary).
4. Place filter sections into a 1.5 ml tube containing 1 ml of 1× TE.
5. Permeabilize by microwaving in a preheated water bath at 65°C for 8 min at 1,000 W (100% power output) (*see* **Note 7**).
6. Cool tubes for 5 min at RT.
7. To stabilize cells for subsequent hybridization, postfix cells in 900 μl of 1× TE and 120 μl formaldehyde (37%) for 5 min at RT.
8. Wash filter sections with 1× TE.
9. Inactivate endogenous peroxidases with 0.1% H_2O_2 in 1× TE for 2 min at RT (*see* **Note 8**).
10. Wash filter sections twice with 1× TE.

3.4 Hybridization of Filter Sections (CARD-FISH) and Counterstaining

1. Mix 1,000 μl hybridization buffer (% formamide depending on probe used) and 3.3 μl HRP-probe working solution in a 1.5 ml tube (*see* **Note 9**).
2. Transfer filter sections to the hybridization mixture.

3. For hybridization place tube into a pre-warmed water bath and microwave at 46°C for 40 min at 500 W in laboratory microwave (*see* **Note 10**).
4. To equilibrate the probe-delivered HRP, transfer filter sections to 50 ml of 1× PBS and wash for 15 min at RT (*see* **Note 11**).
5. Mix 1,000 µl amplification buffer with freshly amended 0.0015% H_2O_2 and 1 µl fluorescein-labeled tyramide in a 1.5 ml tube (*see* **Note 12**).
6. Transfer filter sections to the amplification mixture (*see* **Note 13**) and place tube for 15 min at 46°C in a conventional hybridization oven in the dark (*see* **Note 14**).
7. Wash filter sections five times with Milli-Q water, dehydrate in increasing ethanol concentrations (50%, 70%, and 96%) and let air-dry in the dark.
8. It is possible to store filter sections at −20°C or continue with counterstaining filter sections with a DNA stain (i.e., DAPI-amended mountant solution) (*see* **Note 15**).
9. Put filter sections on glass slide for microscopic enumeration of cells (*see* **Note 16**).

4 Notes

1. Repeated freeze-thawing of probe working solutions will damage the peroxidase and might cause the appearance of numerous brightly fluorescent particles (precipitation of the probe) that do not show any signal in UV (DAPI) excitation. In addition, hybridization signals become dim and background is high.
2. The specific formamide concentration of the hybridization buffer is linked to the probe used. A database of probes and their specific formamide concentrations is available at probeBase (http://www.microbial-ecology.net/probebase). For the exact volume of formamide and Milli-Q water added to the hybridization buffer, refer to Table 1 in [28].
3. Amplification buffer is stored best in small aliquots of 1–2 ml at −20°C.
4. Different fluorochromes are available for CARD-FISH, for example, various Alexa Fluor dyes and coumarin-, fluorescein-, tetramethylrhodamine-, cyanine 3-, and cyanine 5-labeled tyramides. Because these succinimidyl esters can hydrolyze rapidly, all reagents have to be water-free, and the active dye stock as well as the tyramine HCl stock must be prepared a few minutes before use.

5. Due to the size of the HRP molecule, accessibility of probes to the cells may be discriminating. This is, e.g., reflected in the preference for ethanol fixation rather than fixing with the cross-linking agents paraformaldehyde or formaldehyde. The probability that not all organisms can be detected under the same conditions increases with the phylogenetic diversity of the target group. So it is recommended to use the signal amplification method only for probes with a restricted target group for which fixation and hybridization conditions can be readily achieved.
6. Before embedding the filters let the freshly heated agarose cool down to 35–40°C. The temperature for drying the agarose embedded filters is not crucial and can range from 20 to 50°C.
7. For alternatives to permeabilization with 1× TE and a laboratory microwave, see [28].
8. Alternatively incubate filter sections in 50 ml of 0.01 M HCl for 10 min at RT in order to inactivate endogenous peroxidases. Some microorganisms, e.g., from anoxic sediments, may contain peroxidases or enzymes with pseudoperoxidase activity. This can be tested by incubating a filter section in amplification buffer containing H_2O_2 and fluorescently labeled tyramides. Cells with peroxidase activities will show bright fluorescence. These enzymes have to be inactivated, for example, by treatment with hydrochloric acid.
9. The ratio of hybridization buffer to probe working solution (50 ng μl^{-1}) used in FISH is generally 300:1.
10. Alternatively to a laboratory microwave, you might also use a conventional hybridization oven. Length of hybridization time has to be adjusted accordingly (at least double the time as with a laboratory microwave).
11. Gently shaking the tube with 1× PBS during washing for 15 min at RT assists with the removal of unbound probe from the filter sections.
12. The volume of labeled tyramide added strongly depends on the nature of the sample. A ratio of 1:1,000 of fluorochrome to amplification buffer is generally sufficient to get bright signals. If hybridization signals are not sufficient (*see* **Note 16**), increase/decrease the ratio of added tyramide.
13. After washing in 1× PBS, you can remove excess liquid by dabbing filter sections on blotting paper, but do not let filter sections run dry before transferring into the amplification mixture.
14. After transfer of filter sections into amplification mixture, keep filters always protected from direct light due to presence of light-sensitive fluorochrome.

15. On white polycarbonate filters, background fluorescence after DAPI staining is always somewhat worse than on black membrane filters. Black filters, however, show high levels of background fluorescence at green excitation. Use shorter DAPI staining time and/or longer ethanol washing to improve background. Make sure that hybridized filters have been thoroughly rinsed in distilled water before DAPI staining.
16. Enumeration of cells might be hindered by:
    (a) High background fluorescence due to:
        - Too high tyramide concentration. Either decrease the tyramide concentration or increase the blocking reagent concentration.
        - Too high probe concentration. If the background is covered with tiny fluorescent dots, check the probe concentration; 0.2 ng μl^{-1} is plenty.
        - Too short washing after CARD. Prolonged washing in deionized water and/or several changes with freshwater may help.
    (b) Low signal intensity due to:
        - Low ribosome content of the target cells. Increase the tyramide concentration or the temperature during the tyramide signal amplification. A prolonged hybridization time (up to 15 h) may also help.
        - Too low tyramide concentration. Increase tyramide concentration.
        - The probe-delivered HRP has too low or no activity. Check the probe for age; the probe should be thawed only once and should not be stored in the fridge for more than 6 months. Also the pH of the PBS should be around 7.6. Check the H_2O_2 concentration and its age and the reactivity of the tyramide.
        - The HRP is badly coupled to the probe. The amount of unlabeled oligonucleotide can be estimated spectrophotometrically.
        - The HRP-labeled probe cannot penetrate the cell wall. Try different permeabilization protocols.

References

1. Brar SK, Verma M, Surampalli RY et al (2006) Bioremediation of hazardous wastes—a review. Pract Period Hazard Toxic Radioactive Waste Manag 10:59–72
2. Perelo LW (2010) Review: in situ and bioremediation of organic pollutants in aquatic sediments. J Hazard Mater 177:81–89
3. Anneser B, Pilloni G, Bayer A et al (2010) High resolution analysis of contaminated aquifer sediments and groundwater—what can be learned in terms of natural attenuation? Geomicrobiol J 27:130–142
4. Griebler C, Mindl B, Slezak D, Geiger-Kaiser M (2002) Distribution patterns of attached

and suspended bacteria in pristine and contaminated shallow aquifers studied with an in situ sediment exposure microcosm. Aquat Microb Ecol 28:117–129

5. DeLong EF, Taylor LT, Marsh TL, Preston CM (1999) Visualization and enumeration of marine planktonic archaea and bacteria by using polyribonucleotide probes and fluorescent in situ hybridization. Appl Environ Microb 65:5554–5563
6. Glöckner FO, Amann R, Alfreider A et al (1996) An in situ hybridization protocol for detection and identification of planktonic bacteria. Syst Appl Microbiol 19:403–406
7. Schroth MH, Kleikemper J, Bolliger C, Bernasconi SM, Zeyer J (2001) In situ assessment of microbial sulfate reduction in a petroleum-contaminated aquifer using push–pull tests and stable sulfur isotope analyses. J Contam Hydrol 51:179–195
8. Ishii K, Mußmann M, MacGregor BJ, Amann R (2004) An improved fluorescence in situ hybridization protocol for the identification of bacteria and archaea in marine sediments. FEMS Microbiol Ecol 50:203–213
9. Llobet-Brossa E, Rosselló-Mora R, Amann R (1998) Microbial community composition of Wadden Sea sediments as revealed by fluorescence in situ hybridization. Appl Environ Microb 64:2691–2696
10. Långmark J, Storey MV, Ashbolt NJ, Stenström TA (2004) Artificial groundwater treatment: biofilm activity and organic carbon removal performance. Water Res 38:740–748
11. Araya R, Tani K, Takagi T, Yamaguchi N, Nasu M (2003) Bacterial activity and community composition in stream water and biofilm from an urban river determined by fluorescent in situ hybridization and DGGE analysis. FEMS Microbiol Ecol 43:111–119
12. Kalmbach S, Manz W, Szewzyk U (1997) Dynamics of biofilm formation in drinking water: phylogenetic affiliation and metabolic potential of single cells assessed by formazan reduction and in situ hybridization. FEMS Microbiol Ecol 22:265–279
13. Manz W, Szewzyk U, Ericsson P, Amann R, Schleifer KH, Stenström TA (1993) In situ identification of bacteria in drinking water and adjoining biofilms by hybridization with 16S and 23S rRNA-directed fluorescent oligonucleotide probes. Appl Environ Microb 59:2293–2298
14. Albrechtsen H-J, Christensen TH (1994) Evidence for microbial iron reduction in a landfill leachate-polluted aquifer (Vejen, Denmark). Appl Environ Microb 60:3920–3925
15. Albrechtsen H-J, Winding A (1992) Microbial biomass and activity in subsurface sediments from Vejen, Denmark. Microbial Ecol 23:303–317
16. Holm PE, Nielsen PH, Albrechtsen H-J, Christensen TH (1992) Importance of unattached bacteria and bacteria attached to sediment in determining potentials for degradation of xenobiotic organic contaminants in an aerobic aquifer. Appl Environ Microb 58:3020–3026
17. Madsen EL, Ghiorse WC (1993) Groundwater microbiology: subsurface ecosystem processes. In: Ford T (ed) Aquatic microbiology: an ecological approach. Blackwell, Cambridge
18. Brad T, Van Breukelen BM, Braster M, Van Straalen NM, Röling WFM (2008) Spatial heterogeneity in sediment-associated bacterial and eukaryotic communities in a landfill leachate-contaminated aquifer. FEMS Microbiol Ecol 65:534–543
19. Breuker A, Köweker G, Blazejak A, Schippers A (2011) The deep biosphere in terrestrial sediments in the Chesapeake Bay area, Virginia, USA. Front Microbiol 2:156
20. Suárez-Suárez A, López-López A, Tovar-Sánchez A et al (2011) Response of sulfate-reducing bacteria to an artificial oil-spill in a coastal marine sediment. Environ Microbiol 13:1488–1499
21. Witzig M, Boguhn J, Kleinsteuber S, Fetzer I, Rodehutscord M (2010) Influence of the maize silage to grass silage ratio and feed particle size of rations for ruminants on the community structure of ruminal Firmicutes in vitro. J Appl Microbiol 109:1998–2010
22. Grenni P, Gibello A, Barra Caracciolo A et al (2009) A new fluorescent oligonucleotide probe for in situ detection of *s*-triazine-degrading *Rhodococcus wratislaviensis* in contaminated groundwater and soil samples. Water Res 43:2999–3008
23. Kleikemper J, Pelz O, Schroth MH, Zeyer J (2002) Sulfate-reducing bacterial community response to carbon source amendments in contaminated aquifer microcosms. FEMS Microbiol Ecol 42:109–118
24. Pombo SA, Kleikemper J, Schroth MH, Zeyer J (2005) Field-scale isotopic labeling of phospholipid fatty acids from acetate-degrading sulfate-reducing bacteria. FEMS Microbiol Ecol 51:197–207
25. Richardson RE, James CA, Bhupathiraju VK, Alvarez-Cohen L (2002) Microbial activity in soils following steam treatment. Biodegradation 13:285–295

26. Rogers SW, Ong SK, Moorman TB (2007) Mineralization of PAHs in coal–tar impacted aquifer sediments and associated microbial community structure investigated with FISH. Chemosphere 69:1563–1573
27. Kleikemper J, Pombo SA, Schroth MH, Sigler WV, Pesaro M, Zeyer J (2005) Activity and diversity of methanogens in a petroleum hydrocarbon-contaminated aquifer. Appl Environ Microb 71:149–158
28. Pernthaler A, Pernthaler J. (2007) Fluorescence in situ hybridization for the identification of environmental microbes. In: Hilario E, Mackay J (eds) Methods in molecular biology, vol 353. Humana Press, New York, USA, pp 153–164
29. Pernthaler A, Pernthaler J, Amann R (2002) Fluorescence in situ hybridization and catalyzed reporter deposition for the identification of marine bacteria. Appl Environ Microb 68:3094–3101
30. Martin-Laurent F, Philippot L, Hallet S et al (2001) DNA extraction from soils: old bias for new microbial diversity analysis methods. Appl Environ Microb 67:2354–2359
31. Cébron A, Norini M-P, Beguiristain T, Leyval C (2008) Real-Time PCR quantification of PAH-ring hydroxylating dioxygenase (PAH-RHD$_\alpha$) genes from Gram positive and Gram negative bacteria in soil and sediment samples. J Microbiol Methods 73:148–159
32. Powell SM, Ferguson SH, Bowman JP, Snape I (2006) Using real-time PCR to assess changes in the hydrocarbon-degrading microbial community in Antarctic soil during bioremediation. Microbiol Ecol 52:523–532
33. Zhang T, Fang HHP (2006) Applications of real-time polymerase chain reaction for quantification of microorganisms in environmental samples. Appl Microbiol Biotechnol 70:281–289
34. Herrick JB, Madsen EL, Batt CA, Ghiorse WC (1993) Polymerase chain reaction amplification of naphthalene-catabolic and 16S rRNA gene sequences from indigenous sediment bacteria. Appl Environ Microb 59:687–694
35. Kell DB, Ryder HM, Kaprelyants AS, Westerhoff HV (1991) Quantifying heterogeneity: flow cytometry of bacterial cultures. Antonie Van Leeuwenhoek 60:145–158
36. Davey HM, Kell DB (1996) Flow cytometry and cell sorting of heterogeneous microbial populations: the importance of single-cell analyses. Microbiol Rev 60:641–696
37. Amann RI, Binder BJ, Olson RJ, Chisholm SW, Devereux R, Stahl DA (1990) Combination of 16S rRNA-targeted oligonucleotide probes with flow cytometry for analyzing mixed microbial populations. Appl Environ Microb 56:1919–1925
38. Tischer K, Zeder M, Klug R et al (2012) Fluorescence in situ hybridization (CARD-FISH) of microorganisms in hydrocarbon contaminated aquifer sediment samples. Syst Appl Microbiol 35:526–532
39. Takahata Y, Kasai Y, Hoaki T, Watanabe K (2006) Rapid intrinsic biodegradation of benzene, toluene, and xylenes at the boundary of a gasoline-contaminated plume under natural attenuation. Appl Microbiol Biotechnol 73:713–722
40. Thornton SF, Quigley S, Spence MJ, Banwart SA, Bottrell S, Lerner DN (2001) Processes controlling the distribution and natural attenuation of dissolved phenolic compounds in a deep sandstone aquifer. J Contam Hydrol 53:233–267

Studies of the Ecophysiology of Single Cells in Microbial Communities by (Quantitative) Microautoradiography and Fluorescence In Situ Hybridization (MAR-FISH)

Marta Nierychlo, Jeppe Lund Nielsen, and Per Halkjær Nielsen

Abstract

Microautoradiography (MAR) in combination with fluorescence in situ hybridization (FISH) is a powerful method of obtaining information about the ecophysiology of probe-defined single cells in mixed microbial communities. The incorporation of radiolabelled substrates can be quantified by automated image analysis (MARQuant). Quantification of MAR signals can answer more specific questions regarding metabolic activity and function of the microbes. Here, we give an overview of how to use MAR-FISH in various ecosystems and provide a detailed protocol for MAR-FISH, including sampling, incubation with radiotracers, the MAR procedure in combination with FISH and other staining techniques, microscopy, and troubleshooting. A description of the MARQuant image analysis tool, including examples of its application, is also provided.

Keywords: Ecophysiology, FISH, Microautoradiography, Microbial communities, Radiotracers

1 Introduction

Microautoradiography (MAR) provides information about the metabolic activity of single cells, and through its combination with fluorescence in situ hybridization (FISH) for microbial identification, it becomes a very powerful method to obtain information about the ecophysiology of probe-defined single cells in mixed microbial communities [1, 2]. This method has been applied, with minor modifications, in numerous studies during the past 15 years and is now more relevant than ever for testing hypotheses arising from studies based on metagenomes and genomes of uncultured microorganisms (e.g., [3, 4]).

The MAR method was first used in microbial ecology in the 1960s [5, 6]. The method is based on assimilation of radiolabelled substrates by individual cells, which can then be visualized by exposure to a radiation-sensitive silver halide emulsion placed over the radiolabelled bacteria and subsequently processed by standard

T.J. McGenity et al. (eds.), *Hydrocarbon and Lipid Microbiology Protocols*, Springer Protocols Handbooks (2016) 115–130, DOI 10.1007/8623_2015_66, © Springer-Verlag Berlin Heidelberg 2015, Published online: 22 March 2015

photographic procedures. The radiotracers used are typically soft beta emitters, ^{3}H, ^{14}C, and ^{33}P, which allow formation of silver grains on top of the labelled bacteria and can be clearly visualized by bright-field or phase contrast microscopy. Low-energy emitters give the highest resolution, as they produce silver grains deposited close to the source cell. Tritium, for example, has a resolution of approximately 0.5 μm, while it is 2–3 μm for ^{14}C and ^{33}P.

Since the number of silver grains developed by individual cells was shown to be a function of the amount of radiolabelled substrate incorporated by the cell [7], the MAR method can be used in a quantitative manner (qMAR). However, this particular advantage of the MAR technique is not fully exploited in microbial ecology as manual enumeration of silver grains is labor-intensive and time-consuming and is thus considered a bottleneck obstructing the method. A few studies have employed qMAR in the investigation of ecophysiology of bacteria living in mixed communities [7–12], providing important information about the activity level of microorganisms present in environmental assemblages. To overcome the limitations of the qMAR technique and to fully utilize its potential, the "MARQuant" image analysis tool has recently been developed to facilitate the quantification of MAR signal with minimal user input [13].

When MAR is combined with FISH, comprehensive studies of the ecophysiology of probe-defined microorganisms can be carried out in mixed microbial communities. These include, for example, detection of viability, identification and enumeration of bacteria capable of consuming specific organic substrates, studies of autotrophic activity, uptake of orthophosphate, potential use of various electron acceptors, effect of inhibiting substances, and determination of cell-specific uptake rates or half saturation coefficients [14, 15].

Continuous development of variations of the technique such as dual labelling with different isotopes or the heterotrophic uptake of CO_2 ($HetCO_2$-MAR) [14, 16] allows new types of ecophysiological questions to be investigated. In particular, many specific questions about the physiology of microbial communities raised based on continuously emerging genomic, transcriptomic, and proteomic information (e.g., [3, 4]) can be tested by MAR-FISH, providing clear answers with regard to metabolic function of microorganisms in complex microbial ecosystems. Recent examples of MAR-FISH include confirmation of polyphosphate-accumulating ability of *Tetrasphaera* present in activated sludge communities [17], identification of active pollutant degraders in wastewater treatment systems [18], and investigation of utilization of organic compounds by algae in lake water [19]. Multiple examples of MAR-FISH applications in the microbial aquatic ecology field are described in [20].

A detailed description of the procedures for MAR and MAR-FISH can be found in several microbial ecology studies [1, 2, 14, 20–29]. MAR has also been combined with Catalyzed Reporter

Deposition-FISH (CARD-FISH) for increased sensitivity of the FISH signals (e.g., [30, 31]).

This chapter is an extensive upgrade of a previous chapter [27]. It includes a novel protocol for quantitative (q)MAR-FISH and a description of MARQuant image analysis tool as a general procedure to be applied on various types of samples with minor modifications. The overall MAR-FISH procedure is outlined in Fig. 1.

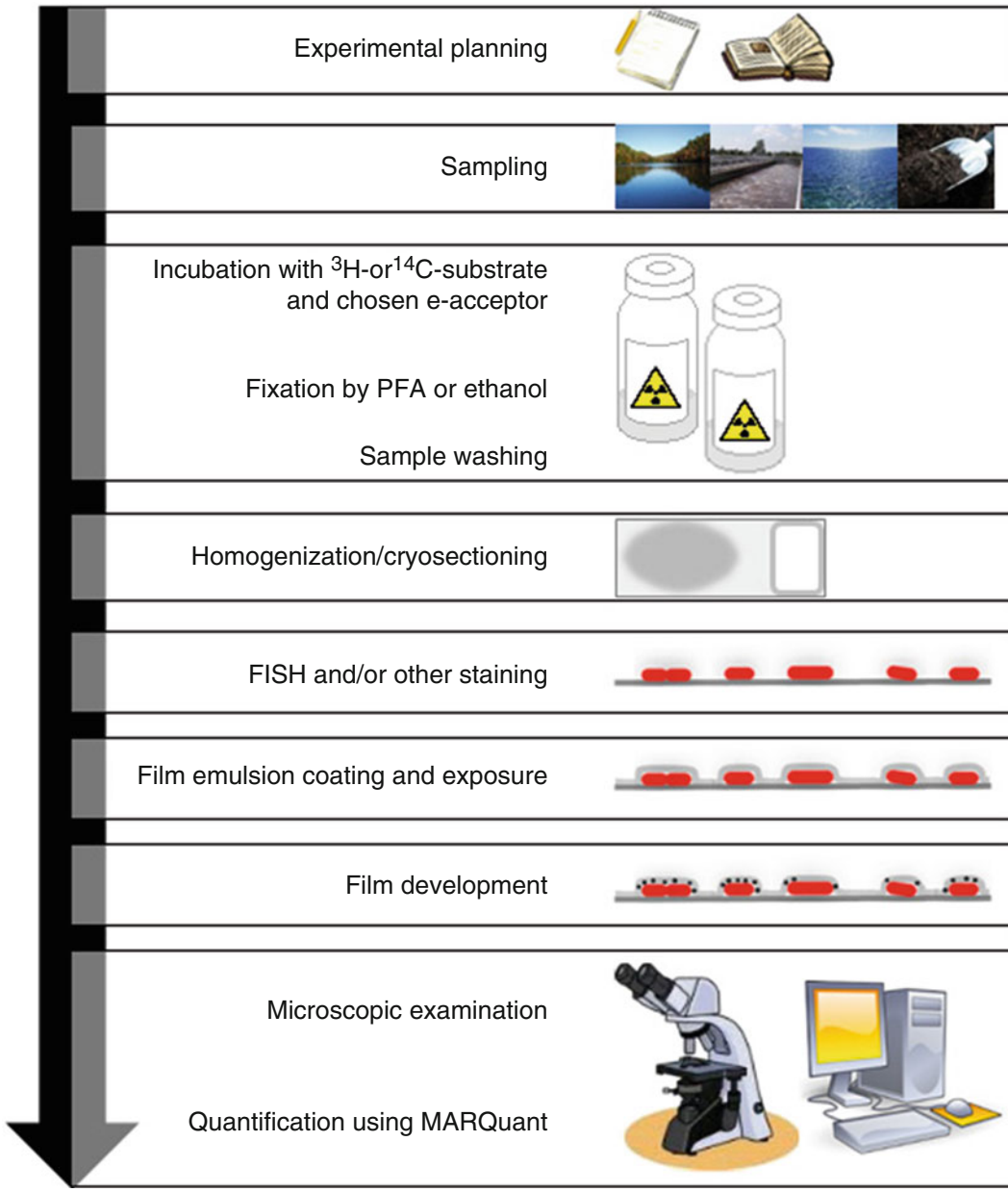

Fig. 1 An overview of the (q)MAR-FISH procedure

The sample is incubated under defined conditions for a period of time to ensure a sufficient uptake of radiotracer by the metabolizing cells. Several factors must be considered while designing the incubation experiment, such as type of specific activity analyzed, concentration of the chosen radiotracer, concentration of unlabelled substrate, concentrations of electron acceptors (oxygen, nitrate, or others) and inhibitors, biomass concentration, incubation temperature, and duration. It is advisable to measure substrate consumption and incorporation into the biomass to ensure that the incubation has been carried out without substrate limitation and with a suitable amount of labelled substrate incorporated into the biomass. Autoradiographic examination is a very sensitive technique, which is based on the incorporation of the radioactive substrates into cellular macromolecules and requires less than 10^{-16} Ci incorporated in a single cell to produce a MAR signal. After the incubation, the samples are fixed in paraformaldehyde (PFA), glutaraldehyde or ethanol and washed to remove excess radiotracer. Depending on the sample, homogenization, cryosectioning, or dilution may be necessary for optimal visualization of the MAR-FISH signal. For FISH, the standard protocols can be followed using oligonucleotide probes labelled with fluorescein or cyanine dyes. The stained MAR-positive bacteria can be examined by a combination of bright field or phase contrast and FISH-positive cells with epifluorescence microscopy. Quantification of the MAR signal is performed using the ImageJ freeware.

2 Experimental Approach

2.1 Sampling and Incubation Planning

A thorough planning of the sampling strategy and the experimental design of the incubation conditions is the most critical step in the (q)MAR-FISH procedure. A sample should be as fresh as possible, and storage/transportation should be kept to a minimum to represent in situ conditions in the system investigated.

Any previous knowledge about the system (e.g., e-acceptor and e-donor) and rates of key processes will be advantageous in the planning of the experiment. Also information on the amount of biomass in the sample should be concordantly analyzed by determination of organic matter, suspended solids (SS), total number of bacteria (DAPI), or FISH. A proper biomass concentration should be found (we have often used 1–2 g SS/L, which usually results in a good biomass/substrate ratio in biofilm/activated sludge samples, but lower concentrations can also be used for oligotrophic environments). Dilution is made using cell-free water from the sample. It is also important to decide whether in situ conditions should be used (intact structure, in situ concentrations, etc.) which will mimic actual in situ activity or if the potential activity of microbes is the aim. The latter often requires gentle homogenization and higher substrate concentrations to ensure non-limiting conditions (see below). The tracer choice should be dictated by the required

level of MAR signal resolution (as discussed above), activity level of bacteria present (^{14}C-labelled substrate will produce a stronger signal than ^{3}H-labelled substrate), the position of the labelled atom in the molecule (should be incorporated into the biomass), and economic considerations (^{14}C-labelled substrates are generally more expensive than ^{3}H-labelled substrates).

The choice of substrate and electron acceptor concentration in the incubation should normally reflect the conditions in the original sample. The length of the incubation should typically represent the time required to incorporate sufficient radiotracer to detect the metabolizing cells. At the same time, it is important that not all the substrate is consumed to ensure the bacteria are labelled during the entire incubation time. An incubation time that is too long can increase the risk of cross-feeding or result in cell propagation. In active systems, 3–6 h-long incubation is typically used and somewhat longer for oligotrophic natural systems with less active cells. The tracer/substrate ratio should normally be kept as low as possible to avoid too fast substrate removal and to minimize the influence of possible radiotracer solvent (e.g., ethanol, xylene, or hydrochloric acid). Typically, 5–40 μCi (=0.185–1.48 MBq) has been used in each incubation (e.g., in 2 mL total sample volume with a biomass content of 1–2 g SS/L).

The environmental samples, the substrate stock, and other solutions required for the experiment are transferred to small serum bottles closed with thick butyl rubber stoppers. For anaerobic experiments, biomass and all the solutions are flushed/evacuated three times, using an evacuation pump and oxygen-free nitrogen prior to the experiment, and are added at time zero using strict anaerobic techniques. In some types of experiments, it is important to monitor the removal of electron donor/acceptor (such as nitrite or nitrate) during the incubation, e.g., in parallel control setups.

A negative control for the examination of adsorption phenomena and chemography is always performed on a pasteurized sample (70°C or 80°C for 10 min). This pasteurization must be made just prior to the experiment (to keep the effect of spore formation to a minimum). An alternative to pasteurization can be an addition of a suitable chemical inhibitory compound which arrests cell metabolic activity and does not react with silver in the film emulsion.

Each MAR incubation should be run in duplicate to ensure reliable results. Triplicate incubation is recommended for new microbial systems under investigation.

2.2 Fixation and Washing

The incubations are terminated by addition of the proper fixation agent. For archaea and Gram-negative bacteria, freshly prepared or recently defrosted 8% PFA is added to the vials (final concentration 3–4%). The fixation should take place at 4°C, and the length varies according to the nature of the cells of interest, typically between 30 min and 3 h. For fixation of Gram-positive bacteria, 1 volume of the sample is mixed with 1 volume of 96% ethanol.

The samples are centrifuged (for biofilm samples 3,800 × g and for single cells 10,000 × g for 10 min), and the pellets are washed three times with sterile filtered tap water or PBS buffer in order to remove the traces of radioactive substrates.

2.3 Homogenization and Glass Slides Preparation

If needed, homogenization can be performed at this point either by using the glass tissue grinder or by spotting the sample on one slide and rubbing it gently against another slide. Glass slides or cover glasses must be coated with an adhesive compound to prevent detachment of the cells. To prepare glass slides (or cover glasses) coated with gelatin, the slides are boiled for approximately 10 min in dH_2O with five drops of detergent (e.g., Prilan Perfect), washed thoroughly in dH_2O to remove the detergent, and placed in an upright position for min. 3 h until dry. 1% gelatin solution containing 0.1 g/L $CrK(SO_4)_2 \cdot 12H_2O$ is heated until both ingredients are dissolved and the slides are dipped in 70°C gelatin solution for 10 min. After that, they must be air-dried and are ready to use. Alternatively, poly-L-lysine coating can be performed.

After spreading the sample onto the coated slides, they are left to air-dry. The remaining sample can be stored at −20°C in a 50% ethanol/50% PBS solution.

Special staining procedures (like Gram or Neisser) can be made at this point.

2.4 FISH Procedure

The (q)MAR-FISH and (q)MAR-CARD-FISH combinations are best performed by following a standard FISH procedure (see below). For standard CARD-FISH procedure, see detailed protocols (e.g., [32]).

First, samples are dehydrated consecutively in 50%, 80%, and 96% ethanol solutions, 2 min each. Then, 2 mL of hybridization buffer with the proper stringency (salt, formamide) for the applied oligonucleotide probe is prepared according to Table 1. Hybridizations are typically designed to occur at 46°C but can be carried out at other temperatures by changing the matching formamide concentration according to the relation: 1% formamide = 0.65°C.

Table 1
Hybridization buffer composition

Reagent	Amount	Final concentration
5 M NaCl	360 µL	0.9 M
1 M Tris-HCl, pH 8.0	40 µL	20 mM
Formamide	0–1,600 µL[a]	0–80%[a]
Distilled H_2O	ad 2 mL	
10% SDS	2 µL	0.01%

[a] depending on the T_d of the probes used

Eight μL of hybridization buffer is transferred onto the slide within a small area (prepare one slide at a time to avoid evaporation of hybridization buffer and thus changed stringency). 1 μL of each gene probe (probe concentration 50 ng/μL) is added and mixed carefully (while mixing, avoid contact with the biomass) with the hybridization buffer. If more gene probes are added on the same slide, the order is immaterial – 1 μL of each of the probes is added to the well. Equimolar concentrations of competitor probe(s) are added if needed. If a large hybridization area is required, double volume of hybridization buffer and the probes can be used.

During hybridization, the slides must be kept horizontally in a moisture chamber (50 mL polyethylene tube with a piece of paper tissue soaked with 1.5 mL hybridization buffer). The slide is hybridized in an oven (46°C) for at least 1½ h (increased hybridization to less accessible regions of the ribosome has been shown to occur upon hybridization for up to 72 h [33]).

Probes with different T_d (requiring different formamide concentrations) cannot be applied together and must be applied in a double hybridization with two subsequent hybridizations, starting with the highest formamide concentration.

During hybridization, the washing buffer is prepared in a 50 mL polyethylene tube (formamide is replaced by NaCl, according to Table 2). The washing buffer is preheated in a 48°C water bath.

After hybridization, the samples are gently rinsed by pouring a few mL of preheated washing buffer over the slide. Each slide is

Table 2
Washing buffer composition

Formamide (%)	1 M Tris-HCl, pH 8.0 (μL)	10% SDS (μL)	5 M NaCl (μL)	0.5 M EDTA (μL)
0	1,000	50	9,000	0
5	1,000	50	6,300	0
10	1,000	50	4,500	0
15	1,000	50	3,180	0
20	1,000	50	2,150	500
25	1,000	50	1,490	500
30	1,000	50	1,020	500
35	1,000	50	700	500
40	1,000	50	460	500
45	1,000	50	300	500
50	1,000	50	180	500
55	1,000	50	100	500

transferred to a tube with the remaining preheated washing buffer and incubated for 15 min at 48°C (water bath).

Following the procedure for FISH or CARD-FISH, the slides must be rinsed by dipping in distilled water and air-dried. The slides must be completely dry before continuing onto the next step. Samples can now be stored at −20°C.

DAPI added prior to the FISH procedure will fade, and combinations of FISH with DAPI staining should now be performed. DAPI solution at a concentration of 1 μg/mL is spread over the biomass, and the cells are stained for 15 min in the dark. The DAPI concentration can be increased (up to 50 μg/mL) to improve brightness of the signal; however, this may also cause increased background fluorescence. After that, slides are rinsed with plenty of distilled water and left to air-dry.

2.5 Autoradiographic Procedure

The following procedures should be carried out in a darkroom equipped with safelight for black and white film development. The film emulsion (e.g., Ilford K5D film emulsion) is melted in a water bath (40°C) for 1 h. The film emulsion is carefully (avoid air bubbles) poured into the Hypercoat dipping vessel. Excess film emulsion can be reused several times without loss of sensitivity, although loss of chemicals, cells, etc., into the film will increase the background noise. Other types of emulsions (e.g., NTB-2, Kodak) can also be applied, but the preparation of the emulsion should be individually optimized before use.

The cover glass/glass slides are dipped carefully in the warm emulsion for 5 s, followed by placing the glass vertically on a folded Kleenex tissue for 5 s in order to get a similar thickness of emulsion on all slides. The back of the slide without the biomass is cleaned with a Kleenex tissue.

The slides are placed horizontally on a plastic tray for minimum 2 h in the dark to dry and solidify before they are placed in a slide box with a water-free silica gel. The slide box is wrapped in aluminum foil and stored at 4°C for the film to be exposed to radiation.

The exposure time is typically 2–20 days, depending on the sample type, labelling type and strength, incubation conditions, etc., and should be determined for each new system investigated. A set of identical samples can be developed (*see* below) with different time intervals to find the best duration of exposure. Optimization of exposure time is crucial for visualization of full range of metabolic activity of the cells present in the sample, which is of great importance if the results are to be quantified. To compare the activity level of bacteria in different samples, it is important to use similar incubation conditions and exposure time. Prolonged exposure time will produce increased background MAR signal.

2.6 Development

The slides are developed at room temperature by placing them in film developer (KODAK D19, final concentration 40 g/L) for 3 min. They are drip-dried before being placed in the stop solution (tap water) for 1 min.

Next, the slides are placed in a fixer (Na thiosulfate, final concentration 300 g/L, room temperature) for 4 min and can be further handled outside the darkroom, although fading of the FISH signals can occur in bright light or with prolonged storage in daylight. Therefore, it is recommended to keep the slides away from the light, if possible.

In order to remove the fixer, the slides are washed two times for 2 min in tap water and three times for 2 min in distilled water.

The slides are then completely air-dried for at least 3 h before microscopic investigation. Use of a fume hood speeds up the drying process.

Storage in the fridge (4°C) preserves MAR slides for at least 1 year, whereas the FISH signal will fade with time.

2.7 Microscopic Observation

Microscopic evaluation of (q)MAR-FISH samples can be best achieved by placing a small drop of antifading mountant on top of the sample, but under a cover glass. The results are visualized by shifting between fluorescent and transmitted light. Dark silver grains are easily observed on top of the radiolabelled DAPI or FISH-stained cells. The cells should have a silver grain density clearly exceeding the background level to be considered MAR positive. Evaluation of the FISH signal might be hampered by the presence of dense layers of silver grains. This can be avoided by carrying out the whole MAR-FISH procedure on thin cover glasses (e.g. 24 × 60 mm) instead of the microscopic glass slides examining the sample through the glass. In this way, the silver grains are underneath the cells rather than covering them, making it easier to visualize the FISH signal.

For the MARQuant analysis, sets of fluorescent micrographs and corresponding bright-field MAR signal images from the same field of view are acquired. Fifty is the recommended minimum number of cells for the analysis in order to obtain statistically reliable results.

2.8 Image Analysis

The MARQuant image analysis tool enables automated quantification of substrate uptake activity in single bacterial cells based on the data contained in fluorescent and bright-field MAR image sets containing fluorescently tagged cells and MAR signals, respectively. Detailed information about the software can be found at www.cmc.aau.dk or [13]. An overview of the image analysis facilitated by the MARQuant program is presented in Fig. 2. The cells (visualized with, e.g. FISH-specific probe) are localized in the fluorescent image, and MAR signal is measured in the bright-field image within user-defined regions around the single cells. The number of silver grains per cell is determined by measurement of the total area of MAR signal associated with the cell, divided by the area of a single

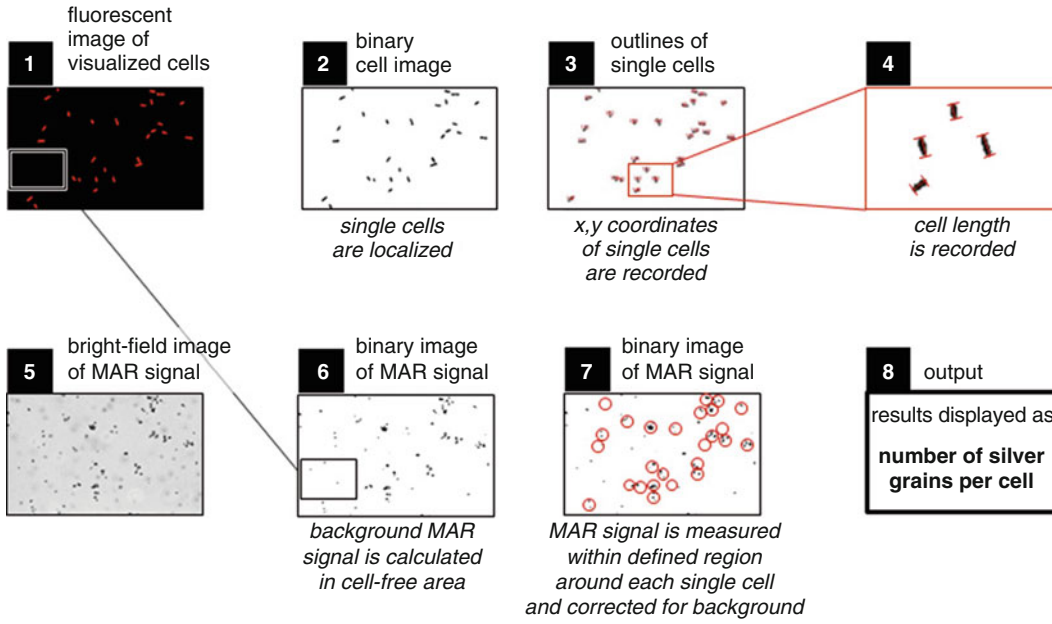

Fig. 2 An overview of image-processing analysis steps employed by the MARQuant tool facilitating quantification of MAR results

silver grain. The area value of the single silver grain is determined for each image by calculation of the average area of all single silver grains localized in the image. Only single detached cells of target bacteria should be analyzed to avoid the risk of false-positive signals from any attached nontarget cells.

For each data set analyzed, a set of manual measurements must be performed in order to determine the pixel range corresponding to the size of the cells and silver grains in the images. Additionally, the area around the cell, within which MAR signal will be measured (called measuring region), must be optimized for each data set investigated. Too small a region can result in underestimation of the silver grains produced by the cell, while too large a region increases the risk of overlap with the MAR signal of other cells. The measuring region is dependent on cell size (length) and the type of tracer used. In order to determine the optimal size of this region, silver grains must be quantified repeatedly for the same set of cells, using measuring regions of increasing diameters. The optimal measuring region is chosen where the increase of the measuring region diameter does not result in a corresponding increase in the number of silver grains (e.g., measuring region with the diameter of 2× cell length is usually optimal to measure MAR signal of ^{3}H-labelled substrates).

After the measured/optimized parameters are implemented to the MARQuant tool script, the image analysis is performed with minimal user input.

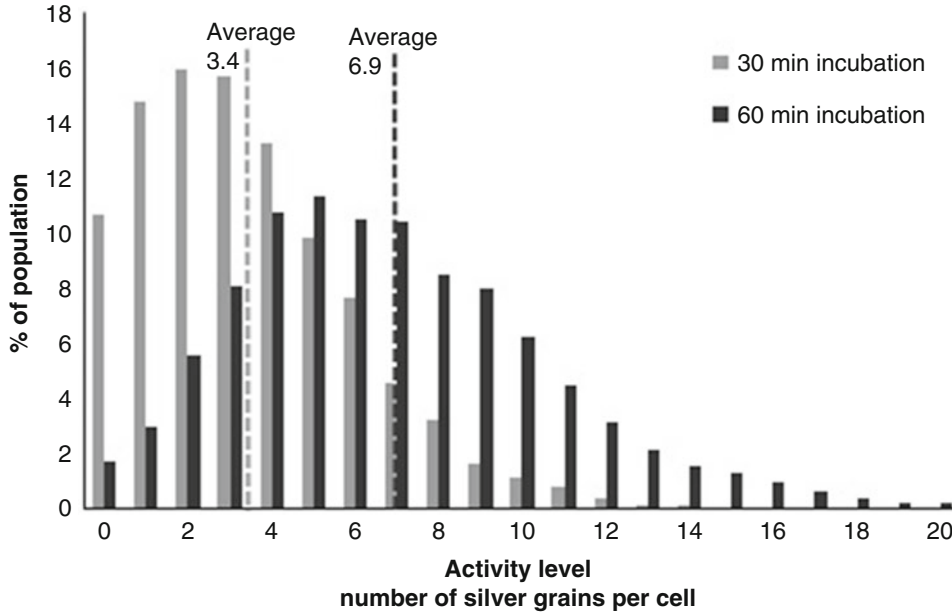

Fig. 3 Substrate uptake quantification in exponentially growing *E. coli* culture incubated for 30 and 60 min with ^{3}H-glucose

Figure 3 presents an example of the results captured using MARQuant image analysis tool. In this data set, ^{3}H-glucose uptake was compared in exponentially growing *E. coli* culture after cells were incubated with the labelled substrate for 30 and 60 min. Since the results are output as number of silver grains per cell, it is possible to construct the distribution of substrate uptake activity across the population. However, a more detailed analysis has shown that for single cells, it is not possible to acquire reliable results since MAR generates a method-related distribution of the observed substrate uptake activity, which can obscure the potential distribution of biological activity. This is caused by the fact that, for cells of a small size, only a limited number of silver grains can be produced around those particular cells. Moreover, to ensure a reliable quantification, silver grains should not overlap so the average number of grains per cell should be around 5. Since each silver grain produced in the film emulsion has a defined probability of being developed, for a set of cells with identical metabolic activity, the number of silver grains developed by these cells can differ by several grains showing an "artificial" distribution. Therefore, only the average substrate uptake per cell should be used to represent the whole population and can be compared between different samples and conditions.

Given that important bacterial cells are often present in filamentous form in the environment, the MARQuant allows quantitative determination of substrate uptake for organisms with this morphology by calculating the number of silver grains per μm of

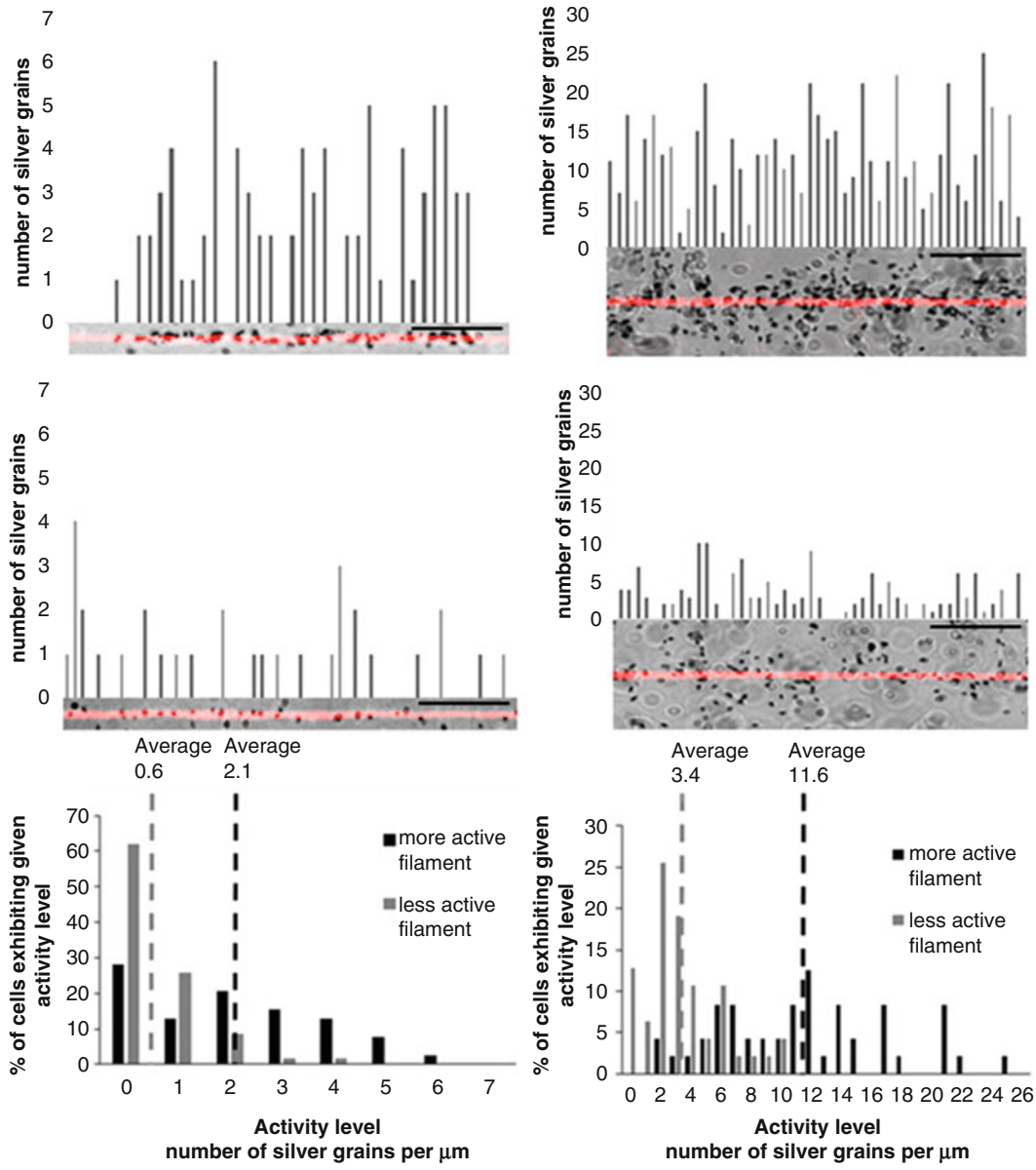

Fig. 4 Example of substrate uptake quantification in filamentous *Thiothrix* incubated with ^{3}H-acetate (*left panel*) and ^{14}C-propionate (*right panel*). Small stretches of the filaments are highlighted in *red*. Scale bar represents 10 μm

the filament. Figure 4 shows an example of how the quantification of substrate uptake is performed for filamentous bacteria. Since the size of the entire filament is considerably larger than single cells, the substrate uptake activity can be compared between filaments belonging to the same sample.

The usefulness of MARQuant tool was demonstrated by confirmation of the ability of polyphosphate accumulation in a novel *Halomonas* present in activated sludge [11] and by confirmation of denitrification capability in three previously unrecognized denitrifiers present in the activated sludge community [12].

2.9 Solutions and Materials

Gelatin and $CrK(SO_4)_2 \cdot 12H_2O$

Isotopes, e.g., ^{3}H-glucose, ^{14}C-trioleic acid (crystalline or aqueous)

Cold (nonradioactive) substrates, electron acceptors, inhibitors, etc.

Paraformaldehyde (8%) (in phosphate-buffered saline, pH 7.0) and/or ethanol 96%

4,6-Diamidino-2-phenylindole (DAPI; 1 mg/mL) and/or FISH oligonucleotide probes targeting specific bacteria (e.g. from Thermo Scientific)

2.9.1 PBS Solution

Film emulsion (e.g., Ilford K5D from Polysciences, Inc.)

Glass slides or cover glasses (gelatin or poly-L-lysine coated)

Developer (e.g., KODAK D19)

Stop and washing solutions (tap and distilled water)

Fixer (sodium thiosulfate)

Darkroom with safelight (using e.g. an Ilford® 906 filter). Safelight filter must be chosen, taking into consideration the type of film emulsion used.

Silica gel

Antifading mountant (e.g., Citifluor®, VECTASHIELD®, or mixtures hereof)

ImageJ software (http://rsbweb.nih.gov/ij/)

2.10 Important Considerations

2.10.1 Soil Samples

MAR on sediment and soil samples with a high content of inorganic particles is difficult to interpret as these particles can resemble the silver grains. Large particle may penetrate the film emulsion and cause variations in the thickness of the film and thus the layer in which silver grains can develop. Separation of cells from the particles by density-gradient centrifugation, e.g., in a Nycodenz cushion density medium [34], and applying only the cell fraction can solve this problem.

2.10.2 Duration of the Experiment

The whole procedure from start of incubation to the microscopic evaluation will typically last 1–3 weeks, depending on the activity of the target organisms. Highly active microbial communities can be examined in as little as a few days, while slow-growing communities require exposure times of several weeks. Careful planning of the incubation conditions can reduce the duration of the exposure time, and especially, optimization of the tracer/substrate ratio for the incubation is important.

2.10.3 Preincubation

Under some conditions, the substrate is taken up and used for growth; under others, it is used to build up storage products, or it is simply not catabolized into the biomass but released, e.g., as CO_2. Under conditions where the bacteria can only form storage compounds from a certain substrate (e.g., the polyphosphate-accumulating organisms [35]), this can be discriminated by performing preincubation steps of different lengths with addition of unlabelled substrate to saturate the storage capacity prior to addition of tracer. Alternatively, careful examination of the concomitant uptake of ^{14}C-bicarbonate (anaplerotic CO_2 fixation by heterotrophic microorganisms), in the presence or absence of an organic substrate, can be used to discriminate between storage and substrate oxidation [16].

2.10.4 Negative Control

Adsorption of hydrophobic tracers/substrates to cell surfaces and inorganic surfaces can cause false-positive MAR signals. This phenomenon can be visualized in the pasteurized control or in controls harvested immediately after addition of the tracer. One solution can be the addition of unlabelled substrate in order to saturate surfaces prior to the addition of labelled substrate.

2.10.5 Homogenization

Large aggregates or particles are often not covered completely by the photographic emulsion, which hampers the formation of silver grains directly above the aggregate, even if sufficient radioactive label is present. This will then result in a false-negative area of microorganisms in the center, often surrounded by a ring of MAR-positive cells. Moreover, aggregates with several layers of microorganisms can cause uncertainty as to the origin of the MAR signal. This can be prevented by homogenization or by cryosectioning of the sample after fixation.

2.10.6 Background Fluorescence

High background fluorescence in the sample can cause difficulties in visualizing the FISH signals. This can often be helped by choosing a fluorophore with high fluorescence, relative to the background fluorescence, or by replacing normal FISH with CARD-FISH (e.g., [31]).

2.10.7 Quantitative MAR Results Interpretation

The MAR signal produced by the cells is a quantitative reflection of cell metabolic activity; however, it must be kept in mind that the number of silver grains produced by the cell is dependent on the amount of radioactive substrate incorporated into cell mass. Since different cells, or even the same cells under different environmental conditions, may use various metabolic pathways to catabolize the substrate, one should be careful when interpreting and directly comparing quantitative MAR results, especially for microorganisms about the metabolism of which little is known.

3 Research Needs

Over the past few years, the field of microbial ecology has seen a continuous expansion of knowledge, thanks to the advanced development and increased availability of the omics techniques deciphering the identity and functions of previously unknown microbes in natural ecosystems. Single cell techniques, such like MAR-FISH and NanoSIMS or micro-Raman [36, 37], are and will stay vital in the future research to test the hypotheses set by the environmental omics data. A combination of these methods allows very detailed studies of single cell microbiology in complex microbial ecosystems to be carried out.

References

1. Lee N, Nielsen PH, Andreasen K, Juretschko S, Nielsen JL, Schleifer K-H, Wagner M (1999) Combination of fluorescent in situ hybridization and microautoradiography – a new tool for structure-function analysis in microbial ecology. Appl Environ Microbiol 65:1289–1297
2. Ouverney CC, Fuhrman JA (1999) Combined microautoradiography-16S rRNA probe technique for determination of radioisotope uptake by specific microbial cell type in situ. Appl Environ Microbiol 65:1746–1752
3. Albertsen M, Hugenholtz P, Skarshewski A, Nielsen KL, Tyson GW, Nielsen PH (2013) Genome sequences of rare, uncultured bacteria obtained by differential coverage binning of multiple metagenomes. Nat Biotechnol 31 (6):533–538
4. Rinke C, Lee J, Nath N, Goudeau D, Thompson B, Poulton N, Dmitrieff E, Malmstrom R, Stepanauskas R, Woyke T (2014) Obtaining genomes from uncultivated environmental microorganisms using FACS–based single-cell genomics. Nat Protoc 9(5):1038–1048
5. Brock TD, Brock ML (1966) Autoradiography as a tool in microbial ecology. Nature 209:734–736
6. Brock ML, Brock TD (1968) The application of micro-autoradiographic techniques to microbial ecology. Fur Theoretishe and Angewandte Limnologie 15:1–29
7. Nielsen JL, Christensen D, Kloppenborg M, Nielsen PH (2003) Quantification of cell-specific substrate uptake by probe-defined bacteria under in situ conditions by microautoradiography and fluorescence in situ hybridization. Environ Microbiol 5 (3):202–211
8. Nielsen PH, de Muro MA, Nielsen JL (2000) Studies on the in situ physiology of *Thiothrix* spp. present in activated sludge. Environ Microbiol 2(4):389–398
9. Sintes E, Herndl GJ (2006) Quantifying substrate uptake by individual cells of marine bacterioplankton by catalyzed reporter deposition fluorescence in situ hybridization combined with microautoradiography. Appl Environ Microbiol 72(11):7022–7028
10. Miura Y, Okabe S (2008) Quantification of cell specific uptake activity of microbial products by uncultured *Chloroflexi* by microautoradiography combined with fluorescence in situ hybridization. Environ Sci Technol 42 (19):7380–7386
11. Nguyen HTT, Nielsen JL, Nielsen PH (2012) "Candidatus Halomonas phosphatis", a novel polyphosphate-accumulating organism in full-scale enhanced biological phosphorus removal plants. Environ Microbiol 14(10):2826–2837
12. McIlroy SJ, Starnawska A, Starnawski P, Saunders AM, Nierychlo M, Nielsen PH, Nielsen JL (2014) Identification of active denitrifiers in full-scale nutrient removal wastewater treatment systems. Environ Microbiol. doi:10.1111/1462-2920.12614
13. Nierychlo M, McIlroy SJ, Larsen P, Nielsen JL, Nielsen PH. MARQuant – a microautoradiography image analysis tool for quantification of substrate uptake of bacterial populations (submitted)
14. Nielsen JL, Nielsen PH (2005) Advances in microscopy: microautoradiography of single cells. In: Leadbetter JR (ed) Methods in enzymology, vol 397. Academic, San Diego, pp 237–256

15. Wagner M, Nielsen PH, Loy A, Nielsen JL, Daims H (2006) Linking microbial community structure with function: fluorescence in situ hybridization - microautoradiography and isotope arrays. Curr Opin Biotechnol 17:1–9
16. Hesselsoe M, Nielsen JL, Roslev P, Nielsen PH (2005) Isotope labeling and microautoradiography of active heterotrophic bacteria based on assimilation of $^{14}CO_2$. Appl Environ Microbiol 71:646–655
17. Nguyen HTT, Le VQ, Hansen AA, Nielsen JL, Nielsen PH (2011) High diversity and abundance of putative polyphosphate-accumulating *Tetrasphaera*-related bacteria in activated sludge systems. FEMS Microbiol Ecol 76 (2):256–267
18. Lolas IB, Chen X, Bester K, Nielsen JL (2012) Identification of triclosan-degrading bacteria using stable isotope probing, fluorescence in situ hybridization and microautoradiography. Microbiology 158(Pt_11):2796–2804
19. Beamud SG, Karrasch B, Pedrozo FL, Diaz MM (2014) Utilisation of organic compounds by osmotrophic algae in an acidic lake of Patagonia (Argentina). Limnology 15(2):163–172
20. Alonso C (2012) Tips and tricks for high quality MAR-FISH preparations: focus on bacterioplankton analysis. Syst Appl Microbiol 35 (8):503–512
21. Meyer-Reil L-A (1978) Autoradiography and epifluorescence microscopy combined for the determination of number and spectrum of actively metabolizing bacteria in natural waters. Appl Environ Microbiol 36:506–512
22. Rogers AW (1979) Techniques of autoradiography. Elsevier, New York
23. Tabor SP, Neihof RA (1982) Improved microautoradiographic method to determine individual microorganisms active in substrate uptake in natural waters. Appl Environ Microbiol 44:945–953
24. Carman K (1993) Microautoradiographic detection of microbial activity. In: Kemp PF, Sherr BF, Sherr EB, Cole JJ (eds) Handbook of methods in aquatic microbial ecology. Lewis, London, pp 397–404
25. Andreasen K, Nielsen PH (1997) Application of microautoradiography for the study of substrate uptake by filamentous microorganisms in activated sludge. Appl Environ Microbiol 63:3662–3668
26. Andreasen K, Nielsen PH (2000) Growth of *Microthrix parvicella* in nutrient removal activated sludge plants: studies of in situ physiology. Water Res 34:1559–1569
27. Nielsen JL, Nielsen PH (2009) Combined microautoradiography and fluorescence in situ Hybridization (MAR-FISH) for the identification of metabolically active microorganisms. In: Timmis KN (ed) Microbiology of hydrocarbons, oils, lipids. Springer, Berlin Heidelberg, pp 4093–4102
28. Okabe S, Satoh H, Kindaichi T (2011) Chapter seven - a polyphasic approach to study ecophysiology of complex multispecies nitrifying biofilms. In: Klotz MG, Stein L (eds) Methods in enzymology. Academic, New York, pp 163–184
29. Wagner M (2011) FISH-microautoradiography and isotope arrays for monitoring the ecophysiology of microbes in their natural environments. In: Murrell JC, Whiteley AS (eds) Stable isotope probing and related technologies. ASM, Washington, pp 305–316
30. Teira E, Reinthaler T, Pernthaler A, Pernthaler J, Herndl GJ (2004) Combining catalyzed reporter deposition-fluorescence in situ hybridization and microautoradiography to detect substrate utilization by bacteria and archaea in the deep ocean. Appl Environ Microbiol 70:4411–4414
31. Nielsen JL, Klausen C, Nielsen PH, Burford M, Jorgensen NOG (2006) Detection of activity among uncultured *Actinobacteria* in a drinking water reservoir. FEMS Microbiol Ecol 55:432–438
32. Pernthaler A, Pernthaler J (2007) Fluorescence in situ hybridization for the identification of environmental microbes. In: Hilario E, Mackay J (eds) Protocols for nucleic acid analysis by nonradioactive probes, vol 353, 2nd edn. Humana Press, Totowa, pp 153–176
33. Yilmaz LS, Ökten HE, Noguera DR (2006) Making all parts of the 16S rRNA of *Escherichia coli* accessible in situ to single DNA oligonucleotides. Appl Environ Microbiol 72:733–744
34. Lindahl V, Bakken LR (1995) Evaluation of methods for extraction of bacteria from soil. FEMS Microbiol Ecol 16:135–142
35. Kong YH, Nielsen JL, Nielsen PH (2005) Identity and ecophysiology of uncultured actinobacterial polyphosphate-accumulating organisms in full-scale enhanced biological phosphorus removal plants. Appl Environ Microbiol 71:4046–4085
36. Behrens S, Lösekann T, Pett-Ridge J, Weber PK, Ng WO, Stevenson BS, Hutcheon ID, Relman DA, Spormann AM (2008) Linking microbial phylogeny to metabolic activity at the single-cell level by using enhanced element labelling-catalyzed reporter deposition fluorescence in situ hybridization (EL-FISH) and NanoSIMS. Appl Environ Microbiol 74:3143–3150
37. Huang WE, Stoecker K, Griffiths R, Newbold L, Daims H, Whiteley AS, Wagner M (2007) Raman-FISH: combining stable-isotope Raman spectroscopy and fluorescence in situ hybridization for the single cell analysis of identity and function. Environ Microbiol 9:1878–1889

Protocol for In Situ Detection of Functional Genes of Microorganisms by Two-Pass TSA-FISH

Kengo Kubota and Shuji Kawakami

Abstract

An approach is presented for the detection of functional genes on chromosomal DNA in prokaryotes by two-pass tyramide signal amplification–fluorescence in situ hybridization (two-pass TSA-FISH). Functional genes are hybridized with 2,4-dinitrophenol (DNP)-labeled polynucleotide probes or digoxigenin-labeled oligonucleotide probes. Horseradish peroxidase (HRP)-labeled antibody is then immunologically bounded, and a first round of TSA with DNP-labeled tyramide is carried out. After the second immunological reaction with HRP-labeled anti-DNP antibody, cells hybridized with the probes are detected upon a second round of TSA with fluorescent-labeled tyramide. As a case study, we describe the use of two-pass TSA-FISH to detect the methanogenesis marker gene *mcrA*, which encodes the alpha subunit of methyl coenzyme M reductase in methanogenic archaea. Practical suggestions for using the two-pass TSA-FISH method are presented as well.

Keywords: Catalyzed reporter deposition, Fluorescence in situ hybridization, Functional genes, Methyl coenzyme M reductase (*mcr*) gene, Prokaryotic cells, Tyramide signal amplification

1 Introduction

Because most microorganisms cannot be cultivated using currently available techniques, molecular approaches for deciphering specific microbial functions at single-cell resolution are urgently needed if we are to understand the ecophysiology of environmental microorganisms. Fluorescence in situ hybridization (FISH) was developed more than 20 years ago for the detection, identification, and enumeration of environmental microorganisms [1]. Microorganisms can also be identified based on specific functions through the detection of functional genes encoded on chromosomal DNA and/or by the detection of specific mRNA [2]. The detection of functional genes gives an indication of microbial functional potential, whereas the detection of specific mRNAs can indicate the transcription of target functional genes.

T.J. McGenity et al. (eds.), *Hydrocarbon and Lipid Microbiology Protocols*, Springer Protocols Handbooks (2016) 131–144,
DOI 10.1007/8623_2015_71, © Springer-Verlag Berlin Heidelberg 2015, Published online: 04 April 2015

A number of methods are available for the detection of prokaryotic functional genes, and these methods fall into three categories: nucleic acid amplification, probe network, and enzymatic signal amplification. Nucleic acid amplification includes methods such as in situ PCR (polymerase chain reaction) [3], in situ LAMP (loop-mediated isothermal amplification) [4], in situ RCA (rolling circle amplification) [5, 6], and CPRINS (cycling primed in situ amplification)-FISH [7]. These methods involve initial amplification of a target functional gene using DNA polymerase, and the gene is detected by subsequent FISH targeting the amplified products. The probe network is also known as RING (recognition of individual gene)-FISH [8], in which high concentrations of RNA polynucleotide probes are used to form a network that is anchored at the targeted sequence. Enzymatic signal amplification utilizes tyramide signal amplification (TSA)-based techniques. TSA is also known as CARD (catalyzed reporter deposition). In TSA, horseradish peroxidase (HRP) mediates the deposition of tyramide, which can be labeled with a variety of fluorescent and hapten molecules. CARD-FISH was initially used for rRNA detection [9, 10] and more recently has been used for detection of mRNAs [11, 12] and functional genes [13–15].

CARD-FISH has limited sensitivity for the detection of mRNAs and functional genes [12, 14, 16]. Two-pass TSA-FISH was developed to overcome this limitation (Fig. 1) [12–14]. In two-pass TSA-FISH, hapten-labeled tyramide is deposited in a first round of TSA. Subsequent to the immunological reaction with an HRP-labeled antibody, a second round of TSA is carried out with fluorescent-labeled tyramide. Detection of the alpha subunit of the methyl coenzyme M reductase gene (*mcrA*) in a methanogen using oligonucleotide probes was the first reported application of two-pass TSA-FISH for the detection of functional genes in prokaryotes [14]. More recently, two-pass TSA-FISH using polynucleotide probes was developed and demonstrated through the detection of *mcrA* and *apsA*, the latter of which encodes the alpha subunit of adenosine-5′-phosphosulfate kinase [13].

Two-pass TSA-FISH enables the detection of functional genes using both oligonucleotide and polynucleotide probes. Advantages and disadvantages of the technique are described elsewhere [17]. In brief, oligonucleotide probes show higher specificity, higher probe design flexibility, and greater ability to penetrate into cells. The major advantage of polynucleotide probes is high sensitivity. In the previous studies, we found that the detection efficiency (*see* **Note 1**) was only 15–20% when two-pass TSA-FISH with oligonucleotide probes targeting a single-copy gene (e.g., *mcrA* gene) on chromosome was applied although single-base mismatches could be distinguished [14]. In contrast, two-pass TSA-FISH with polynucleotide probes achieved very high detection efficiency (>98%) [13]. The length of the polynucleotide

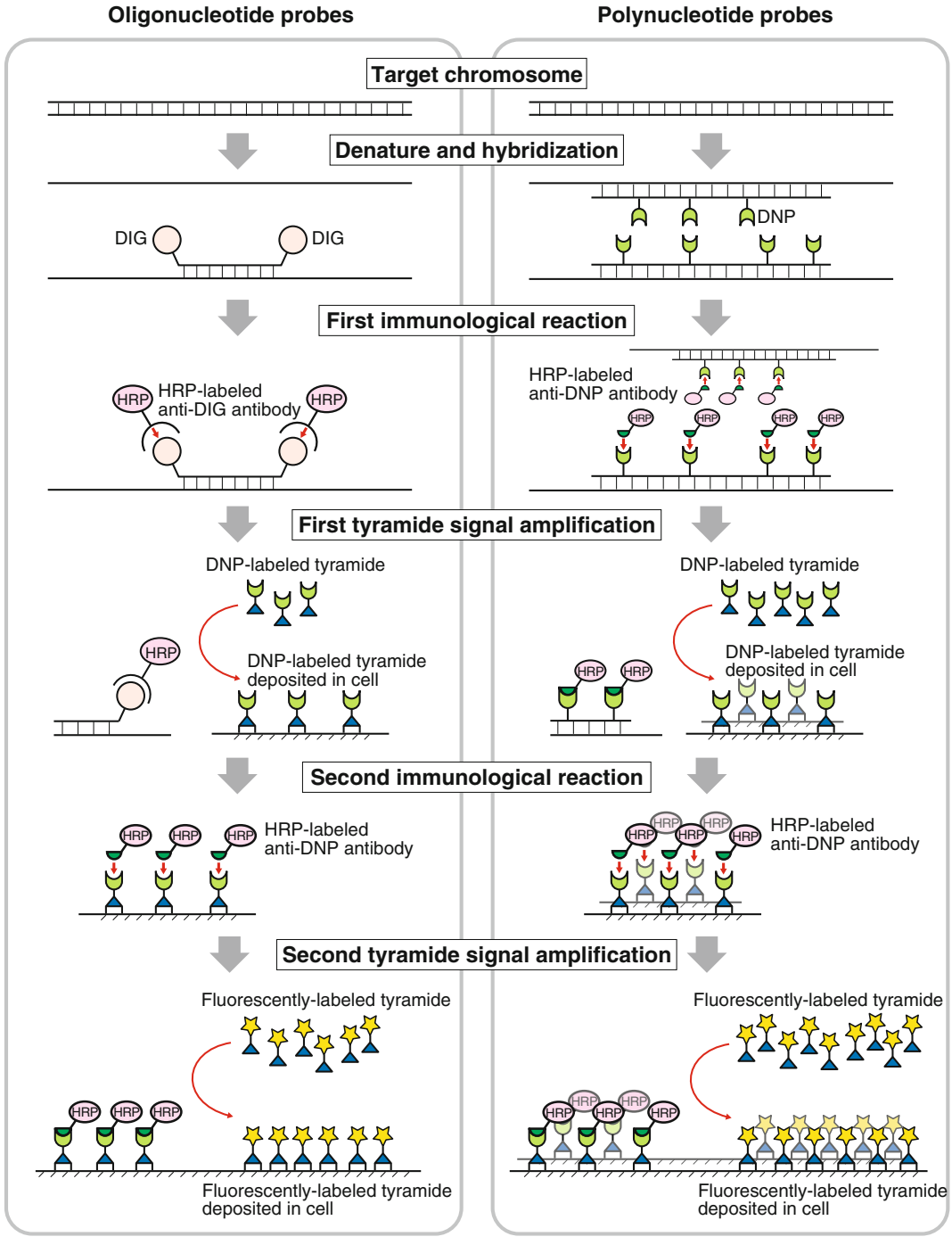

Fig. 1 Schematic flow diagram of two-pass TSA-FISH with oligonucleotide probes (*left*) and polynucleotide probes (*right*)

probe affects the detection efficiency; the longer the probe, the higher the detection efficiency (*see* **Note 2**).

This chapter describes a protocol for the detection of functional genes by two-pass TSA-FISH using either oligonucleotide or polynucleotide probes. As a case study, a protocol for the detection of *mcrA* in methanogens is presented. The *mcrA* gene catalyzes the final step of methanogenesis and is often used as a marker gene.

2 Materials

2.1 Preparation of Polynucleotide Probes

1. *Taq* polymerase and PCR buffer (e.g., AmpliTaq Gold [Applied Biosystems])
2. dATP, dTTP, dCTP, dGTP (Applied Biosystems)
3. DNP-11-dUTP (PerkinElmer)

2.2 Fixation

1. PBS (137 mM NaCl, 8.1 mM Na_2HPO_4, 2.68 mM KCl, 1.47 mM KH_2PO_4, pH 7.4)
2. 4% paraformaldehyde (w/v) solution in PBS
3. Ethanol (absolute ethanol stored at −20°C)

2.3 Embedding and RNase Treatment

1. 0.01% sodium dodecyl sulfate (SDS) (w/v) dissolved in ultrapure water
2. 1% low-melting-point agarose (w/v) dissolved in ultrapure water [e.g., UltraPure Low Melting Point Agarose (Life Technologies)]
3. RNase solution [0.5 mg/mL of RNase A (NIPPON GENE) in 10 mM Tris–HCl (pH 7.5) and 15 mM NaCl]
4. Tris-NaCl-Tween 20 (TNT) buffer [100 mM Tris–HCl (pH 7.5), 150 mM NaCl, 0.05% Tween 20 (v/v)]

2.4 Permeabilization

1. 1 M HEPES (pH 7.0)
2. 1 M dithiothreitol (store at −20°C in small aliquot)
3. 210 mM Na_2S (store at −20°C in small aliquot)
4. Recombinant pseudomurein endopeptidase (rPeiW) enzyme (it is generated as previously described [18], and the activity was measured according to Nakamura et al. [19])

2.5 Two-Pass TSA-FISH with Polynucleotide Probes

1. Formamide
2. 20× SSC [300 mM trisodium citrate (pH 7.5) and 3 M NaCl]
3. 40% dextran sulfate (w/v) (average molecular weight of 500,000, from GE Healthcare Life Sciences) dissolved in ultrapure water

4. 10% blocking reagent (w/v) (Roche) in maleic acid buffer (prepared according to the manufacturer's instructions)
5. 10% SDS (w/v) in ultrapure water
6. 50× Denhardt's solution (Sigma-Aldrich)
7. 10 mg/mL solution of sheared salmon sperm DNA (Ambion)
8. PCR-generated polynucleotide probe (2.5 ng/μL)
9. 10% bovine serum albumin (BSA) (w/v) in PBS
10. HRP-labeled anti-DNP antibody (PerkinElmer)
11. Tyramide-DNP (PerkinElmer)
12. Amplification diluent (PerkinElmer)

2.6 Two-Pass TSA-FISH with Oligonucleotide Probes

1. LNA/DNA oligonucleotide probe (10 pmol/μL)
2. HRP-labeled anti-DIG antibody (Roche)

3 Methods

3.1 Probe Preparation

3.1.1 Polynucleotide Probes

Polynucleotide probes are generated by PCR, during which 2,4-dinitrophenol (DNP)-11-dUTP is incorporated into the probes. Polynucleotide probes ranging from 150 to 850 bp in length have to be used successfully [13]. The longer the probe, the higher the detection efficiency, so it is recommended to prepare longer probes (tested up to approximately 850 bp) (*see* **Note 2**). We generally employ primers used for phylogenetic analyses of functional genes because they are often designed to target conserved regions of a functional gene sequence. Templates can be genomic DNA obtained from pure cultures or genomic DNA extracted from a sample of interest. It should be noted that because of low discrimination power of polynucleotides, it is difficult to detect only a target sequence using polynucleotide probes (detection depends on the stringency of hybridization, but only 70–85% sequence identity can be discriminated [13]). Therefore, polynucleotide probes are useful when the discrimination of alleles is not strictly needed.

To achieve high labeling efficiency and high probe yield, the concentrations of DNP-11-dUTP and Mg^{2+} in the PCR mixture are important. Although the labeling efficiency increases with increasing DNP-11-dUTP concentration, the probe yield decreases [13]. Similarly, although the probe yield increases with increasing Mg^{2+} concentration, the risk of nonspecific amplification is increased [13]. Elongation of PCR extension time sometimes improves the yield of probe (*see* **Note 3**). In the protocol presented here, DNP-11-dUTP is used for probe synthesis; however, fluorescein-12-dUTP (PerkinElmer) can be used, in which case HRP-

labeled anti-fluorescein antibody should be used (PerkinElmer). The concentrations of fluorescein-12-dUTP for probe preparation and HRP-labeled anti-fluorescein antibody for immunological reactions should be optimized as well as the case of using DNP-11-dUTP and HRP-labeled anti-DNP antibody. Alternatively, a PCR digoxigenin (DIG) Probe Synthesis Kit (Roche) can be used. The kit is already optimized for labeling sufficient number of DIG to probe. HRP-labeled anti-DIG antibody (Roche) should be used for the first immunological reaction, and the concentration of HRP-labeled anti-DIG antibody needs to be optimized as well as HRP-labeled anti-DNP antibody.

1. Extract DNA from a sample of interest or a pure culture.
2. Prepare a set of specific primers to amplify the gene of interest. The ME1f (5′-GCM ATG CAR ATH GGW ATG TC-3′)-ME2r (5′-TCA TKG CRT AGT TDG GRT AGT-3′) primer set [20] is used to amplify *mcrA* for the case study.
3. Prepare the PCR mixture as follows: 0.025 U/μL of Taq polymerase; 0.5 pmol/μL of each primer; 200 μM dATP, dCTP, and dGTP; 140 μM dTTP; 60 μM DNP-11-dUTP; and 3.5 mM Mg^{2+} in 1X PCR buffer. The concentrations of DNP-11-dUTP and Mg^{2+} should be optimized for each primer set. The total combined concentration of both dTTP and DNP-11-dUTP is kept at 200 μM.
4. Add template DNA and perform PCR. PCR conditions for the ME1f–ME2r primer set should be as follows: initial denaturation at 95°C for 7 min, followed by 35 cycles of 95°C for 40 s, 55°C for 30 s, and 72°C for 3 min.
5. Evaluate the quality of PCR products using an Agilent 2100 Bioanalyzer or by gel electrophoresis.
6. Purify the PCR products using a MinElute PCR purification kit (QIAGEN) or similar kit.
7. Measure the probe concentration using a photospectrometer or a spectrometer. The number of labeled DNPs per probe can also be calculated based on the molar absorbance coefficient of DNP (*see* **Note 4**).
8. Store the probes at −20°C and adjust the probe concentration to 2.5 ng/μL in 10 mM Tris–HCl (pH 7.5) before use.

3.1.2 Oligonucleotide Probes

The design of oligonucleotide probes is more flexible than that of polynucleotide probes. Oligonucleotide probes can be designed to target either conserved or specific regions of a gene of interest. For oligonucleotide probes used in two-pass TSA-FISH, every second base of the sequence is substituted with locked nucleic acid (LNA) in order to achieve high affinity to the target DNA according to the results of Silahtaroglu et al. [21] who showed LNA substitutions

with every other base give the best results. Probes without LNA substitutions are not suitable because of low binding affinity. There are two patterns of probes that can be considered: LNA substitution starting from the first base and starting from the second base from the 5′ end of the sequence. Check the secondary structure and employ the lower-stability pattern. Labeling of hapten should be done at both the 5′ and 3′ ends of the oligonucleotide probe in order to increase the sensitivity. LNA substitutions increase the binding affinity of the oligonucleotide [21, 22], and thus hybridization stringency should be optimized for each designed probe (*see* **Note 5**). For the case study, DIG-labeled probes are prepared, but either DNP- or fluorescein-labeled probes can be used.

3.2 Sample Fixation (Either Paraformaldehyde or Ethanol)

Paraformaldehyde or ethanol is often used as a fixative. Fixation with paraformaldehyde results in better morphological preservation, but less permeabilized than ethanol fixation. Ethanol fixation renders cells more permeable, but some microorganisms are sensitive to ethanol fixation and will be lost from the sample.

3.2.1 Paraformaldehyde Fixation

1. Harvest cells and wash with PBS.
2. Suspend cells with 1 volume of PBS followed by addition of 3 volumes of 4% paraformaldehyde solution.
3. Incubate for 4–12 h at 4°C.
4. Wash cells twice with PBS and suspend with 1 volume of PBS.
5. Add 1 volume of ice-cold ethanol and store at −20°C (*see* **Note 6**).

3.2.2 Ethanol Fixation

1. Harvest cells and wash with PBS.
2. Suspend cells with 1 volume of PBS, add 1 volume of ice-cold ethanol, and store at −20°C (*see* **Note 6**).

3.3 Embedding and RNase Treatment

1. Mix 1 volume of the fixed cell sample with 1 volume of 0.01% SDS and 7 volumes of PBS. The sample should be adjusted to the appropriate concentration before mixing. Incubate the mixture at 60°C for 20 to 60 s (depends on the amount of the mixture) (*see* **Note 7**).
2. Add 1 volume of pre-warmed 1% low-melting-point agarose to the mixture (*see* **Note 8**). Incubate the mixture at 60°C for 20 to 60 s (depends on the amount of the mixture).
3. Apply the mixture to each well of a glass slide. Generally, we apply 8 μL of mixture to each well of a 10-well glass slide (Matsunami).
4. Dry at 60°C for 10 min in an oven.

5. Dehydrate and desalt through an ethanol series (50, 80, and 95% ethanol for 5, 1, and 1 min, respectively) and then air dry the slide.
6. Treat with RNase A for 30 min at 37°C. To each well add 15–20 μL of RNase solution in the case of a 10-well glass slide. The slide should be placed in a chamber humidified with ultrapure water during incubation.
7. Immerse the glass slide in TNT buffer for 10 min, in ultrapure water for 1 min, and in absolute ethanol for 1 min, and then air dry.

3.4 Cell Permeabilization

Target cells should be permeabilized using either lysozyme, proteinase K, achromopeptidase, rPeiW, or other appropriate method to allow for penetration of probes and antibodies [17]. Treatment with rPeiW [19, 23] is described as a case study. rPeiW works under anaerobic conditions. Moisture chambers are prepared using 50-mL disposable tubes (1 slide per tube) rather than a large box (many slides in a box). All steps should be handled in a fume hood.

1. Prepare a buffer consisting of 50 mM HEPES (pH 7.0), 5 mM dithiothreitol, and 21 mM Na_2S.
2. Prepare a moisture chamber humidified with the buffer and warm the chamber to 60°C.
3. Dissolve rPeiW to a final concentration of 16 U/mL in the buffer.
4. Apply the mixture of rPeiW to the slide and incubate for 15 min at 60°C (*see* **Note 9**). A total of 15 μL should be applied to each well in the case of a 10-well glass slide.
5. Wash in TNT buffer for 10 min and in ultrapure water for 1 min at room temperature.
6. Dehydrate in ethanol for 1 min and then air dry.

3.5 Inactivation of Endogenous Peroxidases

Endogenous peroxidases should be inactivated before in situ hybridization if any are found. Common methods to inactivate endogenous peroxidases include treatment with hydrogen chloride, diethylpyrocarbonate, or hydrogen peroxide (H_2O_2) [17]. Treatment with H_2O_2 in methanol is described as a case study [24].

1. Prepare 50 mL of 0.15% H_2O_2 in methanol.
2. Immerse slides in the solution and incubate for 30 min at room temperature.
3. Wash in ethanol for 3 min and then air dry.

3.6 Two-Pass TSA-FISH

Both polynucleotide and oligonucleotide probes can be used for two-pass TSA-FISH as described above. Basically protocols are similar for both polynucleotide and oligonucleotide probes, but different in probe hybridization part. A detailed protocol of two-pass TSA-FISH with polynucleotide probes is described in Sect. 3.6.1. And the differences between protocols for polynucleotide probes and oligonucleotide probes are pointed in Sect. 3.6.2 to explain the protocol of two-pass TSA-FISH with oligonucleotide probes. Examples of photomicrographs after two-pass TSA-FISH are shown in Fig. 2.

3.6.1 In Situ Gene Detection with Polynucleotide probes

In Situ Hybridization

1. Prepare a moisture chamber humidified with a mixture of 1× SSC and formamide (the concentration should be adjusted to the same as in the hybridization buffer) and warm it to 37°C.
2. Prepare hybridization buffer [1× SSC, 10% dextran sulfate, 1% blocking reagent, 1× Denhardt's solution, 0.2 mg/mL of sheared salmon sperm DNA, 0.01% SDS, and formamide

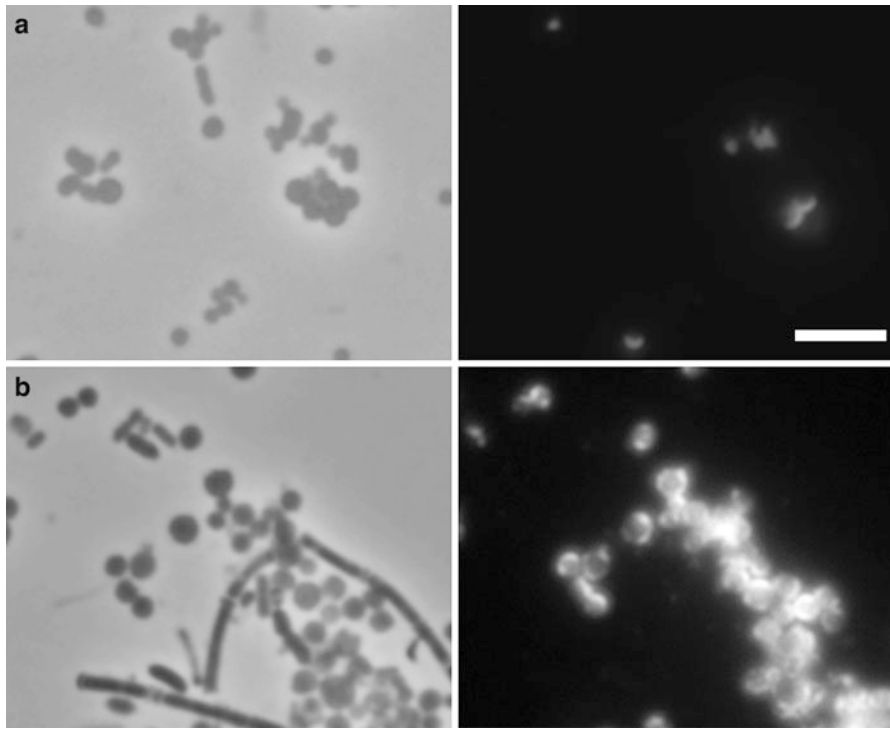

Fig. 2 Detection of *mcrA* gene in *Methanococcus maripaludis* cells by two-pass TSA-FISH with oligonucleotide probes (**a**) and polynucleotide probes (**b**). Photomicrographs of phase contrast (*left panels*) and epifluorescence (*right panels*) show identical fields. *A*, pure culture of *M. maripaludis*; *B*, *M. maripaludis*-spiked granular sludge sample. *Bar* represents 5 μm. Spotty signals were obtained, and the detection efficiency was not high after two-pass TSA-FISH with oligonucleotide probes. On the other hand, strong signals were obtained from whole cells after two-pass TSA-FISH with polynucleotide probes with high detection efficiency (coccoid cells in panel B are *M. maripaludis*)

(*see* **Note 10**)] by mixing the indicated stock reagents (*see* **Note 11**).

3. Apply hybridization buffer to each well of the glass slide and incubate the slide for 30 min at 46°C in the moisture chamber. A total of 15–20 μL of hybridization buffer should be applied to each well in the case of a 10-well glass slide (*see* **Note 12**).
4. Soak up the hybridization buffer by capillary action using Kimwipes. Do not touch the glass surface with the Kimwipes.
5. Mix the polynucleotide probe with hybridization buffer (final probe concentration is 125 pg/μL) and apply the mixture to each well. A total of 15–20 μL of hybridization buffer should be applied to each well in the case of a 10-well glass slide (*see* **Note 12**).
6. Incubate at 95°C for 20 min in the moisture chamber to denature both chromosomes and probe (*see* **Note 13**).
7. Place the moisture chamber into a hybridization oven and incubate at 46°C overnight.
8. Prepare 100 mL of two washing buffers: washing buffer 1 [1× SSC and formamide (the concentration is the same as that used in the hybridization buffer)] and washing buffer 2 (0.1× SSC and 0.01% SDS). Divide each buffer into 50-mL portions and pre-warm to 46°C.
9. After the overnight hybridization, wash slides twice in washing buffer 1 for 30 min each at 46°C.
10. Wash the slides twice in washing buffer 2 for 15 min each at 46°C.

Immunological Reaction

1. Immerse slides in TNT buffer for 10 min at room temperature.
2. Wipe excess buffer off around wells (*see* **Notes 14** and **15**).
3. Apply BB (blocking/BSA) buffer [1% blocking reagent (Roche), 1% BSA in PBS], and incubate for 1 h at room temperature. A total of 15–20 μL of BB buffer should be applied to each well in the case of a 10-well glass slide.
4. Mix BB buffer with HRP-labeled anti-DNP antibody at a ratio of 100:1. Do not vortex; mix gently by pipetting (*see* **Note 16**).
5. Soak up BB buffer by capillary action using Kimwipes. Do not touch the glass surface with Kimwipes.
6. Apply the mixture containing HRP-labeled anti-DNP antibody and incubate for 30 min at room temperature. A total of 15 μL should be applied to each well in the case of a 10-well glass slide.
7. Wash the glass slides twice in TNT buffer for 15 min each, with gentle agitation (*see* **Note 17**).

TSA

1. Prepare amplification buffer for TSA (TSA buffer) containing 0.1% blocking reagent and 20% dextran sulfate in amplification diluent.
2. Mix the TSA buffer with tyramide-DNP at a ratio of 50:1.
3. Wipe excess buffer off around the wells (*see* **Note 14**).
4. Apply the mixture and incubate for 15 min at 37°C. A total of 10–15 μL should be applied to each well in the case of a 10-well glass slide.
5. Wash twice in TNT buffer for 15 min each at 48°C.

Two-Pass TSA

1. Repeat the steps for the immunological reaction described above.
2. Repeat the TSA reaction described above, but use tyramide-Cy3 instead of tyramide-DNP.
3. Wash the slides in ultrapure water for 1 min at room temperature after the second washing in TNT buffer.
4. Immerse the slides in ethanol for 1 min and then air dry.

3.6.2 In Situ Gene Detection Using Oligonucleotide Probes

Replace the following steps:

(5-oligo) Mix oligonucleotide probe with hybridization buffer (the final probe concentration is 0.1 pmol/μL) (*see* **Note 18**). Hybridization stringency should be optimized for the probe used (*see* **Note 5**).

(14-oligo) Mix BB buffer with HRP-labeled anti-DIG antibody at a ratio of 2,500:1 (*see* **Note 16**).

4 Notes

1. The detection efficiency is defined as the percentage of the cells detected after two-pass TSA-FISH is applied to a pure culture sample. All cells should have a target gene, and thus the detection efficiency is supposed to be 100%. Lower detection efficiency is due to low sensitivity of the method, low probe hybridization efficiency to the target gene, low probe and antibody penetrability to target cells, and low immunological reaction efficiencies.
2. Probe length was tested between 135 and 820 bp in the previous study [13]. Longer probe may show lower probe penetration into cells and lower discrimination power. The length of probe should be carefully decided in terms of detection efficiency, discrimination power, and probe penetrability.

3. Elongation of extension time sometimes improves the yield of PCR products. If the efficiency of PCR was not as much as expected, longer extension time may help.
4. The absorption maximum of DNP-11-dUTP is 364 nm and the molar absorbance coefficient is 17,000/M · cm (data available from the product data sheet of the manufacturer).
5. LNA substitutions dramatically increase binding affinity, and thus hybridization requires more stringent conditions (e.g., higher formamide concentration, lower salt concentration, and/or elevated hybridization temperature). In case the optimum hybridization condition is not found due to high binding affinity of LNA-substituted probes, the number of substitutions can be reduced (e.g., every third-base substitution).
6. Do not add ethanol before suspending samples in phosphate-buffered saline (PBS) because the cells may aggregate as a result of the protein-denaturing effects of ethanol.
7. For positive control, clones carrying plasmids containing *mcrA* genes can be used. Preparation of clones has been described by Kawakami et al. [13, 14]. Samples and clones treated with DNase can be used as negative controls.
8. 1% low-melting-point agarose is solidified at room temperature. Heat by microwave to melt it, and keep it approximately 60°C until use.
9. Although rPeiW has its maximum activity at 71°C [18], the treatment was conducted at 60°C to minimize the damage to the samples by high temperature. Treatment time and temperature should be optimized for each sample.
10. The formamide concentration depends on the desired stringency of the hybridization, and it should be optimized for each probe individually.
11. Generally, we prepare 2 mL of hybridization buffer with a series of different concentration of formamide, and use them within a month. The hybridization buffer can be stored at −20°C at least for a month without causing any problems.
12. Solutions with dextran sulfate are viscous, so pipetting must be done carefully.
13. The lid of the chamber is best prepared with Saran Wrap because a plastic lid would be deformed during the denaturation process (95°C for 20 min).
14. For wiping excess buffer from the slides, we use cotton swabs, but absorbent papers such as Kimwipes are also useful.
15. Do not let the samples dry. When a number of slides are being processed, wiping excess buffer from the slides takes time.

In such cases, leave the slides in TNT buffer (washing time does not need to be as strict as shown in the protocol). A little longer immersion in TNT buffer does not have a significant effect on results.

16. The HRP-labeled antibody should be fresh (very important!!!). The antibody concentration needs to be optimized for each sample.
17. The slides are put in a stainless steel slide rack, and then the rack is placed in a beaker filled with TNT buffer. The TNT buffer is agitated using a magnetic stirrer.
18. Probe concentration needs to be optimized for each sample. If higher background was found, lowering probe concentration may work to reduce the background.

Acknowledgment

The authors thank Prof. Hideki Harada of Tohoku University, Prof. Akiyoshi Ohashi of Hiroshima University, and Dr. Hiroyuki Imachi of the Japan Agency for Marine-Earth Science and Technology (JAMSTEC) for their helpful advice regarding protocol development.

References

1. Amann RI, Ludwig W, Schleifer KH (1995) Phylogenetic identification and in situ detection of individual microbial cells without cultivation. Microbiol Rev 59:143–169
2. Wagner M, Haider S (2012) New trends in fluorescence *in situ* hybridization for identification and functional analyses of microbes. Curr Opin Biotechnol 23:96–102
3. Hodson RE, Dustman WA, Garg RP, Moran MA (1995) In situ PCR for visualization of microscale distribution of specific genes and gene products in prokaryotic communities. Appl Environ Microbiol 61:4074–4082
4. Maruyama F, Kenzaka T, Yamaguchi N, Tani K, Nasu M (2003) Detection of bacteria carrying the *stx2* gene by in situ loop-mediated isothermal amplification. Appl Environ Microbiol 69:5023–5028
5. Maruyama F, Kenzaka T, Yamaguchi N, Tani K, Nasu M (2005) Visualization and enumeration of bacteria carrying a specific gene sequence by in situ rolling circle amplification. Appl Environ Microbiol 71:7933–7940
6. Hoshino T, Schramm A (2010) Detection of denitrification genes by in situ rolling circle amplification-fluorescence in situ hybridization to link metabolic potential with identity inside bacterial cells. Environ Microbiol 12:2508–2517
7. Kenzaka T, Tamaki S, Yamaguchi N, Tani K, Nasu M (2005) Recognition of individual genes in diverse microorganisms by cycling primed in situ amplification. Appl Environ Microbiol 71:7236–7244
8. Zwirglmaier K, Ludwig W, Schleifer KH (2004) Recognition of individual genes in a single bacterial cell by fluorescence in situ hybridization – RING-FISH. Mol Microbiol 51:89–96
9. Schönhuber W, Fuchs BM, Juretschko S, Amann RI (1997) Improved sensitivity of whole-cell hybridization by the combination of horseradish peroxidase-labeled oligonucleotides and tyramide signal amplification. Appl Environ Microbiol 63:3268–3273
10. Pernthaler A, Pernthaler J, Amann R (2002) Fluorescence in situ hybridization and catalyzed reporter deposition for the identification of marine bacteria. Appl Environ Microbiol 68:3094–3101
11. Pernthaler A, Amann R (2004) Simultaneous fluorescence in situ hybridization of mRNA

and rRNA in environmental bacteria. Appl Environ Microbiol 70:5426–5433

12. Kubota K, Ohashi A, Imachi H, Harada H (2006) Visualization of *mcr* mRNA in a methanogen by fluorescence in situ hybridization with an oligonucleotide probe and two-pass tyramide signal amplification (two-pass TSA-FISH). J Microbiol Methods 66:521–528
13. Kawakami S, Hasegawa T, Imachi H, Yamaguchi T, Harada H, Ohashi A, Kubota K (2012) Detection of single-copy functional genes in prokaryotic cells by two-pass TSA-FISH with polynucleotide probes. J Microbiol Methods 88:218–223
14. Kawakami S, Kubota K, Imachi H, Yamaguchi T, Harada H, Ohashi A (2010) Detection of single copy genes by two-pass tyramide signal amplification fluorescence *in situ* hybridization (Two-Pass TSA-FISH) with single oligonucleotide probes. Microbes Environ 25:15–21
15. Moraru C, Lam P, Fuchs BM, Kuypers MMM, Amann R (2010) GeneFISH – an in situ technique for linking gene presence and cell identity in environmental microorganisms. Environ Microbiol 12:3057–3073
16. Wagner M, Schmid M, Juretschko S, Trebesius K-H, Bubert A, Goebel W, Schleifer K-H (1998) In situ detection of a virulence factor mRNA and 16S rRNA in *Listeria monocytogenes*. FEMS Microbiol Lett 160:159–168
17. Kubota K (2013) CARD-FISH for environmental microorganisms: technical advancement and future applications. Microbes Environ 28:3–12
18. Luo Y, Pfister P, Leisinger T, Wasserfallen A (2002) Pseudomurein endoisopeptidases PeiW and PeiP, two moderately related members of a novel family of proteases produced in *Methanothermobacter* strains. FEMS Microbiol Lett 208:47–51
19. Nakamura K, Terada T, Sekiguchi Y, Shinzato N, Meng X-Y, Enoki M, Kamagata Y (2006) Application of pseudomurein endoisopeptidase to fluorescence in situ hybridization of methanogens within the family *Methanobacteriaceae*. Appl Environ Microbiol 72:6907–6913
20. Hales BA, Edwards C, Ritchie DA, Hall G, Pickup RW, Saunders JR (1996) Isolation and identification of methanogen-specific DNA from blanket bog peat by PCR amplification and sequence analysis. Appl Environ Microbiol 62:668–675
21. Silahtaroglu AN, Tommerup N, Vissing H (2003) FISHing with locked nucleic acids (LNA): evaluation of different LNA/DNA mixmers. Mol Cell Probes 17:165–169
22. Vester B, Wengel J (2004) LNA (locked nucleic acid): high-affinity targeting of complementary RNA and DNA. Biochemistry 43:13233–13241
23. Kubota K, Imachi H, Kawakami S, Nakamura K, Harada H, Ohashi A (2008) Evaluation of enzymatic cell treatments for application of CARD-FISH to methanogens. J Microbiol Methods 72:54–59
24. Ishii K, Mußmann M, MacGregor B, Amann RI (2004) An improved fluorescence in situ hybridization protocol for the identification of bacteria and archaea in marine sediments. FEMS Microbiol Ecol 50:203–212

Three-Dimensional Visualisation and Quantification of Lipids in Microalgae Using Confocal Laser Scanning Microscopy

Narin Chansawang, Boguslaw Obara, Richard J. Geider, and Pierre Philippe Laissue

Abstract

Fluorescence microscopy and digital imaging allow the selective visualisation and quantification of cellular components and can convey research findings in an appealing and intuitive way. These techniques are regularly used in biomedical research laboratories, but have less widespread application in marine sciences. We present here an approach to label and volumetrically quantify neutral lipids, chloroplasts, DNA and cell volumes in microalgae. Using fluorescence microscopy techniques on "turn-key" systems commonly available to environmental research labs, imaging facilities or accessible groups in other disciplines ensure that this approach can be widely reproduced.

Keywords: Autofluorescence, Chlorophyll, Fluorescence microscopy, Image processing, Lipids, Localisation, Microalgae, Nile red, Quantification, Volumetry

Abbreviations

2D	Two dimensional
3D	Three dimensional
DAPI	4′,6-Diamidino-2-phenylindole
LUT	Look-up table
NA	Numerical aperture
PPFD	Photosynthetic photon flux density
RT	Room temperature
VC	Violet corrected

T.J. McGenity et al. (eds.), *Hydrocarbon and Lipid Microbiology Protocols*, Springer Protocols Handbooks (2016) 145–161, DOI 10.1007/8623_2015_142, © Springer-Verlag Berlin Heidelberg 2015, Published online: 08 September 2015

1 Introduction

Diatoms are microalgae that occur as single cells or colonies in freshwater and marine habitats. Diatoms are found suspended in the water column, in submerged biofilms and in most soils. They have been referred to as "nature's nanotechnologists" because of their ability to produce microscopic, three-dimensional, rigid, silicon dioxide cell walls [1]. Diatoms are the most important photosynthetic organisms in the ocean, where they are estimated to contribute 45% of the total oceanic primary production [2], thus exceeding the contribution of tropical rain forests to planetary photosynthesis. One of the keys to the high productivity of diatoms is the high proportion of cellular biomass that these organisms devote to chloroplasts. Diatoms can accumulate substantial amounts of neutral lipids as energy storage compounds. Lipid production is affected by (1) change in growth phase from exponential to stationary [3], (2) CO_2 concentration [4], (3) concentrations of inorganic nutrients [5–7], (4) salinity [8] and (5) environmental stresses such as elevated temperature and excessively high light [9, 10]. Diatoms also produce natural pigments [11–13], polyunsaturated fatty acids [14–17], biopolymers [18–20] and bioactive compounds [21, 22]. These and other high-value chemicals are important sources that can be used in commercial and industry applications [23].

Thalassiosira weissflogii is a photosynthetic eukaryote of the order Thalassiosirales. This centric diatom is found widely in marine habitats. The minority of genera are presented in freshwater conditions [24]. The main feature of diatoms is their highly ornamented external cell wall made of amorphous silica, called a frustule [18]. The frustule is composed of two plates called thecae; the epitheca fits onto the hypotheca like a lid onto a petri dish. A number of smaller plates called girdle bands link the two thecae. The frustules developed as mechanical protections for the cells from predators in pelagic food webs and biogeochemical cycles [25].

Key advantages of fluorescence microscopy are its high contrast, selectivity and three-dimensional imaging capability (Fig. 1). With the advent of digital cameras and computers, quantified image analysis has become an integral part of bioimaging. This has dramatically increased its value, and images are now considered as multidimensional numerical data. This requires robust methods for extracting quantitative data from microscopic images. Fluorescence microscopy is commonly used in biomedical sciences for imaging either living or fixed tissues that have generally been labelled with one or more fluorescent probes [26]. To date,

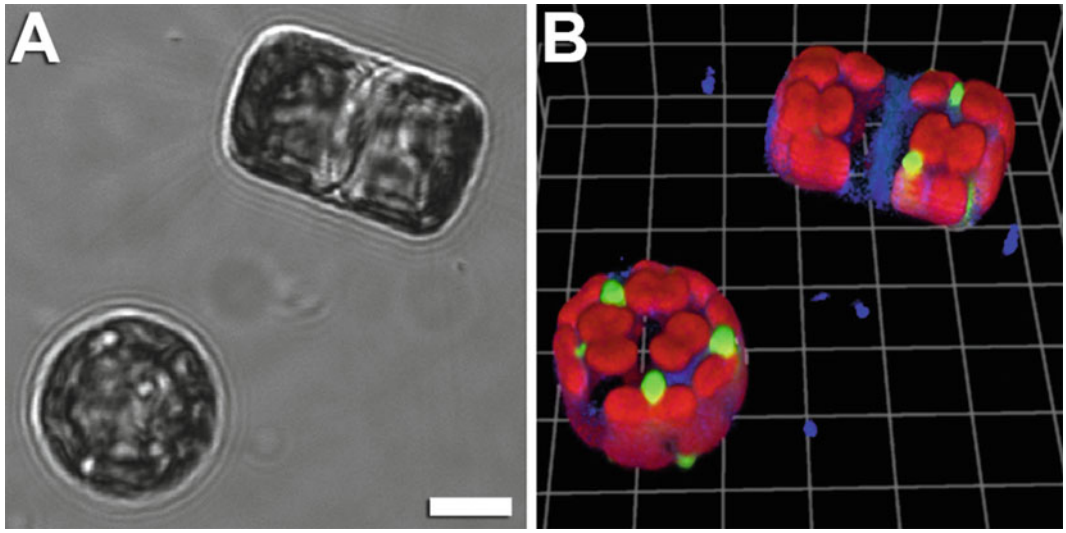

Fig. 1 (**a**) Conventional brightfield image of two *T. weissflogii* diatoms in different orientations. *Scale bar*: 5 μm. (**b**). The same cells imaged with a confocal fluorescence microscope. The three spatial dimensions are shown in perspective. The different colours show chloroplasts (*red*), double-stranded DNA (*blue*) and neutral lipids (*green*). *Grid size*: 5 μm

fluorescence microscopy has found limited use in research on diatoms (Table 1). The aim of this study was to quantify the volume of subcellular structures (chloroplasts, nucleus and neutral lipid droplets) in the diatom *T. weissflogii* using high-resolution microscopy.

2 Materials and Methods

The workflow consists of the steps laid out below:

1. Prepare cell cultures and solutions and stain sample.
2. Mount sample on microscope slide.
3. Acquire microscope images using optimal parameters.
4. Measure cell axes and determine cell volume.
5. Process images for determining subcellular volumes.
6. Statistically evaluate and plot measured volumes.
7. Visualise datasets (merged channels, z-stack montage, etc.).

Throughout the text, instructions and recommendations are in present tense, while procedures, which may vary depending on the instrument, environmental conditions or findings, use past tense.

Table 1
Microalgae research using high-resolution fluorescence imaging

Diatom	Purpose	Contrast method	References
Phaeodactylum tricornutum CCMP2561	Genetic improvement in neutral lipid accumulation	Nile red	[27]
Phaeodactylum tricornutum Pt9 (CCMP 633)	Accumulation of the fluorescent long-chain fatty acid	C_1-BODIPY-C_{12} and Nile red	[28]
Phaeodactylum tricornutum FACHB-863	Neutral lipid accumulation	Nile red	[29]
Asterionella formosa	Neutral lipid accumulation	Nile red and chlorophyll autofluorescence	[30]
Phaeodactylum tricornutum FACHB-863	Analysis of green fluorescent protein (eGFP) reporter gene using expression level in the plastid system	Fluorescent protein construct and chlorophyll autofluorescence	[31]
Phaeodactylum tricornutum UTEX B2089	Lipid storage	BODIPY 505/515	[32]
Cyclotella cryptica CCMP 332	Accumulation of lipid bodies	BODIPY and chlorophyll autofluorescence	[33]
Phaeodactylum tricornutum FACHB-863	Size and number of oil bodies	Nile red	[34]
Actinoptychus senarius	Structure of frustule	Fluorescein isothiocyanate-(3-aminopropyl) trimethoxysilane	[35]
Phaeodactylum tricornutum CCAP 1052/6	Oil-containing lipid bodies	Nile red and chlorophyll autofluorescence	[36]
Phaeodactylum tricornutum	The differentiation of fusiform to oval morphotypes	Fluorescent protein construct and chlorophyll autofluorescence	[37]

2.1 Media and Solutions

2.1.1 Cell Cultures

Cultures of the diatom *T. weissflogii* CCMP 1051 were grown in filter-sterilised (0.2 μm) artificial seawater medium containing 200 μM nitrate, 106 μM silicate, 3 mM carbonate, 1 nM selenite, ¼ concentration of trace elements and ½ concentration of vitamins in *f*/2 medium recipe [38]. Cultures were incubated at 16°C and photosynthetic photon flux densities (PPFD) of 50 μmol photons m^{-2} s^{-1} (low light (LL)) and 500 μmol photons m^{-2} s^{-1} (high

light (HL)) on a 14:10 h light/dark cycle. The cultures were gently stirred with a magnetic stir bar and continuously aerated with filtered air through a 0.22 μm membrane filter. Cells were collected from each of the three replicate cultures during the exponential phase.

2.1.2 Preparation of Nile Red and DAPI

Nile red, a hydrophobic fluorophore with high specificity for neutral lipids [39], binds to lipid-storage droplets in microalgae [40]. A stock solution of fluorescent dye (nile red 99%, Acros Organics™) was prepared by dissolving 500 μg of nile red per mL in acetone under the dim light and in a fume hood. The solution was kept in a brown-coloured bottle and stored in a refrigerator (4–8°C). A stock solution of DAPI (4′,6-diamidino-2-phenylindole, Invitrogen™) was prepared by dissolving 5 mg mL^{-1} in distilled water under dim light, and aliquots stored at −20°C.

2.1.3 Fluorescent Staining

Cells grown under exponential phase were harvested at a cell density of approximately 1.5–2.0 × 10^5 cells mL^{-1}, placed in an autoclaved microcentrifuge (1.5 mL) and then centrifuged at 4,000×*g* for 5 min. The pellet was resuspended using fresh media. DAPI was added to a final concentration of 10 μg mL^{-1}. The sample was mixed gently and kept in the dark at room temperature (RT) for 2 min. Nile red solution was added to yield a final concentration of 10 μg mL^{-1} and kept at RT for 1 min.

2.2 Mounting Samples

Put a drop of the sample culture onto a standard rectangular microscope slide. Cover the drop with a glass coverslip. The sample is viewed through the coverslip, which should face the microscope objective. Since microscopes are available in two orientations, the coverslip should point towards the ceiling for an upright microscope and towards the floor for an inverted. Use coverslips of standard thickness 0.17 mm, also called #1½. Thinner coverslips can also be used (#1), but require an adjustment collar on the objective. Make sure you do not put on two coverslips sticking together.

The volume of the drop ranges from 20 to 50 μL, depending on the size of the coverslip. Too little liquid will cause the inclusion of air bubbles between the slide and coverslip. Too much liquid will cause cells to float around, making imaging impossible. If your coverslip is floating on top of the slide, suck away some liquid with a tissue paper until it adheres to the slide. During imaging, liquid evaporates (especially in high light), so it is useful to seal the coverslip on its sides. We recommend rubber cement (e.g. "Fixogum", Marabuwerke GmbH & Co., D-71732 Tamm, Germany). A 20 μL pipette tip on the nozzle allows for careful framing of the coverslip. Pointing the nozzle upwards after use allows the rubber cement in the pipette tip to flow back into the tube. The weight of the coverslip can fracture a diatom's frustule, or even crush it (Fig. 2). The use of spacers is thus recommended (see also Sect. 4.2, Avoiding Cell Breakage).

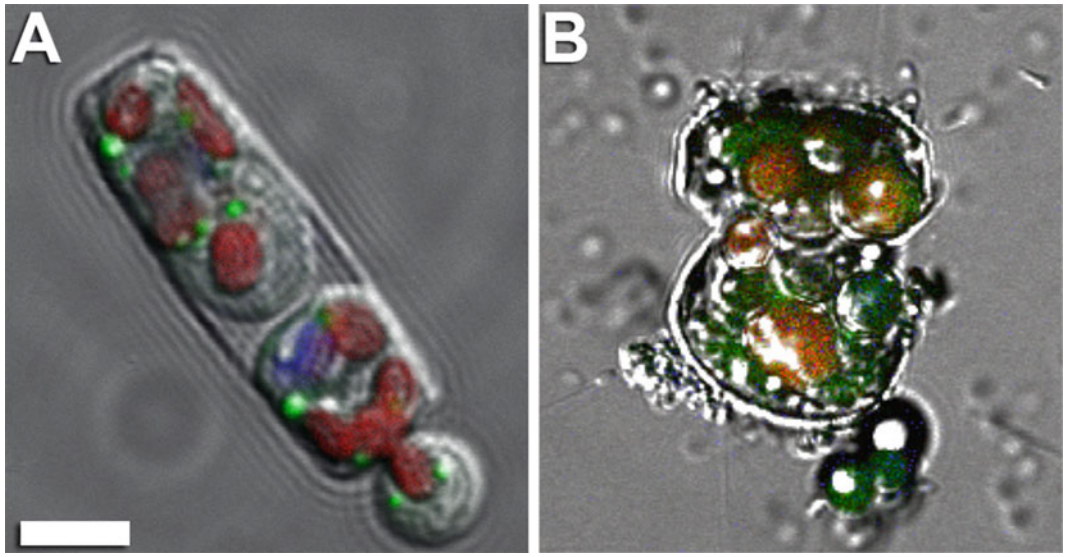

Fig. 2 For fragile specimens, using spacers prevents the coverslip from crushing the sample. (**a**) Damaged frustule leads to protuberance of cytosol, plasmalemma and a chloroplast. (**b**) Crushed frustule. *Scale bar*: 5 μm

2.3 Image Acquisition

For image acquisition, a Nikon A1si confocal laser scanning microscope (CLSM) was used with a plan-apochromatic VC 1.4 NA 60× magnifying oil-immersion objective (Nikon Corp., Tokyo, Japan). Images were acquired in four channels, using one-way sequential line scans. Nile red was excited at 488 nm, and its emission collected from 500 to 550 nm. Chlorophyll autofluorescence in chloroplasts was excited at 637 nm, and its emission collected from 662 to 737 nm. DAPI labelling dsDNA was excited at 405 nm, and its emission collected from 425 to 475 nm.

Differential interference contrast images for cellular outlines were acquired using the transmitted light detector. In all cases, no offset was used, and the scan speed was ¼ frames/s (galvano scanner). The pinhole size was 34.5 μm, approximating 1.2 times the airy disk size of the 1.4 NA objective at 525 nm. Scanner zoom was centred on the optical axis and set to a lateral magnification of 55 nm/pixel. Axial step size was 140 nm, with 30–50 image planes per z-stack. 50–70 cells with average to fair signal strength in all channels were examined.

2.3.1 Use Identical Acquisition Parameters

Acquisition parameters need to be identical in order to make a valid comparison between samples reared in different conditions (e.g. HL compared to LL). Changing image acquisition parameters (e.g. higher laser intensity or detector gain for LL samples) will influence volumetric measurements and invalidate a comparison. Using the same microscope and objective, retain a constant value for laser intensity, detector gain, scanning speed (also denoted as pixel dwell time or frames per second), image size, zoom factor and pinhole size.

2.3.2 Avoid Overexposed Pixels

Overexposed pixels should be avoided, as they cannot be used for quantification. Look-up tables (LUTs) colour-coding the maximum greyscale value are commonly implemented in microscope image acquisition software. This allows the detection of saturated pixels. Adjust laser power and/or detector gain to avoid saturation before acquiring datasets.

2.3.3 Use Nyquist Sampling

Datasets should be acquired with the correct 3D sampling parameters. These are determined by the Nyquist–Shannon reconstruction theorem [41, 42]. Briefly, this means that the smallest structure in an image, as determined by the microscope's resolution using Abbe's criterion, should be represented by at least two pixels, although three to four are also acceptable. Undersampling (e.g. just one pixel for the smallest structure) must be avoided. It also allows the removal of single-pixel high-frequency noise through post-acquisition filtering (e.g. spatial deconvolution). Adjusting these parameters (x, y and z resolution) correctly is implemented in many image acquisition softwares, often designated as simply "Nyquist".

2.3.4 Minimise Optical Aberrations

Image defects (i.e. optical aberrations) should be minimised in the imaging setup. This can be done using objectives corrected for spherical ("plan") and chromatic aberrations (achromatic, apochromatic and apochromatic violet corrected (VC), depending on the number of colours corrected for). Furthermore, unidirectional, not bidirectional scanning, zooming into the centre of the field of view and separating colours in line scanning rather than full-frame mode are good measures for minimising aberrations.

2.4 Approximation of Cellular Volume

The cellular volume can be approximated by measuring a cell's long (L, length) and short (W, width) axes and deriving a cylindrical volume from these parameters. Axes and formula for this approximation are shown in Fig. 3. Half the width represents the radius of the cylinder, so to obtain the volume, it must be squared and multiplied with the length L and the number π.

2.5 Quantifying the Volume of Subcellular Structures

The proposed approach uses MATLAB software (version R2012b with Image Processing Toolbox; Math Works Inc., Natick, Massachusetts, USA). All steps are based on analysis in 3D. The algorithm is divided into three stages: (1) pre-filtering, (2) thresholding and (3) post-filtering. The noise level in the input image is reduced by convolving the image with a 3D Gaussian kernel. The kernel size is controlled by a user-defined sigma (σ), which denotes the standard deviation of the distribution. The filtered image is then segmented using the Otsu method for global thresholding [43]. This thresholding separates each colour channel image into foreground (i.e. the objects of interest, circled red in Fig. 3, middle

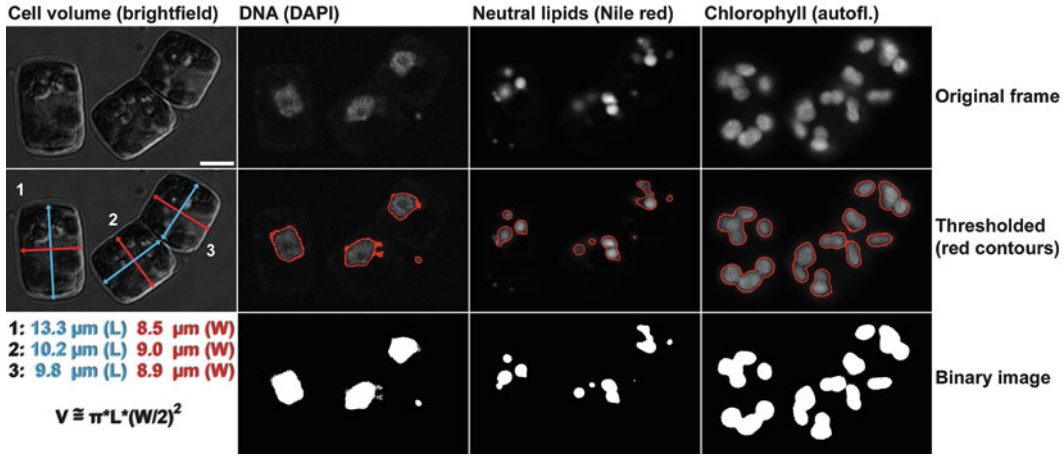

Fig. 3 *Top row*: The four acquired channels, DIC for cell volume, DAPI for DNA, nile red for neutral lipids and autofluorescence of chlorophyll for chloroplasts. Long (L) and short axes (W) are determined in DIC images (*first column*), and cell volume (V) approximated using a cylindrical model. The volume of the subcellular, fluorescent components is determined by global thresholding (*middle row*) and measurement of binary image series (*bottom row*). *Scale bar*: 5 µm

row) and background (i.e. the "noise"). This allows binary images to be generated (Fig. 3, bottom row), in which objects are white and background is black. These binary images are "cleaned" by removing the smallest structures in the image. To this end, we use the method of morphological opening by reconstruction with a disk structuring element [44]. The structuring element size, which determines just how small the removed structures are, is controlled by a user-defined radius (r). Parameters σ and r are normalised according to image size. The resulting binary image stacks are then used to determine the volume of the objects of interest in each colour channel. The MATLAB algorithm used in this study is available upon request from the corresponding authors. The combined routines – Gaussian filtering, global thresholding, morphological filtering and volume measurement – are however generic and available in many open-source and commercial software packages (*see* **Notes**).

2.6 Statistical Evaluation of Volumetry

Cell volumes incubated at low light (LL) were significantly larger than those incubated at high light (HL) (Table 2). Cells grown in LL showed the highest volume, which was approximately 740 ± 34 (mean ± SE) µm^3. Chloroplasts at LL were significantly larger (t-test and Mann–Whitney test, $p < 0.05$), with on average 1.6-fold greater volumes compared to HL. In contrast, neutral lipids presented the highest volumes at HL with an average of 46 ± 3 µm^3. This was twice as much as average lipid volume at LL (21 ± 2 µm^3), thus showing the largest difference between

Table 2
Shown are the mean values, standard deviation and standard error for each of the three replicate cultures of *T. weissflogii* maintained under low light (LL) and high light (HL)

	Cell volume		DNA volume		Lipid volume		Chloroplast volume	
Light treatment	LL	HL	LL	HL	LL	HL	LL	HL
Average	740	528	90	80	21	46	585	374
Standard deviation	247	204	78	46	12	26	158	145
Standard error	34	24	11	5	2	3	22	17

treatments in the parameters used in this study. Volumes of DNA stained with DAPI, which in essence represents nuclei, were similar in LL and HL conditions.

Volumes are shown as bar charts (Fig. 4), boxplots (Fig. 5) and scatterplots (Fig. 6) to illustrate different options for communicating results.

2.7 Visualisation

It is useful to provide a description of the datasets regarding the localisation of subcellular structures. In the case of *T. weissflogii*, the nucleus was often found in the middle of the cell's long axis and close to the cell wall. Chloroplasts were adjacent to the cell wall and never deep inside the cell's cytoplasm. Neutral lipids were scattered throughout the cell, often adjoining the cell wall (Fig. 7).

Visualisation deals with different approaches for presenting the acquired microscope images [45]. When visualising 3D datasets, movies rotating the sample can give a good impression of the 3D structure. In the case of printed media however, one faces the problem of having to show multiple colours and three spatial dimensions in 2D images. We show here different options to achieve this (Fig. 7).

2.7.1 Visualisation of a Single Frame with Multiple Colour Channels

Splitting a multichannel image into its components (Fig. 7a) is a clear way to visualise localisation of the different spectral information. To show where the same location in one channel can be found in another, synchronised arrowheads can be used.

Merging channels produces a single image (Fig. 7b). The brightfield image (often DIC or phase contrast) can be included; however, it weakens the contrast of the fluorescent channels.

2.7.2 Visualisation of Multiple z-Frames with Multiple Colour Channels

A z-series of *merged channels* (Fig. 7c) can be used to show all optical sections through one cell. This is often called a *montage* or *gallery view* and provides a good overview of the localisation of subcellular components. The brightfield image can also be included in this approach. The drawback is that the serial images become smaller the more z-frames are shown (40 frames of 140 nm thickness in z-stack montage example (Fig. 7b) for one entire cell). Some

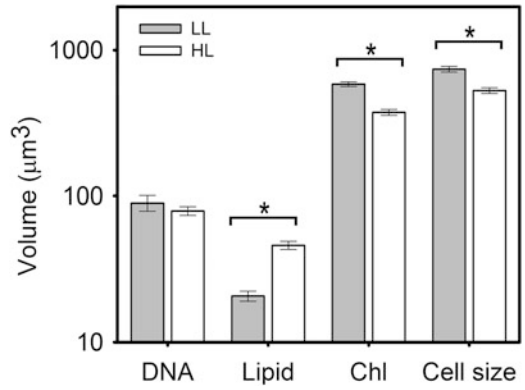

Fig. 4 Bar chart of neutral lipid (Lipid), DNA, chloroplast (Chl) and cell volume content in *T. weissflogii*. Shown are the mean values and standard error for each of the three replicate cultures maintained under low light (LL) and high light (HL). Using *t*-test ($p < 0.05$) between parameter and volume is indicated with the *asterisk*

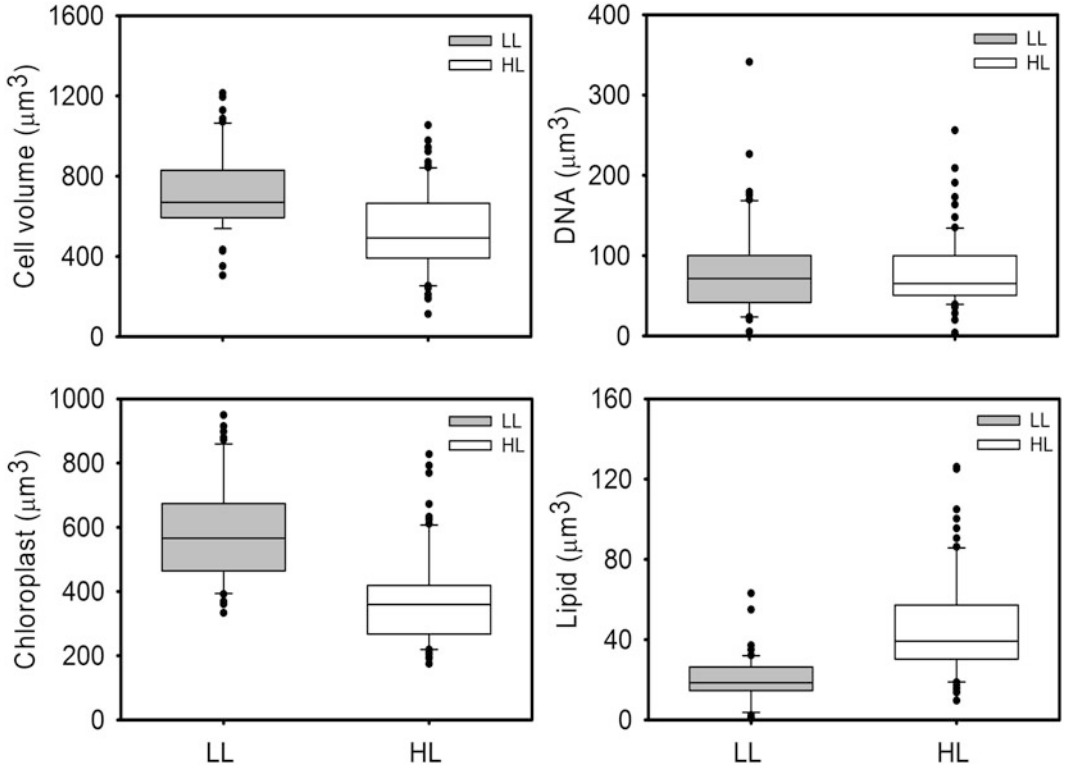

Fig. 5 Boxplots of volumetry in *T. weissflogii* maintained under low light (LL) and high light (HL). Clockwise, from *top left*: volumes of cells, nuclei (DNA stained with DAPI), lipids and chloroplasts. The *horizontal line* in each *box* represents the median value, while standard deviation is shown by the *whiskers. Black dots* represent outliers

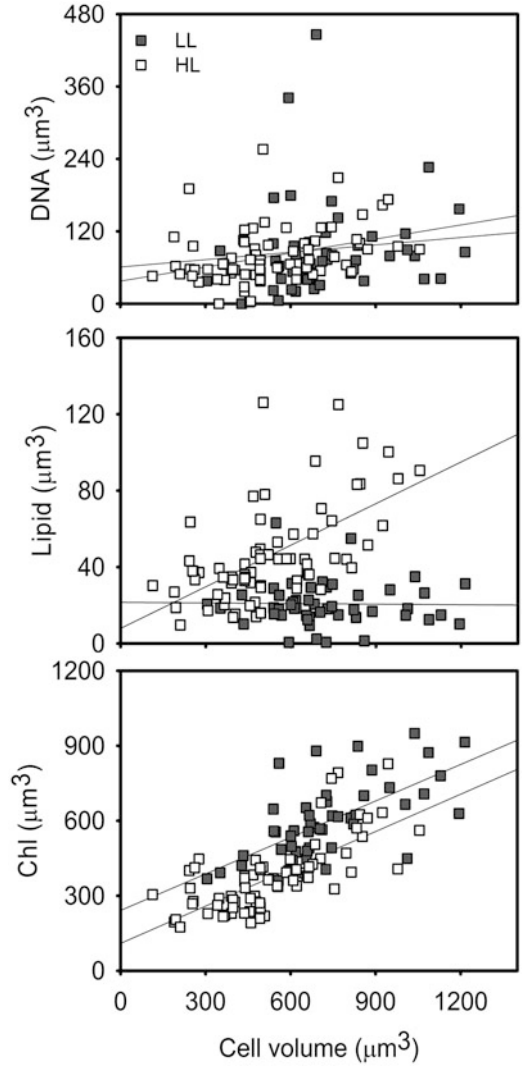

Fig. 6 Scatterplots of DNA (*top*), neutral lipid (*middle*) and chloroplast volumes ("Chl", *bottom*) plotted against the cellular volume in *T. weissflogii* maintained under low light (LL) and high light (HL). *Lines* indicate least square linear regression curves for the different populations

visualisation software packages allow to bypass this problem by offering the possibility to include only every *n*-th image of a stack, allowing fewer, but larger, micrographs to be used.

The "slices" view (Fig. 7d) uses a crosshair on the xy image. This indicates where the planes for xz and yz visualisations lie. One can imagine a knife slicing along the crosshair lines and the cross sections being shown on the sides. When visualising 3D datasets as a whole (unlike approaches mentioned above), only the fluorescence channels should be used. Brightfield z-series are not suited

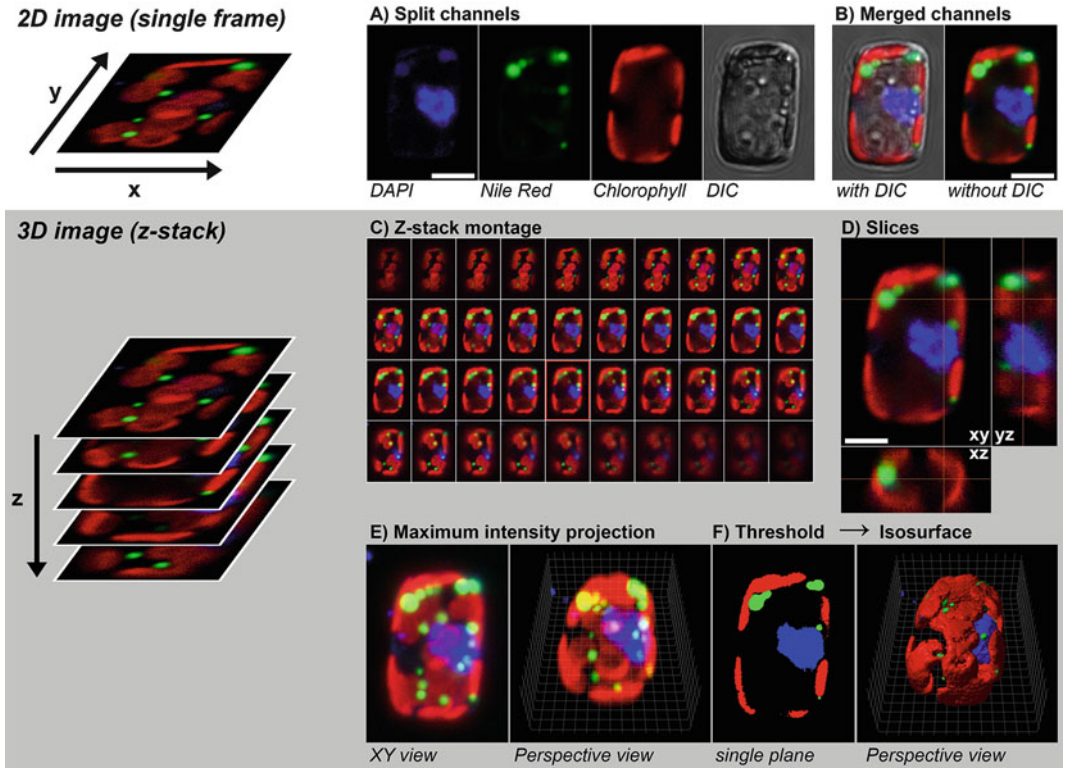

Fig. 7 Visualisation of single diatoms. (**a**) Split channels. (**b**) Merged channels. (**c**) Z-stack montage. (**d**) Slices. (**e**) Maximum intesity projection. (**f**) Isosurface model through thresholding. *Scale bars*: 5 μm. *Grid size*: 1 μm. See Sect. 2.7 for details

for 3D visualisation, as they do not generate optical sections. Hence, brightfield images should not be used in the "slices" view.

2.7.3 Perspective Visualisation

This is an intuitive way to present data. It is also seductive, but can tend to visualise 3D content less clearly compared to the approaches mentioned above. Common ways to visualise 3D datasets in perspective are maximum intensity projection, perspective view, and isosurface models.

A *maximum intensity projection* (Fig. 7e) collapses an image stack into a single image plane. It is an effective way to visualise a 3D dataset in a single frame (as seen from "above"). It must however be noted that, as the third spatial dimension is reduced, subcellular structures in two different channels may falsely appear to overlap.

3D datasets can also be visualised in *perspective view* by tilting the 3D dataset. In this case, a grid should be included to show the correct dimensions. Subcellular components can be visualised using the unprocessed datasets and a projection algorithm such as maximum intensity projection, implemented in many image processing programmes. As with all maximum intensity projections, it can

produce the false impression of overlapping (colocalising) subcellular structures in two different channels.

By setting a threshold (Fig. 7f) in each channel, subcellular structures can be segmented as binary images (cf. Fig. 3). The resulting binary file can be used to create an *isosurface model*. This can also be tilted for a perspective view. The surface model lighting can also be changed to highlight certain features. In some programmes, the surface can be made transparent.

3 Discussion

We present here a technique based on 3D imaging of subcellular components. It allows visualisation and volumetry in single-celled organisms. The approach is sensitive – significant differences were found using as few as 50 cells for one condition. An alternative approach, flow cytometry, has been used extensively in oceanography to rapidly measure large numbers of cells in large samples [46]. One recently described approach uses imaging flow cytometry to determine lipid and chloroplast quantity by area measurements [33]. But these images lack the third spatial dimension (z) and may thus misrepresent the true localisation of labelled and autofluorescent subcellular structures. In addition, the vast majority of flow cytometers and cell sorters do not acquire images and hence do not allow to assess cellular integrity. High-resolution microscopy emerges thus as an accurate alternative to high-throughput imaging of neutral lipid and chloroplast content in diatoms. This suggests that, at least in our case, variance is reduced by increasing resolution.

In *T. weissflogii*, a large part of the cellular volume is occupied by chloroplasts. We used DNA as an internal control, since its content is not expected to change significantly between light treatments. Indeed, there was no significant difference in DNA-labelled volumes between LL and HL conditions (Figs. 4, 5 and 6). The impact of PPFD (LL = 50 µmol photons m^{-2} s^{-1} versus HL = 500 µmol photons m^{-2} s^{-1}) on all other measured biovolumes of *T. weissflogii* was however significant: On the one hand, chloroplast volumes were greater in LL than in HL and corresponded to the cell volumes (Fig. 6). On the other hand, the size of neutral lipid droplets was twice as great in cells grown under HL compared to cells grown under LL. Statistical evaluation was similar using both *t*-test and Mann–Whitney (Table 2).

These results are consistent with the common pattern of photoacclimation in microalgae, which involves downregulation of the capacity for light absorption (e.g. reduced pigment content and chloroplast size) and accumulation of energy storage reserve (e.g. starch and/or neutral lipids) in response to increases of the PPFD [47].

Previous observations also found reduced lipid content in LL conditions, e.g. *Isochrysis galbana* of class Haptophyceae [48], for *Nannochloropsis* sp. of class Eustigmatophyceae [49] and for *Pavlova lutheri* of class Pavlovophyceae [50]. Subcellular structures and their localisation, determined with scanning electron microscopy, were also described in the vegetative cell of *Melosira varians* [51] and *T. weissflogii* [52]. Using the approach described in this chapter, we can visualise the localisation of subcellular structures in cells grown in different environmental conditions. More importantly, accurate quantification of these subcellular volumes is achieved by using simple sample preparation, conventional microscopy and modest image processing.

4 Notes

4.1 Sealing the Slide (See Sect. 2.2, Mounting Samples)

Nail varnish is not recommended as it can affect cells and their fluorescence [53]. A good alternative to the recommended rubber cement is vacuum grease [54].

4.2 Avoiding Cell Breakage (see Sect 2.2, Mounting Samples)

For optimal image quality, working cleanly is important. Avoid putting fingerprints on the imaged area of the clean glass slides. Do not spill liquid onto the glass, especially the coverslips. If using vacuum grease to seal the coverslip, be sure to use it only on the edges. Treat your samples carefully, as diatoms can break easily. Cells with damaged frustules should not be used for quantification. If most cells are broken upon viewing, make a new slide using spacers [54]. Spacers are put on the slide and prevent the coverslip from crushing the cells. They can be made from vacuum grease [54], chewing gum [55], double-sided tape [56] or torus-shaped stickers for ring binders [57]. For this study, we achieved best results using small pieces of coverslips cut with a diamond scribe (Agar Scientific Ltd, UK) as spacers.

4.3 Choice of Microscope (See Sect. 2.3, Image Acquisition)

All datasets acquired in this study were obtained with a confocal laser scanning microscope (CLSM). With its capability to take optical sections and zoom in on a cell, CLSM is suitable for high-resolution 3D imaging of subcellular, live morphology. Good optical sectioning can also be obtained using widefield fluorescence microscopy (WFM) in combination with spatial deconvolution and objectives with high numerical aperture (NA). In addition, WFM can be used for repeated imaging of the same cell to follow the redistribution of subcellular structures in different conditions. CLSM causes photodamage with its focussed laser beam and is not recommended for longer-term live imaging studies.

4.4 Image Processing for Volumetry (See Sect. 2.5, Quantifying the Volume of Subcellular Structures)

Gaussian filtering, global thresholding, morphological filtering and volume measurement are commonly available image processing routines. Hence, these operations can be reproduced using corresponding implementations in image processing software such as the freely available open-source programme Fiji [58]. A good open-source plug-in for Fiji/ImageJ is available for threshold-based separation of subcellular organelles from the background and subsequent volumetry [59]. Documentation and downloads can be found at http://fiji.sc/Squassh.

4.5 Pruning (See Sect. 2.6, Statistical Evaluation)

Before image processing, all datasets should be checked for cellular integrity and signal strength. Cells that appear damaged, have poor contrast or move during image acquisition need to be excluded from analysis. Rigorous pruning after image processing is also crucial, as the method is affected by outliers. If volumetric values of a subcellular structure (lipid, chloroplast or nucleus) in a particular dataset are markedly different from the other values in the same cohort, check the original dataset and the binary stack associated with the subcellular structure in question; exclude dataset if the extraordinary values are due to a poor sample or questionable image processing.

Acknowledgements

N. C. acknowledges support from the Royal Thai Government for sponsoring her PhD research. R. J. G. and P. P. L. acknowledge NERC for supporting algal ecophysiology research and environmental fluorescence microscopy, respectively.

References

1. Bradbury J (2004) Nature's nanotechnologists: unveiling the secrets of diatoms. PLoS Biol 2(10)
2. Yool A, Tyrrell T (2003) The role of diatoms in regulating the ocean's silicate cycle. Global Biogeochem Cycles 17(4):1103–1124
3. Fidalgo JP, Cid A, Torres E, Sukenik A, Herrero C (1998) Effects of nitrogen source and growth phase on proximate biochemical composition, lipid classes and fatty acid profile of the marine microalga *Isochrysis galbana*. Aquaculture 166:105–116
4. Wang XW, Liang JR, Luo CS, Chen CP, Gao YH (2014) Biomass, total lipid production, and fatty acid composition of the marine diatom *Chaetoceros muelleri* in response to different CO_2 levels. Bioresour Technol 161:124–130
5. Shifrin NS, Chisholm SW (1981) Phytoplankton lipids: interspecific differences and effects of nitrate, silicate and light-dark cycles. J Phycol 17(4):374–384
6. Illman AM, Scragg AH, Shales SW (2000) Increase in *Chlorella* strains calorific values when grown in low nitrogen medium. Enzyme Microb Technol 27:631–635
7. Liu ZY, Wang GC, Zhou BC (2008) Effect of iron on growth and lipid accumulation in *Chlorella vulgaris*. Bioresour Technol 99:4717–4722
8. Chen GQ, Jiang Y, Chen F (2008) Salt-induced alterations in lipid composition of diatom *Nitzschia laevis* (Bacillariophyceae) under heterotrophic culture condition. J Phycol 44:1309–1314
9. Hegarty SG, Villareal TA (1998) Effects of light level and N:P supply ratio on the competition between *Phaeocystis* cf. pouchetii (Hariot) Lagerhelm (Prymnesiophyceae) and five diatom species. J Exp Mar Bio Ecol 226 (2):241–258

10. Converti A, Casazza AA, Ortiz EY, Perego P, Del Borghi M (2009) Effect of temperature and nitrogen concentration on the growth and lipid content of *Nannochloropsis oculata* and *Chlorella vulgaris* for biodiesel production. Chem Eng Process Process Intensif 48:1146–1151
11. Pennington F, Guillard RR, Liaaen-Jensen S (1988) Carotenoid distribution patterns in Bacillariophyceae (diatoms). Biochem Syst Ecol 16(7):589–592
12. Bertrand M (2010) Carotenoid biosynthesis in diatoms. Photosynth Res 106(12):89–102
13. Xia S, Wang K, Wan L, Li A, Hu Q, Zhang C (2013) Production, characterization, and antioxidant activity of fucoxanthin from the marine diatom *Odontella aurita*. Mar Drugs 11 (7):2667–2681
14. Tonon T, Harvey D, Larson TR, Graham IA (2002) Long chain polyunsaturated fatty acid production and partitioning to triacylglycerols in four microalgae. Phytochemistry 61 (1):15–24
15. Wen ZY, Chen F (2003) Heterotrophic production of eicosapentaenoic acid by microalgae. Biotechnol Adv 21(4):273–294
16. Jiang H, Gao K (2004) Effects of lowering temperature during culture on the production of polyunsaturated fatty acids in the marine diatom *Phaeodactylum tricornutum* (Bacillariophyceae). J Phycol 40(4):651–654
17. Chautona MS, Reitan KI, Norskerc NH, Tveteråsd R, Kleivdale HT (2015) A techno-economic analysis of industrial production of marine microalgae as a source of EPA and DHA-rich raw material for aquafeed: research challenges and possibilities. Aquaculture 436:95–103
18. Hoagland KD, Rosowski JR, Gretz MR, Roemer SC (1993) Diatom extracellular polymeric substances-function, fine-structure, chemistry, and physiology. J Phycol 29:537–566
19. Wolfstein K, Stal LJ (2002) Production of extracellular polymeric substances (EPS) by benthic diatoms: the effect of irradiance and temperature. Mar Ecol Prog Ser 23:613–622
20. Underwood GJ, Paterson DM (2003) The importance of extracellular carbohydrate production by marine epipelic diatoms. Adv Bot Res 40:183–240
21. Mimouni V, Ulmann L, Pasquet V, Mathieu M, Picot L, Bougaran G, Cadoret JP, Manceau AM, Schoefs B (2012) The potential of microalgae for the production of bioactive molecules of pharmaceutical interest. Curr Pharm Biotechnol 13(15):2733–2750
22. de Jesus Raposo MF, de Morais RMSC, de Morais AMMB (2013) Bioactivity and applications of sulphated polysaccharides from marine microalgae. Mar Drugs 11(1):233–252
23. Pulz O, Gross W (2004) Valuable products from biotechnology of microalgae. Appl Microbiol Biotechnol 65(6):635–648
24. Stoermer EF, Julius ML (2003) Centric diatoms. In: Wehr JD, Sheath RG (eds) Freshwater algae of North America. Academic, Amsterdam
25. Hamm CE, Merkel R, Springer O, Jurkojc P, Maier C, Prechtel K, Smetacek V (2003) Architecture and material properties of diatom shells provide effective mechanical production. Nature 421(6925):841–843
26. Paddock SW (1999) Confocal microscopy methods and protocols. In: Paddock SW (ed) Methods in molecular biology. Humana, New Jersey
27. Xue J, Niu YF, Huang T, Yang WD, Liu JS, Li HY (2015) Genetic improvement of the microalga *Phaeodactylum tricornutum* for boosting neutral lipid accumulation. Metab Eng 27:1–9
28. Guo L, Sui Z, Zhang S, Liu Y, Du Q (2014) Preliminary comparison of quantification efficiency between DNA-derived dataset and cell-derived dataset of mixed diatom sample based on rDNA-ITS sequence analysis. Biochem Syst Ecol 57:183–190
29. Ma YH, Wang X, Niu YF, Yang ZK, Zhang MH, Wang ZM et al (2014) Antisense knockdown of pyruvate dehydrogenase kinase promotes the neutral lipid accumulation in the diatom. Microb Cell Fact 13(1):100
30. Mekhalfi M, Amara S, Robert S, Carrière F, Gontero B (2014) Effect of environmental conditions on various enzyme activities and triacylglycerol contents in cultures of the freshwater diatom, *Asterionella formosa* (Bacillariophyceae). Biochimie 101:1–10
31. Xie WH, Zhu CC, Zhang NS, Li D, Yang WD, Liu JS et al (2014) Construction of novel chloroplast expression vector and development of an efficient transformation system for the diatom *Phaeodactylum tricornutum*. Mar Biotechnol 16:538–546
32. Wong DM, Franz AK (2013) A comparison of lipid storage in *Phaeodactylum tricornutum* and *Tetraselmis suecica* using laser scanning confocal microscopy. J Microbiol Methods 95 (2):122–128
33. Traller JC, Hildebrand M (2013) High throughput imaging to the diatom *Cyclotella cryptica* demonstrates substantial cell-to-cell variability in the rate and extent of triacylglycerol accumulation. Algal Res 2(3):244–252
34. Yang ZK, Niu YF, Ma YH, Xue J, Zhang M, Yang WD et al (2013) Molecular and cellular

mechanisms of neutral lipid accumulation in diatom following nitrogen deprivation. Biotechnol Biofuels 6(1):67

35. Friedrichs L, Maier M, Hamm C (2012) A new method for exact three-dimensional reconstructions of diatom frustules. J Microsc 248:208–217
36. Horst I, Parker BM, Dennis JS, Howe CJ, Scott SA, Smith AG (2012) Treatment of *Phaeodactylum tricornutum* cells with papain facilitates lipid extraction. J Biotechnol 162:40–49
37. De Martino A, Bartual A, Willis A, Meichenin A, Villazán B, Maheswari U et al (2011) Physiological and molecular evidence that environmental changes elicit morphological interconversion in the model diatom *Phaeodactylum tricornutum*. Protist 162(3): 462–481
38. Guillard RR, Ryther JH (1962) Studies of marine planktonic diatoms. I. *Cyclotella nana* Hustedt, and *Detonula confervacea* (Cleve) Gran. Can J Microbiol 8:229–239
39. Greenspan P, Fowler SD (1985) Spectrofluorometric studies of the lipid probe, nile red. J Lipid Res 26:781–789
40. Cooksey KE, Guckert JB, Williams SA, Callis PR (1987) Fluorometric determination of the neutral lipid content of microalgal cells using Nile Red. J Microbiol Methods 6 (6):333–345
41. Nyquist H (1928) Certain topics in telegraph transmission theory. AIEE 47(2):617–644
42. Shannon CE (1949) Communication in the presence of noise. Proc IRE 37:10–21
43. Otsu N (1979) A threshold selection method from Gray-level. IEEE Trans Syst Man Cybern 9(1):62–66
44. Serra J (1982) Image analysis and mathematical morphology. Academic, New York
45. Walter T, Shattuck DW, Baldock R, Bastin ME, Carpenter AE, Duce S et al (2010) Visualization of image data from cells to organisms. Nat Methods 7(30):S26–S41
46. Collier JL (2000) Flow cytometry and the single cell in phycology. J Phycol 36:628–644
47. Berner T, Dubinsky Z, Wyman K, Falkowski PG (1989) Photoadaptation and the "package" effect in *Dunaliella tertiolecta* (Chlorophyceae). J Phycol 25:70–78
48. Brown MR, Dunstan GA, Jeffrey SW, Volkman JK, Barrett SM, LeRoi JM (1993) The influence of irradiance on the biochemical composition of the prymnesiophyte *Isochrysis* sp. (clone T-ISO). J Phycol 29(5):601–612
49. Sukenik A, Carmeli Y, Berner T (1989) Regulation of fatty acid composition by irradiance level in the eustigmatophyte *Nannochloropsis* sp. J Phycol 25(4):686–692
50. Guihéneuf F, Mimouni V, Ulmann L, Tremblin G (2009) Combined effects of irradiance level and carbon source on fatty acid and lipid class composition in the microalga *Pavlova lutheri* commonly used in mariculture. J Exp Mar Bio Ecol 369(2):136–143
51. Crawford R (1973) The protoplasmic ultrastructure of the vegetative cell of *Melosira varians* C.A. Agardh. J Phycol 9(1):50–61
52. Bayraktaroğlu E, Legović T, Velasquez ZR, Cruzado A (2003) Diatom *Thalassiosira weissflogii* in oligotrophic versus eutrophic culture: models and ultrastructure. Ecol Modell 170:237–243
53. Rodighiero S, Bazzini C, Ritter M, Fürst J, Botta G, Meyer G et al (2008) Fixation, mounting and sealing with nail polish of cell specimens lead to incorrect FRET measurements using acceptor photobleaching. Cell Physiol Biochem 21:489–498
54. Shaw PM, Jones GJ, Smith JD, Johns RB (1989) Intraspecific variations in the fatty acids of the diatom Skeletonema costatum. Phytochemistry 28(3):811–815
55. Michels J (2007) Confocal laser scanning microscopy: using cuticular autofluorescence for high resolution morphological imaging in small crustaceans. J Microsc 227:1–7
56. Exposito-Rodriguez M, Laissue PP, Littlejohn GR, Smirnoff N, Mullineaux PM (2013) The use of HyPer to examine spatial and temporal changes in H_2O_2 in high light-exposed plants. Methods Enzymol 527:185–201
57. Laissue PP, Reiter C, Hiesinger PR, Halter S, Fischbach KF, Stocker RF (1999) Three-dimensional reconstruction of the antennal lobe in *Drosophila melanogaster*. J Comp Neurol 405:543–552
58. Schindelin J, Arganda-Carreras I, Frise E, Kaynig V, Longair M, Pietzsch T et al (2012) Fiji: an open source platform for biological image analysis. Nat Methods 9(7):676–682
59. Rizk A, Paul G, Incardona P, Bugarski M, Mansouri M, Niemann A et al (2014) Segmentation and quantification of subcellular structures in fluorescence microscopy images using Squassh. Nat Protoc 9(3):586–596

A Correlative Light-Electron Microscopy (CLEM) Protocol for the Identification of Bacteria in Animal Tissue, Exemplified by Methanotrophic Symbionts of Deep-Sea Mussels

Sven R. Laming and Sébastien Duperron

Abstract

Bacterial symbionts associated with animal tissues play major roles in the functioning of various ecosystems. Identification of bacteria often relies on marker gene comparative sequence analysis and fluorescence in situ hybridization (FISH). However, analysis of bacteria and host ultrastructure using transmission electron microscopy (TEM) can be equally important to understand the localization of bacteria and the degree of host-symbiont integration. We here provide a protocol which allows both FISH and TEM to be performed sequentially on a single section of tissue. Observations can then be superimposed, allowing ultrastructural investigation to be coupled with proper FISH-based identification of bacteria.

Keywords: Correlative microscopy, Fluorescence in situ hybridization, Symbiosis, Transmission electron microscopy

1 Introduction

Fluorescence in situ hybridization (FISH) is very often used in the assessment of microbial symbioses to identify bacteria associated with animals [1]. It most often uses 16S rRNA phylotype-specific oligonucleotide probes labeled with fluorochromes (FISH, DOPE-FISH) or enzymes that allow signal amplification (CARD-FISH) [2, 3]. However, FISH is constrained by poor resolution due to an upper threshold determined by the emission wavelength of the target signal observed and by the limits placed on separation power by fluorescence microscopy, preventing the visualization of fine structural details. Such information may be of importance when assessing the degree to which microbial symbionts are integrated into host tissues, for example, their intra- or extracellular localization. It is also important when investigating eventual ultrastructural differences between distinct symbionts in terms of size, internal structures, or the presence

T.J. McGenity et al. (eds.), *Hydrocarbon and Lipid Microbiology Protocols*, Springer Protocols Handbooks (2016) 163–174,
DOI 10.1007/8623_2015_85, © Springer-Verlag Berlin Heidelberg 2015, Published online: 16 June 2015

of inclusions [4]. It may therefore be desirable to examine the ultrastructure of tissues in more detail, using electron microscopy. Symbiosis studies often use low- and high-resolution approaches in tandem to examine discrete, complementary aspects of symbioses [5]. These are typically carried out on separate sections of tissue, as hybridization and counterstaining techniques for fluorescence and transmission electron microscopy (TEM), respectively, are assumed to be mutually exclusive. However, due to the relative size of microbial symbionts, neighboring sections cut in sequence will almost never feature the same bacterium. Consequently, any biological inferences made using FISH and TEM will not be based on the same set of bacteria. By making careful adjustments to each protocol (**Note 1**) and accepting certain technical compromises (**Note 2**), it is possible to employ correlative light-electron microscopy (CLEM) on a single section to overcome this problem, by first performing FISH and, following some washing and counterstaining steps, TEM [6]. If a sufficient number of micrographs are captured following each procedure, FISH and TEM image mosaics of identical regions in the same semi-thin section can then be superimposed directly upon one another for direct visual correlation, using the protocol presented below. This protocol is exemplified by methanotrophic symbionts present in gills of deep-sea cold seep mussels, though it can be adapted to other types of bacteria and animal tissues.

2 Materials

1. Ultramicrotome and accessories.
2. Epifluorescence microscope.
3. Hydrophobic PAP pen, available at Sigma Aldrich cat: Z377821.
4. Hybridization oven.
5. Liquid nitrogen.
6. Gelatine capsules (size 00, Electron Microscopy Sciences, UK) and holder.
7. LR white medium-grade resin (London Resin Company, UK).
8. Toluidine solution.
9. Carbon Film 200 Mesh, Nickel TEM grids and grid holders.
10. Precision forceps for handling EM grids.
11. Filter paper.
12. 8 mm diameter circular coverslips or coverslips of equivalent size.
13. Eppendorfs (PCR type).
14. Hybridization buffer containing 900 mM NaCl, 20 mM Tris HCl, 0.01% SDS, and 10–60 %vol. formamide depending on the probe(s) used (Table 1).

Table 1
Composition of hybridization buffer depending on the formamide concentration employed

Formamide used	10%	20%	30%	40%	50%	60%
NaCl (5 M)	1.08	1.08	1.08	1.08	1.08	1.08
Tris HCl (1 M)	0.12	0.12	0.12	0.12	0.12	0.12
Milli-Q	4.2	3.6	3	2.4	1.8	1.2
SDS (20%)	0.003	0.003	0.003	0.003	0.003	0.003
Formamide	0.6	1.2	1.8	2.4	3	3.6

Concentrations of stock solutions are displayed, and volumes are given in mL for a final volume of ~6 mL, to be used for wetting tissue in hybridization chambers and for mixing with probes

Table 2
Composition of washing buffer depending on the formamide concentration employed during hybridization

Formamide used	10%	20%	30%	40%	50%	60%
NaCl (5 M)	900	430	204	92	36	8
Tris HCl (1 M)	200	200	200	200	200	200
EDTA (0.5 M)	0	100	100	100	100	100
SDS (20%)	5	5	5	5	5	5
Milli-Q	8,900	9,300	9,500	9,600	9,650	9,700

Concentrations of stock solutions are displayed, and volumes are given in μL for a final volume of 10 mL

15. Washing buffer, composition depends on formamide concentration used for hybridization (Table 2).
16. Anti-fade mounting medium, such as SlowFade with DAPI available at Life Technologies cat: S36938, with or without DAPI.
17. Proper DNA probes labeled with various fluorochromes in their 5′ end can be ordered from various companies such as Eurogentec (examples in Duperron [8], this volume, Table 3).
18. Uranyl acetate solution containing 1.25 g uranyl acetate per 25 mL Milli-Q water. Prepare on the day of use and keep in the dark.
19. Lead (II) citrate solution containing 0.1 mL NaOH (10 M) and 0.02 g lead (II) citrate per 10 mL CO_2-free Milli-Q water.
20. Plastic petri dishes.
21. Pelletized potassium hydroxide.

22. Extraction hood.
23. Glass microscope slides.
24. Install ImageJ and plugin MosaicJ on a computer [7].

3 Methods

3.1 Tissue Fixation, Embedding, and Grid Preparation for CLEM

Tissue fixation using formaldehyde with serial transfer to 80% ethanol is recommended (detailed Duperron [8]; this volume, Sect. 4.2.3). The resin used for embedding animal tissue intended for CLEM-type analyses must meet specific FISH and TEM requirements in order to optimize both techniques. The protocol below uses thermal-cured LR white medium-grade resin, a low toxicity, ultralow viscosity polyhydroxy-aromatic acrylic. Once polymerized, the resin is both hard and hydrophilic, permitting the cutting of sections sufficiently thin for TEM, while ensuring probe permeability during FISH. Several means of polymerization exist for this resin; however, only anaerobic thermal curation is presented here.

1. Bring LR white resin to room temperature.
2. In a suitable capsule holder, prepare two uncapped gelatin capsules (size 00) for each tissue sample to be embedded.
3. Half-fill first capsule with unpolymerized LR white.
4. Remove target tissue from ethanol (**Note 3**), blot dry with filter paper, and immerse in resin in first capsule.
5. Leave for 30 min so resin can infiltrate.
6. Remove used resin completely with transfer micropipette. If tissue samples are small, the use of a dissecting microscope can help to prevent their accidental removal.
7. Place the waste LR white into a dedicated container to be disposed of later following polymerization into a solid.
8. Refill the capsule containing the tissue with fresh resin.
9. Repeat **steps 6–8** eight more times, excluding **step 9** on the eighth and last repeat.
10. Half-fill the second capsule with fresh unpolymerized LR white and carefully transfer the fully infiltrated tissue into it.
11. Once the tissue has sunk to the bottom, orientate using a stiff hair or nylon thread by rolling the tissue into position (under a dissecting microscope if necessary).
12. Fill capsule to brim with resin until a convex meniscus is formed, and carefully replace the cap down fully until it clicks, catching overflowing resin with tissue. This minimizes the volume of air trapped at the top. Ensure the exterior is cleaned of resin.

13. Carefully place the sealed capsule securely in the holder in a vertical position, and relocate to an oven preheated to 55°C to polymerize, for a minimum 20 h.
14. Following polymerization, gelatin can be removed with hand-hot water.
15. Having trimmed the resin pellet, wet-cut sections on a suitable ultramicrotome (glass knives with boats are sufficient), employing periodic toluidine staining to identify the cutting axis and suitability of tissue for CLEM analyses, according to standard TEM protocols.
16. When target tissue region is located (i.e., well-preserved suitable host tissue and the presence of putative symbionts), ramp down to 300 nm and begin cutting semi-thin sections until cut consistency and iridescent hue becomes uniform (300 nm sections should be slightly transparent and somewhere between purple and blue green).
17. Let sections rest in the boat for a period of time, to minimize compression effects during cutting.
18. Transfer sections onto the darker, coated side of Carbon Film 200 Mesh, nickel grids, avoiding pleats (**Note 5**).
19. Leave the grid to air-dry and carefully transfer to and store in a dust-free grid holder.

3.2 CLEM Part 1: Adapted FISH Protocol and Fluorescence Imaging

As with standard FISH, symbiont- or group-specific oligonucleotide probes targeting ribosomal RNA (usually 16S or 23S) are applied during CLEM-type FISH. Probe specificity and suitable formamide concentrations are best assessed on a tissue by tissue basis according to the same criteria. This can be done in advance of CLEM using the standard FISH protocol, but carried out on thinner 300-nm LR white sections on Superfrost Plus slides (rather than grids, for simplicity) with an extended hybridization step of 20 h. Once the formamide concentration has been established (**Note 5**), FISH can be performed on the grid-mounted samples. Note that in the following protocol, the composition of the hybridization and washing buffers is prepared as indicated in Tables 1 and 2 (i.e., Tris HCl is retained, contrary to Halary [6]).

1. If not already, bring grids to room temperature in their holder.
2. Preheat hybridization chambers containing a piece of tissue wetted with hybridization buffer to 46°Cs.
3. Using a PAP pen on microscope slides (they need not be Superfrost Plus), trace an empty encircled area (min diameter 5 mm) for each of the grid-loaded sections to be hybridized, with a maximum of 4 per slide.
4. Note what each circle is intended to hold with regard to buffer, grid, and associated probes. At least one of the encircled areas should be for a control on each slide (refer again to **Note 3**).

5. First distribute the hybridization buffer and probes chosen for each encircled area, ensuring adjacent aliquots do not mix (1:15 dilution of the 50 ng/μL probe stock solution in buffer). Several probes with distinct fluorochromes can be mixed: each probe contributes to the overall aliquot volume, which is best kept below 30 μL. Probes are light sensitive, so the following steps should be performed under low, indirect light.
6. Using precision forceps suitable for handling TEM grids, place grids section-side down floating on buffered, probe-loaded aliquots.
7. Once all grids are loaded, place the glass slides into preheated hybridization chamber carefully, close and gently seal chamber, and leave to hybridize for 20 h at 46°C in darkness.
8. Prior to the end of the hybridization, prepare two Eppendorfs filled with washing buffer for each grid being processed (volume depends on incubation approach, **Note 6**) and preheat them to 48°C.
9. Carefully retrieve the slides from the hybridization chambers. Using fine forceps, carefully extract each grid, touch grid edge to filter paper to remove retained hybridization buffer, and quick dip several times in the first washing buffer Eppendorf tube. Then transfer the grid to the second washing buffer Eppendorf tube, seal it, and incubate for 15 min in the dark. Wipe the forceps clean between grids.
10. Remove grids carefully from Eppendorfs using forceps, touch grid edge to filter paper to remove retained washing buffer, and quick dip several times in Milli-Q water (RT). Leave each grid to dry on filter paper, keeping note of which grid is which throughout.
11. Place a small amount of anti-fade (1–2 μL) on the underside of each grid while inverted (opposite side to the tissue section), to minimize trapped microbubbles.
12. Place up to four grids (section-side up) on each slide, spaced apart, resting on the small droplet of anti-fade.
13. Add a similar volume of anti-fade to the section side of each grid near their edges and gently cover with coverslip; the smaller the coverslip, the easier it is to remove later (individual 8 mm diameter circular coverslips work very well, **Note 4**).
14. Press each coverslip down gently until it begins to resist lateral movement and remove excess anti-fade using a filter paper edge, if necessary.
15. Store at −20°C until observation. Overnight storage often improves the signal-to-noise ratio by decreasing tissue autofluorescence.

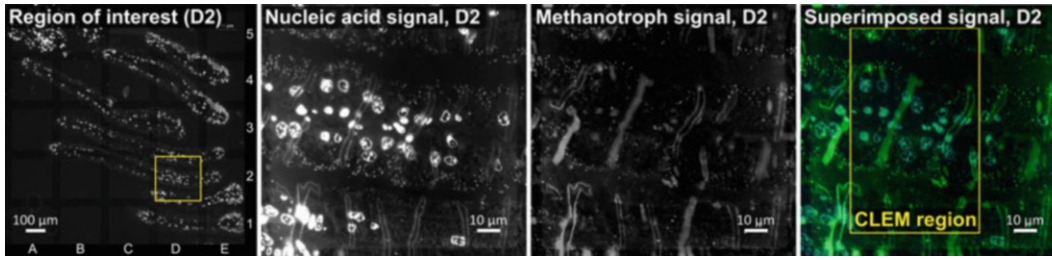

Fig. 1 FISH imaging of bacteria upon bivalve gill filaments using micrograph mosaics. The images from left to right are of mosaics made up of individual aligned micrographs either at 20× (first) or 100× objectives (remaining images). Pictured are views of gill tissue in sagittal section from a chemosymbiotic bivalve, *Idas modiolaeformis*. The latter three micrographs are magnified views of region D2 in the first reference micrograph, labeled accordingly. The overlaid methanotroph-specific signal upon DAPI in the last image reveals corresponding signal between the two labeling techniques (and also a general eubacterial probe, which is not pictured). The "CLEM region" refers to the region imaged with TEM, allowing correlative imaging to be performed (*see* Figs. 2 and 3). The methanotroph signal was obtained using probe MedM-138 [9]

Sections can then be observed under an epifluorescence microscope (suitability of confocal microscopy may depend on the plane of laser excitation, as completely flat grids are rare), and images are acquired using excitation wavelengths corresponding to the different fluorochromes (Fig. 1). In order to construct mosaic images for CLEM, sequences of overlapping images are captured manually under the 100× objective to permit the alignment of tiled images of target tissues, identified during fluorescence imaging (*see* Fig. 1). This procedure can be automated on microscopes equipped with a motorized stage. At this magnification, four overlapping images will cover one grid square. Mosaics can be created using Adobe Photoshop (*File* > *Automate* > *Photomerge* > *Reposition only* or *Interactive layout*) or by using the MosaicJ plugin of ImageJ, discussed in more detail later using the TEM images [7]. Ideally several target squares within which target tissue and symbionts appear should be imaged in this way for each grid and each emission wavelength.

3.3 CLEM Part 2: Grid Removal and Temporary Storage

1. Plunge the coverslip to be removed into liquid nitrogen, and once the nitrogen ceases to boil, remove the slide, and using a scalpel or feather blade, lever off the coverslip. The grid should remain in place.
2. Remove grid using fine forceps (heating the underside of the glass with a finger tip if necessary) and rinse with ultrapure water and dry on filter paper.
3. Place in a dust-free grid holder and store in the fridge.

3.4 CLEM Part 3: TEM Protocol and Imaging

Pre-embedding contrast staining using osmium tetroxide must be omitted by necessity when performing CLEM. Although it is not explored here, in theory it may be feasible to include a post-FISH

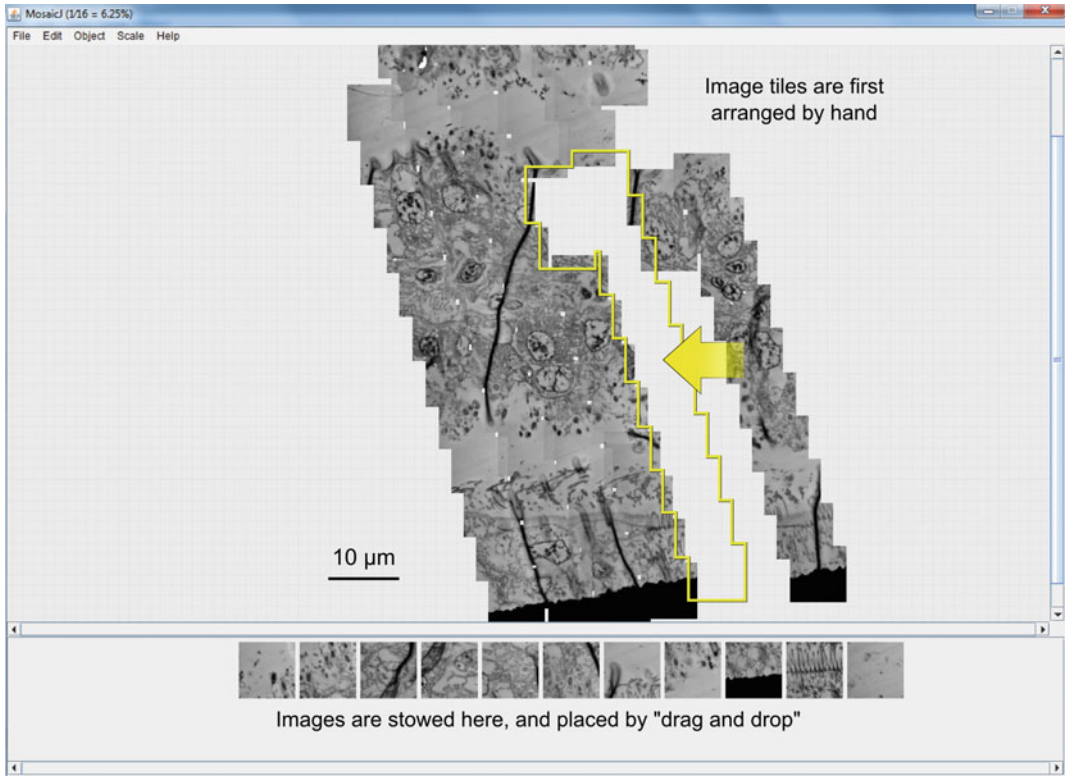

Fig. 2 Using MosaicJ in ImageJ. The screenshot shows the TEM images midway through the process of creating the mosaic, made up of individual hand-aligned micrographs at a relatively high magnification (2,000×), in the main window pane. These images correspond to a region in square D2 indicated in Fig. 1. Images can be dragged as groups seen here in *yellow*. The images stowed in the scrolling pane beneath are yet to be added. Final precision alignments and moderate blending are performed automatically

osmium tetroxide treatment on individual grids at this stage. However, the contrast staining described here involves uranyl acetate and lead (II) citrate only.

1. Prepare two plastic petri dishes under an extraction hood: the first is for uranyl acetate staining and must be in complete darkness, and the second is for lead citrate staining, which is performed in the absence of CO_2 (**Note** 7). Turn the hood's fan on.
2. Prepare the uranyl acetate and lead (II) citrate solutions fresh.
3. Prepare a washing solution of 50% ethanol (aqueous) and a separate one of Milli-Q.
4. Immediately prior to use, filter the uranyl acetate solution (e.g., using a 20-µm syringe filter) and dilute in absolute ethanol (1:1).

5. Add as many separate aliquots of each solution as there are grids to be stained, to the base of their respective petri dish staining chambers. Replace the lid of the second CO_2-free dish immediately.
6. Float the grids section-side down on the aliquots of the uranyl acetate, replace the lid, and leave in complete darkness for 7 min.
7. Remove the lid (first dish), lift each grid and dip several times in the 50% ethanol solution, and touch-dry on filter paper.
8. Open the second petri dish and float each grid section-side down on the aliquots of lead (II) citrate and return the Parafilm-sealed lid immediately. Leave for 7 min.
9. Remove the lid (second dish), lift each grid and dip several times in the Milli-Q, and touch-dry on filter paper.
10. Place in a dust-free grid holder and store in the fridge.

Sections can then be observed under a transmission electron microscope so long as the power of the microscope is sufficient to penetrate 300-nm sections. As this is not always the case, be sure to confirm this with the operating technician. Using the lowest magnification that entirely fills the field of view (i.e., no circular border from the microscopes narrowest aperture), take sequences of overlapping images to cover the grids selected during FISH imaging. This may involve a large number of images and is far easier to perform if it can be automated sequentially between saved grid references. Specific microbes and target host tissues visible in reference FISH images can then be selected and viewed at full magnification. If a mosaic-type feature is not available (or fails to work) in the TEM software, mosaics can be created using Adobe Photoshop (*File* > *Automate* > *Photomerge* > *Reposition only* or *Interactive layout*), though with large numbers of images, mosaics are best reconstructed using the MosaicJ plugin of ImageJ (Abramoff et al. [7], Fig. 3). The images can be dragged and dropped into the MosaicJ window once the plugin is running. Initially, images will appear in the scrolling window below. These can then be selected and dragged into the upper window for rough alignment by hand. The sequence of images is best named and ordered incrementally. When complete, the plugin aligns overlapping tiles more precisely based on to the registration engine TurboReg, which must be installed independently of MosaicJ. For details see http://bigwww.epfl.ch/thevenaz/mosaicj/. It remains to identify the overlapping regions of the FISH and CLEM mosaics and superimpose one upon the other. The superimposed images in Fig. 4 were performed manually in a vector graphics package (Inkscape v. 0.48).

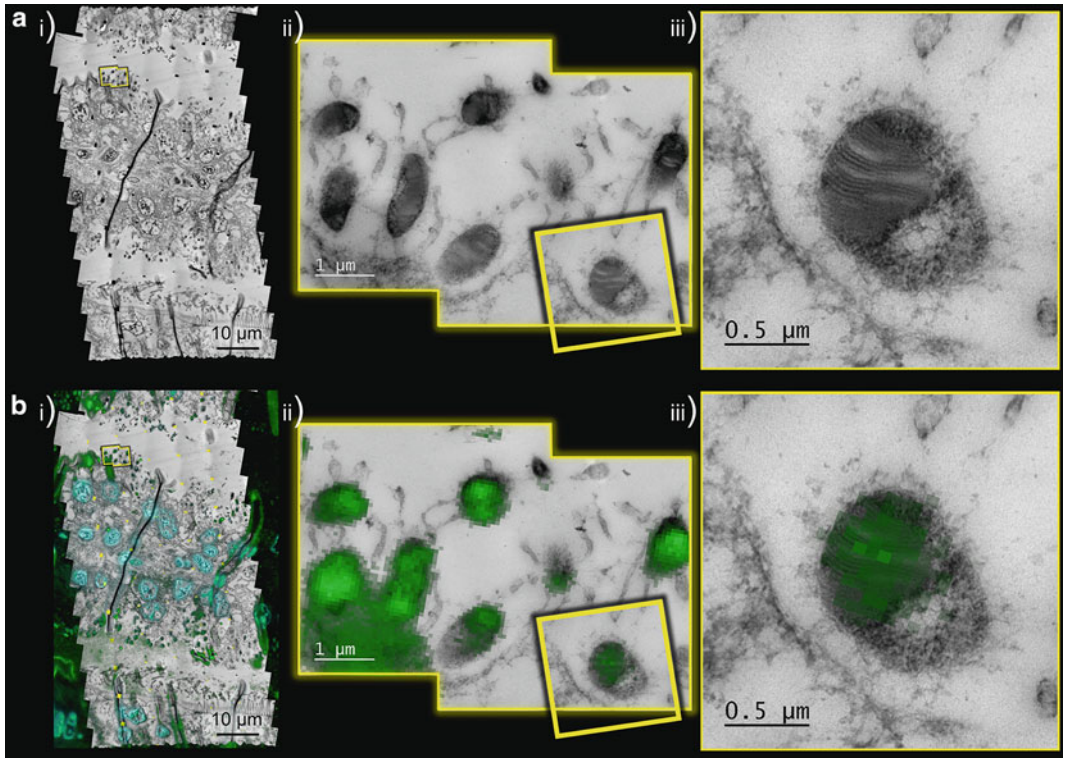

Fig. 3 Manual CLEM superimposition of FISH and TEM mosaics. Images are (**a**) TEM mosaics or single images at increasing magnifications from (i)–(iii). Regions of interest are indicated in *yellow* in the preceding image from left to right. In (**b**) the same TEM mosaics are overlaid with FISH image mosaics (see full images in Fig. 1) which correspond to the same region. In (i) both a blue signal (DAPI) and a green signal (methanotroph probe) have been overlaid on top. In (ii) and (iii) only methanotroph signal is shown for clarity. Ultrastructural details from high-resolution TEM images thus augment the data available from the specific fluorescent labeling through FISH. In this case, intracellular stacked membranes seen in both figures (iii) are typical of type I methanotrophic Gammaproteobacteria, supporting the phylogenetic relatedness already identified using specific FISH probes. Note that FISH signal is highest in intact bacteria. Images were superimposed in the vector graphics software Inkscape, having removed the black background in Photoshop CS6

4 Notes

1. Main adjustments include the following: (a) the use of a hard methacrylate embedding resin and an ultramicrotome for semi-thin sectioning; (b) FISH hybridizations being performed upon sections mounted on custom TEM grids, resistant to corrosion; (c) the extension of FISH hybridization times to accommodate reduced section thicknesses; (d) the washing of grids immersed in Eppendorfs rather than as sections on slides in a rack/falcon tube; (e) transitory sample treatment to allow post-FISH counterstaining for TEM; and (f) an electron microscope powerful enough to penetrate semi-thin sections.

2. Principal compromises include (a) semi-thin sections (300 nm) at thicknesses falling between those employed in FISH and TEM as standard; (b) the retention of embedding resin and use of TEM grids during FISH, which can result in refracted-light aberrations and variability in focal planes, respectively; and (c) the complete omission of osmium tetroxide counterstaining.
3. When using LR white, tissue stored in ethanol at >70% does not need to be dehydrated any further prior to infiltration within resin. However if preferred, serial transfer to higher-% ethanol grades will not affect the quality of embedding adversely.
4. This can be achieved either by drawing the grid upward, from below the water's surface in the knife boat, or by using a suitable EM loop and transferring the section to a grid on a dry slide, drawing the excess water laterally (because of impermeable carbon film) by touching filter paper to the edge.
5. A default concentration of 30% formamide is recommended as a starting point.
6. The best is to use PCR-type Eppendorfs placed in a thermocycler set at 48°C (the temperature will be stringently controlled in this way). Alternatively, larger Eppendorfs may be used in a rack, placed in a water bath maintained at 48°C. In either case use caution: due to the viscosity of the washing buffer, the grids will likely sink. Retrieval is best achieved using forceps, having gently rotated the grid to access its edge if necessary. Avoid bending the grid.
7. Cover the first petri dish with an opaque lid, since the uranyl acetate solution is photolabile. Fifteen mins ahead of use, place KOH pellets within the second dish at the perimeter of the base, balance a square of Parafilm so as to cover the open rim, and replace the lid on top to seal the petri dish. The KOH absorbs CO_2 which otherwise readily forms precipitous, electron dense lead carbonate.

References

1. Dubilier N, Bergin C, Lott C (2008) Symbiotic diversity in marine animals: the art of harnessing chemosynthesis. Nat Rev Microbiol 6:725–740
2. Pernthaler A, Pernthaler J, Amann R (2002) Fluorescence in situ hybridization and catalysed reporter deposition for the identification of marine bacteria. Appl Environ Microbiol 68:3094–3101
3. Stoecker K, Dorninger C, Daims H, Wagner M (2010) Double labeling of oligonucleotide probes for fluorescence in situ hybridization (DOPE-FISH) improves signal intensity and increases rRNA accessibility. Appl Environ Microbiol 76:922–926
4. Cavanaugh CM, Levering PR, Maki JS et al (1987) Symbiosis of methylotrophic bacteria and deep-sea mussels. Nature 325:346–347
5. Distel DL, Lee HKW, Cavanaugh CM (1995) Intracellular coexistence of methano- and thioautotrophic bacteria in a hydrothermal vent mussel. Proc Natl Acad Sci U S A 92:9598–9602

6. Halary S, Duperron S, Boudier T (2011) Direct image-based correlative microscopy technique for coupling identification and structural investigation of bacterial symbionts associated with metazoans. Appl Environ Microbiol 77(12):4172–4179
7. Abramoff MD, Magalhaes PJ, Ram SJ (2004) Image processing with ImageJ. Biophoton Int 11:36–42
8. Duperron S (2015) Characterization of bacterial symbionts in deep-sea metazoans: protocols for conditioning, fluorescence in situ hybridization, and image analysis. In: Mc Gentity TJ, Timmis KN, Nogales B (eds) Hydrocarbons and lipid microbiology protocols. Springer. doi:10.1007/8623_2015_73
9. Duperron S, Halary S, Lorion J et al (2008) Unexpected co-occurrence of 6 bacterial symbionts in the gill of the cold seep mussel Idas sp. (Bivalvia: Mytilidae). Environ Microbiol 10:433–445